



HAL
open science

Lipid transporters in the morphogenesis of the opportunistic human fungal pathogen *Candida albicans*

Miguel Angel Basante-Bedoya

► **To cite this version:**

Miguel Angel Basante-Bedoya. Lipid transporters in the morphogenesis of the opportunistic human fungal pathogen *Candida albicans*. Molecular biology. Université Côte d'Azur, 2021. English. NNT : 2021COAZ6030 . tel-04318930

HAL Id: tel-04318930

<https://theses.hal.science/tel-04318930>

Submitted on 2 Dec 2023

HAL is a multi-disciplinary open access archive for the deposit and dissemination of scientific research documents, whether they are published or not. The documents may come from teaching and research institutions in France or abroad, or from public or private research centers.

L'archive ouverte pluridisciplinaire **HAL**, est destinée au dépôt et à la diffusion de documents scientifiques de niveau recherche, publiés ou non, émanant des établissements d'enseignement et de recherche français ou étrangers, des laboratoires publics ou privés.

THÈSE DE DOCTORAT

Transporteurs lipidiques dans la
morphogénèse du champignon
pathogène opportuniste
de l'Homme *Candida albicans*.

Miguel Ángel BASANTE-BEDOYA

Institut de Biologie de Valrose (iBV)

Présentée en vue de l'obtention

du grade de docteur en Sciences de la vie
et de la santé - Interactions moléculaires et
cellulaires

d'Université Côte d'Azur

Dirigée par : Dr. Martine BASSILANA

Soutenue le : 10 décembre 2021

Devant le jury, composé de :

Dr. Martine Bassilana, CNRS DR, iBV,
Université Côte d'Azur

Dr. Robert Arkowitz, CNRS DR, iBV
Université Côte d'Azur

Dr. Derek McCusker, CNRS DR, IBGC,
Université de Bordeaux

Pr. James Konopka, Stony Brook
University, NY, USA

Dr. Cathy Jackson, CNRS DR, Inst.
Jacques Monod, Paris

Dr. Guillaume Drin, CNRS DR, IPMC,
Université Côte d'Azur

Transporteurs lipidiques dans la morphogenèse du champignon pathogène opportuniste de l'Homme *Candida albicans*

Jury :

Président du jury

Dr. Robert Arkowitz, CNRS DR, iBV Université Côte d'Azur

Rapporteurs

Dr. Derek McCusker, CNRS DR, IBGC, Université de Bordeaux

Pr. James Konopka, Stony Brook University, NY, USA

Examineurs

Dr. Cathy Jackson, CNRS DR, Inst. Jacques Monod, Paris

Dr. Guillaume Drin, CNRS DR, IPMC, Université Côte d'Azur

RÉSUMÉ

Candida albicans est un champignon pathogène opportuniste de l'homme qui peut causer des infections superficielles ou systémiques; sa capacité à passer d'une forme ovoïde à une forme filamenteuse est associée à sa virulence. Pendant cette croissance filamenteuse hautement polarisée, une accumulation de vésicules (Spitzenkörper), caractéristique des champignons filamenteux, ainsi qu'une distribution enrichie de lipides, tels que l'ergostérol, les dérivés phosphorylés du phosphatidylinositol (PI(4)P, PI(4,5)P₂) et la phosphatidylsérine (PS) est observée à l'apex des filaments. Cependant, l'importance de l'asymétrie de ces lipides dans la bicouche membranaire est méconnue. Les flippases (P4-ATPases) transportent les lipides à travers la bicouche membranaire pour générer et maintenir son asymétrie. *C. albicans* a 5 flippases, incluant Drs2 qui est critique pour la croissance filamenteuse et la distribution de phosphatidylsérine (PS). De plus, un mutant de délétion *drs2* est hypersensible au fluconazole et au cuivre et nous montrons ici qu'un tel mutant est aussi critique à la virulence dans un modèle murin d'infection systémique. Pour préciser le rôle de Drs2 pendant la croissance filamenteuse de *C. albicans*, nous avons étudié la distribution de cette ATPase, ainsi que celle de lipides et régulateurs clés, pendant l'initiation et le maintien de ce processus de croissance. Nous avons également caractérisé des mutants ponctuels de Drs2, analogues à ceux altérés pour le transport de PS chez *S. cerevisiae*. De plus, nous avons examiné l'importance d'autres flippases, telles que Dnf1-3, dans la croissance filamenteuse invasive ainsi que le rôle de transporteurs de lipides appartenant à la famille des « oxysterol binding protein » (Osh). Nos résultats indiquent que Drs2 joue un rôle unique dans le maintien de la croissance filamenteuse de *C. albicans*, qui paraît particulièrement critique après la formation du premier septum, et indiquent qu'une interaction entre Drs2 et Osh4, via PI(4)P, joue un rôle essentiel pour la croissance filamenteuse.

Mots clés : *Candida albicans*, croissance invasive, croissance polarisée, transporteurs lipidiques, flippases, phospholipides.

ABSTRACT

Candida albicans is a human opportunistic fungal pathogen that can cause superficial or systemic infections; its ability to change from an ovoid to a filamentous form is associated with its virulence. During this highly polarized filamentous growth, an accumulation of vesicles (Spitzenkörper), characteristic of filamentous fungi, as well as a polarized distribution of lipids, such as ergosterol, phosphorylated derivatives of phosphatidylinositol (PI(4)P, PI(4,5)P₂) and phosphatidylserine (PS) is observed at the apex of filaments. However, the importance of the asymmetry of these lipids in the membrane bilayer is not completely understood. Flippases (P4-ATPases) transport lipids across the membrane bilayer to generate and maintain its asymmetry. *C. albicans* has 5 flippases, including Drs2 which is critical for filamentous growth and phosphatidylserine (PS) distribution. Furthermore, a *drs2* deletion mutant is hypersensitive to fluconazole and copper. We show here that such a mutant is also critical to virulence in a mouse model of systemic infection. To clarify the role of Drs2 during *C. albicans* filamentous growth, we studied the distribution of this ATPase, as well as that of key lipids and regulators, during the initiation and maintenance of this growth process. We also characterized point mutants of Drs2, analogous to those altered for PS transport in *S. cerevisiae*. In addition, we examined the importance of other flippases, such as Dnf1-3, in invasive growth and the role of lipid transporters belonging to the oxysterol binding protein (Osh) family. Our results indicate in particular that Drs2 plays a unique role in the maintenance of invasive filamentous growth of *C. albicans*, which appears to be more critical after the first septum formation, and that an interaction between Drs2 and Osh4, *via* PI(4)P, plays an essential role during invasive filamentous growth.

Key words: *Candida albicans*, invasive growth, polarized growth, lipid transporters, flippases, phospholipids.

CONTENTS

RÉSUMÉ.....	i
ABSTRACT	ii
Acknowledgements	iv
List of abbreviations.....	vii
INTRODUCTION.....	1
Chapter I: The fluid mosaic	2
1. Lipid classification.....	2
2. Membrane composition: the importance of charged lipids.....	6
3. Fluidity and organization of the mosaic:	10
Chapter II. How lipid composition is established and maintained.	13
1. Vesicular transport:	14
2. Non-vesicular transport: Lipid transporter proteins (LTPs)	17
3. Membrane asymmetry:	24
Chapter III: <i>Candida albicans</i>	33
1. Virulence.....	34
2. <i>Candida albicans</i> morphogenesis	36
3. Lipids in <i>C. albicans</i>	52
THESIS OBJECTIVES.....	61
MATERIAL AND METHODS	62
Growth conditions	63
Plasmid construction.....	64
Strain construction.....	68
Microscopic analyses.....	75
RESULTS.....	94
Additional results.....	155
DISCUSSION	165
CONCLUSION	174
BIBLIOGRAPHY	175

Acknowledgements

I would like to sincerely thank the members of the jury for accepting this role and evaluating my PhD project.

I always thought that this section was going to be the easiest, but actually, when I think of all the people who collaborated, professionally and personally, to make this thesis a success, the task becomes more complicated...

Ça fait six ans (déjà !) que j'ai rencontré ce labo. Je suis vraiment reconnaissant que ce soit dans ce labo que j'ai acquis, dans la pratique, mes premières connaissances en recherche. La bonne ambiance, le travail d'équipe et le soutien de tous les membres ont fait paraître ce boulot plus facile de ce qu'il l'est vraiment. Je tiens donc à vous remercier, Rob et Martine, de m'avoir donnée la chance, pas seulement une fois, de rejoindre l'équipe Arkowitz pour ma formation, et de m'avoir aidé à participer dans différents congrès et formations. Martine, je voulais t'adresser un gros MERCI pour toute la confiance déposée en moi, pour avoir été toujours très franche et directe quand je pouvais faire mieux de ce que j'étais en train de faire, tu m'as poussé de la bonne manière à arriver plus loin pendant ces années que j'ai été à ta charge.

Cette équipe a changé tellement de taille, quand je suis arrivé en était presque quinze personnes maintenant beaucoup de gens sont parti et des nouveaux sont arrivés. Cela peut paraître un peu triste, mais en même temps j'ai eu la chance de rencontrer des excellent.e.s scientifiques et encore meilleures personnes. Rocío, je dois commencer par toi, pas seulement parce que tu as été la première scientifique avec qui j'ai travaillé côte à côte, mais parce que tu as contribué énormément à ma formation, tu m'as appris beaucoup pendant si peu de temps, et grâce à toi, pas seulement j'ai eu une excellente fin de licence à Madrid, mais aussi, tu m'as servi d'exemple de persévérance pour continuer dans ce boulot et tu m'as toujours soutenu, tu as eu plus de confiance en moi que je n'en ai eu en moi-même. Muchísimas gracias, de corazón.

Celui qui dit que le travail d'équipe n'est pas indispensable pour faire une thèse n'a pas apprécié la meilleure partie de ce boulot. J'ai eu la meilleure équipe et toi, Steph, tu as été mon compagnon de guerre pendant toutes ces années, tu as été là pour m'écouter et me conseiller, pour me remonter le moral, pour les fous rire. Merci d'avoir contribué autant à ce travail et d'avoir fait en sorte que l'on soit tous une grande famille qui travaille ensemble.

I think I am very lucky; I came to France because I wanted to learn French and at the same time, I wanted to continue my career. This lab was the best I could have found, not only because of the scientific skill I gained, but also because I learned how to communicate in so many languages... Hayet, Rohan, Pat, Nadia, Charlitos, thank you for sharing with me a bit of your culture, for making me a better speaker and for all the international laughs and great moments together!

Charlitos, I am very thankful for everything you taught me (believe me, it was more than what you think), in and out of the lab, you and Maggy made me an English speaker and a snowboard beginner! “CON TACONES!!!!”.

There are so many people I would like to thank; Antonio, last arriver but already your support has been very important! Ma petite Marine, j’ai l’impression de te connaître depuis des années, tu as toujours eu un gros sourire pour moi, et je te remercie énormément que même depuis la distance tu aies toujours un petit mot au bon moment pour m’encourager.

Le soutien et la bonne compagnie ne venaient pas seulement des gens de ce bâtiment ou des personnes liées au travail. Après mon arrivée en France, il a fallu très peu de temps pour me faire une place dans un groupe très chaleureux qui a joué le rôle d’une deuxième famille et des profs de français. Merci ONEP d’avoir été là pour moi. Et merci aussi à tous mes collègues de promo et grand.e.s ami.e.s (ça va même pour toi, Baptiste), on a survécu les gars !

Tengo que decir, que la suerte me ha llovido de todos lados. Desde el principio ha habido mucha gente que aportaron su granito de arena para que hoy pueda mirarlos y decirles con orgullo, gracias. A mis profesores de instituto de los que heredé el gusto por la biología, Lidia, ¡espero haber conseguido el diez! Graciela, creo que los golpes de borrador en la pizarra me sentaron bien al final, ¡gracias! Il y a aussi bien évidemment celle qui m’a fait adorer cette langue et qui m’a toujours encouragé pour venir en France et continuer à apprendre, Pilar, merci de m’avoir donné la clé pour ouvrir la première porte, celle qui m’a amené à cet endroit où j’ai tant grandi.

Marina, Nadia, después de tanto tiempo me cuesta hablar de vosotras como mis mejores amigas, creo que ya hace un buen rato que sois parte de mi familia, siempre estáis ahí, siempre he contado con vosotras, y siempre os encuentro cuando vuelvo a casa. Gracias por haberme apoyado durante este tiempo y por haberme dado fuerzas como habéis podido durante estos años de lejanía. Nadia, ha sido un honor haber compartido tantos años de carrera juntos, siento haberte abandonado en la última etapa, pero bueno, ¡no podía quedarme atrás! Siempre te he

admirado muchísimo, espero que lo sepas. Marina, vete pensando en cómo vamos a grabar este logro con tinta, ¡quién mejor que tú para tal tarea!

Michele, ciao, lo sai che ti meriti 1000 pagine. Sai anche molto bene che questo lavoro mi è piaciuto soprattutto perché l'ho condiviso con te in questi due anni, mi hai sempre aiutato a vederlo da un'altra prospettiva, e che mi hai sempre dato la forza necessaria per continuare, ancora e ancora. Grazie, grazie mille per tutto. Bau.

A mi padre, porque siempre fuiste un ejemplo de trabajo duro, adaptación y cuidado de los tuyos. A mi madre, quien me enseñó lo importante que es estar siempre ahí para los tuyos, que nunca hay que olvidarse a sí mismo. Vosotros dos me habéis enseñado que hay que dar siempre lo mejor de sí en todo. Nano, aunque no lo creas, también me has enseñado mucho, eres todo un luchador, y siempre he admirado eso. Sé que nunca fui un amante del balón, pero este gol os lo dedico a vosotros. Este trabajo es vuestro, fruto de vuestro trabajo, y de vuestra educación. Gracias, infinitamente.

I know I haven't mentioned everyone, but that doesn't mean I haven't thought of you. All of you who have worked with me, who will be watching me online on the D-day or coming here to see how this story ends, all of you who were there when I needed you and will be there to celebrate, thank you!

List of abbreviations

Abbreviation	Meaning
ABC	ATP-Binding Cassettes
ABP1	Actin Binding Protein
ADP	Adenosine-diphosphate
ALS	Agglutinin-Like Sequence
cAMP	Cyclic Adenosine Monophosphate
AP1-4	Adaptor protein 1-3
ARF	ADP-Rybolisation Factor
ARG4	Arginine 4
ARL	ARF-Like
Arp2/3	Actin Related Protein 2/3
ATP	Adenosine-triphosphate
BAR domain	Bin/Amphiphysin/Rvs domain
Bem1	Bud emergence protein 1 (scaffold)
Bni1	Spitzenkorper formin
BWP17	Wild-type <i>C. albicans</i> strain
Cdc	Cell division Cycle
CDK	Cyclin-dependent kinases
CERT	Ceramide transfer protein
COPI/II	Coat protein complex I/II
CORVET	Core class C vacuole/endosome tethering
CRIB	Cdc42/Rac Interactive-Binding

DAG	Diacylglycerol
DIC	Differential interference contrast (transmission image)
Dnf1-3	Drs2p/Neo1p family 1-3
Drs2	deficient in ribosomal subunits
ECE1	Elongation Cell 1
ER	Endoplasmic reticulum
ERES	ER exit sites
ESCRT	Endosomal sorting complex required for transport
F-actin	Filamentous actine
FAPP1/2	Four-phosphate-adaptor protein 1 and 2
FCS	Fetal calf serum
FFAT	two phenylalanine in an acidic tract
FM4-64	N-(3-Triethylammoniumpropyl)-4-(6-(4-(Diethylamino) Phenyl)
G-actin	Globular actin
GAP	GTPase Activating Protein
GAP	Guanine nucleotide Exchange Factor
GDP	Guanosine diphosphate
GFP	Green Fluorescent Protein
GNB	GFP nanobody
GPI	Glycosylphosphatidylinositol
GTP	Guanosine triphosphate
GUT	Gastrointestinally Induced Transition
HGC1	Hyphal G cyclin 1
HIS1	Histidine 1

Hwp1	Hyphal Wall Protein 1
HYG	Hygromycine
LTD	Lipid transfer domain
LTP	Lipid transporter proteins
MAP	Mitogen activated protein
MAPK	Mitogen activated protein kinase
MAPKK	Mitogen activated protein kinase kinase
MAPKKK	Mitogen activated protein kinase kinase kinase
MCC	Membrane Compartment of Can1
MCP	Membrane Compartment of Pma1
MCS	membrane contact sites
MDR	Multi-Drug-Resistance
Mlc1	Myosin Light Chain 1
mSc	mScarlet red fluorescent protein
MT	Microtubules
MTL	Mating Type like Locus
NAT	Nourseothricin N-acetyl transferase
NBD-DAG	Nitrobenzoxadiazole-labeled Diacylglycerol
Neo1	Neomycin resistant 1
ORD	OSBP Related Domain
ORF	Open Reading Frame
ORP	OSBP-related proteins
OSBP	Oxysterol Binding Proteins
OSH	OSBP homologous

PA	Phosphatidic acid
pACT1	Actin 1 promoter
pADH1	Alcohol dehydrogenase 1 promoter
PAK	p21 activated kinases
PC	Phosphatidylcholine
PCR	Polymerase Chain Reaction
PE	Phosphatidylethanolamine
PH	Pleckstrin Homology
PI	Phosphatidylinositol
PI(4)P	Phosphatidylinositol-4-phosphate
PI(4,5)P ₂	Phosphatidylinositol-4,5-biphosphate
PIP	Phosphatidylinositol phosphate
PKA	Protein Kinase A
PKC	Protein Kinase C
PLC	Phospholipase C
PM	Plasma membrane
PS	Phosphatidylserine
Ras	Rat sarcoma
RBCs	Red blood cells
Rho	Ras homology
RT-PCR	Reverse Transcription Polymerase Chain Reaction
SAP	Secreted Aspartyl Proteinase
SAT1	Streptothricin Acetyltransferase
SL	Sphingolipids

SLEDs	SL-enriched domains
SM	Sphingomyelin
SNARE	Soluble N-ethylmaleimide-sensitive-factor Attachment protein REceptor
SPK	Spitzenkörper
SRD	sterol-rich domains
START	Steroidogenic Acute Regulatory Transfer
TAG	triacylglycerol
TGN	<i>trans</i> -Golgi network
TM	Transmembrane domain
URA3	Uracile 3
VASt	StART-like analogous
VSC	Vesicle Supply Center
WGD	whole genome duplication
YEPD + Uri	Yeast extract peptone dextrose media with uridine

INTRODUCTION

Chapter I: The fluid mosaic

Key to separate the inside of a cell from its external environment, the cell membrane -or plasma membrane- is a structure present in all organisms, prokaryotes as well as eukaryotes. The existence of the cell membrane was established in 1890 and in 1900, when Charles Ernest Overton proposed the "Overton Biomembrane Model". In 1925, based on studies of erythrocytes, Gorter and Grendel proposed the theory of the lipid bilayer (Gorter and Grendel, 1925). Ten years later, the "paucimolecular model" of Danielli and Davson, which prevailed until 1972, incorporated the presence of proteins, stating that the lipid bilayer is found inside two layers of globular proteins, which would create the tension on the surface of lipid bilayers (Danielli and Davson, 1935).

These were the premises leading to the current model, the "fluid mosaic model", first proposed in the 70s by Singer and Nicolson (Singer and Nicolson, 1972), stating that membranes are composed of a lipid bilayer with a hydrophobic inner part and a hydrophilic outer one. Proteins (the "mosaic" pieces) are found floating within this lipid bilayer. They can interact with the polar parts on the outside, such as peripheral proteins, or with both parts of the membrane on the inside, *via* the presence of non-polar amino acids that cross the entire lipid bilayer. As these components can move laterally, the mosaic is defined as a dynamic, "fluid" entity. The next chapters will delineate the characteristics of both lipid-lipid and lipid-protein interactions, main actors of the "fluid mosaic" model.

1. Lipid classification

The functions of lipids are numerous. Key to the structuring of biological membranes, they are also involved in energy storage and in cell signaling. Biomolecules such as lipids and proteins can interact in a non-covalent and highly dynamic way. The physical properties of cell membranes are based on the various molecular characteristics of the lipids, such as the length

and saturation of the carbon chains, the charges present in the polar heads and the asymmetric distribution of lipids between the two leaflets of the membrane. As an example of protein-lipid crosstalk, it was shown that, whether through direct lipid-protein interactions or strong lipid-lipid interactions, lipids can regulate protein localization and activity (Janmey and Kinnunen, 2006). The numerous functions of lipids are based on their great diversity and their ubiquitous distribution, as lipids have hydrophobic or amphipathic properties. Technologies such as liquid chromatography and mass spectrometry, which are used in Lipidomics, have enabled the classification of lipids according to their structure (**Table 1**).

By the classification in LIPID MAPS® Lipidomics Gateway, lipids are separated in (i) lipids synthesized by the condensation of thioesters derived from carbanions (molecules of an organic origin with negative charge), such as acetyls (e.g., acetyl-CoA), and (ii) lipids synthesized by condensation of carbocations derived from isoprenes (e.g., Isopentenil-PP) (Fahy et al., 2011, 2009, 2005).

In the first group, there are lipids such fatty acyls, glycerides, sphingolipids, saccharolipids and polyketides, while sterols and prenol lipids are in the second group (**Table 1**).

- **Fatty acyls** constitute the most abundant group of biological lipids in cells. Among them, there are fatty acids, carboxylic acids with a carbon chain of 4 to 48 carbon atoms, which can be saturated or unsaturated. These fatty acids can also be “conjugated”. The fatty acyls include for instance alcohols or fatty esters.

- **Glycerides**, glycerolipids or acylglycerols are based on a glycerol molecule esterified with one, two or three fatty acids. Triglycerides, the most abundant glycerides, are found in all living organisms, and are part of animal and vegetable fats.

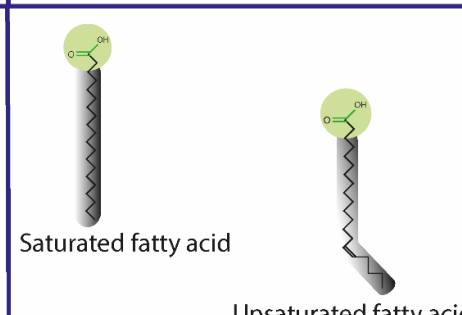
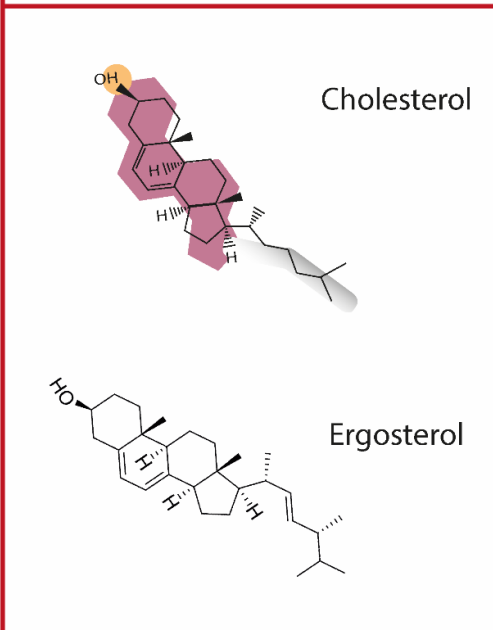
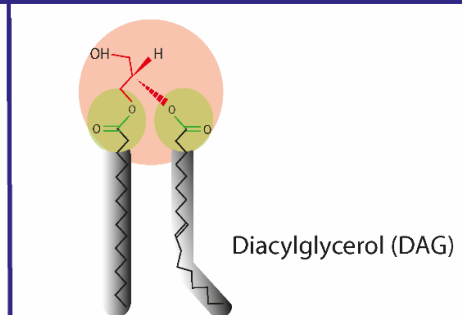
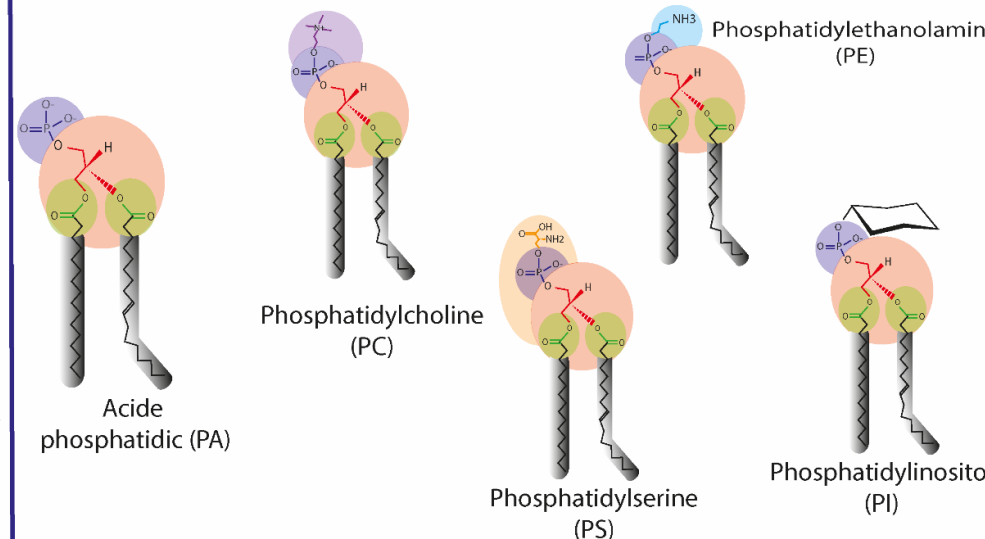
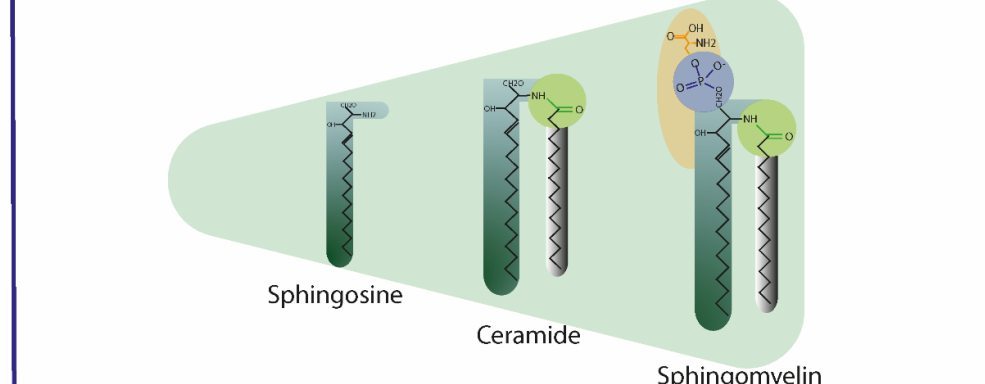
- **Glycerophospholipids** or phospholipids have a glycerol molecule in their composition. This glycerol has one of the hydroxyl groups esterified with a phosphate, originating a

phosphatidic acid. The phosphate groups of the phosphatidic are esterified with several types of molecules, such as inositol, and amino acids, such as ethanolamine, choline, and serine. The phospholipids constitute the minimum structure of the biological membranes, with *(i)* a strongly hydrophilic polar head and *(ii)* chains of esterified fatty acids as the hydrophobic part.

- **Sphingolipids** are complex lipids with a common structural axis, sphingosine, an amino alcohol derived from serine, and a fatty acid with a long carbonic chain. The polar part of sphingosine may be associated with a substituent such as hydrogen, phosphocholine or a monosaccharide, giving respectively a ceramide, a sphingomyelin, or a glycosphingolipid.

- **Sterols** are steroids with 27-29 carbon atoms that derive from sterane. Sterols are grouped according to their function: *(i)* cholesterol and derivatives, essential components of biomembranes; notably, **ergosterol** is found in fungi; *(ii)* steroids, which are considered hormones because of their roles in cell signaling; *(iii)* secosteroids, which include vitamin D.

Table 1. Lipid classification. Schematic representation of lipid groups. Classification is based on their structure and synthesis pathway. Condensation of thioesters give rise to fatty acids, glycerides, glycerophospholipids and sphingolipids. Sterols are synthesized by condensation of isoprene units

	Condensation of thioesters	Condensation of isoprene units
Fatty acids	 <p>Saturated fatty acid</p> <p>Unsaturated fatty acid</p>	 <p>Cholesterol</p> <p>Ergosterol</p>
Glycerides	 <p>Diacylglycerol (DAG)</p>	
Glycerolphospholipids	 <p>Acide phosphatidic (PA)</p> <p>Phosphatidylcholine (PC)</p> <p>Phosphatidylethanolamine (PE)</p> <p>Phosphatidylserine (PS)</p> <p>Phosphatidylinositol (PI)</p>	
Sphingolipids	 <p>Sphingosine</p> <p>Ceramide</p> <p>Sphingomyelin</p>	

2. Membrane composition: the importance of charged lipids

Most lipids are hydrophobic and composed mainly of hydrocarbon chains, such as triglycerides, non-polar lipids involved in energy storage. Polar lipids, which have positive or negative charges associated with hydrophobic or non-polar parts, are **fatty acids, phospholipids, and sphingolipids**. Fatty acids have a polar head composed of a carboxylic group and a carbon chain whose degree of saturation and length confer the physical properties to form lipid bilayers. Unsaturated acyl chains are curved and reduce the level of membrane compaction. In contrast, the saturated chains are tightly bound to each other (Lodish, 2008). Fatty acids, together with phospholipids and sphingolipids, are the main lipids that composed cell membranes.

Phospholipids are composed of a diglyceride, a phosphate group that constitutes the negatively charged fraction, and an organic fraction. Depending on the composition of the polar head, there are zwitterionic phospholipids, such as phosphatidylcholine (PC) and phosphatidylethanolamine (PE), or negatively charged lipids such as phosphatidylserine (PS) and phosphatidylinositol (PI). Apart from their polar heads, these phospholipids are also distinguished by the length and saturation of the aliphatic chains (Fahy et al., 2005; Holthuis and Menon, 2014)

▪ Lipid interactions

The membrane fluidity is determined by the lipids and their interactions (Janmey and Kinnunen, 2006). Similar to fatty acids, phospholipids promote the grouping of aliphatic chains, but the presence of a polar head and a two-chain aliphatic part can modify the morphology of the membrane. Phospholipids such as PI form structures with a positive curvature, such as micelle-forming lipids. PC, which represents 50% of phospholipids in eukaryotes, form cylindrical structure with a tendency to form a flat, stable, and fluid bilayer. Other phospholipids, such as

PE, have a conical shape, but inverted from that of PI, which leads to negative curvatures (**Figure 1**) (Holthuis and Menon, 2014; Janmey and Kinnunen, 2006; McMahon and Boucrot, 2015). These lipid properties give membranes the level of curvature necessary to regulate cell shape, organelles formation, vesicle transport and protein activation (McMahon and Boucrot, 2015).

The properties of membranes such as order, elasticity and fluidity are dependent on lipid conformation and their interactions (Pöyry and Vattulainen, 2016). The dynamics of each lipid is different, *e.g.*, the lateral diffusion of the phosphatidylinositol biphosphate (PIP₂) is slower compared to other lipids, which is most likely due to the interactions between the basic C-terminal of proteins around and the anionic head of this lipid (Pöyry and Vattulainen, 2016). Membrane fluidity is regulated by cholesterol, which also has a high affinity for cylindrical anionic lipids, such as sphingolipids (*e.g.*, sphingomyelin (SM)), or PE (van Meer et al., 2008).

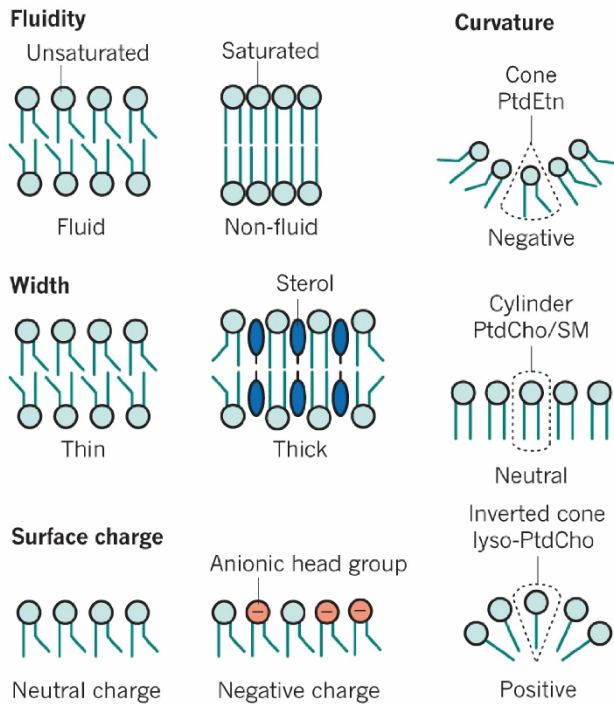


Figure 1. Physical properties of membranes based on lipid composition. The saturation state of lipids confers fluidity to membranes. Saturated lipids tend to make compacted zones in the membrane, while the unsaturated lipid chains confer fluidity by inhibiting a solid gel formation. Membrane thickness is associated with the acyl-chain length and the presence of sterol. Surface charge is based on the content in anionic lipids, such as PS or PI. The curvature is determined by lipid shape, as lipid's area ratio (polar head/ acyl chain) result in different shapes: a cone locally induces a negative curvature, while a cylinder and an inverted cone induce neutral and positive curvatures, respectively. From Holthuis and Menon, 2014

- **The interactions between lipids and proteins:**

Lipids and proteins are both involved in the organization and function of the plasma membrane. One role of lipids is purely structural: the wide range of lipids and physico-chemical properties form lipid bilayers favorable for the distribution, the function and the regulation of proteins (Harayama and Riezman, 2018; Simons and Sampaio, 2011; van Meer et al., 2008). However, lipids are more than a fluid scaffold, as protein-lipid interaction is also essential for the activity of proteins and, ultimately, their biological functions (Harayama and Riezman, 2018).

As reviewed in (Sezgin et al., 2017), to avoid the hydrophobic tails of lipids to be exposed to polar environments, lipids diffuse laterally according to their acyl chain length. Thus, lipids with a similar acyl chain length will group, generating zones of the membranes with different transversal thickness. These zones can generate hydrophobic mismatches and result in protein segregation (see lipid raft section). Moreover, it has been shown that the presence of charged lipids in the membrane impacts the level of maturation of transmembrane proteins. For example, *(i)* Interactions with lipids can alter the dimerization of protein complexes, such as rhodopsin. This protein must interact with a 16-carbon aliphatic chain PC for a correct monomer organization, as an interaction with PC having longer or shorter chains results in a tendency to form dimers and a decrease in diffusion through the bilayer (Kusumi and Hyde, 1982; Nicolson, 2014). *ii)* Other studies show the involvement of PS, PI and phosphorylated derivatives, or PA as recognition patterns for proteins that harbor domains such C2, PH (Pleckstrin homology) and FFAT (two phenylalanines (FF) in an acidic tract), *e.g.*, an Oxysterol Binding Protein function is dependent on the concentration of PI4P (Stefan et al., 2017; van Meer et al., 2008) (see section lipid transporters). PS negative charges also contribute to stabilize Rho GTPases at the plasma membrane in yeast (Haupt and Minc, 2017; Sartorel et al., 2018).

In summary, biological functions are not exclusively dependent on proteins, as lipid physical properties are essential for protein distribution and generation of suitable microenvironment.

3. Fluidity and organization of the mosaic:

- **Lipid movements:**

The fluid mosaic model is based on the dogma “everything can move” (Singer and Nicolson, 1972). The amphipathic properties of lipids and their differences in size, charge and form make biomembranes a malleable and versatile matrix in which proteins are embedded. Several studies indicate that lipids move in three main directions: *(i)* rotation on their own axis, *(ii)* lateral diffusion, with these two movements occurring inside one of the monolayers, or *(iii)* transverse movement, or “flip-flop”, by which lipids move from one side of the membrane to the other (Berg et al., 2002; Jacobson et al., 2019; Pomorski and Menon, 2016). Rotation and lateral diffusion are very fast lipid movements, for example, one lipid rotates in its own axis in ~ 1 ns, or laterally diffuses ~ 0.01 nm/ns (Pomorski and Menon, 2016). In contrast, flip-flop implies that a single amphipathic molecule traverses the hydrophobic core of the plasma membrane (PM) and, compared to the lateral diffusion where lipid movement is in 2D, flip-flop must break a stronger energy barrier. The principal consequence of this energy requirement is a slower rate (one phospholipid molecule flip-flops once in several hours) compared to the diffusion coefficient of lipids of $2\mu\text{m}^2$ in 1s. The first analysis of lipid spontaneous flip-flopping was done in 1971 on synthetic vesicles (McConnell and Kornberg, 1971). The translocation was monitored by measuring the appearance of unreduced lipids on an outer bilayer that was previously reduced with ascorbate, and reported a frequency of $\sim 10^{-5} \text{ s}^{-1}$ at 30°C (reviewed in Pomorski and Menon, 2016). With this approach at different temperatures, they established that an initially asymmetric bilayer loses asymmetry very slowly, with each lipid translocating in

~100h. “Thus, a phospholipid molecule takes about 10^9 times as long to flip-flop across a membrane as it takes to diffuse a distance of 50 Å in the lateral direction” (Berg et al., 2002; Contreras et al., 2010; van Meer et al., 2008).

The hydrolysis of sphingolipids and glycerophospholipids produces lipid second messenger like Diacylglycerol (DAG) that promotes the recruitment of distinct proteins. The trans-bilayer movement of fluorescent nitrobenzoxadiazole-labeled DAG (NBD-DAG), observed in artificial lipid vesicles, is 63s^{-1} (Berg et al., 2002; Contreras et al., 2010; van Meer et al., 2008). Other lipids, such as cholesterol in animal PMs, show flip-flop rates below milliseconds and this rate is important to regulate the Sphingomyelin (SM)-high-concentrated membrane fluidity; reciprocally, interaction with SM restricts cholesterol flip-flop rate (Gu et al., 2019).

Lateral movements and lipid-lipid interactions are based on the lipid tail length and compaction, and are key for organization into lipid domains or lipid rafts that are rich in saturated lipids, sterols and SM (Sezgin et al., 2017).

- **Lipid rafts**

There are more than a thousand different lipids present in eukaryotic cells (Fahy et al., 2009, 2005; van Meer et al., 2008). This diversity results in countless different interactions allowing lipid compartmentalization within the same membrane, where the boundaries are drawn by the higher affinity between certain lipids. According to the following definition, “*Membrane rafts are small (10–200 nm), heterogeneous, highly dynamic, sterol- and sphingolipid-enriched domains that compartmentalize cellular processes. Small rafts can sometimes be stabilized to form larger platforms through protein-protein and protein-lipid interactions*” (Pike, 2006).

Lipid rafts form a platform where proteins can be selectively included or excluded by their “raftophilic” properties, based on the specific length and charge mismatches between lipid aliphatic chains and protein transmembrane domains (Diaz-Rohrer et al., 2014; Sezgin et al.,

2017; Simons and Ikonen, 1997). Alpha helices with hydrophobic amino-acid side chains are present in most of transmembrane proteins. For these proteins to be stably anchored in the PM, a hydrophobic match with the surrounding lipids is critical and lipid rafts, with longer and saturated chains, can provide such an environment. The actin cytoskeleton plays an important role in the diffusion and stabilization of lipids, by anchoring part of the membrane to specific sites, *e.g.*, GPI-anchored proteins interact with lipids such as PS and the actin cytoskeleton anchors through scaffold proteins. These interactions favor the clustering of the GPI-anchored proteins in the PM (Sezgin et al., 2017). Segregation of different membrane components to optimize their interaction and activity is the most axiomatic function of these lipid domains. As an example, specific interactions with raft-enriched lipids such as cholesterol may change protein conformation (Bogdanov et al., 2008; Kusumi and Hyde, 1982; Lingwood et al., 2011).

In fungi, lipids are also organized into domains. Several fungi have SL-enriched domains (SLEDs), which are quite rigid, sterol-depleted, and distinct from lipid rafts. These domains play a role in membrane maturation events in endosomes, lysosomes and vacuoles in yeast (Hurst and Fratti, 2020; Santos et al., 2020). However, lipid rafts, which are rich in ergosterol and sphingolipids, are an important topic in research; ergosterol lipids are absent in mammalian cells, thus making them potential targets for antifungal drugs. Ergosterol levels are different in specialized microdomains such as the Membrane Compartment of Can1 (MCC)/eisosomes, which facilitate a spatially confine endocytosis, and the MCP (containing Pma1)(Grossmann et al., 2007; Lanze et al., 2020; Malinsky et al., 2013). In fungal PMs, sterol-rich domains (SRDs) are observed at the filamentous cell tip in *Candida albicans* or *Aspergillus nidulans*, as well as at the septum and mating projection (shmoos) in *Saccharomyces cerevisiae* or *Schizosaccharomyces pombe* (Alvarez et al., 2007; Martin and Konopka, 2004).

Chapter II. How lipid composition is established and maintained.

Eukaryotic cells are defined by the presence of endomembranes that allow a compartmentalization of cell functions and are associated with specific lipid compositions that depend on where lipids are synthesized, modified and degraded, and on how they reach their final destination. Most of the lipids are produced in the endoplasmic reticulum (ER), yet not much of the lipids remain in this organelle. The Golgi is also site of lipid production, in particular for the synthesis of Sphingolipids (Holthuis and Menon, 2014; van Meer, 2011).

In the secretory pathway, the vesicles that are generated by budding in early organelles will fuse with later ones and one of the main differences between these early and late organelles is the lipid composition. For example, PS and PI are more concentrated in the trans Golgi and PM inner leaflets, while in the *cis*-Golgi and the ER, these phospholipids face the lumen (Kobayashi and Menon, 2018). Although synthesized in the ER, sterol is limited in this organelle (5 mol% of lipids), compared to the PM (30–40 mol%) (Holthuis and Menon, 2014). The PM is enriched in SM, yet most of the sphingolipids are synthesized at the Golgi. Furthermore, ceramides, which are precursors of Sphingolipids, are supplied by the ER, making lipid transport essential for maintaining lipid composition (Holthuis and Menon, 2014; van Meer, 2011; van Meer et al., 2008).

Fine-tuning of lipid distribution is critical for membrane specific properties. The plasma membrane is characterized by an enrichment in anionic and unsaturated lipids in the inner leaflet (Lorent et al., 2020; van Meer et al., 2008). Even once lipids reach the membrane they were synthesized for, they can be modified in order to maintain their correct distribution. For example, the concentration of PI is regulated by its phosphorylation into PI(4)P and PI(4,5)P₂, which takes place at the Golgi and the PM (Del Bel and Brill, 2018; Holthuis and Menon, 2014; Klug and Daum, 2014; van Meer, 2011). Other authors suggest that modifications such as the

acyl chain length of PM lipids take place directly at the PM (Lorent et al., 2020; Makarova and Owen, 2020).

In the following sections I will discuss studies on the role of lipid and protein transport in cell growth through three main sections: how lipids and proteins reach the targeted membrane; how specific lipid composition is generated; and how it is maintained.

1. Vesicular transport:

New material is continuously needed for membrane biogenesis to occur and understanding this process during cell development and growth has been the aim of a number of research groups during the last decades. The baker's yeast *Saccharomyces cerevisiae* is a useful model to study the intracellular organization, including the secretory pathway, which is key for membrane biogenesis (Feyder et al., 2015).

In the endocytic pathway, vesicles budding off the PM form early endosomes that mature ultimately into lysosomes in mammalian cells (Mahmutefendić et al., 2018), or vacuoles in yeast, where the molecules internalized from the external medium and the plasma membrane are degraded. Organelles, such as mitochondria, chloroplasts and peroxisomes do not appear to contribute substantially to these vesicular transports, and other ways of communication connect these organelles, such as direct contacts between their membranes or lipid pipelines with specific lipid transporters (Horvath and Daum, 2013; Prinz, 2010).

The vesicular pathway plays an important role in the remodeling of cell membranes. Aside from this role, the biological importance of this pathway is reflected also in processes such as neural synapsis formation (Binotti et al., 2021; Cooper, 2000), pheromone communication (Martin, 2019a, 2019b; Yashiroda and Yoshida, 2019), host-pathogen interactions (Naglik et al., 2019) or polarized growth (Campanale et al., 2017; Chiou et al., 2017; Martin and Arkowitz, 2014).

In other words, vesicular traffic serves to deliver specific materials to different compartments and thus enables an organelle to have an identity and carry out its function.

- **Anterograde transport:**

In the anterograde vesicle transport, there are distinct steps. First, COPII-type coated vesicles bud from the ER and are delivered to the Golgi. Some areas of the reticulum are favorable for COPII assembly, with specific lipid composition and localized dynamic remodeling of PIs (Schink et al., 2016). Proteins transported *via* these vesicles display sorting signals to differentiate proteins destined to the ER or other membranes such as the PM (Feyder et al., 2015). Moreover, the COPII machinery, as well as COPI and clathrin, cooperates in the formation of vesicles by creating tensions and folding the membrane and selects the proteins to be at the specific ER exit sites (ERES) (Gomez-Navarro and Miller, 2016; Has and Das, 2021). From the *trans*-Golgi Network (TGN), vesicles are directed to the plasma membrane or to the late endosome-lysosomes/vacuoles. Vesicle budding mechanisms are different as a function of the vesicle final destination and content. For example, material is delivered to the plasma membrane through SEC vesicles that are transported by tropomyosin on actin cables and tethered at the PM via the exocyst complex, composed of Sec3/5/10/6/8/15 and Exo70/84 in yeast (Feyder et al., 2015; Mei and Guo, 2018). Moreover, as recently demonstrated in HeLa cells, Exo70 would be critical not only for tethering but also for defining whether the vesicle will partially or completely fuse with the PM (An et al., 2021).

Lipid composition and shape are critical for vesicular budding. While cargoes leaving the TGN for endosomes are sorted by coat-dependent mechanisms (Kim and Gadila, 2016), cargo proteins destined to the plasma membrane are sorted at TGN into exocytic vesicles that are rich in SL and sterol lipid raft which select specific cargoes (Surma et al., 2012).

- **Retrograde transport:**

To maintain the cell shape during membrane remodeling, retrograde vesicular transport is critical to recycle as well as to internalize material. Vesicles bud off of PM regions where clathrin is concentrated, *via* adaptor proteins, and high concentration of PI(4,5)P₂ facilitates these adaptor proteins interactions (Feyder et al., 2015; Li et al., 2020; Mahmutefendić et al., 2018). Retrograde transport, which also returns resident molecules from the source compartment, is mediated by a class of coating proteins, called COPI, that will form vesicles and select molecules to be returned to the ER.

Retrograde and anterograde vesicular-transported cargos are selected at different levels, *(i)* vesicle coats populate the vesicle with specific cargo proteins by sequence-based recognition, as an example, the yeast heteropentameric complex called retromer, together with ESCRT (endosomal sorting complex required for transport) and the sorting nexins, is necessary for discriminating PM-recycled and Golgi retrograde-transported proteins at the endosomes (Ma and Burd, 2020). *(ii)* Lipids facilitate membrane protein segregation in and out of vesicles (Holthuis and Menon, 2014). The first evidence of this lipid-dependent sorting is based on the study of an artificial lipid raft protein FusMid that allowed the quantification of lipids in the secretory vesicles (Klemm et al., 2009). Other authors demonstrated that plasma membrane proteins, such as Pma1 and GPI-anchor proteins, like Gas1, are transported in these SL- and sterol-rich vesicles (Surma et al., 2011). In clathrin-independent endocytic pathways, where endocytosis depends on BAR domain-containing proteins (*e.g.*, endophilin) that mediate the membrane curvature, lipids such as PI(3,4)P₂ are necessary for endophilin recruitment at the PM of mammalian migrating cells (Shafaq-Zadah et al., 2020).

In summary, factors, such as sequence-based recognition, lipid raft affinities, as well as retrograde vesicular transport, are efficient mechanisms to retain proteins in specific organelles.

As described in the next section, maintaining lipids at specific locations is also critical to maintain membrane identity.

2. Non-vesicular transport: Lipid transporter proteins (LTPs)

One of the main challenges of having such dynamic vesicular transport is to maintain the membrane composition necessary for a proper compartmentalization of function. Lipids provide the membrane with specific thickness, fluidity and landmarks and membranes provide in turn the microenvironment necessary for correct protein function (Harayama and Riezman, 2018; Holthuis and Menon, 2014; Lenoir et al., 2021) .

As a result, synthesis, degradation, modification of lipids must be constantly regulated in time and space. A process such as vesicular transport tends to equilibrate lipid composition of different compartments by mixing membranes while apportioning new material (Delfosse et al., 2020; Lenoir et al., 2021). Moreover, some organelles such as mitochondria or chloroplasts do not substantially participate in vesicular transport, so alternative mechanisms are necessary to control the lipid composition in these compartments (Horvath and Daum, 2013; Prinz, 2010). Lipid transfer proteins (LTPs) have been described for more than 40 years as capable of overcoming the hydrophilic barrier that lipids face to get from one endomembrane to the other. This is possible by the presence of a hydrophobic cavity where lipids bind and are transported between two membranes (Delfosse et al., 2020; Lipp et al., 2020). LTPs fine-tune lipid transport and bypass vesicular transport (Delfosse et al., 2020; Lipp et al., 2020). LTPs participate in a variety of processes, as the lipids they transport can serve as cofactors for other enzymes, activate transcription factors or regulate other lipid transporters (Chiapparino et al., 2016).

The variety of functions of these transporters is accompanied by a high diversity of LTPs. Indeed, in humans, there are about 125 genes encoding different LTPs. All of them contain a specific Lipid Transfer Domain (LTD) that confers specificity for the transported lipids, and

most of them have domains necessary for their localization (Chiapparino et al., 2016; Lipp et al., 2020). These characteristics are common for all Eukaryotic LTPs; for instance, Ceramide transporters acting between the Golgi and the ER (CERT), and the OxySterol Binding Proteins (OSBP) are well conserved in yeast and other fungi (**Figure 2**). CERTs have distinct domains: a START (Steroidogenic Acute Regulatory Transfer) domain able to recognize Ceramides with a specific acyl chain length (Bohnert, 2020; Kudo et al., 2008), a FFAT (two phenylalanine in an acidic tract) and a PH (Pleckstrin Homology) domain, which allow specific recognition of proteins in the ER and PI(4)P in the Golgi, respectively, establishing contact sites between these two organelles (Bohnert, 2020; Lev, 2012). Similarly, in *S. cerevisiae*, OSBP function is regulated by specific domains: it localizes at the Golgi by interaction with PI(4)P and GTP-Arf1 through its PH domain and interacts at the ER with the VAP-A protein through a FFAT domain (**Figure 2**)(Lipp et al., 2020).

Domains similar to the ligand-binding domain of OSBP are termed ORD (OSBP Related Domain); they contain a conserved EQVSHHPP motif and are found in all eukaryotes(Delfosse et al., 2020) . Humans have 12 OSBP-related proteins (ORP), compared to yeast, where only 7 ORP genes were identified and termed OSBP homologous (Osh) proteins. The PH and FFAT domains are only present in Osh1-3 and other members, such as Osh4-7, contain only the ORD domain, suggesting that the localization of these LTPs are dependent on its substrates (**Figure 2**) (Lipp et al., 2020; Tong et al., 2016).

Blocking the secretory pathway in yeast has almost no effect on sterol transport (Baumann et al., 2005; Heino et al., 2000; Urbani and Simoni, 1990), suggesting a non-vesicular transport as a main path for sterol distribution. Several LTP members have a LTD able to recognize sterols (Chiapparino et al., 2016). Some members of the START (Steroidogenic Acute Regulatory Transfer) family are LTPs for sterol (Wilhelm et al., 2017), however these proteins are not

present in fungi and Archaea, where other StART-like analogous (VAsT) proteins have been shown to transport Ergosterol (Marek et al., 2020).

With only an ORD domain, *S. cerevisiae* Osh4 is one of the simplest Osh proteins (**Figure 2**). It has been studied for its implication in the regulation of sterol gradient from the ER to the PM and in the secretory pathway by modulation of PI(4)P levels at the Golgi (de Saint-Jean et al., 2011; Filseck et al., 2015; Georgiev et al., 2011; Ling et al., 2014; J. Moser von Filseck et al., 2015; Smindak et al., 2017; Stefan et al., 2011). In a first place, PI(4)P concentration plays a role in vesicle maturation, since decreasing the PI(4)P levels is necessary for loading docking-related proteins into the vesicles (Ling et al., 2014; Mizuno-Yamasaki et al., 2010; Schink et al., 2016; Smindak et al., 2017). In a second place, low levels of PI(4)P and high concentration of sterol both favor vesicle fusion with the PM (Smindak et al., 2017). The Osh4-mediated exchange of PI(4)P/Ergosterol (**Figure 3**) in yeast is ensured by the interconversion of PI(4)P and PI by the phosphatase Sac1 at the ER, and the kinase Pik1 at the Golgi, respectively (de Saint-Jean et al., 2011; Filseck et al., 2015).

Figure 3 illustrates a schematic for Osh4 function in *S. cerevisiae*. The PI(4)P backbone, PI, synthesized at the ER is transported to the Golgi by the LTP of the CRAL-Trio superfamily, Sec14 (Sugiura et al., 2019), where it is phosphorylated by the PI-4 kinase, Pik1, to generate PI(4)P (Audhya et al., 2000). PI(4)P concentration being higher at the Golgi than at the ER, Osh4 transports PI(4)P to the ER along its concentration gradient and the energy generated is used to transport ergosterol in the opposite direction. PI(4)P is dephosphorylated by the phosphatase Sac1 at the ER (Filseck et al., 2015; Joachim Moser von Filseck et al., 2015).

In vesicular transport from the Golgi to the PM, Osh4 would function in a similar fashion, participating in the maturation of secretory vesicles (Ling et al., 2014; Mizuno-Yamasaki et al., 2010; Smindak et al., 2017) (**Figure 4**).

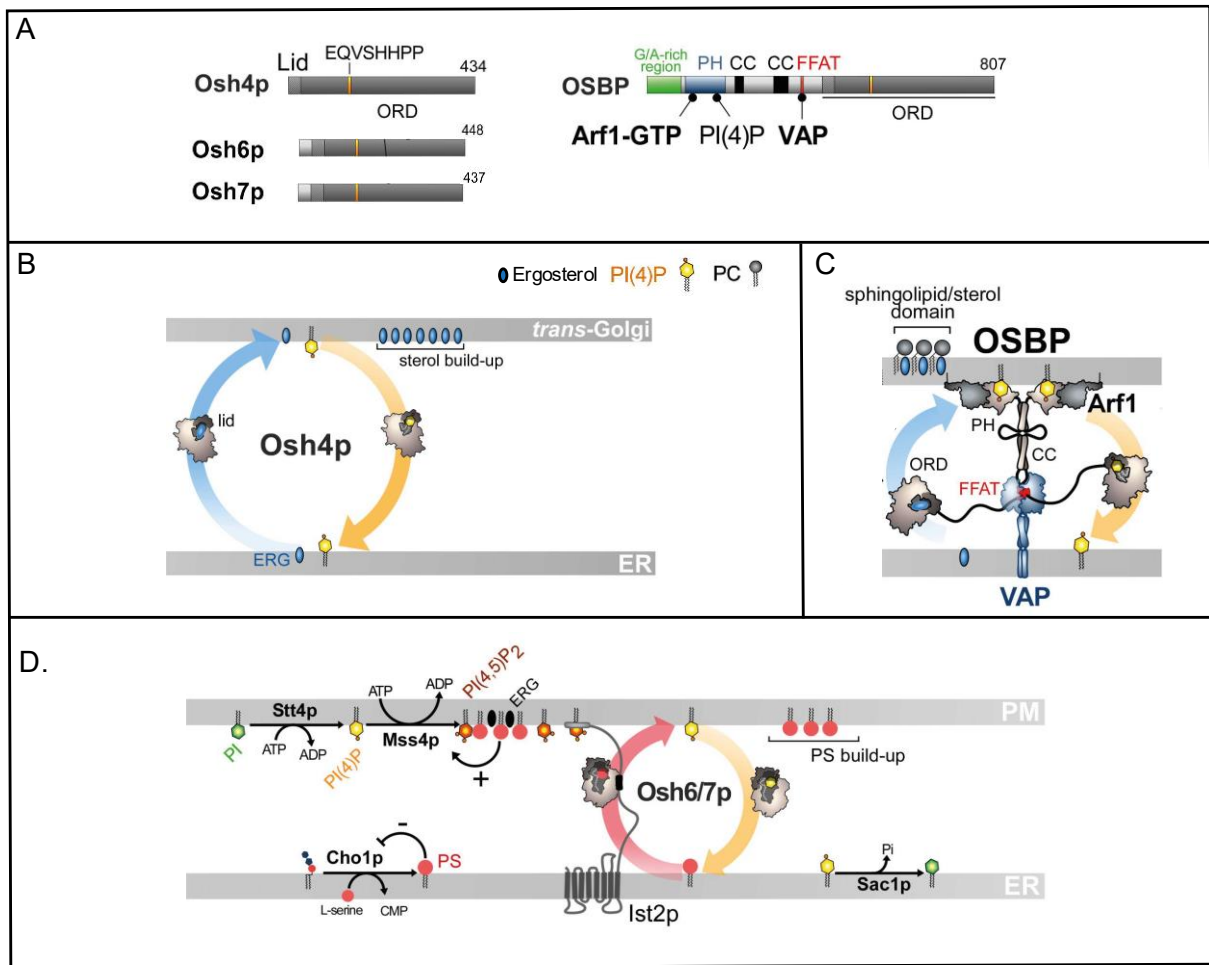


Figure 2. Domain composition of different LTPs. **A.** Comparison between a yeast OSBP-homologous (Osh4) protein and the human OSBP. Osh4p contains only an ORD containing a lid and the EQVSHHPP signature as indicated. The interaction between the domains of OSBP with PI(4)P and other Arf1 and VAP proteins are shown by black lines. PH, Pleckstrin Homology domain, FFAT, two phenylalanine in an acidic tract domain. **B.** In yeast, Osh4p exchanges ergosterol from the ER and PI(4)P from the trans-Golgi. **C.** OSBP interacts *via* its PH domain with PI(4)P and Arf1-GTP and, through its FFAT motif, with ER-resident VAP receptors forming ER-Golgi contact sites. **D.** PS is transferred by Osh6p/7p to the PM by using a PI(4)P gradient maintained by Stt4p and Sac1p. PI(4,5)P₂ production by Mss4p is favored by PS- and sterol-rich domains. PI(4,5)P₂ enables the recruitment of Ist2p to the PM. Ist2p-Osh6/7 interaction anchors Osh6/7 to the ER-PM contact-sites (from Lipp et al., 2020).

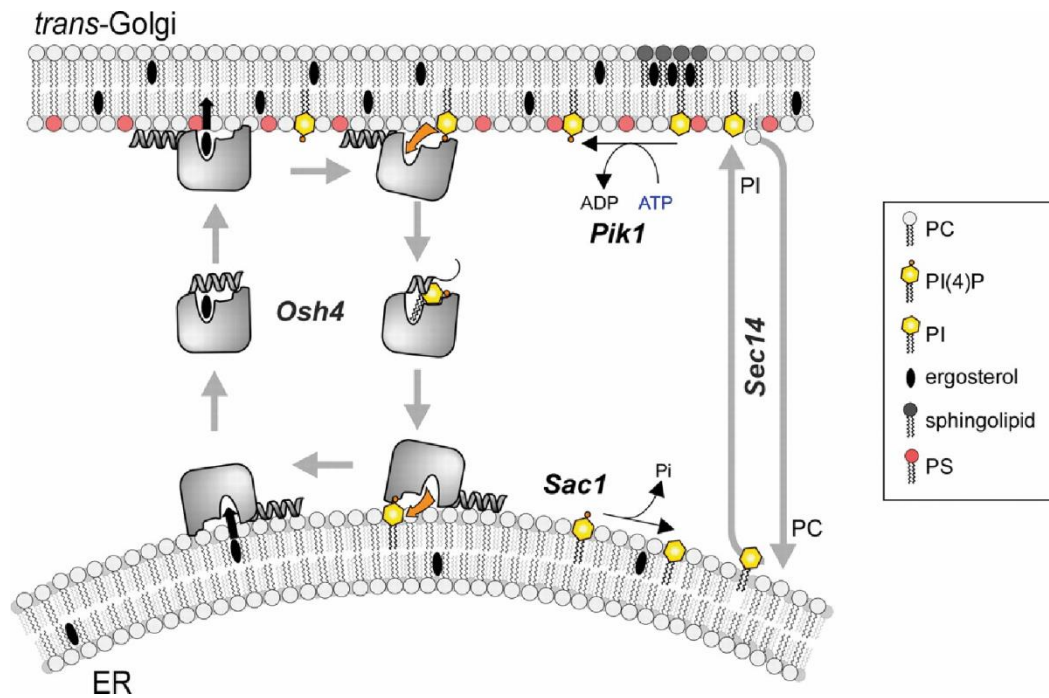


Figure 3. Sterol and PI(4)P exchange by Osh4. (i) PI/PC exchange between ER and Golgi is performed by Sec14. The kinase Pik1 phosphorylates PI to generate PI(4)P at the Golgi. (ii) PI(4)P is transported by Osh4 to the ER. The energy generated by this PI(4)P transfer along its concentration gradient is used for the transport of ergosterol in an opposite direction. (iii) The low concentration of PI(4)P at the ER is maintained by the phosphatase Sac1, which reduces PI(4)P to PI. From de Saint-Jean et al., 2011.

Osh4 would participate in vesicular maturation and fusion, by progressively decreasing the level of PI(4)P (**Figure 4(a.)**) and by forming transient membrane contact sites (MCS) between vesicles and the PM (**Figure 4(b.)**), respectively. Osh4 would exchange PI(4)P for ergosterol at the PM, facilitating vesicle fusion with the PM (Smindak et al., 2017).

S. cerevisiae has six more Osh family members with overlapping function (Beh et al., 2001), and PI(4)P is a common ligand for all these proteins (Maeda et al., 2013; Manik et al., 2017; J. Moser von Filseck et al., 2015). Osh6/7 exchange PI(4)P and PS between the ER and the PM, where they localize (D'Ambrosio et al., 2020; Maeda et al., 2013; Schulz et al., 2009). Osh6/7 exchange PS by using the PI(4)P gradient that is sustained by Sac1 at the ER, and the PI-4 kinase Stt4 at the PM (**Figure 2D**) (Lipp et al., 2020). Interestingly, Osh6/7-mediated transport is dependent on the binding capacity of PI(4)P and the PI(4)P levels, as deletion of Sac1 results in a loss of PI(4)P gradient and Osh6 activity (J. Moser von Filseck et al., 2015).

In filamentous fungi, the role of these transporters is poorly understood. In *C. albicans*, it has been suggested that Osh3 is required for invasive growth in specific nutrient-poor media (Hur et al., 2006). *A. nidulans* has five Osh proteins (OshA-OshE) and *oshC* and *oshD* deletion mutants show altered branching events (Bühler et al., 2015). In *A. nidulans*, OshA-E proteins are localized at different sites and, for instance, the Osh4 homologous, OshC, is in the cytoplasm and showed a subapical clustered localization in a small population of cells (Bühler et al., 2015).

Compared to the in-depth studies of the Osh proteins in *S. cerevisiae*, much remains to be discovered about the role of these proteins in other fungi, for example during morphogenesis and highly polarized hyphal growth.

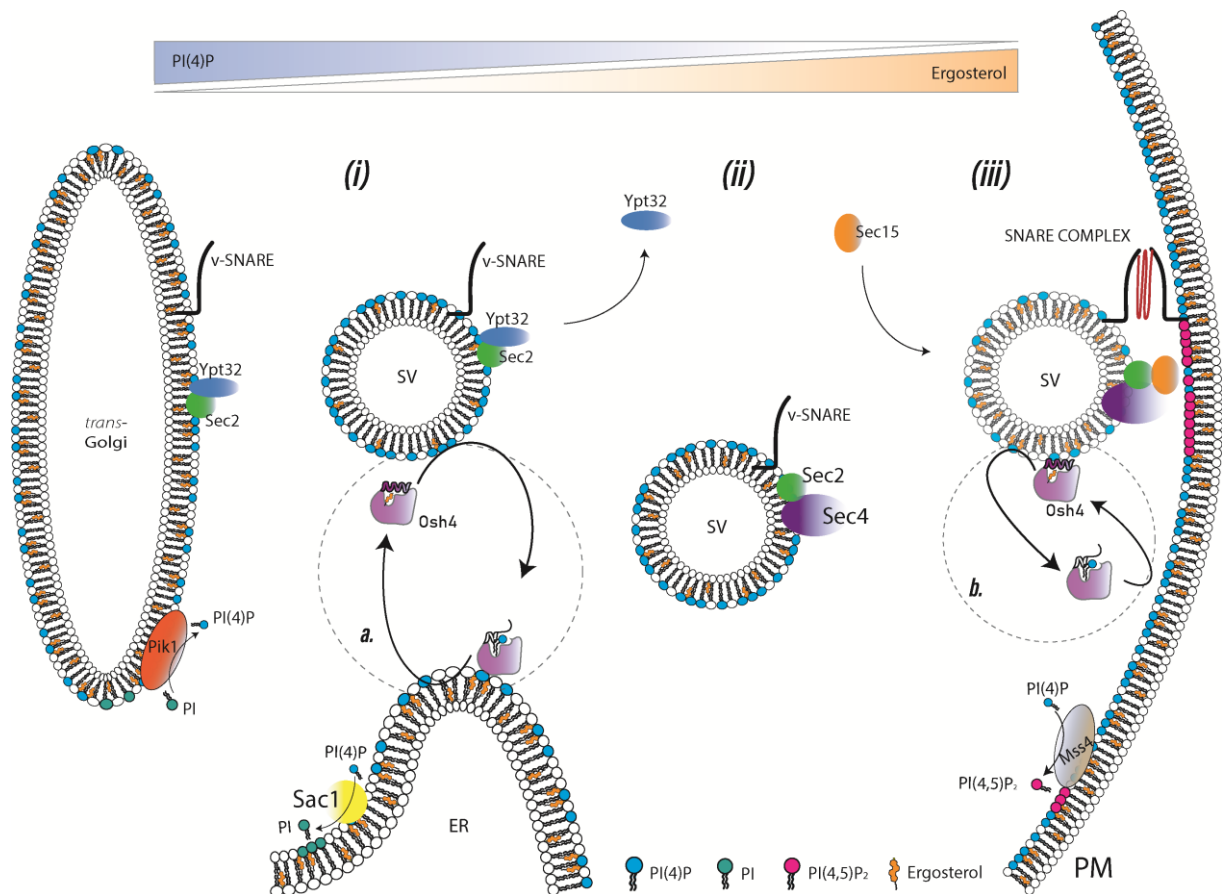


Figure 4. Role of Osh4 in *S. cerevisiae* vesicle maturation. (i) Vesicles budding off the Golgi and enriched in PI(4)P and Ypt32 recruit Sec2. (ii) The recruitment of Sec4 is then facilitated by the presence of Sec2 and a decrease in PI(4)P concentration *via* Osh4 (a.). Ypt32 is released from the vesicles when PI(4)P concentration is reduced. (iii) Sec2 interacts with Sec15, the effector of Sec4. Once the mature vesicle is anchored to the PM, Osh4 would continue exchanging PI(4)P for ergosterol (b.), favoring the SNARE-mediated fusion to continue. The vesicle tethering is mediated by the exocyst including Sec15 and other subunits at the PM (not represented). The exocyst subunits Exo70 and Sec3 can bind PI(4,5)P₂ at the PM. Vesicle tethering is followed by vesicle fusion with the PM, mediated by the SNARE fusion machinery. Figure based on the models proposed by Smindak et al., 2017; Ling et al., 2014; Schink et al., 2016 and Mizuno-Yamakasi et al, 2010.

3. Membrane asymmetry:

Lipid asymmetry refers to the unequal composition between the two leaflets of a bilayer (Bretscher, 1973). Red blood cells (RBCs) are an excellent model to study PM properties, as they are a simple structure lacking endomembranes. In this model, recent lipidomics studies confirm a PC and SM enrichment in the exoplasmic membrane, and PE, PS and PI, in the inner one (Lorent et al., 2020). Moreover, acyl chains interaction has been speculated to participate in “Interleaflet coupling” across the PM (Doktorova et al., 2020). The aliphatic length and saturation of lipids are different between the two leaflets and mass spectroscopy analyses reveal that the level of unsaturation is higher in the inner leaflet, which means that membrane asymmetry does not rely only on the difference between the polar heads of the bilayer (Lorent et al., 2020). Membrane asymmetry, which is ATP-dependent, requires not only transport but also *in situ* modifications of the lipid acyl chain length (Doktorova et al., 2020; Lorent et al., 2020; Makarova and Owen, 2020).

Most eukaryotic cells have endomembranes, where lipid asymmetry is also present. In these cells, there are lipid asymmetries at the PM, the Golgi and the endosomes, while the ER has a symmetric lipid distribution, except for PS (Doktorova et al., 2020; Holthuis and Menon, 2014; Kobayashi and Menon, 2018; Lorent et al., 2020; van Meer et al., 2008). New models have emerged to understand the extent and importance of lipid asymmetry among eukaryotes *in vivo* (Ikeda et al., 2006; Klose et al., 2012; Santos and Riezman, 2012; Santos et al., 2020), as well as *in vitro* (Florek et al., 2018; Lorent et al., 2020).

Yeasts share with most eukaryotic cells having phosphatidic acid (PA), phosphatidylcholine (PC), phosphatidylethanolamine (PE), phosphatidylinositol (PI), phosphatidylserine (PS), diacylglycerol (DAG) being the most abundant lipids at the PM, and triacylglycerols (TAG) and sterol esters (SE) serving as storage lipids. Yeasts have Sphingolipids and PC in the outer

leaflet, and PS and PE in the inner leaflet of the plasma membrane. The major yeast sterol is ergosterol (Erg) and, based partly on lipidomic approaches, it was shown that the dynamics of lipid metabolism change with environmental conditions, such as changes in growth conditions (Klose et al., 2012). Mating in *S. cerevisiae* is dependent on the asymmetric distribution of sphingolipid-enriched lipid rafts (Proszynski et al., 2006). Some steps in the endocytic pathway are dependent on the phospholipid asymmetry generated and maintained by P4-ATPases (presented below), as the absence of these proteins alter the FM4-64 endocytic tracer uptake (Pomorski et al., 2003).

Several mechanisms generate the asymmetric lipid distribution. As mentioned earlier, lipid exchange *via* LTPs, such as ORPs, is an example of how asymmetric distribution can be generated. Once a lipid is transported to a membrane, it can be trapped. For instance, at the Golgi, ceramides are transformed into sphingolipids and PI is phosphorylated into PI(4)P. The metabolic conversion of these lipids ensures that the transport is unidirectional. On the other hand, lipids, such as PS, with negatively charged polar heads, can interact with polybasic domains of membrane proteins at the PM, or *via* calcium-mediated interactions with luminal proteins at the ER (Kobayashi and Menon, 2018; Lorent et al., 2020).

Maintenance of membrane asymmetry is crucial for cell viability, as extracellular exposure of PS can result in cell death through apoptotic and non-apoptotic pathways (Shlomovitz et al., 2019). Membrane asymmetry is also critical for the distribution of membrane proteins (Lorent et al., 2020; Makarova and Owen, 2020). Charged lipids can be implicated in their topology, as proteins tend to position their positively charged amino acids in the inner leaflet of the PM. Furthermore, proteins are organized in such way that the larger domains are in the inner side of the membrane, as this side is less compact and more fluid because of its lipid composition (Doktorova et al., 2020; Lorent et al., 2020). This suggests that lipid asymmetry play an important role in the asymmetric protein conformation.

In summary, lipid asymmetry is a common aspect of biomembranes, and such asymmetry must be maintained in an active and energy-dependent fashion. To this end, eukaryotes have evolved over the course of evolution a series of lipid transporters that generate and maintain membrane asymmetry.

- **Lipid asymmetry and requirement for an active transport**

Transmembrane lipid transporters differ by the substrate selectivity, transport direction and energy consumption. Flip-flop of lipid's polar head through a membrane bilayer is an energetically unfavorable movement. Scramblases transport lipids along their concentration gradient. Different scramblases are found for example in the ER, one of the most symmetrical endomembranes (Daleke, 2003; Hankins et al., 2015b; Kobayashi and Menon, 2018). These scramblases are regulated by Ca^{2+} (Daleke, 2003). For instance, in mouse fibroblasts, PS is evenly distributed between the ER-monolayers, when Ca^{2+} is present, due to the action of a Ca^{2+} -dependent scramblase, TMEM16K (Tsuji et al., 2019). In contrast, floppases and flippases actively transport lipids, with flippases transporting lipids towards the cytoplasmic side and floppases to the side exposed to the extracellular media or the lumen of the organelles. Flippase and floppase functions are ATP-dependent and they belong to the P4-ATPases and the ATP-Binding Cassettes (ABC) transporters, respectively (**Figure 5**) (Kobayashi and Menon, 2018; López-Marqués, 2021; Lyons et al., 2020; Pomorski and Menon, 2016). Importantly, some members of the ABC superfamily have been implicated in antifungal drug resistance, for instance, the *C. albicans* drug resistant proteins 1 and 2 (CaCdr1/2) or the Multi-Drug-Resistance (MDR) proteins, as well as in the dynamics of *Candida* infections (Banerjee et al., 2021).

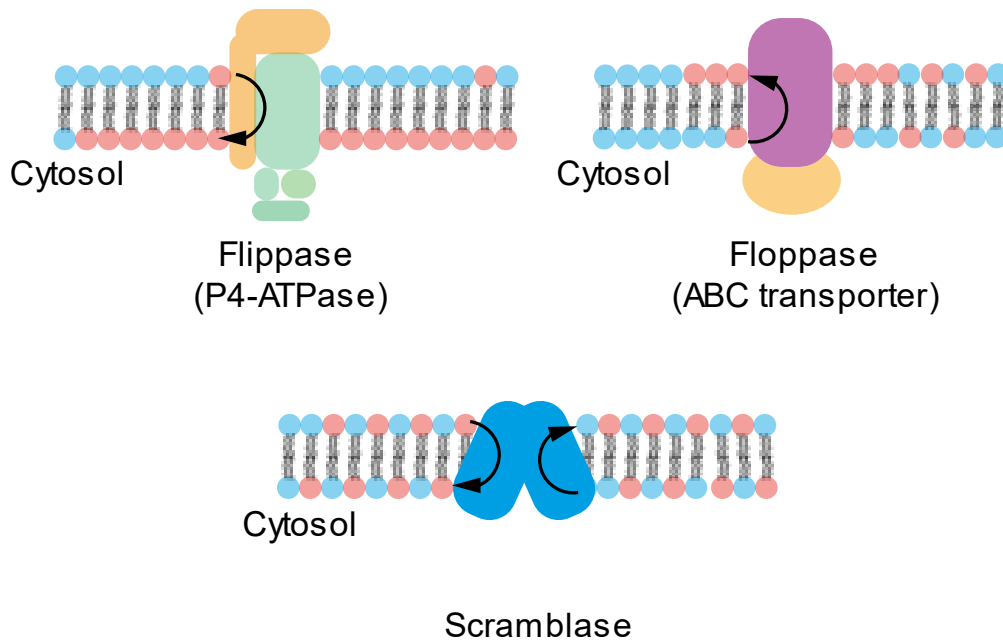


Figure 5. Flippases, Floppases and Scramblases. Phospholipids such as PS (pink) are accumulated at the cytosolic leaflet of membranes by flippases, which belong to the P4-ATPase family. ATP-binding cassette (ABC) transporters, or floppases, facilitate membrane lipid transport in the opposite direction, from the cytosolic to the exoplasmic/luminal leaflet. Flippases and floppases function in an ATP dependent manner. Lipid scramblases translocate lipids down their concentration gradients, without using ATP.

P4-ATPases translocate phospholipids from the exoplasmic to the cytosolic leaflet of membranes (Kobayashi and Menon, 2018; López-Marqués, 2021; Lyons et al., 2020; Pomorski and Menon, 2016)(**Figure 5**). Well conserved among eukaryotes, P4-ATPase function and ultrastructure have been characterized in *S. cerevisiae* (Bai et al., 2019; Baldrige and Graham, 2013, 2012; Pomorski et al., 2003; Takar et al., 2019; Timcenko et al., 2021, 2019; Tsai et al., 2013). Collectively, *S. cerevisiae* has five members of this family, Neo1 (Neomycin resistant 1), Drs2 (Deficient for Ribosomal Subunit 2), Dnf1 (Drs2/Neo1 family), Dnf2, and Dnf3. Their localizations are different in *S. cerevisiae* budding cells: Neo1 localizes broadly at the Golgi and endosomes and transports PE and PS (Takar et al., 2016); Drs2, which is specific for PS and PE, localizes with Dnf3 at the TGN and post-Golgi secretory vesicles (Alder-Baerens et al., 2006; Hua et al., 2002; Pomorski et al., 2003), and Dnf1 and Dnf2 at the PM and the endocytic membranes, where they transport PC and PE (Alder-Baerens et al., 2006; Hankins et al., 2015a; Hua et al., 2002; Pomorski and Menon, 2016). Several studies have uncovered different regulatory mechanisms for the function of flippases. For instance, Drs2 is positively regulated by PI(4)P (Natarajan et al., 2009; Timcenko et al., 2019), as well as by the interaction with both the Arf-like protein Arl1 and the guanine nucleotide exchange factor Gea2 (Chantalat et al., 2004; Natarajan et al., 2009; Timcenko et al., 2019; Tsai et al., 2013). Moreover, other flippases such as Dnf1/2 are activated upon kinases-mediated phosphorylation by Flippase kinase 1 (Fpk1) and Fpk2 (Frøsig et al., 2020; Nakano et al., 2008; Roelants et al., 2010).

P4-ATPases belong to the P-type ATPase superfamily (P1-5), in which P1-3 ATPases are transporters of ion and heavy metals. Na^+/K^+ and Ca^{2+} -ATPases are well characterized, and their mechanism of transport is based on a canonical binding pocket (Zhang and Zhang, 2019). P5 ATPases do not appear to have defined ligand, but P4-and P5-ATPases are only found in eukaryotic genomes (Huang et al., 2021). P-type ATPases have 4 functional domains, including 3 cytosolic domains, *i.e.*, the Actuator Domain (A), the Nucleotide-binding domain (N), the

phosphorylation domain (P) and a transmembrane domain (TM) (Bai et al., 2019; Timcenko et al., 2021, 2019). These proteins also function with a non-catalytic subunit of the ligand-effect modulator/the cell division cycle (Lem3/Cdc50) family (Furuta et al., 2007; Lenoir et al., 2009; Saito et al., 2004). The yeast Lem3/Cdc50 family is composed by Cdc50, Lem3 and Crf1, which interact with Drs2, Dnf1/2 and Dnf3, respectively (Furuta et al., 2007; Saito et al., 2004). Formation of the heterodimeric complex activates and targets these flippases to their correct organelle localization, with the absence of one of the two heterodimeric members resulting in the ER-retention of the other one (Furuta et al., 2007; Lenoir et al., 2009; Saito et al., 2004). Consistent with this, mutation of either the catalytic or the non-catalytic part results in similar phenotypes (Chen et al., 2006; Kato et al., 2002).

The catalytic cycle of these proteins (Post-Albers cycle), involves several intermediate stages depending on the substrate binding and the phosphorylation state, E1, E1P, E2P and E2 (**Figure 6**) (Bai et al., 2019; Baldrige and Graham, 2013; Lyons et al., 2020). Recently, the *S. cerevisiae* P4-ATPase Drs2 has been studied by cryo-electron microscopy in 3 conformations: auto-inhibited, fully active and intermediate conformations (Timcenko et al., 2019). These structures reveal in particular how the Drs2 carboxy-terminus could inhibit the Drs2-Cdc50 complex activity and the auto-inhibition relief by PI(4)P (Bai et al., 2019; Baldrige and Graham, 2013; Lyons et al., 2020; Timcenko et al., 2019). This suggests that the mechanisms involved in PI(4)P regulation may directly affect the function of this flippase.

In P4-ATPases, the phospholipid binding site is different from the canonical substrate binding site in cation pumps. This was demonstrated by characterizing two *S. cerevisiae* P4-ATPases, Dnf1 and Drs2 (which bind PC/PE and PS/PE, respectively) and by showing that the domains implicated in substrate specificity are indeed located outside of the canonical binding region (Baldrige and Graham, 2013, 2012). The specificity of these flippases depends on a few amino acids, as in Dnf1, for instance, the mutation Y618F in TMD4 increases PS flipping activity,

and, conversely, mutations in Drs2 (such as F511Y), reduce PS flipping activity (Baldrige and Graham, 2012). Based on directed mutagenesis and genetic approaches, the authors identified residues located on the entry (cluster located in and between TMD1-2 on the exofacial side) and exit gates (cluster located in TMD3-4 near the cytosolic side) and proposed that these gates act cooperatively for phospholipid selection and transport (Baldrige and Graham, 2013).

P4-ATPases are implicated in a number of processes. In neurological disorders in humans, some brain malfunction results from flippase dysfunction (Martín-Hernández et al., 2016). In some parasites, these ATPases can capture lipids, which cannot be synthesized by these organisms, in the extracellular medium (Bansal et al., 2005). In plants, the ATPase ALA3 participates in secretion from the Golgi and is involved in the control of polarized growth of roots and shoots in *Arabidopsis* (Poulsen et al., 2008). In fungi, the endomembrane organization and protein transport rely to some extent on ATPases, as deletion of these flippases are often related with defects in membrane trafficking in different organisms (Hankins et al., 2015b; Pomorski et al., 2003; Schultzhaus et al., 2017, 2015; Takar et al., 2016; Wu et al., 2016). Moreover, membrane protein transport and localization of peripheral membrane proteins, such as the small G-proteins, depend on lipids. For instance, it was reported that the Rho GTPase Cdc42, a master regulator of polarized growth, depends on PS asymmetric distribution for membrane localization (Das et al., 2012; Haupt and Minc, 2017; Lopez-Marques et al., 2014; Meca et al., 2019; Saito et al., 2007). In filamentous fungi, P4-ATPases have been associated with sporulation (Schultzhaus et al., 2019, 2017, 2015) and to some extent with the secretion of compounds related with fungal pathogenicity (Balhadère and Talbot, 2001; Gilbert et al., 2006; Hu et al., 2017; Hu and Kronstad, 2010; Labbaoui et al., 2017; Yun et al., 2020). Consequently, flippases are proteins with great potential as candidates in the regulation of polarized growth and virulence of these organisms.

In the next section, I will discuss the human fungal pathogen *C. albicans* as a model to study polarized growth and the importance of flippases and of lipid distribution.

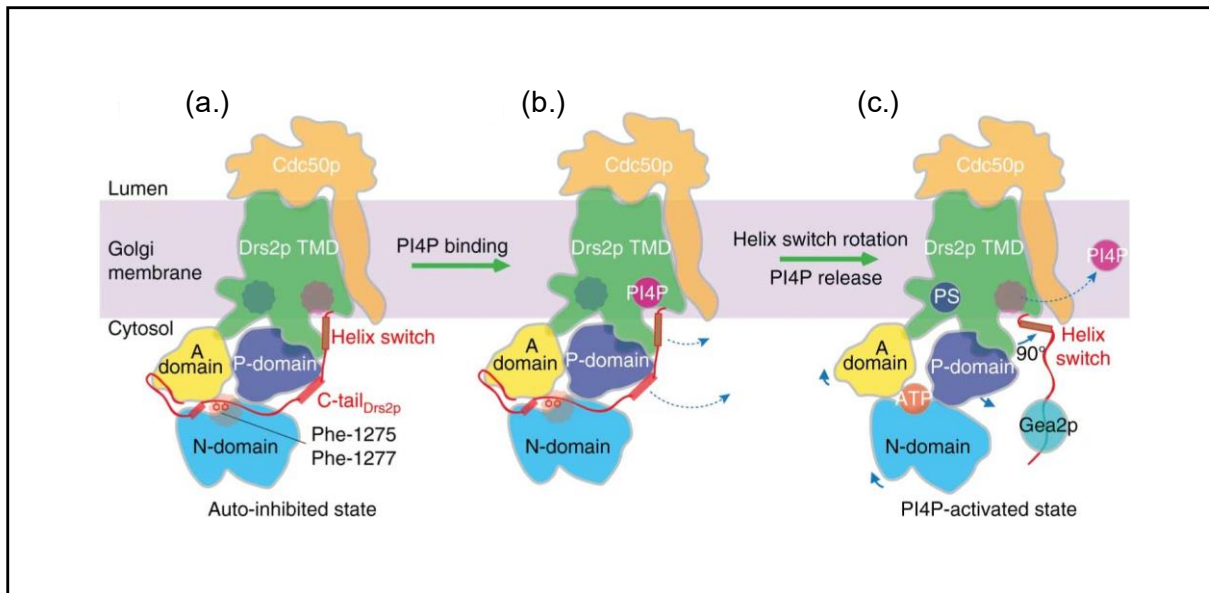


Figure 6. Model for Drs2p-Cdc50p autoinhibition and activation by PI4P from Bai et al., 2019. (a.) Auto-inhibited state (without the PI(4)P activator). Autoinhibition is done through the C-terminus wrapping around the cytosolic A, P, and N domains, occupying the ATP-binding pocket. (b.) PI(4)P activates Drs2p-Cdc50p by binding a positively charged pocket in cytosolic leaflet of the membrane. (c.) This activation consists in a 90° rotation of the helix switch uncovering cytosolic domains (A,P and N) and the interaction of the helix with Gea2. Once activated, ATP and the substrate PS bind to Drs2p and PI4P diffuses away from the flippase.

Chapter III: *Candida albicans*

Candida albicans is an opportunistic human fungal pathogen that belongs to the *Candida* genus. In general *Candida spp.* are harmless commensal yeasts commonly populating the human mucosa, that can be pathogenic in specific conditions. *Candida spp.* belong to the *Ascomycota* phylum, *Saccharomycotina* sub-phylum and *Saccharomycetales* order (McManus and Coleman, 2014). Among the 16 families, the *Saccharomycetales incertae sedis* family contains the CTG clade. As part of this clade, *C. albicans* expresses the CTG codon as serine instead of leucine. The genus *Saccharomyces*, which includes *Saccharomyces cerevisiae*, belongs to the *Saccharomycetaceae* family, also called the whole genome duplication (WGD) clade, as the genomes of these species have been duplicated (Diezmann et al., 2004; Fitzpatrick et al., 2006; Wolfe and Shields, 1997). Focusing on the diversity of these phyla, it is interesting to notice that, although *C. albicans* and *S. cerevisiae* are both yeasts that can be found in ovoid budding form, *C. albicans* has diverged from *S. cerevisiae* about 800 million years ago (Fitzpatrick et al., 2006; Hedges, 2002). Yeasts reproduce by budding, fission and/or sexual reproduction, each of these growth modes are triggered by specific environmental conditions. The genus *Candida* includes more than 150 species (Calderone, 2012). The majority of *Candida* species belong to the CTG codon clade, such as *C. lusitaniae*, *C. guilliermondii*, *C. parapsilosis*, *C. tropicalis* and *C. dubliniensis*, which are the species most closely related to *C. albicans* (Fitzpatrick et al., 2006); *C. glabrata*, on the other hand, belongs to the WGD clade (Fitzpatrick et al., 2006). Most *Candida* species, about 65%, are adapted to their environmental niche and able to grow at a temperature of 37°C, which is important for commensal organisms (Calderone, 2012; Pappas et al., 2018). The genome of *C. albicans* is completely sequenced (<http://www.candidagenome.org>) and consists of 8 pairs of chromosomes that code for about 6400 genes (Jones et al., 2004). Unlike *S. cerevisiae*, *C. albicans* is an obligate diploid and is

the most prevalent among *Candida spp.* to cause infections (Moyes et al., 2015; Pappas et al., 2018), making the study of this organism particularly medically relevant.

1. Virulence

As introduced above, *Candida spp.* are harmless commensal yeasts present in the oral, gastrointestinal, and urogenital mucosa in 60% of healthy individuals (Pappas et al., 2018). However, these organisms can become pathogenic in response to environmental stress, such as an imbalance of the intestinal flora or an immunodeficiency of the host, resulting in superficial infections, such as vaginal infections (Moyes et al., 2016). *C. albicans*, *C. glabrata*, *C. parapsilosis*, *C. tropicalis* and *C. krusei* are the 5 major *Candida spp.* that are isolated from blood or mucosal samples of immunocompromised patients, but *C. albicans* and *C. glabrata* are the two most virulent and common nosocomial diseases (Brunke and Hube, 2013). When *C. albicans* invades the host tissues and infiltrates into the bloodstream, resulting in systemic infection (Pappas et al., 2018), which is particularly problematic for immunocompromised patients, such as patients with AIDS, transplant patients or those undergoing chemotherapy (Moyes et al., 2016; Pappas et al., 2018).

C. albicans transition from a commensal to a pathogen is triggered by different environmental and biological cues. *C. albicans* growth is limited by the presence of bacteria that induce the secretion of *Candida spp.*-growth inhibitory factors by the mucosa, thus extensive or long-term use of antibiotics may indirectly favor *C. albicans* development (Kullberg and Arendrup, 2015; Pappas et al., 2018). Other factors, such as mucositis (inflammation of the mucosa), surgery and intravenous catheters can facilitate bloodstream infection in immunosuppressed patients, resulting in candidemia (Kullberg and Arendrup, 2015; Pappas et al., 2018). *C. albicans* also exhibits specific properties, such as adhesion, secretion and invasive growth to facilitate

pathogenicity (Kullberg and Arendrup, 2015; Moyes et al., 2016; Noble et al., 2017; Pappas et al., 2018).

- **Adhesion:**

The first step in the interaction with epithelial tissues is adhesion, mediated *via* epithelial cell receptors and *Candida* adhesins (Moyes et al., 2016). The most common adhesins expressed by *C. albicans* belong to the Als (Agglutinin-Like Sequence) family, encoding for cell wall-associated proteins (Hoyer and Cota, 2016) and the cell wall protein Hwp1 (Hyphal Wall Protein) (Staab et al., 2004; Sundstrom et al., 2002; Zhu and Filler, 2010). Both Als proteins and Hwp1 are Glycophosphatidylinositol (GPI)-anchored to the PM but their roles in adhesion are different. For instance, by using the loss-of-function mutants *als1*, *als2* and *als3*, it was shown that Als1 has no role in adhesion, Als2 an intermediate role, and Als3 a critical role: indeed, *als3* cells are not able to adhere and to infect epithelial cells *in vitro* (Zhao et al., 2005, 2004).

- **Secretion and invasion:**

The epithelial and endothelial host cell invasion by *C. albicans* can be facilitated by distinct mechanisms: (i) The induction of phagocytosis by epithelial cells, with the adhesins/invasins Als3 and Ssa1 expressed on the surface of *C. albicans* being recognized and bound by E-cadherin and other epithelial cell receptors (Moyes et al., 2015; Swidergall and Filler, 2017). (ii) Active penetration, which is thought to be facilitated by mechanical forces generated during the hyphal growth, coupled to an adhesin-mediated anchoring (Moyes et al., 2015; Swidergall and Filler, 2017). (iii) The secretion of proteins can also play an important role in *Candida* pathogenesis. For example, the Secreted Aspartyl Proteinase (SAP) family can damage the epithelium, hence increasing the probability of penetration through epithelial cells (Moyes et

al., 2015; Swidergall and Filler, 2017; Zhu and Filler, 2010). *SAP1-3* contribute to superficial infections; *SAP4-6* are important to escape from macrophages and for systemic infections (Naglik et al., 2004, 2003), and to invade epithelial cells *in vitro* (Dalle et al., 2010; Zhu and Filler, 2010). Another secreted protein, candidalysin, which is a cytolytic peptide toxin, can induce epithelial cell damage (Allert et al., 2018; Moyes et al., 2016). The *ECE1* (extent of cell elongation) gene encodes this toxin that is necessary for efficient host infection, although not essential for hyphal formation *per se* (Allert et al., 2018; Moyes et al., 2016).

Candida hyphal development is essential for biofilm formation (Cavalheiro and Teixeira, 2018). Biofilms are microbial communities of bacteria, fungi, or both, that confer different properties than those of individual cells, such as drug resistance (Cavalheiro and Teixeira, 2018; Rodríguez-Cerdeira et al., 2020). The first step of a biofilm formation is adhesion to the host tissues, therefore *Candida* adhesins such as Hwp1, Als1, and Als2 play a crucial role in this process (Rodríguez-Cerdeira et al., 2020). Consistently, mutants of transcription factors, such as Efg1 and Cph1 that control the expression of *ECE1*, *HWP1*, and *ALS3*, are critical for biofilm formation (Cavalheiro and Teixeira, 2018; Ramage et al., 2002; Rodríguez-Cerdeira et al., 2020).

2. *Candida albicans* morphogenesis

C. albicans can be found as budding yeasts (white cells), morphologically similar to *S. cerevisiae* cells, opaque cells, gray cells, and GUT (Gastrointestinally Induced Transition) cells (Noble et al., 2017). Opaque cells are produced from white cells that are homozygous (a/a or α/α) for the Mating Type like Locus (MTL)(Perry et al., 2020). This transition occurs in 1 in 10,000 cell divisions and passes through an intermediate stage, gray cells (Perry et al., 2020). Opaque cells are competent for mating and the GUT cells, which are also competent for mating, are thought to be a morphology adapted to commensalism (Noble et al., 2017; Pande et al.,

2013). Despite the mating competence of opaque cells, *C. albicans* was considered as an asexual organism, since no meiosis or sporulation has been observed (Noble et al., 2017). Indeed, mating is thought to be a very rare event due to the high frequency (~97%) of MTL heterozygous cell (Perry et al., 2020). However, opaque cells can undergo homothallic mating (between two opaque cells of the same mating type) in a glucose poor media or during oxidative stress (Perry et al., 2020). This is the case of the sexual biofilm where, in the deepest layer isolated from the surface, there are less nutrient and oxygen, and homothallic mating is favored (Noble et al., 2017; Perry et al., 2020). As in all sexual organisms, mating in *C. albicans* allows for the cells to adapt faster to different environmental conditions by generating genetic variability, and once adapted, the asexual budding and filamentous growth allows the cellular spreading (Perry et al., 2020).

The yeast-to-hyphae transition is a virulence trait in *C. albicans*, but filamentous growth is not required for all *Candida spp.*'s ability to infect a host; for instance, *C. glabrata* does not form hyphae but is the second most common pathogen among *Candida spp.* (Brunke and Hube, 2013). In *C. albicans*, mutants locked in either the filamentous or yeast form are less virulent, thus, the ability to switch between the two morphological states is essential for virulence (Braun et al., 2001, 2000; Lo et al., 1997; Murad et al., 2001; Pappas et al., 2018; Schweizer et al., 2000; Zheng et al., 2004). In addition, most of the infection steps detailed above, such as active penetration and induced endocytosis occur during *C. albicans* hyphal state (Dalle et al., 2010; Moyes et al., 2015; Naglik et al., 2004, 2003; Noble et al., 2017; Swidergall and Filler, 2017; Zhu and Filler, 2010) and the genes implicated are mostly hyphal specific genes. For example, *ALS3*, which is only expressed in hyphae, induces *C. albicans* endocytic uptake by epithelial cells through Als3-E-cadherin interactions. Yeast forms colonize the surface of the tissue, without apparent damage (Moyes et al., 2015; Noble et al., 2017; Swidergall and Filler, 2017). Furthermore, recent work supports the idea that filamentous growth is dispensable for virulence

in specific infection models (Dunker et al., 2021). A *C. albicans* strain lacking the Epithelial Escape and Dissemination 1 (*EDDI*) gene is able to form germ tubes but does not undergo hyphal extension, resulting avirulent in an *in vivo* murine model of intraperitoneal infection (Dunker et al., 2021). However, this mutant is fully virulent in a mouse model of systemic infection, most likely due to rapid proliferation supported by enhanced metabolic adaptation (Dunker et al., 2021). In summary, while filamentation is most of the times a key trait for virulence, specific cases exist in which efficient host infection happens in absence of any filamentation.

- **Hyphal gene induction**

While *C. albicans* budding growth is triggered by internal cues, similar to *S. cerevisiae*, hyphal growth is triggered by external cues (Bassilana et al., 2020). In contrast to budding growth, which is cell cycle-dependent, hyphal growth can be initiated at any cell cycle stage (Hazan et al., 2002) and the expression of hyphal specific genes is regulated by several key transcription factors (Arkowitz and Bassilana, 2019; Chen et al., 2020; Kornitzer, 2019; Sudbery, 2011) (**Figure 7**). For instance, *in vitro*, in response to the presence of serum, *C. albicans* changes from a budding yeast cell of about 5 μ m to a filamentous cell with a filament extension rate of $\sim 0.3\mu$ m/min (Silva et al., 2019). The presence of serum activates signaling pathways that depend on Ras1 and trigger in particular a mitogen-activated protein kinase (MAPK) cascade, which ultimately converges on the activation of the transcription factor Cph1 (Chen et al., 2020; Kornitzer, 2019; Sudbery, 2011). Among the hyphal specific genes, the Hyphal G cyclin 1 (*HGCI*) gene, encoding for a cyclin associated with the G1 phase, is critical for hyphal growth (Wang, 2016) and *HGCI* is further regulated by *UME6* (Carlisle and Kadosh, 2010). The *hgc1* and *ume6* deletion mutants are both defective in maintaining hyphal growth and are reduced in

virulence in a murine model for systemic candidiasis (Zheng et al., 2004) (Banerjee et al., 2008; Mendelsohn et al., 2017). Cln3, a G₁ cyclin essential for cell cycle, is a suppressor of hyphal morphogenesis by inhibiting Ume6 (Mendelsohn et al., 2017). Other hyphal specific genes are implicated in *C. albicans* virulence such as **HWPI** (Hyphal Wall Protein) (Fan et al., 2013; Staab et al., 2004, 1999), **ALS** (Agglutinin Like Sequence) genes, (Hoyer and Cota, 2016), **SAP** (Secreted Aspartyl Protease) genes (Allert et al., 2018; Zhu and Filler, 2010) and **ECE1** (extent of cell elongation, candidalysin) (Allert et al., 2018; Moyes et al., 2016). Negative regulation of hyphal formation is mediated by the Tup1-mediated regulatory pathway. Tup1, Nrg1 and Rfg1 are DNA binding proteins able to repress half of the hyphal genes. These repressors are activated by the quorum sensing molecule, farnesol, and inhibited during hyphal formation. Their absence results in constitutive pseudohyphal growth (Chen et al., 2020; Cleary et al., 2016; Kornitzer, 2019). Therefore, up or downregulation of some of these genes can be used as indicators of virulence defects in *C. albicans* mutated strains.

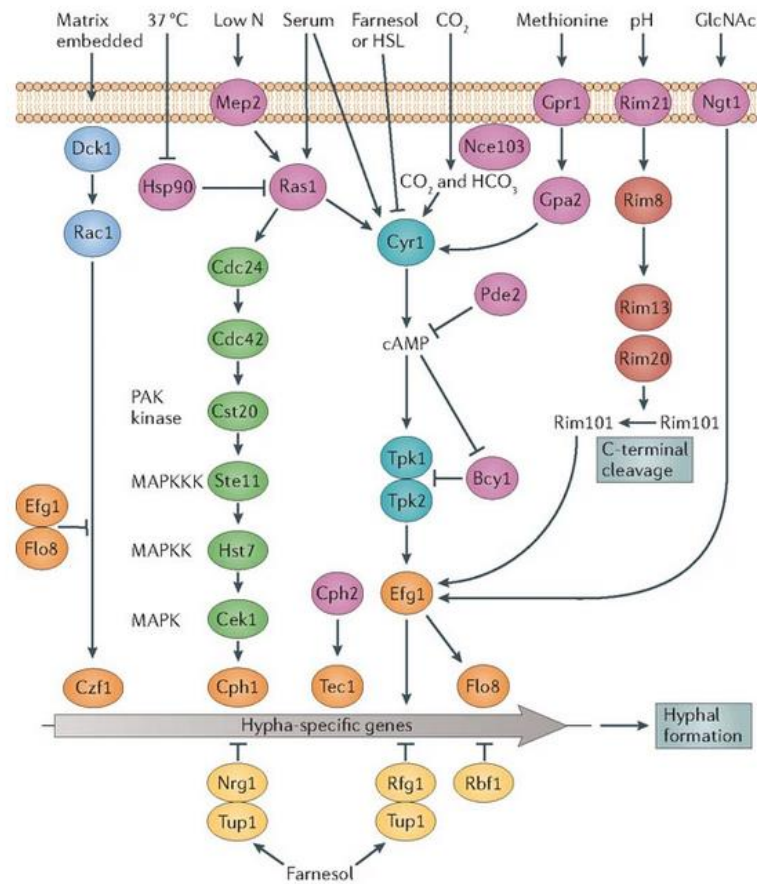


Figure 7. Pathways for Hypha-specific gene induction. Signals perceived by receptor molecules are trigger the corresponding signaling cascade, which results in the activation of hypha specific transcription factors. This leads to the transition from budding to filamentous growth. High concentration of the quorum sensing molecule, farnesol, activates Tup1 which negatively regulates hyphal specific gene expression and thus, the yeast to hypha transition does not occur. From Sudbery, 2011

- **Germ tube initiation:**

Filamentous growth consists in the initiation and maintenance of filament apical growth; thus, it is a highly polarized process. As conserved in other fungi, included *S. cerevisiae* polarized growth, *C. albicans* filamentous growth requires polarity establishment proteins, *i.e.*, Cdc42/Cdc24/Bem1 (Bassilana et al., 2005, 2003a; Brand et al., 2014; Corvest et al., 2013; Pulver et al., 2013). Cdc42 is a highly conserved Rho GTPase, which was initially described in *S. cerevisiae* (Johnson and Pringle, 1990), and its activation depends on the formation of a polarity establishment complex (Chiou et al., 2017; Woods and Lew, 2019) comprised of (i) the Guanine nucleotide exchange factor (GEF), Cdc24, which is the sole activator of Cdc42, (ii) p21 activated kinases (PAKs), which are Cdc42 effectors, and (iii) Bem1, which is a SH3 domain containing scaffold protein. Bem1 and the PAKs participate in a positive feedback loop, resulting in the formation of a polarity patch of Cdc42-GTP (Bassilana et al., 2020; Butty et al., 2002; Chiou et al., 2017; Woods and Lew, 2019). The recruitment of either Cdc24 or Bem1 appears to be sufficient to initiate a Cdc42 polarity patch (Witte et al., 2017). Bem1 is also a Cdc42-GTP effector (Grinhagens et al., 2020) that is implicated in the actin-independent localization of the exocyst subunit Exo70 (Miller et al., 2019). Inactivation of Cdc42 is promoted by the GTPase activating proteins (GAPs) Rga1/2 and Bem3 (Smith et al., 2002).

Cell polarity is a dynamic process that allows cells to adapt to their environment in response to external cues. Cdc42 is critical for filamentous growth in fungi, for instance, it controls germ tubes directional growth in *N. crassa* (Lichius et al., 2014). In *C. albicans*, it was shown that activated Cdc42 is recruited to the incipient germ tube and remains at the filament apex during filament extension (Corvest et al., 2013). However, the scaffold protein, Bem1, although essential, it can still form hyphae when its expression levels are downregulated (Bassilana et al., 2003a). In contrast, Cdc42, Cdc24 are essential and its downregulation results in an

impaired hyphal growth (Bassilana et al., 2005, 2003a). Moreover, the active Cdc42-GTP was lethal when expressed in a constitutive manner (Ushinsky et al., 2002) and caused loss of polarity when conditionally expressed in hyphae (Brand et al., 2014; Court and Sudbery, 2007). In *S. cerevisiae* Cdc42-GTP has been shown to interact with several proteins, such as the exocyst component Sec3, thereby promoting polarized secretion (Zhang et al., 2008), and the formin Bni1p, critical for actin polymerization. In *C. albicans*, the formin Bni1 is localized to the Spitzenkörper and necessary for hyphal growth maintenance (Li et al., 2005; Martin et al., 2005). Sec3 is necessary for *C. albicans* hyphal growth maintenance upon septum formation (Li et al., 2007). Interestingly, upon optogenetic disruption of active Cdc42 localization, Sec3 localization at the hyphal tip is perturbed (Silva et al., 2019).

- **Hyphal extension:**

Hyphal growth is independent of cell cycle, yet its maintenance is regulated by the Cyclin-dependent kinases (the Cdk Cdc28) (Desai, 2018; Wang, 2016). *C. albicans* has three G1 cyclins (Ccn1, Cln3, and Hgc1) and two B-type mitotic cyclins (Clb2, Clb4), their expression oscillates during the cell cycle and differently regulate the same target kinase, Cdk1, which is always active but finely tuned (Desai, 2018). Decoupling hyphal growth from the cell cycle allows for cell tip continuous growth, thus Cdc28 is also finely regulated by the different cyclins. The forkhead transcription factor Fkh2 is phosphorylated by the Ccn1/Cln3-Cdc28 complex during hyphal growth (Greig et al., 2015). Fkh2 activity is independent from the cell cycle and targets *HGC1*. *HGC1* and *UME6* are critical for filament extension (Desai, 2018; Zheng et al., 2004). The complex Hgc1-Cdc28 also phosphorylates Rga2, inactivating this Cdc42 GAP at the hyphal tip to maintain Cdc42 activity (Zheng et al., 2007). Rga2 localization at the septum probably contributes to restricting Cdc42 activity at the hyphal apex. Interestingly, deletion of this GAP does not impair filamentation (Court and Sudbery, 2007).

Hgc1-Cdc28 phosphorylates (i) the polarisome protein Spa2, which recruits the actin-binding proteins Bni1, Bud6, and Aip5 (Li et al., 2005; Martin et al., 2005; Xie et al., 2020) and (ii) the exocyst subunit Exo84 and the Rab GTPase Sec4 GEF Sec2, promoting their localization at the filament apex (Bishop et al., 2010; Caballero-Lima and Sudbery, 2014; Wang et al., 2016).

Other proteins such as septins are regulated by Hgc1-Cdc28-mediated phosphorylation (Sinha et al., 2007). Septins play important roles in *C. albicans* morphogenesis and virulence (Douglas and Konopka, 2016; González-Novo et al., 2009; Warena et al., 2003; Warena and Konopka, 2002). The hypha-specific phosphorylation that regulates the septin Cdc11 depends on the Cdc28-Ccn1 and Cdc28-Hgc1 during initiation and extension, respectively (Sinha et al., 2007). The septum formation is particularly regulated during hyphal growth since no cell separation occur after cell division and Hgc1-Cdc28 also targets the Sep7 septin, whose phosphorylation prevents cytokinesis (González-Novo et al., 2009, 2008) and Efg1, a transcription factor that competes with Ace2, another transcription factor implicated in septum degradation post-cytokinesis (Wang et al., 2009). At the septum, septins act as barriers to retain the machinery necessary for septum formation (*e.g.*, the polarisome, the exocyst subunit Sec3, as well as the actomyosin ring) (Douglas and Konopka, 2016; González-Novo et al., 2009). In *S. cerevisiae*, septins are a conserved family of GTP-binding proteins that serve as scaffolds or as diffusion barriers between mother and daughter cells, and are used as markers of cell division progression (Cheffings et al., 2016; Douglas and Konopka, 2016; González-Novo et al., 2009). Septins can delimit active Cdc42 region by recruiting its GAPs (Chiou et al., 2017). Septins also recruit proteins implicated in the actomyosin ring during cytokinesis in budding yeast (Cheffings et al., 2016; González-Novo et al., 2009). In *C. albicans* filamentous cells, septins mark the germ tube site. Just before septation, the septin cap at the tip generates a ring, that remains in a fixed position as the tip continues to elongate (Douglas and Konopka, 2016; González-Novo et al., 2009). When mitosis is completed, one nucleus segregates back to the mother cell. At this point,

the septin ring splits to allow the septum construction (**Figure 8**) (Finley and Berman, 2005; Thomson et al., 2016). Thus, septins are critical to regulate *C. albicans* cell division and morphogenesis.

Time (min)	Event
0	Site of Septum 1 is marked by Cdc3-GFP
41	Nucleus 1 divides (Nop1-YFP)
44	Nucleus 2 crosses Septum 1
	Mlc1-YFP transported from Spitzenkörper at tip to Septum 1
60	Septin rings separate at Septum 1
67	Septum 1 is closed by chitin
	Mlc1-YFP transported from Septum 1 to Spitzenkörper

Figure 8. Temporal and spatial sequence of cell-division events during hyphal growth in *Candida albicans* (Thomson *et al.*, 2016).

- **Hyphal organization:**

Hyphal growth is a highly polarized process which requires a rapid extension of the tip of the hypha. This implies the need for an apical organization of different structures involved in the initiation and maintenance of hyphal growth. In *C. albicans*, Cdc42-GTP is maintained at the apex of the germ tube and filament, where it promotes the activation and/or recruitment of critical effector proteins for cytoskeleton organization and membrane traffic regulating apical tip organization (Bassilana et al., 2020, 2005; Brand et al., 2014; Chen et al., 2020; Corvest et al., 2013; Court and Sudbery, 2007; Pulver et al., 2013).

The exocyst:

In *S. cerevisiae*, the exocyst complex is comprised of Sec3, Sec5, Sec6, Sec8, Sec10, Sec15, Exo70, and Exo84 (TerBush et al., 1996), and Cdc42 interacts with Sec3 (Zhang et al., 2008). In *C. albicans*, exocyst subunits localize to a crescent at the hyphal apex, while secretory vesicles associated proteins, the Rab-type GTPase Sec4, its GEF Sec2 and the myosin light chain protein 1 (Mlc1) localize to a subapical cluster (Bishop et al., 2010; Crampin et al., 2005; Jones and Sudbery, 2010; Li et al., 2007; Weiner et al., 2019) which is consistent with the model in **Figure 9**. Sec15 has been shown to interact with Rsr1, Bem1 and the myosin V, Myo2 (Guo et al., 2016). Several members of the exocyst have been shown to be essential for a correct hyphal growth. For example, phosphorylation of Exo84 by the Hgc1-Cdc28 is required for correct recycling to the PM (Caballero-Lima and Sudbery, 2014) and Sec3 is necessary for maintaining hyphal growth upon septum formation (Li et al., 2007).

The polarisome:

The *S. cerevisiae* polarisome complex includes Spa2, Pea2 (Valtz and Herskowitz, 1996), the formin Bni1 and the formin-actin-binding proteins Bud6 and Aip5 (Xie et al., 2019). These proteins are conserved in *C. albicans* (Crampin et al., 2005; Xie et al., 2020). As an example,

Bud6 and Spa2 form an apical crescent at the filament apex (Crampin et al., 2005). In filamentous fungi such as *Ashbya gossypii* and *N. crassa*, the crescent localization of Spa2 depends on the growth rate; during the slow growth phase, Spa2 becomes a "cap" in *Ashbya gossypii*. In *N. crassa* during fast growth, Spa2 localizes as patches (Araujo-Palomares et al., 2009; Köhli et al., 2008). In *C. albicans*, the spatiotemporal localization of the polarisome is altered during hyphal growth, where Cdc28-Clb2 and Cdc28-Hgc1 cooperate to phosphorylate Spa2, allowing the polarisome to be maintained at the filament tip (Wang et al., 2016). Additionally, deletion of SPA2 disrupts filamentous growth, resulting in formation of thick filaments in the mutant (Wang et al., 2016; Zheng et al., 2003). The polarisome member Bni1 is a Cdc42-GTP effector implicated in actin cable polarization in *S. cerevisiae* (Chen et al., 2012; Grinhagens et al., 2020). In *C. albicans*, it was shown that deletion of *BNII* causes cells to be able to initiate but not to maintain polarized hyphal growth (Li et al., 2005; Martin et al., 2005), suggesting a specific role in hyphal extension.

The Spitzenkörper:

The organization of the secretory pathway can have specific functions in distinct cell types. For example, there is an accumulation of vesicles in presynaptic cells ready to be secreted upon electrical stimulus (Binotti et al., 2021). In the yeast *Schizosaccharomyces pombe*, during mating, it is proposed that Cdc42-GTP zones dictate regions of pheromone secretion that are ultimately stabilized when the cell encounter pheromones from cells of opposite sex (Martin, 2019b; Merlini et al., 2016).

In filamentous fungi the secretory pathway is highly organized and compartmentalized at the apex of the filaments, which is the site of growth (Bassilana et al., 2020; Riquelme et al., 2018; Takeshita, 2016). The secretory vesicles, prior to anchoring and fusion with the plasma membrane, accumulate at the apex of the filaments and this accumulation is called the Spitzenkörper (SPK) (Riquelme et al., 2018; Takeshita, 2016). The SPK, first identified in

1924, was observed in fixed samples of *Coprinus narcoticus* and *Coprinus sterquilinus* as an iron hematoxylin stained apical body (Brunswik, 1924), and subsequently observed as a dense portion at the *Polystictus versicolor* filament tip by phase contrast microscopy (Girbardt, 1957).

Although it is a common structure among different fungi (Crampin et al., 2005; Jones and Sudbery, 2010; Pantazopoulou and Peñalva, 2009; Riquelme and Sánchez-León, 2014; Schultzhaus et al., 2015; Steinberg, 2007; Weiner et al., 2019), the SPK composition varies from fungus to fungus and is proposed to be a Vesicle Supply Center (VSC) (Riquelme et al., 2018). For example, in *Neurospora crassa*, the SPK is formed by different types of secretory vesicles, a central core of microvesicles surrounded by macrovesicles (Riquelme and Sánchez-León, 2014). In other fungi, such as *Candida albicans*, the SPK is composed of vesicles homogeneous in size (Weiner et al., 2019), loaded with the Rab8 homolog Sec4 and its GEF Sec2, the myosin light chain Mlc1, the formin Bni1, and the Rab11 homolog Ypt31 (Crampin et al., 2005; Jones and Sudbery, 2010; Silva et al., 2019). Very recent work in the laboratory showed that a SPK is observed in the absence of Mlc1, yet, in such mutants the filaments are wider and extend faster (Puerner et al., 2021b). This SPK is present in *C. albicans* hyphal cells during all stages of the cell cycle, including septum formation (Crampin et al., 2005). Perturbation of actin cables or secretion disrupted the Spitzenkörper (Crampin et al., 2005; Jones and Sudbery, 2010; Li et al., 2007; Weiner et al., 2019), its integrity and polarized localization are also dependent on the polarisome member Spa2 and Bud6 (Crampin et al., 2005). In *C. albicans*, as in other fungi, the absence of SPK results in reduced filamentous growth (Puerner et al., 2021b; Zheng et al., 2020). Interestingly, a cluster of vesicles that has all the components present in the SPK is observed in the absence of tip growth and is highly dynamic moving by hops and jumps, suggesting that such a cluster can form in the absence of directional growth (Silva et al., 2019).

The actin cytoskeleton:

In filamentous fungi, **actin cytoskeleton** and microtubules are keys for material delivery to the growing apex (Riquelme et al., 2018; Takeshita, 2016). In *C. albicans*, drugs such as latrunculin A or cytochalasin A, which inhibit actin polymerization, alter filamentous growth (Hazan and Liu, 2002; Jones and Sudbery, 2010). In filamentous fungi, such as *A. nidulans*, secretory vesicles transport requires microtubules (Riquelme et al., 2018). This long-distance transport is not critical in *C. albicans*, where microtubules are dispensable for hyphal formation (Rida et al., 2006). Instead, in *C. albicans*, it is suggested that the secretory pathway organization, with the ER extending along the filament, a sub-apical Golgi and a SPK comprised of vesicles of uniform size, facilitates short-range delivery (Weiner et al., 2019) (**Figure 9**).

The actin cytoskeleton is comprised of 3 principal structures. *(i)* **The cortical actin** patches form a subapical ring during hyphal development in *A. nidulans* and *N. crassa* (Araujo-Bazán et al., 2008; Berepiki et al., 2011; Delgado-Álvarez et al., 2010; Upadhyay and Shaw, 2008). In *C. albicans*, a collar 2 micrometers back from the filament tip was observed (Ghugtyal et al., 2015; Sudbery, 2011). The actin-binding protein Abp1, which is implicated in clathrin mediated endocytosis (Epp et al., 2013a; Ghugtyal et al., 2015), localizes to this endocytic collar, yet *ABP1* is not essential and hyphal morphogenesis was not altered in *abp1* deletion mutants (Caballero-Lima et al., 2013; Ghugtyal et al., 2015; Martin et al., 2007). In contrast, the AP-2 endocytic adaptor complex is required for *C. albicans* hyphal morphology and the recycling of the chitin synthase Chs3 (Chapa-y-Lazo et al., 2014; Knafler et al., 2019). The Arp2/3 (Actin Related Protein) complex is also required for *C. albicans* hyphal formation but, in contrast to *S. cerevisiae*, not for viability, indicating that actin-driven polymerization during endocytosis can occur *via* Arp2/3-independent routes (Epp et al., 2013a, 2010). *(ii)* **The actin cables** are also independent of Arp2/3 in *C. albicans* (Epp et al., 2013a, 2010). It was recently shown in *C. albicans* that the *S. cerevisiae* Aip5 homolog binds G-actin, Bni1, and Bud6 to form the

nucleation complex to polymerize F-actin (Xie et al., 2020). Beside Bni1, another formin is present in *C. albicans*, Bnr1, which functions at the division site and is partially redundant with Bni1 (Crampin et al., 2005; Dünkler and Wendland, 2007; Martin et al., 2005). Actin cables, which serve as rails for the transport of organelles such as secretory vesicles and the Golgi, are disrupted with specific drugs, resulting in a growth inhibition and in a blocked filamentation (Crampin et al., 2005; Hazan and Liu, 2002; Jones and Sudbery, 2010; Pointer et al., 2015). This filament arrest was concomitant with a disruption of Cdc42 localization, which was not observed in budding growth after latrunculin A treatment (Hazan and Liu, 2002), suggesting a specific requirement of actin cytoskeleton for Cdc42 localization during hyphal growth (Hazan and Liu, 2002). **(iii) The actomyosin ring**, which is a contractile structure composed of actin and myosin II in *S. cerevisiae* (Cheffings et al., 2016). Myosin II and I are regulated by the Myosin light chain (Mlc1) protein (Stevens and Davis, 1998). In *S. cerevisiae*, Mlc1 is recruited at the site of cytokinesis and interacts with Myo1 (Boyne et al., 2000), where it functions in parallel with the septins (Graziano et al., 2014). In *C. albicans*, Mlc1 is recruited at the SPK and also at the actomyosin ring (Crampin et al., 2005). In the *mlc1* mutant, unfinished cytokinesis results in the formation of chains of cells (Puerner et al., 2021b). In contrast, *mlc1* mutant has a faster hyphal extension rate than a WT strains, even though the cell were wider (Puerner et al., 2021b).

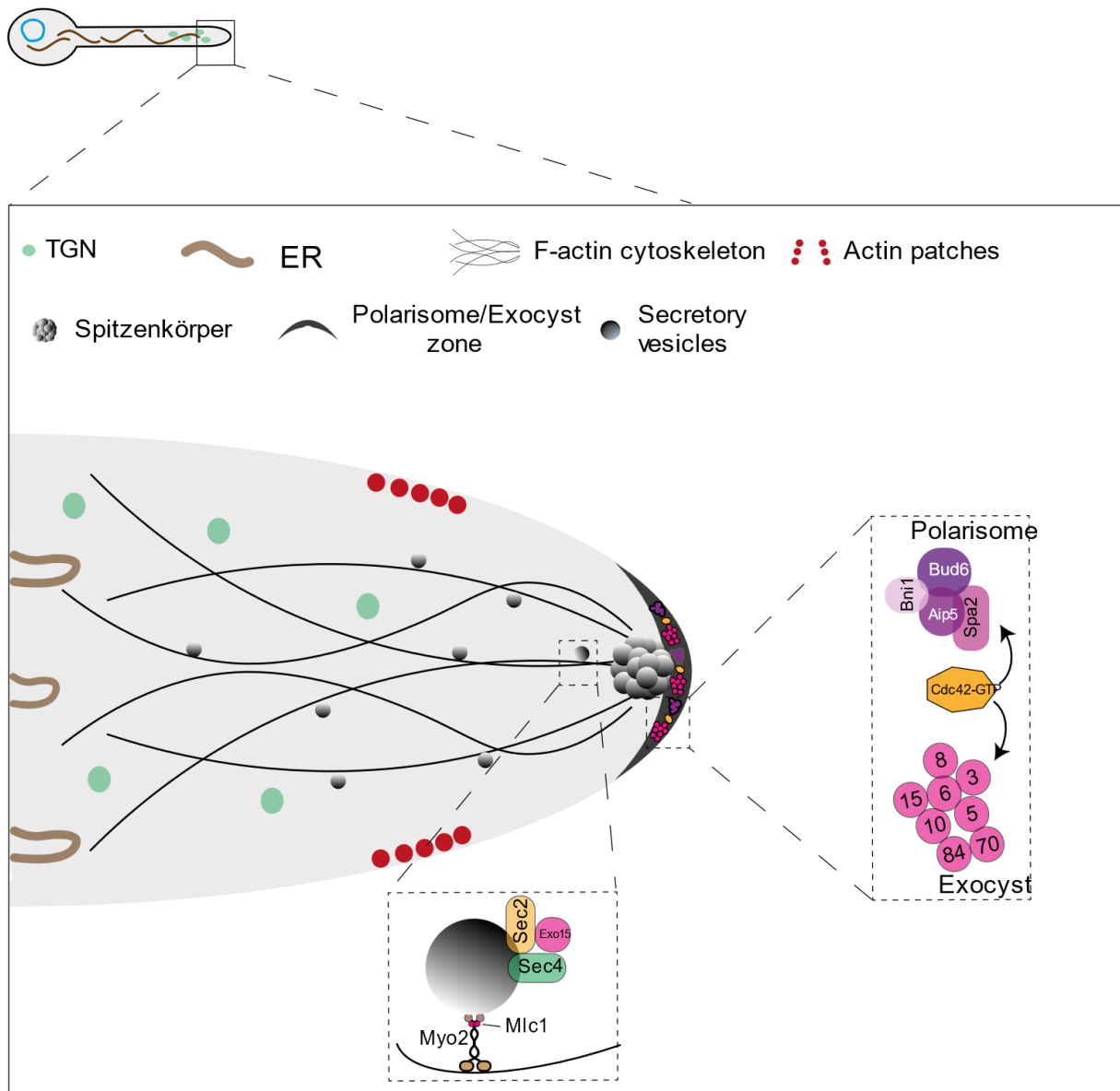


Figure 9. Schematic of *C. albicans* hyphal tip structural organization. In *C. albicans*, the ER (shown in brown) and the Trans Golgi Network (TGN; depicted as green spheres) extend to the hyphal tip to constitute an “on-site secretory vesicles delivery” by which vesicles are locally budded and delivered, resulting in a short-range trafficking within the tip region (Weiner et al., 2019). Secretory vesicles (represented as grey spheres), loaded with the Rab-type GTPase Sec4 and the GEF Sec2, are transported on actin cables (black strings) by the class V myosin Myo2/Mlc1 complex and accumulate at the Spitzenkörper (SPK) located at the hyphal tip. Actin cable nucleation is generated by the formin Bni1, which is assisted by the polarisome composed by Spa2, Aip5 and Bud6 (molecular components of this structure are schematized in the inset magnification). From the SPK, the vesicles are delivered to the PM. The exocyst, which is composed of Sec3, Sec5, Sec6, Sec8, Sec10, Sec15, Exo70 and Exo84, participates in vesicle docking before fusion. Endocytosis takes place at the endocytosis collar, an accumulation of actin patches (red rounds in the scheme) located 1-3 μ m sub-apically from the apex. Based on models from Sudbery, 2011 and Weiner et al., 2019.

3. Lipids in *C. albicans*.

The major lipids in fungi, based on *S. cerevisiae*, are sphingolipids, sterols and glycerophospholipids (Klug and Daum, 2014); the latter group includes the phosphatidic acid (PA) and phosphatidylcholine (PC), which are less abundant than phosphatidylserine (PS), phosphatidylethanolamine (PE), phosphatidylinositol (PI) and its phosphorylated derivatives (PIPs), these three latest are ~80% of phospholipids at the PM. Phosphatidylinositol-4-Phosphate (PI(4)P) and phosphatidylinositol-4,5-bis-phosphate (PI(4,5)P₂) at the plasma membrane result from the phosphorylation of PI by the single kinases Stt4 and Mss4 (Cutler et al., 1997; Desrivères et al., 1998; Homma et al., 1998; Trotter et al., 1998; Yoshida et al., 1994), while Golgi PI(4)P is produced by another kinase, Pik1 (Flanagan et al., 1993; Garcia-Bustos et al., 1994). A single synthase, encoded by the *CHO1* gene, converts CDP-DAG (CDP-diacylglycerol) to PS (K. Atkinson et al., 1980; K. D. Atkinson et al., 1980; Letts et al., 1983). These enzymes are conserved among fungi, with some exceptions, as an example, *A. nidulans* and *Cryptococcus neoformans* appear to have a Stt4 PI-4-kinase that is essential for viability, however, Pik1 orthologs are absent (De Souza et al., 2013; Lee et al., 2016).

During *C. albicans* yeast-to-hyphal transition, lipids, especially phospholipids and ergosterol, are redistributed and enriched at the growing apex (Ghugtyal et al., 2015; Labbaoui et al., 2017; Martin and Konopka, 2004a; Vernay et al., 2012). The enzymes abovementioned implicated in phospholipid synthesis are also present in *C. albicans* (**Figure 10**), and their downregulation has a very deleterious effect in hyphal growth (Chen et al., 2010; Ghugtyal et al., 2015; Vernay et al., 2012). Suggesting an essential role of phospholipids in *C. albicans* morphogenic transition (Chen et al., 2010; Ghugtyal et al., 2015; Vernay et al., 2012).

Ergosterol is the major sterol in the budding yeast and ergosterol synthesis is a target for antifungal agents (**Figure 11**) (Bhattacharya et al., 2018). Equivalent to cholesterol in

mammals, ergosterol concentration in the ER is low but increases along the secretory pathway up to the PM (Klug and Daum, 2014). In *S. cerevisiae*, 25 known ER-enzymes encoded by the ERG genes regulate ergosterol biosynthesis (Bhattacharya et al., 2018). Misregulation of these enzymes results in altered susceptibilities to antifungal drugs such as fluconazole (Bhattacharya et al., 2018). Fluconazole blocks 14- α -dymethylation of lanosterol in the ergosterol biosynthetic pathway (Bhattacharya et al., 2018).

▪ **Lipid function in *C. albicans*:**

In *C. albicans*, blocking the synthesis of ergosterol and sphingolipid results in a filamentous growth defect (Martin and Konopka, 2004a). Ergosterol filament apex polarization is dependent on the AP-2 complex implicated in clathrin-dependent endocytosis (Knafler et al., 2019), which supports the idea of the “raftophilic” cargo-sorting function of lipids rafts during vesicular transport (Alvarez et al., 2007; Martin and Konopka, 2004b). Similar to ergosterol, PI(4)P, PI(4,5)P₂, and PS are dramatically enriched at the end of filament (Ghugtyal et al., 2015; Labbaoui et al., 2017; Vernay et al., 2012) and the enzymes implicated in their synthesis are essential for *C. albicans* morphogenesis, as the repression or deletion of these enzymes impairs filamentous growth (Chen et al., 2010; Ghugtyal et al., 2015; Vernay et al., 2012). These phospholipids are important to localize and/or stabilize key components for polarized growth in fungi:

- **PI(4,5)P₂**. In *S. cerevisiae*, this lipid is important for the function and proper localization of proteins such as the MAPK scaffold Ste5 during formation of mating projections (Garrenton et al., 2010, 2006) and invasive growth (Adhikari and Cullen, 2015; Guillas et al., 2013). In *C. albicans*, during hyphal growth, PI(4,5)P₂ forms a steep gradient with the highest concentration at the subapical zone of the filament. This gradient is generated and maintained by a local production at the tip, where the PI-4 kinase Mss4 is localized (Vernay

et al., 2012) and by clearing of PI(4,5)P₂ at the back of the cell. As the levels of PI(4,5)P₂ decrease in the rest of the cell, this lipid gets accumulated at the germ tube tip (Vernay et al., 2012). The downregulation of Mss4 impairs yeast-to-hyphal transition. In addition, this kinase is required to stabilize active Rho1 at the growth site during budding growth (Corvest et al., 2013). These data indicate a close functional link between phospholipids and the localization of key proteins regulating hyphal morphogenesis.

- **PI(4)P.** In *S. cerevisiae*, PI(4)P, which is found principally at the Golgi and plasma membranes, participates in vesicle budding, maturation and fusion (Bard and Malhotra, 2006; Moser von Filseck and Drin, 2016; Smindak et al., 2017). PI(4)P facilitates the recruitment of proteins implicated in polarized growth, such as the Cdc42 effector, Cla4 (Wild et al., 2004). As in *S. cerevisiae*, there are two functionally independent pools of PI(4)P in *C. albicans*, one at the Golgi and another one at the PM (Audhya et al., 2000; Ghugtyal et al., 2015; Santiago-Tirado et al., 2011). Golgi PI(4)P levels in *C. albicans* are important for vesicular traffic, as down-regulation of the Pik1 kinase alters the number of Golgi cisternae and their dynamics (Ghugtyal et al., 2015). Indeed, the *pik1* repressible mutant shows reduced Golgi PI(4)P levels when *PIK1* gene is downregulated, which results in perturbed secretory vesicle budding and decreased secretory vesicle targeting to the site of growth (Ghugtyal et al., 2015). PM PI(4)P was observed as a tight cap at the hyphal filament tip (Ghugtyal et al., 2015). This polarized localization has been proposed to be maintained by the action of phosphatases, such as Sac1, rather than by endocytic recycling (Ghugtyal et al., 2015). Both PI(4,5)P₂ and PI(4)P shows very polarized distribution (Ghugtyal et al., 2015; Vernay et al., 2012). However, a less dramatic defect in filamentation is observed upon reduction of the PI-4-kinase Stt4, responsible for the synthesis of the PI(4)P pool at PM (Vernay et al., 2012), raising questions about the dispensability of this pool for the yeast-to-hyphal transition.

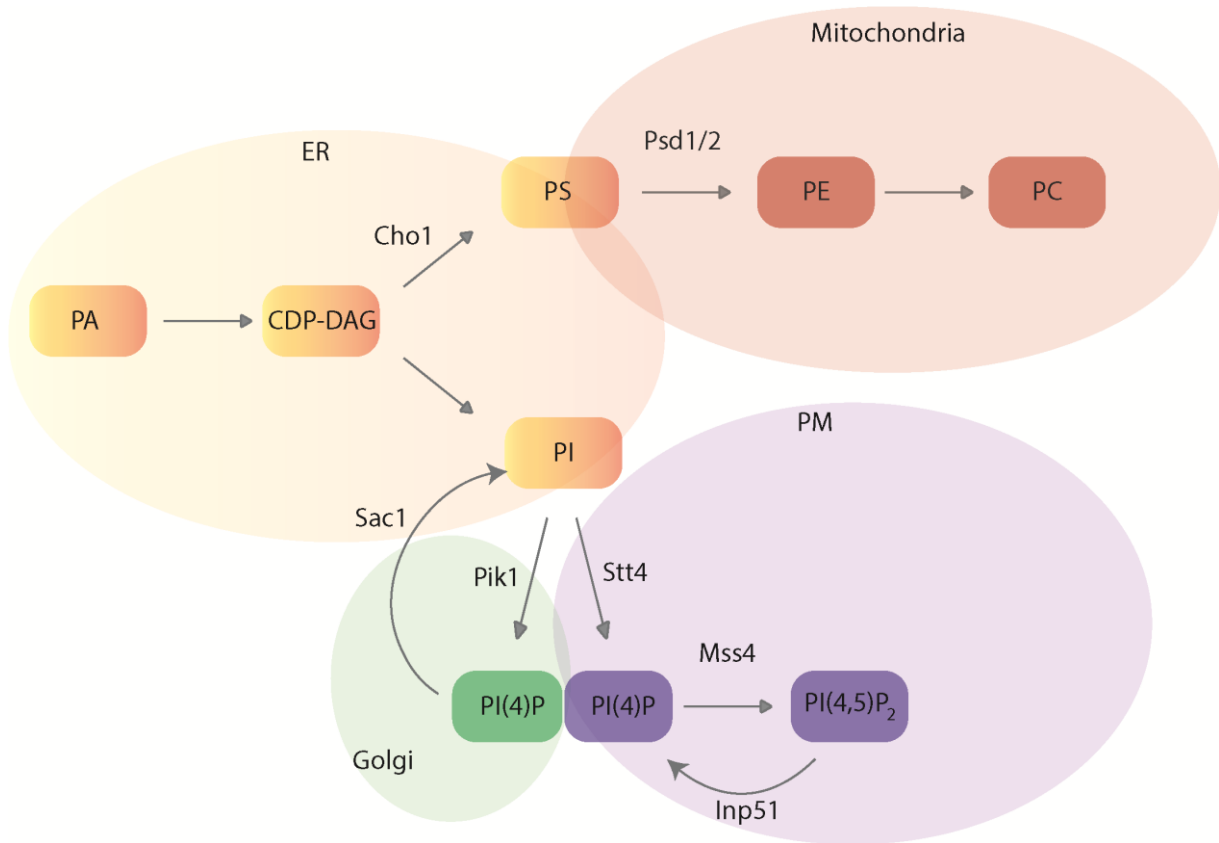


Figure 10. Phospholipids and enzymes implicated in their synthesis in *C. albicans* Schematic representation of the main phospholipids distributed in *C. albicans* endoplasmic reticulum (ER), mitochondrial membrane, Golgi or cellular plasma membrane (PM). Arrows show the biochemical direction of phospholipid production; enzyme regulating each biochemical step are indicated next to the

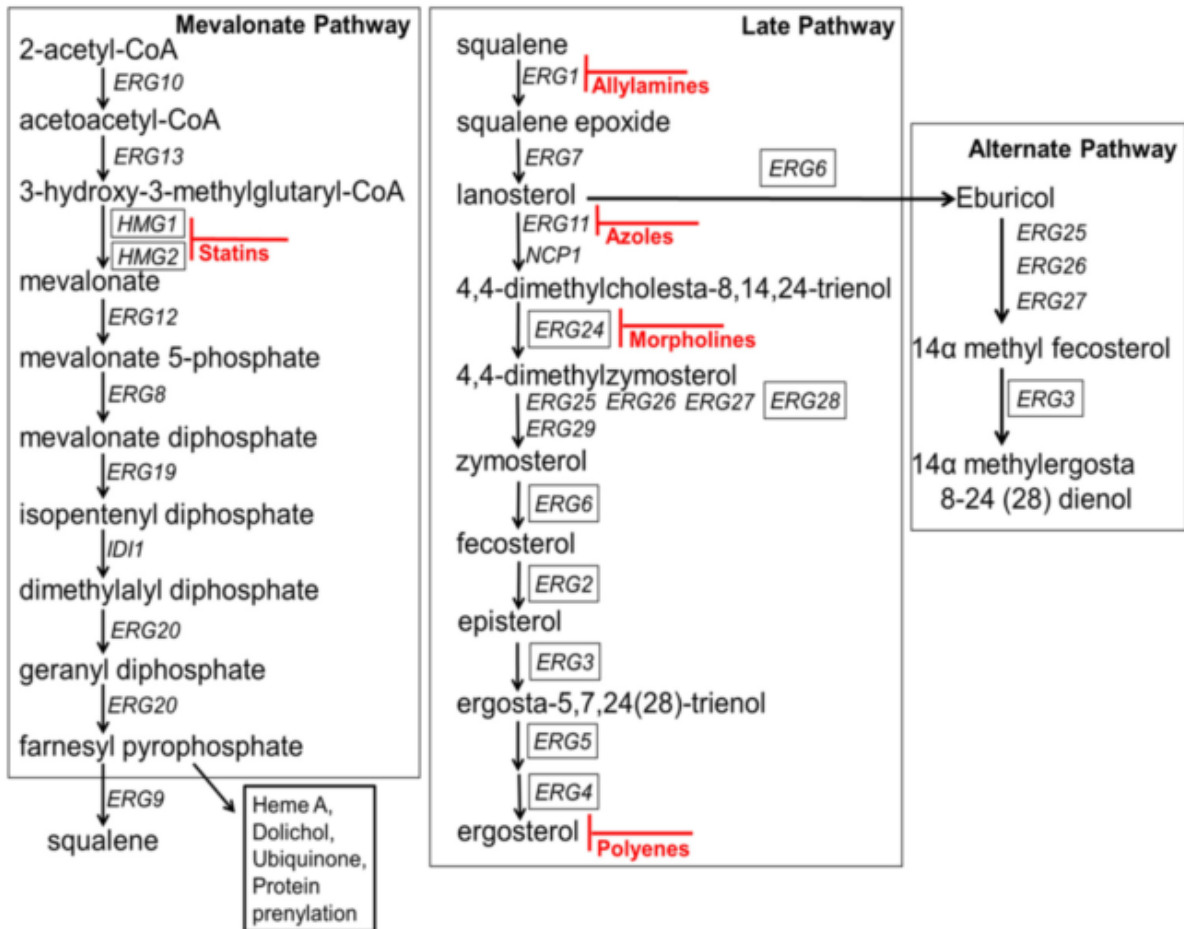


Figure 11. Biochemical pathway for the synthesis of Ergosterol. Genes required for each biochemical step are indicated next to the arrows; boxed genes are nonessential ones. Antifungal drugs are showed in red. The box on the right represents an alternate pathway leading to the toxic fungistatic sterol. Reproduced from Bhattacharya et al., 2018.

- **PS:** Phospholipids are important for membrane electrostatic properties (Lenoir et al., 2021). As introduced above, PS is the most abundant among the anionic phospholipids at the PM and, together with PI(4)P, it is enriched at the cytosolic leaflet from late secretory organelles to the PM in *S. cerevisiae* (Holthuis and Menon, 2014; Klug and Daum, 2014; Lenoir et al., 2021). In *S. cerevisiae*, deletion of the unique PS synthase Cho1 impairs polarized endocytosis (Sun and Drubin, 2012). PS is critical for Cdc42 and Bem1 polarized localization in *S. cerevisiae* (Fairn et al., 2011; Meca et al., 2019) and for Rho1 localization in *S. pombe* (Haupt and Minc, 2017). However, in *S. cerevisiae* cell viability is not affected in the *cho1* mutant, indicating that the essential function of Cdc42 is not compromised upon Cho1 loss (Fairn et al., 2011; Sun and Drubin, 2012). Together, these results suggest that the interactions between the PM and Bem1 is based on more general lipid properties. In fact, it was shown that Bem1 localization can be partially rescued by synergic lipid-protein interactions between Bem1 and other anionic lipids such as PI(4)P and PI(4,5)P₂ (Meca et al., 2019). In *C. albicans*, an enriched distribution of PS is observed at the hyphal apex (Labbaoui et al., 2017) and deletion of the PS synthase Cho1 results in a reduced ability to form filaments and in an altered cell wall structure (Chen et al., 2010; Davis et al., 2014). Indeed, the *cho1* mutant shows an increased cell wall thickness (Chen et al., 2010) and β (1-3)-glucan unmasking (Davis et al., 2014). Furthermore, mutants lacking Cho1, or the PS decarboxylases (Psd1 and Psd2) have a similar compromised virulence in murine models (Chen et al., 2010; Davis et al., 2018). Both *cho1* and *psd1/2* mutant virulence were rescued after providing these mutants with the capacity to capture higher concentrations of ethanolamine (Davis et al., 2018). However, the rescue of the *cho1* mutant was not due to PE itself, but to a reverse Psd1/2 enzymatic reaction that produce PS when the concentration of PE is high enough (Davis et al., 2018). Recent work has shown that the absence of PS in the *cho1* mutant improved copper-stress resistance (Douglas and Konopka, 2019). As

copper level increase is an immune response against pathogens, these results suggest a critical role for PS in *C. albicans* pathogenesis and virulence.

- **The P4-ATPase Drs2:**

PS asymmetric distribution with strong enrichment at the cytosolic leaflet is regulated by proteins from the P4-ATPase family (Hankins et al., 2015a; Lenoir et al., 2021; Lopez-Marques et al., 2014; Pomorski et al., 2003; Roland and Graham, 2016)(See section II.3. Membrane asymmetry). One of the five P4-ATPases in *S. cerevisiae*, Drs2, was identified, together with 6 others (Drs1-Drs7), in a deficient in ribosomal subunits mutant screening (Ripmaster et al., 1993), and was visualized for the first time at the Golgi, co-localizing with another P4-ATPase Dnf3 (Chen et al., 1999; Hua et al., 2002).

Among the five genes encoding the P4-ATPases, a certain degree of redundancy has been demonstrated for the *DRS2/DNF* genes, yet *NEO1* is the sole required for cell viability in *S. cerevisiae* (Hua et al., 2002). Although Drs2 and Neo1 transport PS and PE, little to none functional overlap has been shown (Takar et al., 2016). Nonetheless, overexpression of *NEO1* can suppress a cold sensitivity defect of the *cdc50* mutant (Saito et al., 2004) and Drs2 and Neo1 are redundant in the absence of the PQ-loop protein Any1 (Takar et al., 2019), suggesting a segregation of Drs2 and Neo1 function induced by the Any1-Neo1 interaction (Takar et al., 2019). In contrast, in filamentous fungi, Neo1 homologs are not essential. The *A. nidulans* homologous, DnfD, which localizes to the late Golgi, is also dispensable for viability and necessary for conidia formation (Schultzhaus et al., 2019). In *C. albicans*, the *neo1* mutant is also viable and has an increased sensitivity to duramycin, indicating a defect in PE asymmetry at the PM (Douglas and Konopka, 2019).

Drs2 was associated with clathrin-dependent vesicle budding (Chen et al., 1999), protein transport in clathrin-dependent vesicles from TGN to the PM, and AP3-dependent budding to

the vacuole in *S. cerevisiae* (Gall et al., 2002; Hua et al., 2002). Drs2 is necessary for Golgi organization. The *drs2* mutant, similar to clathrin mutants, accumulates aberrant Golgi structures called “Berkeley bodies” (Chen et al., 1999), and has a reduced number of post-Golgi exocytic vesicles (Gall et al., 2002); Moreover, Drs2 participates in the generation of membrane curvature in the TGN/Early endosome membranes (Xu et al., 2013) and in the recruitment of the golgin Imh1 in *S. cerevisiae* (Tsai et al., 2013). Drs2, the GEF Gea2 and its effector Arl1 form a complex regulated by PI(4)P, that is implicated in the activation of Drs2 and in budding of clathrin vesicles associated to AP1 adaptor protein (Chantalat et al., 2004; Natarajan et al., 2009). PM-proteins Pma1 and Can1 sorting and localization of ergosterol are restored after deletion of the OSBP-homologous protein, Osh4, in the *drs2* mutant (Hankins et al., 2015b; Muthusamy et al., 2009). Thus, lipid homeostasis seems to be more important than the presence of the lipid transporters *per se* (Hankins et al., 2015b; Muthusamy et al., 2009).

The role of P4-ATPases has been previously investigated in filamentous fungi. In *A. nidulans*, PS distribution is dependent on the flippases DnfA and DnfB, the respective homologues of Dnf1 and Drs2 (Schultzhaus et al., 2015). Enriched at the SPK, PS shows a very polarized distribution at the hyphal site of growth, in contrast to its homogeneous distribution in subapical regions or PM of nongrowing cells. Thus, PS distribution correlates with DnfA/B localization. Consistently, the absence of DnfA reduces PS localization to the DnfB-loaded microvesicles (Schultzhaus et al., 2015). DnfA/B have been implicated in endocytosis in *A. nidulans* and *F. graminearum*, as they interact with the AP-2 complex (Martzoukou et al., 2017; Zhang et al., 2019), which is essential for hyphal maintenance in fungi, including *C. albicans* (Knafler et al., 2019).

The regulation of these P4-ATPases by their non-catalytic subunits is conserved and essential for a correct function. Indeed, the deletion of the Lem3/Cdc50 members phenocopies the flippase deleted mutants (Chen et al., 2006; Kato et al., 2002; Schultzhaus et al., 2017; Xu et

al., 2019). In *A. nidulans*, Cdc50 deletion impairs viability (Schultzhaus et al., 2017). A similar defect was observed upon deletion of both DnfA and DnfB (Schultzhaus et al., 2015), suggesting that Cdc50 regulates both flippases (Schultzhaus et al., 2017). In *Cryptococcus neoformans*, the Drs2 homologue Apt1 can complement a *drs2* mutant of *Saccharomyces cerevisiae* (Hu and Kronstad, 2010). Moreover, based on phenotypic similarities of the *cdc50* and *apt1* mutants, Cdc50 has been proposed to function together with Apt1 to contribute to flippase function (Hu et al., 2017; Hu and Kronstad, 2010). In *C. albicans*, deletion of *DRS2* results in defect of filamentous growth, altered distribution of PS and hypersensitivity to fluconazole (Labbaoui et al., 2017). A similar phenotype has been reported for a *cdc50* mutant (Xu et al., 2019). In addition, in a *drs2* deletion mutant, sensitivity to copper is increased and this phenotype is more drastic than that of a *dnf1* or *neo1* mutant (Douglas and Konopka, 2019), indicating a role of PS in copper sensitivity.

THESIS OBJECTIVES

Candida albicans hyphal growth is associated with a filament tip enrichment of lipids, including ergosterol, the phosphorylated derivatives of phosphatidylinositol (PI(4)P, PI(4,5)P₂) and phosphatidylserine (PS). Deletion of the lipid flippase Drs2 results in altered distribution of PS and defect in hyphal growth, when *C. albicans* is exposed to serum. In contrast, budding growth is not affected. The aim of my project was to determine the function of Drs2 in hyphal growth and the importance of PS asymmetry in this process. To this end, I localized Drs2 during hyphal growth and further characterized the *drs2* deletion mutant by analyzing the distribution of different lipids and key regulators of hyphal growth, such as active Cdc42. I also analyzed mutants analogous to those in *S. cerevisiae* that are altered for PS flippase activity. In addition, I investigated the importance of other flippases in hyphal invasive growth, as well as that of Oxysterol-binding proteins, using loss-of-function mutants. Furthermore, I examined potential genetic interactions between these transporter encoding genes and *DRS2*.

MATERIAL AND METHODS

Growth conditions

The media and buffer composition used for this work are illustrated in **Table 2**.

- **Budding growth:** The yeasts are grown at 30°C in a rich (YEPD: Yeast extract peptone dextrose) or selective synthetic media, in liquid or solid media containing 2% agar. The effect of different compounds is tested on YEPD agar medium in the presence of 50mM of PIPES buffer, at pH 5.5 containing:
 - Cell wall perturbants: Congo red (400 µg/ml), Calcofluor white (25 µg/ml)
 - Antifungal agents: fluconazole (10 µg / ml), caspofungin (125 ng / ml), Amphotericin B (3µg / ml).
 - Toxins: papuamide A (1µg / ml), duramycin (50 µg/ml)

Serial dilutions of cells in exponential growth [$OD_{600nm} = 0.6-0.8$] are spotted (5-7µl of culture) and incubated at 30°C for 2 to 6 days.

- **Filamentous growth:** Filamentation is induced in liquid or agar containing media in the presence of Serum (FCS, fetal calf serum), in general 50% (Basilana et al., 2005) or in low carbon source containing media (Spider medium) (Calera et al., 2000).
 - For filamentous growth in liquid media, the cells in exponential growth ($DO_{600nm}=0.6$) are incubated with 50% FCS at 37°C for 45, 60, 90 or 120 minutes.
 - For filamentous growth in 2% agar and 50% FCS containing media, the colonies are visualized after 4 to 7 days of incubation at 30°C.
 - For time-lapse experiments, cells are added on 0.5% agar and 75% FCS containing media on microscope slides (pads) (Basilana et al., 2005). Cells at $OD_{600nm} 0.4$ are added to FCS in 1:1 ratio.

- **Growth of bacteria:** The bacteria are grown at 37°C in rich media (TYE, **Table 2**) or selective (TYE Amp, **Table 2**) in liquid or 2% agar containing media.

Plasmid construction

The plasmids generated are illustrated in **Table 3**.

Plasmids pExpARG4:

- For plasmids containing *DRS2* and *OSH4* under the control of their own promoter, genomic DNA fragments containing *the* ORFs (Open Reading Frame) and 1000 base pairs upstream and downstream were amplified by PCR, using the oligonucleotide pairs CaDrs2pup1000SalI/CaDrs2m5963NotI and CaOsh4pup1000SalI/CaOsh4m3268NotI (**Table 4**), which contain the unique restriction sites, SalI and NotI in 5' and 3', respectively. The amplification was done using Phusion DNA polymerase and the Thermocycler Biometra Trio according to the program:

1. 98°C 30 sec
2. 98°C 15 sec
3. 55°C 20 sec
4. 72°C 30 sec/1 kb 30 cycles
5. 72°C 10 min
6. 10°C pause

Given that SalI and XhoI are compatible restriction sites, PCR products digested with SalI and NotI were inserted by ligation into the plasmid *pExpARG4XhoI-pARL3ARL3-NotI* (Labbaoui et al., 2017), generating *pExpARG4pDRS2DRS2* and *pExpARG4pOSH4OSH4*.

- **Single directed mutagenesis (SDM)** was used to introduce mutations (Drs2^{F511Y} and Drs2^{QO}) in Drs2, similar to that specifically altered phosphatidylserine flipping in *S. cerevisiae* (Baldrige and Graham, 2012). The plasmids **pExpARG4pDRS2DRS2^{F511Y}** and **pExpARG4pADH1DRS2^{F511Y}** were generated from *pExpARG4pDRS2DRS2* and *pExpARG4pADH1DRS2* (Labbaoui et al., 2017), respectively. The mutation *F511Y* corresponds by sequence alignment to the mutation *F520Y*. In this work, the mutation *F520Y* will be called *F511Y* by analogy with *S. cerevisiae*.

The Primers CaDrs2F511Yp/ CaDrs2F511Ym (**Table 4**) are used to introduce this mutation, as well as a silent mutation for a KpnI restriction site, allowing to screen the transformants.

The **SDM** is done using the Pfu DNA polymerase, according to the program:

1. 95°C 30 sec
2. 95°C 30 sec
3. 55°C 1 sec
4. 68°C 15min 15 cycles
5. 65°C 5 min
6. 10°C pause

Following amplification, the samples are treated with DpnI, which digests methylated DNA. This step is necessary to reduce the transformation background, as the plasmid that served as a matrix, unlike PCR products, is methylated. The program used is as follows:

1. 37°C 1h
2. 68°C 20min
3. 10°C pause

4µL of product are used to transform competent XL1-Blue *E. coli* cells prepared by the calcium chloride method (Inoue et al., 1990) (section “PLASMID AMPLIFICATION”).

To verify the presence of the mutation in *DRS2*, after **plasmid amplification** a first screening is carried out using primers CaDrs2p1336 / CaDrs2m1732 to amplify a fragment of about 400pb containing the silent restriction site KpnI. Plasmids containing KpnI digested fragments were confirmed by sequencing (Eurofins MWG Operon, Esbersberg, Germany).

A similar procedure was used to generate *pExpARG4pDRS2DRS2^{QQ}*, *pExpARG4pADH1DRS2^{QQ}*. For the SDM we used primers CaDrs2QQp691/CaDrs2QQm755 to mutate in GA→QQ (Baldrige and Graham, 2013), and to introduce a silent deletion of a restriction site ClaI. To verify the presence of the mutation in *DRS2*, we used primers CaDrs2p446/CaDrs2m940 to amplify a fragment that we digested with ClaI. Plasmids containing fragments that were not digested with ClaI were confirmed by sequencing.

- To visualize the distribution of ergosterol, we used the genetically encoded biosensor D4H [Marek *et al.*, 2020]. D4H was amplified from plasmid pSM2244 (Marek *et al.*, 2020), using primer pair D4HpAscIBamHI / D4HmMluI and cloned into plasmid *pExp-pACT1-mScarlet-CtRac1* (Silva *et al.*, 2019), using AscI and MluI unique restriction sites, yielding *pExp-pACT1-mScarlet-D4H*. This plasmid was linearized with NcoI and integrated into the *RP10* locus.

Plasmids pDup:

To select cell transformation by plasmids *pDup3* and *pDup5* (Gerami-Nejad *et al.*, 2013), the Nourseothricin resistance gene *SAT1* or the auxotrophy marker *URA3* were used, respectively.

- Plasmids *pDup3pDRS2DRS2* and *pDup3pDRS2DRS2^{F511Y}* were generated from *pExpARG4pDRS2DRS2*, *pExpARG4pDRS2DRS2^{F511Y}*, respectively, after PCR amplification of a fragment containing the ORF and 1000 bp upstream and downstream using the oligonucleotide pair CaDrs2pup1000SpeI / CaDrs2m5963NotI (**Table 4**). PCR products digested by SpeI and NotI were inserted into *pDup3* (Gerami-Nejad *et al.*, 2013).

- For plasmids overexpression, the *ORFs* *DRS2*, *OSH4* and *DNF2* were amplified using primers *CaDRS2p1AscI* / *CaDRS24963mMluI*, *CaOSH4p1AscI* / *CaOSH4m1293MluI*, *CaDNF2p1AscI* / *CaDNF2m5151MluI*, which have the unique restriction sites MluI and AscI in 5' and 3', respectively. After amplification as above, the PCR products were digested by MluI / AscI and inserted into the plasmid *pDup3pADH1mSCARLETctRAC1tADH* (Silva et al., 2019). Similar procedure was used to generate the plasmid *pDup3pADH1-GFP*LactC2 after GFP-LactC2 PCR amplification with primers LactC2mMluI / yeGFP3pAscI from *pExpArgpACTIGFPyeLactC2* (Labbaoui et al., 2017).

- For the construction of plasmids containing *pDNF2DNF2* (6Kb), PCR amplification was done in two steps: first, the *pDNF2* promoter was amplified from gDNA, using primers *CaDnf2pup1000XmaI* / *CaDnf2mup21AscI*, as in section “Plasmids pExpARG4”. PCR products were digested by XmaI and AscI to be inserted into *pDup3-(XmaI)-pTEF1-(AscI)-CRYlinker-GFPγ-CDC42-(SbfI)-tTEF1* (Silva et al., 2019) generating the intermediate plasmid *pDup3-(XmaI)-pDNF2-(AscI)-CRYlinker-GFPγ-CDC42-(SbfI)-tTEF1*. Then, the ORF of *DNF2* was similarly amplified, using primers *CaDnf2p1AscI* / *CaDNF2m5151SbfI*. PCR products were digested by AscI and SbfI to be inserted into *pDup3-(XmaI)-pDNF2-(AscI)-CRYlinker-GFPγ-CDC42-(SbfI)-tTEF1*, generating *pDup3-pDNF2DNF2*.

The plasmids *pEApDRS2DRS2*, *pEApDRS2DRS2^{F511Y}*, *pEApOSH4OSH4*, *pEApADH1DRS2^{QQ}* were linearized with StuI for *RP10* locus integration. The plasmids *pDup3pDRS2DRS2*, *pDup3pDRS2DRS2^{F511Y}*, *pDup3pDNF2DNF2*, *pDup3pADHOSH4*, *pDup3pADH1DRS2* were linearized by NgoMIV for a *NEUT5L* integration.

All constructions were sequenced by Eurofins MWG Operon in Esbersberg, Germany.

Plasmid amplification

The amplification of plasmids was done by transformation of competent XL1-Blue *E. coli* cells prepared by the calcium chloride method (Inoue et al., 1990). About 0.2 µg of plasmid DNA are mixed with 100 µl of competent bacteria and subjected to:

- A heat shock: The mixture is put on ice for 10 minutes, then switch to 42°C for 2 minutes and on the ice for 2 to 5 minutes.
- An incubation period to express beta-lactamase: An equivalent volume of TYE medium is added and the suspension is incubated at 37°C for one hour to express beta-lactamase, an enzyme capable of degrading antibiotics containing the beta-lactam cycle, as is the case of ampicillin.
- The mixture is then spread on agar containing TYE + ampicillin (100µg/ml) media and incubated at 37°C for 12 hours.

Plasmid were extracted using a NucleoSpin Plasmid Kit (Macherey-Nangel) from the colonies grown on ampicillin.

Strain construction

Transformation of *C. albicans*: electroporation

- A colony of *C. albicans* is inoculated in 5 ml of YEPD + Uri and grown at 30°C overnight. This preculture is diluted 10 times in YEPD + Uri and grown again to a DO₆₀₀ of 2-4.
- The suspension is centrifuged at 3000 rpm, 3 min at 4°C. The pellet is resuspended in 8 ml of H₂O + 1 ml of lithium acetate 1M + 1 ml of TE 10X (100mMTris-HCL, 10mM EDTA, pH7.5), incubated at 30°C, 45min, before adding 250µl of DTT 1M and incubation at 30°C for 15 min.

- Cells are then submitted to 3 wash steps: first with 50 ml of iced water, then 25 ml of iced water and finally 10 ml of iced sorbitol 1M. The final pellet is resuspended in 100µl of sorbitol. To 40 µl of these competent cells are added 5µg of the DNA of interest.
- After electroporation at 1800V, the cells are centrifuged (1.5 min at 3000 rpm) and resuspended in 400 µl of LM2 before inoculation on selective medium. When an antibiotic resistance gene is used (Nourseothricin or Hygromycin), 1ml of YEPD + Uri is added instead with additional incubation at 30°C for 4 hours, followed by centrifugation (1.5 min at 3000 rpm) and resuspension in 400µl of LM2 as before.
- Colonies appear 2-3 days after incubation at 30°C.

Generation of *C. albicans* strains

- **Loss of function Mutants**

The mutants $\Delta dnf1/\Delta dnf1$ (*dnf1*), $\Delta dnf2/\Delta dnf2$ (*dnf2*), $\Delta dnf3/\Delta dnf3$ (*dnf3*), $\Delta osh2/\Delta osh2$ (*osh2*), $\Delta osh3/\Delta osh3$ (*osh3*), $\Delta osh4/\Delta osh4$ (*osh4*), $\Delta osh7/\Delta osh7$ (*osh7*), and $\Delta drs2/\Delta drs2\Delta osh2/\Delta osh2$ (*drs2osh2*), $\Delta drs2/\Delta drs2\Delta osh3/\Delta osh3$ (*drs2osh3*), $\Delta drs2/\Delta drs2\Delta osh4/\Delta osh4$ (*drs2osh4*), $\Delta drs2/\Delta drs2\Delta osh7/\Delta osh7$ (*drs2osh7*), as well as intermediate *heterozygous strains* (**Table 7**) were generated by homologous recombination from the original strain BWP17 (Wilson et al., 1999) (see primers for KO mutants in **Table 5**). The mutant $\Delta drs2/\Delta drs2$ (*drs2*) was previously *generated* (Labbaoui et al., 2017).

- For the mutants *osh2*, *osh3*, *osh4*, the two copies of the genes were replaced sequentially by the auxotrophy markers *HIS1* and *URA3*. These markers were amplified by PCR from plasmids *pGEMHIS1*, *pGEMURA3* (Wilson et al.,

- 1999) using the primers CaOSH2mKO/CaOSH2pKO, CaOSH3mKO/CaOSH3pKO and CaOSH4mKO/CaOSH4pKO, respectively.
- For the mutant *osh7*, a copy of *OSH7* was replaced by *SAT1* (Basso et al., 2010; Schaub et al., 2006) and the other by *HIS1*, amplified from plasmids *pFa-SAT1* (Schaub et al., 2006) and *pGEM-HIS1*, using primer pairs, CaOsh7alphKOS1/CaOsh7alphKOS2 and CaOSH7A.mKO/CaOSH7A.pKO, respectively.
 - The *dnf1* mutant was generated by replacing the two alleles with *SAT1* and *HYGB* (which allows resistance to Hygromycin) amplified from *pFA-SAT1* and *pHBIS* (Lai et al., 2016) using primers CaDNF1.S1pKO/ CaDNF1.S2mKO. Similar deletion of *DNF1* in the mutant *dnf2* resulted in the *dnf1dnf2* mutant.
 - The *dnf2* mutant was generated by replacing the two alleles with *ARG4* and *HIS1* amplified from *pGEM-cdARG4* (Bijlani et al., 2019) and *pFA-HIS1* using primers CaDNF2mKO-pGEM/CaDNF2pKO-pGEM and CaDNF2.S1pKO/ CaDNF2KOS2, respectively.
 - The *dnf3* mutant was generated by replacing the two alleles with *SAT1* and *URA3* amplified from *pFA-SAT1* or *pFA-URA3* using primers CaDNF3.S1pKO/CaDNF3.S2mKO.

The double-mutants *drs2osh2*, *drs2osh3*, *drs2osh4*, *drs2osh7* and *drs2sac1* were generated from the mutant *drs2* (Labbaoui et al., 2017), in which *URA3* was previously replaced by *SAT1*: *SAT1* was amplified from *pFa-SAT1* using primers CaURAexchS1/CaURAexchS2. Then, the two copies of *OSH2*, *OSH3*, *OSH4*, *OSH7a/α* or *SAC1* were sequentially replaced by *URA3*, *ARG4* or *HYGB*, using *pGemURA3* and primers CaOSH4mKO/CaOSH4pKO or CaOSH7A.mKO/CaOSH7A.pKO, or *pFa-ARG4* and *pFa-HYGB* with primers CaOsh2KOS1/CaOsh2KOS2, CaOsh3KOS1/CaOsh3KOS2, CaOsh4KOS1/CaOsh4KOS2,

CaOsh7alphKOS1/CaOsh7alphKOS2 and CaSAC1.S1/CaSAC1.S2. A second clone *drs2osh4* was obtained from an independent clone of *drs2* (PY3361, **Table 7**) using *pFA-SAT1* and *pFa-HYGB* with primers CaOsh4KOS1 / CaOsh4KOS2.

To make strains prototroph the following plasmids were used (see ref in **Table 3**):

- ***pBN (ARG-URA)*** (Ghugtyal et al., 2015) digested with NotI for *RP10* insertion of *ARG4* and *URA3*.
- ***pDup5empty*** (Gerami-Nejad et al., 2013) digested with NgOMIV for *NEUT5L* insertion of *URA3*.
- ***pExpARG4*** (Bassilana et al., 2003a) digested with StuI for *RP10* insertion of *ARG4*.
- ***pGEM-HIS1*** digested with NruI to reintroduce *HIS1* in its own locus.

- **Strains expressing fluorescent reporters:**

For localization of Drs2, Dnf2 and Osh4, strains expressing Drs2-GFP γ , Dnf2-GFP γ and Osh4-GFP γ were generated by integration of GFP γ 3' of the *DRS2*, *DNF2* and *OSH4* ORFs, respectively. The fragment GFP γ -*HIS1* was amplified using primer pairs CaDRS2.P1(S1AFP)/CaDRS2.P2(S2), CaDNF2.S1AFP/CaDNF2.S2 and CaOsh4S1-AFP/CaOsh4S2, respectively, and plasmids ***pFA-GFP γ -HIS1***, ***pFA-GFP γ -URA3***, or ***pFA-GFP γ -ARG4*** (Zhang and Konopka, 2010) (**Table 3**). These cassettes were integrated by homologous recombination in the heterozygous strain for each of the genes (Δ /+*DRS2*, Δ /+*DNF2* and Δ /+*OSH4*).

For localization of Mlc1, Sec7, Cdc10, Sec3 and Abp1, the strains were generated by amplifying a DNA fragment encoding a fluorescent reporter (AFP, Any Fluorescent Protein),

integrated in 3' of the ORF of interest by homologous recombination. To do so, the following primers (see **Table 6**) and plasmids (from refs in **Table 3**) were used:

- Mlc1-AFP: mScarlet-*ARG4* was amplified using primers CaMlc1pFA/CaMlc1mFA and *pFA-mScarlet-ARG4* (Puerner, 2020).
- Sec7-AFP: x3mScarlet-*ARG4* was amplified using primers CaSec7xFP_S1/CaSec7xFP_S2 and *pFA-x3mScarlet-ARG4* (Puerner, 2020).
- Cdc10-AFP: mScarlet-*ARG4* was amplified using primers CaCdc10pFa_S1AFP/CaCdc10mFA_S2.
- Sec3-AFP: x3mScarlet-*ARG4* was amplified using primers CaSec3longxFP_S1/CaSec3longxFP_S2 and *pFA-x3mScarlet-ARG4*.
- Abp1-AFP: GFP γ -*ARG4* was amplified using primers CaAbp140xFP_S1/CaAbp140xFP_S2 and *pFA-GFP γ -ARG4*.

To generate the strains expressing GFP-Sec4, the plasmid *pGFP-Sec4-utr* (Li et al., 2007) linearized by HindIII, was integrated in 5' of the *SEC4* ORF by homologous recombination and transformants screened for the URA3 marker. *CDR1-GFP* was integrated in the *CDR1* locus after linearization of the plasmid pCDR1G4 (Ghugtyal et al., 2015) with XhoI and SacI by homologous recombination.

pExpArg-pACT1GFPRID and *pExpArg-pACT1CRIBGFP* (Corvest et al., 2013) *pExpArg-pADH1-PHFAPP1^(E50A,H54A)-GFP*, *pExpARG-pACT1-GFP-PHOSH2^(H340R)-PHOSH2^(H340R)-GFP* (Ghugtyal et al., 2015), *pExpARGpADH1-GFP-PHPLC δ 1-PHPLC δ 1-GFP* (Vernay et al., 2012), and *pExpARG-pACT1-GFP-LactC2* (Labbaoui et al., 2017) were linearized by StuI and integrated at the *RP10* locus. *pEApACT1mScarletD4H* was also integrated at the *RP10* locus after linearization with NcoI. The pDup plasmids (Gerami-Nejad et al., 2013) including

pDup3pTEF1-ss-mCherryPHR2-GPI (Labbaoui et al., 2017) and *pDUP3-pADHGFPLACTC2* were integrated at the NEUTL5 locus after digestion with NgoMIV.

- **GFP-nanobody (GNB) strains:**

The miR-GNB tag was amplified by PCR from pFA-CamiRFP670-CaGNB-URA3 (Puerner et al., 2021b), using primers CaMlc1pFA/CaMlc1mFA. This miR-CaGNB-URA3 cassette was introduced 3' of the *MLC1* ORF in strains expressing Drs2-GFP, Dnf2-GFP and Osh4-GFP to attempt to sequester the GFP fusion proteins at the SPK (Puerner et al., 2021b).

Verification of *C. albicans* mutants

The strains are verified by PCR and / or RT-PCR.

- **Genomic DNA extraction:**

→ To visualize DNA fragments shorter than 2kb: 5µl of cells grown overnight at 30°C in YEPD were added to 100µl of YEPD and centrifuged at 13000 rpm for 2min. Pellets were resuspended in 100µl of LitAct-SDS lysis solution (see solution **Table 2**). Prior to incubation at 70°C for 5min for cell lysis and two successive washes (in 300µl of ethanol 96% then 500µl of ethanol 70%). After centrifugation 15000g for 3min, pellets were dried at 50°C, 20-30min, then resuspended in 50µl of TE1X.

→ To visualize DNA fragments longer than 2kb: 2 ml of cells grown overnight were centrifuged for 2 min at 13000 rpm. The cells were broken by vortexing (4 min) in the presence of acid-washed beads (0.3 g, 425-600 µm, Sigma), TENS-TX buffer (200 µl) and a solution of PCIA (200 µl), before centrifugation at room temperature for 5 min at 13000 rpm. The aqueous phase, containing DNA and RNA, was transferred to a new tube and a second extraction with PCIA (200µl) was carried out. The aqueous phase was then mixed by inversion in the presence

of 1ml of ice-cold ethanol 99% and centrifuged for 10 min at 13000 rpm. Pellets were dried for 5-10 min at 50 ° C and resuspended in TE buffer (400 µl) with 3 µl of RNase (10 mM) and incubated 10 min at 37 ° C. The DNA was subsequently precipitated in ammonium acetate 4M (10 µl) and ethanol 99% (1 ml). After centrifugation (13000 rpm, 5min at ambient T °), pellets were dried at 50 ° C and resuspended in 20 µl of TE 1X buffer.

- **Verification of strains by PCR:**

The PCR reaction contains a pair of primers diluted to 1/200 (1.25µl of each primer [1 mM]), 5 µl of HF buffer (5X), 0.5µl of dNTP (10mM), 0.25µl of the phusion enzyme (1/10) and 1 µl of genomic DNA for a final volume of 25µl. The following PCR program was used:

1. 98°C 30 sec
2. 98°C 15 sec
3. 55°C 20 sec
4. 72°C 30 sec/1 kb 35 cycles
5. 72°C 10 min
6. 10°C pause

Transcriptional analysis: RT-PCR

For the RNA extraction, the protocol of the Pure Yeast RNA purification Master Kit (epicenter) was used.

- **Complementary DNA preparation (cDNA):**

To 4 µg of mRNA in 6 µl were added 1 µl of RNase out (40 U / µl, Invitrogen), 1 µl of DNase RQ1 (1U/µl, Promega) and 2 µl of MMLV-RT buffer (5X, Invitrogen). The mixture was incubated at 37 ° C 30 min, inactivated at 70 ° C 5 min, then put on ice 5 min. 2µl of random primers (random primers 100 ng / µl) were added to the mixture before incubation 10 min at 70 ° C then 5 min on ice, and addition of 4µl of MMLV-RT buffer (5X, Invitrogen), 1.25µl of

dNTP (10mM), 2 μ l of DTT (0.1 M), 1 μ l of RNase out and 6 μ l of H₂O ultrapure (Qbiogen). This mixture was incubated at 37 ° C 2 min before addition of 1 μ l of MMLV-RT (Moloney Murine Leukaemia Virus Reverse Transcriptase, 200 U / μ l, Invitrogen), and incubation at 37 ° C 50 min before inactivation of the reaction at 70 ° C 10 min. cDNA were kept at -20°C (Hope et al., 2010; Bassilana et al., 2005).

- **RT-PCR:**

The RT-PCR reaction was carried out similar to the PCR reaction described above, using the same PCR program with 29 or 32 amplification cycles. Specific primers for amplifying fragments less than ~ 100 bp were used (see **Table 10**. RT-PCR primers).

Microscopic analyses

- **Images of colonies:**

After 3-6 days of incubation at 30°C, the edge of colonies were imaged using an ImagingSource DMK 23UX174 sCMOS camera and a Leica MZ6 binocular magnifying glass at X20 magnification (Bassilana et al., 2003a).

- **Images of cells:**

→Time lapses and fluorescent images were obtained using a spinning disk confocal microscope (inverted IX81 Olympus microscope with a 100X objective and a numerical aperture 1.45) and an EMCCD camera (Andor technology, UK). Z-stacks (images of 0.4 micron sections) were acquired every 5 min, as described [Ghugtyal et al., 2015]. Maximum or sum intensity projections were generated from 21 or 16 z-sections with ImageJ software. Laser illuminations of 445 nm (Turquoise), 488 nm (GFP), 561 nm (mScarlet) and 670 nm (miRFP) were used. CRIBGFP distribution experiments were carried out as described [Corvest et al., 2013]. For the

time-lapses, cells were grown on minimum media (SC-Arg) with agar (0.5%) for budding growth or supplemented with 75% FCS for hyphal growth (Basilana et al., 2005).

→For filipin analyses, widefield images were acquired on an inverted ZEISS Axio Observer Z1 microscope with a 100X (1.3 NA) objective.

→Huygens professional software version 18.04 (Scientific-Volume Imaging) was used to deconvolve z-stack images of cells expressing PH-FAPP1^[E50A,H54A]-GFP. Bars are 5 microns.

→Filament lengths and diameters were measured from DIC images, using ImageJ software. Golgi cisternae were quantitated from deconvolved MAX projection images.

→Quantitation of PI(4)P distribution was performed on SUM projections, using the Matlab program HyphalPolarity (Ghugtyal et al., 2015). Quantitation of PS plasma membrane and internal mean signals was performed on central z-sections, also using the Matlab program HyphalPolarity. Unless indicated otherwise, error bars represent the standard error media.

Table 2. Media and buffers

Growth media	
Media	Composition for 1L
YEPD + Uri	2.2% bacto peptone, 1.1% yeast extract, 2% Agar, 2% glucose, 0.1% Uridine
LM2	8g Yeast nitrogen base, 55mg adenine, 55mg tyrosine
TYE	5g NaCl, 16g bactotryptone, 10g yeast extract
TYE + Ampicillin	5g NaCl, 16g bactotryptone, 10g yeast extract, 100 µg/ml
SPIDER	10g nutrient (1%), 10g Mannitol (1%), 2g K ₂ HPO ₄ (0.2%), 15g Agar 1.5%
FCS	50% YEPD + 50% FCS

Selective media	
Media	Composition for 1L
-Ura	LM2, glucose 2%, 1/100 volume of -leu+leu drop out
-His-Ura	LM2, glucose 2%, 1/100 volume -His drop out
-His+Ura	LM2, glucose 20%, uridine(80mg), 1/100 volume -His dropout
-His-Ura-Arg	LM2 + 20% glucose + 1/100 volume of -His-Arg drop out.
YEPD + NAT	2.2% bacto peptone, 1.1% yeast extract, 2% Agar, 2% glucose, 0.1% Uridine, 200µg/ml NAT
YEPD + HYG	2.2% bacto peptone, 1.1% yeast extract, 2% Hagar, 2% glucose, 0.1% Uridine, 1mg/ml hygromicin

Buffers and solutions	
TENS-TX	10mM TrisHCl pH8.0, 1mM EDTA pH8.0, 100mM NaCl, 1%(w/v) SDS, 2% (v/v) Triton X100
PCIA (PhenolChloroform IsoamylAlcohol)	25ml Phenol, 24ml Chloroform, 1ml Isoamyl Alcohol
TE 1X (Tris-EDTA)	10mM Tris HCl pH8.0, 1mM EDTA pH8.0
Sorbitol	1M
PBS	Phosphate Buffer Saline 1M
LitAct-SDS	Lithium acetate 200mM, 1%SDS

Table 3. Plasmids

Name	Reference
pBN(ARG-URA)	(Ghugtyal et al., 2015)
pCAU98	(Nakayama et al., 2000)
pCDR1G4	(Ghugtyal et al., 2015)
pDUP3empty	(Gerami-Nejad et al., 2013)
pDup3-pADH1-DNF2	This study
<i>pDup3-pADH1-DNF2^{N550S}</i>	This study
pDup3-pADH1-DRS2	This study
pDUP3-pADH1-GFP-LACTC2	This study
pDup3-pADH1-OSH4	This study
<i>pDup3-pDNF2-CryLinker-GFP-Cdc42-TEFt</i>	This study
pDup3-pDNF2-DNF2	This study
<i>pDup3-pDNF2-DNF2^{N550S}</i>	This study
pDup3-pDRS2-DRS2	This study
pDup3-pDRS2-DRS2 ^{F511Y}	This study
<i>pDup3-pDRS2-DRS2^{QQ}</i>	This study
pDUP3-pTEF1-ss-mCherry-PHR2-GPI	(Silva et al., 2019)
<i>pDup3-pTEF-CryLinker-GFP-Cdc42-tTEF</i>	(Silva et al., 2019)
pDup5empty	(Gerami-Nejad et al., 2013)
<i>pEA-pDRS2-DRS2^{QQ}</i>	This study
pExpARG4empty	(Bassilana et al., 2003a)
pExpARG4-GFP γ -ctRAC1	(Puerner et al., 2021b)
pExpARG4-pACT1-CRIB-GFP	(Corvest et al., 2013)

pExpARG4-pACT1-GFP-lactC2	(Labbaoui et al., 2017)
pExpARG4-pACT1-GFP-PH _{OSH2(H340R)} -PH _{OSH2(H340R)} -GFP	(Ghugtyal et al., 2015)
pExpARG4-pACT1-GFP-RID	(Corvest et al., 2013)
pExpARG4-pACT1-mScarlet-D4H	Provided by H. Labbaoui
pExpARG4-pADH1-DRS2	(Labbaoui et al., 2017)
pExpARG4-pADH1-DRS2 ^{F511Y}	This study
pExpARG4-pADH1-PH _{FAPP1(E50A,H54A)} -GFP	(Ghugtyal et al., 2015)
pExpARG4-pARL3-ARL3	(Labbaoui et al., 2017)
pExpARG4-pDRS2-DRS2	(Labbaoui et al., 2017)
pExpARG4-pDRS2-DRS2 ^{F511Y}	This study
pExpARG4-pOSH4-OSH4	This study
pExpARGpADH1-GFP-PHPLC δ 1-PHPLC δ 1-GFP	(Vernay et al., 2012)
pFA-CaARG4	(Schaub et al., 2006)
pFA-CaHIS1	(Schaub et al., 2006)
pFA-GFP γ -ARG4	(Zhang and Konopka, 2010)
pFA-GFP γ -HIS1	(Zhang and Konopka, 2010)
pFA-GFP γ -URA3	(Zhang and Konopka, 2010)
pFA-HIS1	(Schaub et al., 2006)
pHB1S	(Lai et al., 2016)
pFA-miRFP670-GNB-URA3 (GNB-A3)	(Puerner et al., 2021b)
pFA-mScarlet-ARG4	(Puerner, 2020)
pFA-mScarlet-URA3	(Puerner et al., 2021b)
pFA-x3mScarlet-ARG4	(Puerner, 2020)
pFA-SAT	(Schaub et al., 2006)

pFA-URA3	(Schaub et al., 2006)
pGem-CdARG4	(Bijlani et al., 2019)
pGEM-HIS1	(Wilson et al., 1999)
pGEM-URA3	(Wilson et al., 1999)
pGFP-SEC4-utr	(Li et al., 2007)

Table 4. Primers for plasmid construction

Name	Sequence
CaDNF2m2 204	GAATAATACATCCCCACATCAG
CaDNF2m5 151_SbfI	ATCCTGCAGGTTAATTCATTGAAGATACTCTTTTTTG
CaDnf2m51 51MluI	ATACGCGTTTAATTCATTGAAGATACTCTTTTTTG
CaDnf2mup 21AscI	TATAGGCGCGCCAAGAGTGTGGATAGCAATTCG
CaDNF2N5 50Sm1968	GACAAACAATAAAAATAAAATTTAACAAGACATAATAAGACAATTC TCGAGACATTCTTGATTGTTTAGTTGGCGTTACCCCAGC
CaDNF2N5 50Sp1885	GCTGGGGTAACGCCAACTAAACAATCAAGAATGTCTCGAGAATTG TCTTATTATGTCTTGTTAAATTTTATTTTATTGTTTGTC
CaDNF2p1 724	CCAATAGAATGAATAACTCACAATC
CaDnf2p1A scI	GGCGCGCCATGACTAAAAATAAGCACAATTTACGCG
CaDnf2pup 1000XmaI	TACCCGGGCTGGTGTAGGGTATAGCCTAC
CaDrs2F51 1Ym	ATATTTGATCAATTCAACCGTGACATACAATGAAATGGGTACCAA TTGGAAAATAAAATCC
CaDrs2F51 1Yp	GGATTTTATTTTCCAATTTGGTACCCATTTTCATTGTATGTCACGGTT GAATTGATCAAATAT
CaDrs2m17 32	CATTTCTGGTTAATGTACCGG
CaDrs2m49 64NotI	TATAGCGGCCGCGgagttggttaataacaaaatcag
CaDrs2m94 0	GGACAACATCTCCCCTTG
CaDRS2m MluI	ATACGCGTTTACTTACTTTCTGATAATTCCCC
CaDrs2p13 36	CGTACTGATGTGGAAAGAATC
CaDrs2p44 6	CGTCACGAGATTTTGATATAACCC
CaDRS2pA scI	GGCGCGCCATGTCCAATTATAATCGGACAG
CaDrs2pup 1000SalI	ATGTCGACctttaaataatagccgaattccccg
CaDrs2pup 1000SpeI	TAACTAGTCTTTTAATATAGCCGAATTCCCCG
CaDrs2QQ_ m755	CTATTTGTGGGGGAAACATGAGGTACTGCTCCAATAATTGATGTAA CAAGGAAAAATAAATTGGC
CaDrs2QQ_ p691	GCCAATTTATTTTTCCTTGTTACATCAATTATTGGAGCAGTACCTCA TGTTTCCCCCACAAATAG
CaOSH4m1 293MluI	ATACGCGTTTAAAAGACTATTTCTTTTTCATCTTCC

CaOSH4m3 268-NotI	TATAGCGGCCGCGGTTAGTAACGCTCTTAGAACGTTGG
CaOSH4p1 AscI	GGCGCGCCATGTCAAACCTCAAATCCAGTTCTG
CaOSH4pu p1000SalI	ATGTTCGACAAAACAACACAAGAAAGAGCTGCTGCTG
D4H .P1 D4HpAscI BamHI	ACGGCGCGCCGACTAGTGGATCCAAGGGAAAAATAAACTTAGATC ATAGTGGAGCC
D4H.P2 D4HmMluI	GATACGCGTTAATTGTAAGTAATACTAGATCCAGGG
LactC2mMl uI	ATACGCGTCGTACGCGTTTAAACAACCC
yeGFP3pAs cI	GGCGCGCCATGTCTAAAGGTGAAGAATTATTCAC

Table 5. Primers for KO mutants

Name	Sequence
CaDNF2pKO	cacctaatttactttatccaatttcgaattgctatccacactttatgactaaaaataagcacaatttca cgcTGTGGAATTGTGAGCGGATA
CaDNF2mKO	gtatgtgtgtttgtgtctataatgtttctttatgttatgcaaatgaaattgctgtaattcattgaagat actcTTTCCCAGTCACGACGTT
CaDNF2mTETOKin	TggtgatcactagggtcgtcattgttattaaCtccatcactactattatttagcgtgaaattgtgcttat ttttagtcacTAGTTTTCTGAGATAAAGCTG
CaDNF2pTETOKin	Gtctagtgggtgccatattttctattttttttttttttttttttttgcacgttgggtataattttcaacaatc aaatacAGGAATTGATTTGGATGG
CaOSH2mKO	caatcaacaattaaaacagtcataaatatgtctcccgtgttcgccaatcttgtgctttcttctagge caatacTTTCCCAGTCACGACGTT
CaOSH2pKO	ccataataaactgataaaacactaacaactttagaataaacagctaaaatcatgaatgattcacc ccaactaagtgcTGTGGAATTGTGAGCGGATA
CaOSH3mKO	ggattctatgatctaaataatataacgtctaatagatatgaaaaagacaaagaaatagtaaaattac cacaatttaacTTTCCCAGTCACGACGTT
CaOSH3pKO	cccactcaatcccattattttttcccttgacagttgaactttccataccaacttgaaatggaact ttagaagTGTGGAATTGTGAGCGGATA
CaOSH4mKO	gatgtactactattataaacattattttacgaaattgaaaaacactactctaaattcatttaaagactat ttcTTTCCCAGTCACGACGTT
CaOSH4pKO	ctatattttaaaataacacatcgtcttcaagccaacagtatattttttgtcatgtcaaacccaatcca ggtctgaagTGTGGAATTGTGAGCGGATA

CaOSH7A.mKO	cgatttctaactctaaactaaagataaatatataaagaagtacattaaattgcaatataatcaaaaaacga attaagtttcttcTTTCCCAGTCACGACGTT
CaOSH7A.pKO	cccttcattaaatctccctgagatttggtgtttttatctgtattcagtacgaagtcaggccaccatgg gtttaaTGTGGAATTGTGAGCGGATA
CaDNF2mKO-pGEM	gtatgtgtgtttgtgtctataatgtttctttatgttatgcaaatgaaaattgctgtaattcattgaagat actctttttgatttctgtagcttattctagatgctcTTTCCCAGTCACGACGTT
CaDNF2pKO-pGEM	cacctaaactactttatccaattcgaattgctatccacactcttatgactaaaaataagcacaatttca cgctaataatagtagtgatggagTGTGGAATTGTGAGCGGATA
CaOsh2KOS1	ccataataaactgataaaacactaacaactttagaataaacagctaaaatcatgaatgattcacc ccaactaagtgcGAAGCTTCGTACGCTGCAGGTC
CaOsh2KOS2	caatcaacaattaaacagctctaaaatagctctcccgttcccaaatctgtgctttctctagge caatacTCTGATATCATCGATGAATTCGAG
CaOsh3KOS1	cccactcaatcccattatttcttcccttgacagttgaacttcccataccaacttgaaataggaaact ttagaagGAAGCTTCGTACGCTGCAGGTC
CaOsh3KOS2	ggattctatgatctaaataatataacgtctaatagatgaaaaagacaaagaaatagtaaattac cacaatttaacTCTGATATCATCGATGAATTCGAG
CaOsh4KOS1	ctatattttaaataaacacatcgttctcaagccaacagtatattttttgcatgtcaaaactccaaatcca gttctgaagGAAGCTTCGTACGCTGCAGGTC
CaOsh4KOS2	gatgtactactattataaacattattttacgaaattgaaaaacactactctaaattcatttaaagactat ttcTCTGATATCATCGATGAATTCGAG
CaOsh7alphKOS1	ccagcgaacatgcaacttttcttctgttgagggttcaggtaatcagatgggattaacagctaaattag ataagGAAGCTTCGTACGCTGCAGGTC
CaOsh7alphKOS2	taaattagacaactactgttcttaattcaaaatctattaatgaccgtatattaaaagccaacaa ttaattacTCTGATATCATCGATGAATTCGAG
CaDNF2.S1pKO	CAC CTA ATT CTA CTT TAT CCA ATT TCG AAT TGC TAT CCA CAC TCT TAT GAC TAA AAA TAA GCA CAA TTT CAC GCG AAG CTT CGT ACG CTG CAG GTC
CaDNF2KOS2	ctgtatgtgtgtttgtgtctataatgtttctttatgttatgcaaatgaaaattgctgtaattcattgaa gatactcTCTGATATCATCGATGAATTCGAG
CaDNF1.S1pKO	CAAGTGACAACCTCTCCAGTTAGCTCCTATTATTTGCATCGA CCAAATCTAGAAGATCTTACTAGAACATCGAAAGTTGGAG TGACCATTTGCTGAAGCTTCGTACGCTGCAGGTC
CaDNF1.S2mKO	CGAAAAATGTAAAACCGAAATCAAATGCAATGATACAATA AACTGAAACCCAATTACCACATAAAGTAGGTTAAGGATTC AAAGCTACACTATTCCTCTGATATCATCGATGAATTCGAG

CaDNF3.S1pKO	CTACAGATTCAACTTTATAGAATCCTACATTGAGTCACCTG TCTCATCATTTGGTCATTAATTTACAACACTACAGTGAATCAT ACAATTAGATTTGGAAGCTTCGTACGCTGCAGGTC
CaDNF3.S2mKO	GCTCGGGTGAATTGAGACAATTTTGATGTATCTTGTATATT TGTATAAATACTTAGATGTACATTTCTTTTGGTTTTGGAAA CTCAATAGACACCTCTGATATCATCGATGAATTTCGAG
CaURAexchS2	tgtggaattgtgagcggataacaatttcacacaggaacagctatgacatgattacgccaagctc ggTCTGATATCATCGATGAATTTCGAG
CaURAexchS1	tttcccagtcacgacgttgaaaacgacggccagtgaattgtaatacgaactactataggcgaatt ggGAAGCTTCGTACGCTGCAGGTC
CaSAC1.S1	AATATAAACACTATTTTTTCCACTTTCTTTAATCTAACCTTA TACGCAACTATACAATTATATAACAGAAAATGGTGTTAGA AGCTTCGTACGCTGCAGGTC
CaSAC1.S2	ATCTATTATATAAAAATAAGCAGCTACAACCTAAAGACAAC TTCTAAAAAACAACCCCCACAGCTAATCAATTCTT TCTGATATCATCGATGAATTTCGAG

Table 6. Primers for KI strains

CaCdc10pFa_S1AFP	caatcaaccaagatttgaagaacacctctggtgtgccaaatgctcctatgttccaatcaactacaggtc tgctgctgctagaGGTGCTGGCGCAGGTGCTTC
CaCdc10mFA_S2	CGCGTTTTGCTTTTCAACAAACACACAAAAGAAGAGGAATAC AAAAAAGTAAAATCACATTATATCAATAACAAACctgatcatcgat gaattcgag
CaMlc1pFA	gatgagttataaaaggggtcaatgtaactctgatggaatgtggattatgtgaattgtcaaatcaattt agaccaaGGTGCTGGCGCAGGTGCTTC
CaMlc1mFA	CGAACAAGACTATACAATAACTATAATTTGTAAAACCTTGTAGT ATATATATTTCAATGGTTAATTGTAAATTTCTTTTATtctgatcat cgatgaattcgag
CaAbp140xFP_S1	GTGAAAAGGGTCCTTTTAAAAAGGAAAAAATTGCCACGGATA GAAGATTATTAGTCAATAGAAAGAAACAATTGAAAATGTACC GTAATTGGCTACAGGCTGTATTTAGAGGAaggctgctggcaggtgcttc
CaAbp140xFP_S2	GTCTCATCCTTATATTCAAGGTATTGATGTAACCTTCATTAATG AATCAACTGATACGAGAAATTTGGCAATTATTCAAACATTTAG ATAATTTTTTATATATTACTCTAActgatcatcgatgaattcgag
CaDRS2.P1(S1AFP)	caagttgaaggtcaagatcaagataaaattgtagattatgataactactaaaaaagaggagttttgg ggaattatcagaagtaagGGTGCTGGCGCAGGTGCTTC

CaDRS2.P2(S2)	gggagtgagatagttgtatatcaaacagttctatagctttaataataaaaaaaaaaacattcattgattgcat taataactactcactctatttaTCTGATATCATCGATGAATTCGAG
caSec3longxFP_S1	GGAAATGATATAGGGTCTGCTTTGAATGAAGTGGATAATATG ACTCAGATTTTCCAGAAGATGGAGGTGAGATTGAACTTGTA CGAAATGAGCTACAAAGTTCTGCTACTGCTgggtgctggcgcaggtgcttc
caSec3longxFP_S2	GTTGTATATGTAGTAGAGAAAGCAGTACTAAAAACAGTATTA ATTAATTAAGCTATACTATACAAACCTTAATAATTACTATACT CTTGATAAAAAGACTTGCTCCATTtctgatatcatcgatgaattcgag
caSec7xFP_S1	GGCAATGAAAGCTTTTTTAACTAGAGTGGGTGAAGAGTTTGTT AGTATTTCTGACAACAATAAGGAAAGAAGGgggtgctggcgcaggtgctt c
caSec7xFP_S2	GTAATGATACTTACAGTTGTTTTAACATAATTGATAAATT ATTATTATACATTATTCCTACTTTCAtctgatatcatcgatgaattcgag
Ca.Dnf2.S1AFP	GGTAGCTACAGAAGAAATTCCATTAGAAGATTTTGATGATGA ACAAAAAAGAGCATCTAGAATAAGCTACGAAAATCAAAAAA GAGTATCTTCAATGAATGGTGCTGGCGCAGGTGCTTC
CaDNF2.S2	CCTCTCATTCTTTATATAAATATGCTTGAAATTCTTGTATGTGT GTTTGTTGTCTATAATGTTTTCTTTTATGTTATGCAAATGAAAA TTGCTGTTATCTGATATCATCGATGAATTCGAG
CaOsh4S1-AFP	GGAACCTTGAAAGACTCAAAGTATGACCATGGTGAAGCCAAG CATTGGAGAGTTAACTTGAAAAAGTTGGAAGATGAAAAAGAA ATAGTCTTTGGTGCTGGCGCAGGTGCTTC
CaOsh4S2	GTAATCCTTCTATAGTAAACTGTTTATATTTAAATGATGTACT ACTATTATAAACATTATTTTACGAAATTGAAAAAACCTACTCT AAATTCATTTATCTGATATCATCGATGAATTCGAG

Table 7. KO mutant and complemented strains.

STRAIN	RELEVANT GENOTYPE	REFERENCE
BWP17	<i>ura3Δ::λimm434/ura3Δ::λimm434</i> <i>his1Δ::hisG/his1Δ::his arg4::hisG/arg4Δ::hisG</i>	(Wilson et al., 2000)
PY3303-3304	Same as BWP17 with <i>DRS2Δ::URA3/DRS2</i>	(Labbaoui et al., 2017)
PY3310	Same as PY3303 with <i>DRS2Δ::URA3 / DRS2Δ::HIS1</i>	(Labbaoui et al., 2017)
PY3361	Same as PY3304 with <i>DRS2Δ::URA3/ DRS2Δ::HIS1</i>	Provided by H. Labbaoui
PY3375	Same as PY3310 with <i>RP10::ARG4</i>	(Labbaoui et al., 2017)
PY3377	Same as PY3361 with <i>RP10::ARG4</i>	Provided by H. Labbaoui
PY3869	Same as BWP17 with <i>OSH2Δ::HIS1/OSH2</i>	This study
PY3882-84	Same as BWP17 with <i>OSH4Δ::URA3/OSH4</i>	This study
PY3908-09	Same as BWP17 with <i>OSH3Δ::URA3/OSH3</i>	This study
PY3921	Same as PY3882 with <i>OSH4Δ::URA3/ OSH4Δ::HIS1</i>	This study
PY3945	Same as PY3908 with <i>OSH3Δ::HIS1/ OSH3Δ::URA3</i>	This study
PY3974-76	Same as PY3921 with <i>RP10::ARG4</i>	This study
PY3977-79	Same as PY3945 with <i>RP10::ARG4</i>	This study
PY3995-96	Same as PY3869 with <i>OSH2Δ::HIS1/ OSH2Δ::URA3</i>	This study
PY4002-04	Same as PY3995 with <i>RP10::ARG4</i>	This study
PY4168	Same as BWP17 with <i>OBPAΔ::SAT1/OBPalpha</i>	This study
PY4671-72	Same as PY3310 with <i>DRS2Δ::HIS1/ DRS2Δ::SAT1</i>	This study

PY4861	ura3Δ::λimm434/ura3Δ::λimm434 his1::hisG/ HIS1::his1::hisG arg4::hisG/URA3::ARG4::arg4::hisG	(Basilana et al., 2003a)
PY4889-91	Same as BWP17 with <i>DNF1Δ::SAT1/DNF1</i>	This study
PY4946	Same as PY4889 with <i>DNF1Δ::SAT1/ DNF1Δ::HYGB</i>	This study
PY5003-04	Same as PY3375 with <i>NEUTL5::SAT1- pDup3pADHDNF2</i>	This study
PY5005	Same as PY4861 with <i>NEUTL5::SAT1- pDup3pADHDNF2</i>	This study
PY5042-41,43	Same as PY3310 with <i>RP10::ARG4- pExpARGpDRS2DRS2</i>	This study
PY5045-44,46	Same as PY3310 with <i>RP10::ARG4- pExpARGpDRS2DRS2^{F511Y}</i>	This study
PY5204-07	Same as PY4671 with <i>OSH4Δ::URA3/OSH4</i>	This study
PY5231	Same as PY4671 with <i>OSH2Δ::URA3/OSH2</i>	This study
PY5232-5233	Same as PY4671 with <i>OSH3Δ::URA3/OSH3</i>	This study
PY5242	Same as 4671 with <i>OSH7alphaΔ::HYGB/OSH7A</i>	This study
PY5246	Same as PY4168 with <i>OSH7Δ::SAT1/ OSH7alpha::HIS1</i>	This study
PY5256-58	Same as 5246 with <i>RP10::URA3-ARG4</i>	This study
PY5296	Same as 5204 with <i>OSH4Δ::URA3/OSH4::HYGB</i>	This study
PY5297-5300	Same as 5242 with <i>OSH7alphaΔ::HYGB/OSH7A::URA3</i>	This study
PY5539-41	Same as PY5296 with <i>RP10::ARG4</i>	This study
PY5674-76, PY6401	Same as PY5296 with <i>RP10::ARG4- pExpARGpOSH4OSH4</i>	This study
PY5677-79	Same as BWP17 with <i>DNF2Δ::HIS1/DNF2</i>	This study
PY5680-82	Same as PY3361 with <i>OSH4Δ::HYGB/OSH4</i>	This study
PY5683-84	Same as BWP17 with <i>DNF3Δ::URA3/DNF3</i>	This study

PY5691-92	Same as PY5680 with <i>OSH4Δ::HYGB/ OSH4Δ::SAT1</i>	This study
PY5724-25	Same as PY5691 with <i>RP10::ARG4</i>	This study
PY5738-37, 39	Same as PY5691 with <i>RP10::ARG4-pExpARGpOSH4OSH4</i>	This study
PY5741-43	Same as PY5683 with <i>DNF3Δ::URA3/DNF3::SAT1</i>	This study
PY5801-03	Same as PY5741 with <i>RP10::ARG4 / HIS1::his1::hisG</i>	This study
PY5804-06	Same as PY5677 with <i>DNF2Δ::HIS1/ DNF2::ARG4</i>	This study
PY5814-15	Same as PY5804 with <i>NEUT5L::URA3</i>	This study
PY5816-17	Same as PY5806 with <i>NEUT5L::URA3</i>	This study
PY5818-19	Same as PY5804 with <i>DNF1Δ::URA3/DNF1</i>	This study
PY5821-20	Same as PY5806 with <i>DNF1Δ::URA3/DNF1</i>	This study
PY5871-72	Same as PY5821 with <i>DNF1Δ::URA3/ DNF1::HYGB</i>	This study
PY5919-21	Same as PY5814 with <i>NEUT5L::SAT1-pADHDNF2</i>	This study
PY5922-24	Same as PY5871 with <i>NEUT5L:: SAT1-pADHDNF2</i>	This study
PY6015-17	Same as PY5871 with <i>NEUTL5::SAT1-pDup3pDNF2DNF2</i>	This study
PY6235	Same as 4946 with <i>HIS1::his1::hisG/ URA3::ARG4::arg4::hisG</i>	This study
PY6260-61	Same as PY3310 with <i>RP10::ARG4-pExpARGpDrs2Drs2²⁰⁰</i>	This study
PY6400	Same as PY5818 with <i>DNF1Δ::URA3/ DNF1::HYGB</i>	This study
PY6408-09	Same as PY5231 with <i>OSH2Δ::URA3 / OSH2::HYGB</i>	This study
PY6431	Same as PY5233 with <i>OSH3Δ::URA3 / OSH3::HYGB</i>	This study

PY6428-27	Same as BWP17 with <i>SAC1::HYGB /SAC1</i>	This study
PY6430-29	Same as PY4671 with <i>SAC1::HYGB /SAC1</i>	This study
PY6432-35	Same as PY6430 with <i>SAC1Δ::HYGB / SAC1::ARG4</i>	This study
PY6436-38	Same as PY6428 with <i>SAC1Δ::HYGB / SAC1::ARG4</i>	This study

Table 8. Strains with KI and protein reporters:

PY2263	Same as BWP17 with <i>RP10::ARG4-pExpArgACT1pCRIB-GFP</i>	(Bassilana et al., 2005)
PY3785	Same as BWP17 with <i>ABP1/ABP1::ABP1-GFPγ- ARG4</i>	Provided by H. Labbaoui
PY4665-64	Same as PY3303 with <i>DRS2Δ::URA3/DRS2::DRS2-GFPγ-HIS1</i>	This study
PY4676-75	Same as PY4671 with <i>SEC4/SEC4::GFP-SEC4-URA3</i>	This study
PY4677	Same as BWP17 with <i>SEC4/SEC4::GFP-SEC4-URA3</i>	This study
PY4928-31,51,52	Same as PY4665 with <i>MLC1/MLC1::MLC1-mScarlet-ARG4</i>	This study
PY4972, PY5792, 76-77, 93	Same as PY3310 with <i>RP10::ARG4-pExpArgACT1pCRIB-GFP</i>	This study
PY5063-65	Same as PY4676 with <i>RP10::ARG4-pExpARGpDRS2DRS2</i>	This study
PY5097-100	Same as PY3310 with <i>ABP1/ABP1::ABP1-GFPγ-ARG4</i>	This study
PY5218-22	Same as PY4676 with <i>MLC1/MLC1::MLC1mScarlet-ARG4</i>	This study
PY5349,47-50	Same as PY4677 with <i>MLC1/MLC1::MLC1mScarlet-ARG4</i>	This study
PY5385	Same as BWP17 with <i>MLC1/MLC1:: MLC1-miRFP670GNB-URA3</i>	Puerner
PY5507-06,08	Same as BWP17 with <i>CDR1/CDR1::CDR1-GFP-SAT1</i>	This study

PY5524-26	Same as PY3310 with <i>CDR1/CDR1::CDR1-GFP-SAT1</i>	This study
PY5569-70	Same as BWP17 with <i>CDC10/CDC10::CDC10-mScarlet-ARG4</i>	This study
PY5571-73, PY5137-41,	Same as PY3310 with <i>CDC10/CDC10::CDC10-mScarlet-ARG4</i>	This study
PY5613-14	Same as PY5569 with <i>NEUT5L::SAT1-pDup3ADH1pmiRFP670ctRac1</i>	This study
PY5615-16	Same as PY5571 with <i>NEUT5L::SAT1-pDup3ADH1pmiRFP670ctRac1</i>	This study
PY5746-44,45	Same as PY5677 with <i>DNF2Δ::HIS1/DNF2::DNF2-GFPγ-URA3</i>	This study
PY5865-63,64	Same as PY5385 with <i>DRS2 /DRS2::DRS2-GFPγ-HIS1</i>	This study
PY5875, 73-76	Same as PY3882 with <i>OSH4Δ::URA3/OSH4::OSH4-GFPγ-ARG4</i>	
PY5877-78	Same as PY5385 with <i>DNF2/ DNF2::DNF2-GFPγ-ARG4</i>	This study
PY5879-81	Same as PY5385 with <i>OSH4/OSH4::OSH4-GFPγ-ARG4</i>	This study
PY5885-87	Same as PY5865 with <i>DRS2::cdARG4/DRS2::DRS2-GFPγ-HIS1</i>	This study
PY5889-88,90	Same as PY5680 with <i>OSH4Δ::HYGB/OSH4::OSH4-GFPγ-ARG4</i>	This study
PY5915-13,14	Same as PY5746 with <i>MLC1/MLC1::MLC1-mScarlet-ARG3</i>	This study
PY5925-27	Same as PY4665 with <i>DRS2Δ::ARG4/DRS2::DRS2-GFPγ-HIS1</i>	This study
PY5931-32	Same as PY5879 with <i>OSH4Δ::HYGB/OSH4::OSH4-GFPγ-ARG4</i>	This study
PY6239-40	Same as PY5746 with <i>NEUT5L::SAT1-pDup3ADHpmScarletCtRac1ADH1t</i>	This study
PY6241-42	Same as PY4665 with <i>NEUT5L::SAT1-pDup3ADHpmScarletCtRac1ADH1t</i>	This study

PY6393-94	Same as PY4861 with <i>RP10::SAT1-CDR1pCDR1GFP</i>	This study
PY6395	Same as PY3375 with <i>RP10::SAT1-CDR1pCDR1GFP</i>	This study

Table 9. Strains with lipid reporters:

PY1206= PY5566	Same as BWP17 with <i>RP10::ARG4-pADHGFP-PH^{PLCδ1}-PH^{PLCδ1}-GFP</i>	(Vernay et al., 2012)
PY2045	Same as BWP17 with <i>RP10::ARG4-pADHI-PH^{FAPP1[E50A,H54A]}-GFP</i>	Provided by Ghugtyal
PY3239	Same as BWP17 with <i>RP10::ARG4-pACT1GFPyeLactC2</i>	(Labbaoui et al., 2017)
PY3362	Same as PY3310 with <i>RP10::ARG4-pACT1GFPyeLactC2</i>	(Labbaoui et al., 2017)
PY3873	Same as PY3310 with <i>RP10::ARG4-pADHI-PH^{FAPP1[E50A,H54A]}-GFP</i>	This study
PY4050	Same as PY3310 with <i>RP10::ARG4-pADHGFP-PH^{PLCδ1}-PH^{PLCδ1}-GFP</i>	This study (Labbaoui)
PY5134-36	Same as PY3310 with <i>NEUT5L::SAT1-pDup3pADHGFPyeLactC2</i>	This study
PY5151-53	Same as PY5134 with <i>RP10::ARG4-pExpARGpDRS2DRS2</i>	This study
PY5254-55	Same as PY5246 with <i>RP10::ARG4-pACT1GFPyeLactC2</i>	This study
PY5336-34,35,37	Same as PY3921 with <i>RP10::ARG4pACT1GFPyeLactC2</i>	This study
PY5364-37,65	Same as PY5296 with <i>RP10::ARG4pACT1GFPyeLactC2</i>	This study
PY5373	Same as PY5297 with <i>RP10::ARG4pACT1GFPyeLactC2</i>	This study
PY5156, 54,55 5470-73,	Same as PY5134 with <i>RP10::ARG4-pExpARGpDRS2DRS2^{F511Y}</i>	This study
PY5568, 5551	Same as PY3310 with <i>RP10::ARG4-pACT1-GFP-(PH^{OSH2[H340R]})₂-GFP</i>	This study

PY5619-21	Same as BWP17 with <i>RP10::ARG4-pACT1-GFP-(PH^{OSH2[H340R]})₂-GFP</i>	This study
PY5626-27,29	Same as PY3921 with <i>RP10::ARG4-pACT1-GFP-(PH^{OSH2[H340R]})₂-GFP</i>	This study
PY5630, 28, 31-32	Same as PY5296 with <i>RP10::ARG4-pACT1-GFP-(PH^{OSH2[H340R]})₂-GFP</i>	This study
PY6037, PY6073-75	Same as BWP17 with <i>RP10::ARG4-pExpARGpACTmScarletD4H</i>	This study
PY6076-78	Same as PY3921 with <i>RP10::ARG4-pExpARGpACTmScarletD4H</i>	This study
PY6083-82,84	Same as PY3310 with <i>RP10::ARG4-pExpARGpACTmScarletD4H</i>	This study
PY6213-15	Same as PY6083 with <i>NEUT5L::SAT1-pDup3pAct1turquoisectRac1</i>	This study
PY6218-16,17	Same as PY6083 with <i>NEUT5L::SAT1-pDup3pDRS2DRS2</i>	This study
PY6237-36	Same as PY6037 with <i>NEUT5L::SAT1-pDup3pAct1turquoisectRac1</i>	This study
PY6238	Same as PY6083 with <i>OSH4Δ::HYGB/OSH4</i>	This study
PY6284-83,85	Same as PY5134 with <i>RP10::ARG4-pExpARGpDRS2DRS2^{QQ}</i>	This study
PY6286	Same as PY6238 with <i>OSH4Δ::HYGB/OSH4::SAT1</i>	This study
PY6407-05,06	Same as PY5568 with <i>NEUT5L::SAT1-pDup3pDRS2DRS2</i>	This study

Table 10. RT-PCR primers

ACT1mTM	ACATTTGTGGTGAACAATGG
ACT1pTM	ATGTTCCCAGGTATTGCTGA
CaDRS2p3485TM	CGGCATTAGTGGTTACCATGT
CaDRS2m3547TM	GCAGGATACCAACCTAACCATAA

CaDnf2p2280	TGACAAGACCGGGACATTA
CaDnf2m2386	TCCGTAACCCAGCCAAT
CaDnf1p1794	GCACAATCAACGGGAAGTCATAC
CaDnf1m1867	AATGCCTGCACGTTTATCCAA
CaOsh4p618_TM	TTTGATTACTGCTGCTCCTT
CaOsh4m687_TM	AATGTGACCACTGGATGCTT
CaDnf3p2205_TM	AAGCATCAATGGCAGGTCATC
CaDnf3m2309_TM	GCTGCCGTGCTTGTTCCTG
CaUME6p401_TM	TGGCTCCACTTACAAATCATAGTGA
CaUME6m490_TM	GCTTTACCAATCCTAGTCCCAACTC
CaOBPAp54_TM	TGAAGCAGCTGTCAAATCTAATGTG
CaOBPAm138_TM	CTGTCCCTCGTTATCCATTTTCATC
CaOBPalphap545_TM	GTAACTCGTCTGCAGCAATCATG
CaOBPalpham610_TM	CCTCGTTGTCCCATTACCAA
CaOsh2p3797TM	AAGCCAGAAAACAGAGGGAAGAT
CaOsh2m3871TM	TCACTGGATGCTTTCTCTTAACAAA
CaOsh3p2253TM	GGGTAAACTTGCACCTACGGATT
CaOsh3m2327TM	GCAGTGTCTGTATCTCCCTTTTCA
CaSAC1.p17Tm	CCCATTCCACAGCAACAGATG
CaSAC1.m448Tm	TTCAACACCACCTCCCAGTGT

RESULTS

The following section gathers the results of this work, divided into two parts. The first part is consisting in the paper “Two distinct lipid transporters together regulate invasive filamentous growth in the human fungal pathogen *Candida albicans*”, to be submitted shortly, while the second part shows additional results that further support the data included in the paper. The virulence assays in murine candidiasis model were performed in collaboration with Dr. Rocío García-Rodas and Dr. Óscar Zaragoza from the Mycology Reference Laboratory, National Centre for Microbiology, Health Institute Carlos III, Majadahonda, Madrid, Spain.

Stéphanie Bogliolo, from our laboratory, participated in the following experiments: the phenotypic quantification shown in Figure 1C,D and in Figure 4C,D; the generation and verification of the *drs2osh2*, *drs2osh3*, *sac1*, and *drs2sac1* mutant strains (Figure 9 and S2A); and the RT experiments in Figure 2, S1 and S2.

Manuscript in preparation

Two distinct lipid transporters together regulate invasive filamentous growth in the human fungal pathogen *Candida albicans*

Miguel A. Basante-Bedoya¹, Stéphanie Bogliolo¹, Rocio Garcia-Rodas^{1,2}, Oscar Zaragoza², Robert A. Arkowitz¹ and Martine Bassilana^{1*}

¹Université Côte d'Azur, CNRS, INSERM, iBV, Parc Valrose, Nice, FRANCE.

² Mycology Reference Laboratory. National Centre for Microbiology. Health Institute Carlos III. Majadahonda, Madrid, Spain.

* Corresponding author
E-mail: mbassila@unice.fr

Short title: Lipid transporters in *C. albicans* morphogenesis

Abstract

Flippases transport lipids across the membrane bilayer to generate and maintain asymmetry. The human fungal pathogen *Candida albicans* has 5 flippases, including Drs2, which is critical for filamentous growth and phosphatidylserine (PS) distribution. Furthermore, a *drs2* deletion mutant is hypersensitive to the antifungal drug fluconazole and copper ions. We show here that such a flippase mutant also has an altered distribution of phosphatidylinositol 4-phosphate, PI(4)P, and ergosterol. Analyses of additional lipid transporters, *i.e.* the flippases Dnf1-3, and oxysterol binding protein (Osh) family lipid transfer proteins, *i.e.* Osh2-4 and Osh7, indicate that they are not critical for filamentous growth. However, deletion of Osh4 alone, which exchanges PI(4)P for sterol, in a *drs2* mutant can bypass the requirement for this flippase in invasive filamentous growth. In addition, deletion of the lipid phosphatase Sac1, which dephosphorylates PI(4)P, in a *drs2* mutant results in a synthetic growth defect, suggesting that these proteins function in parallel pathways. Together, our results indicate that a balance between the activities of two different classes of lipid transporters regulates invasive filamentous growth, *via* PI(4)P. In contrast, deletion of *OSH4* in *drs2* does not restore growth on fluconazole, nor on papuamide A, a toxin that binds PS in the outer leaflet of the plasma membrane, suggesting that Drs2 has additional role(s) in plasma membrane organization, independent of Osh4.

Introduction

Polarized growth is an essential process that is regulated in particular by cooperative interactions between key establishment proteins and specific lipids at the plasma membrane (PM). For instance in the baker yeast *Saccharomyces cerevisiae*, the activity and dynamic nanoclusters of the Rho-GTPase Cdc42 is regulated by multivalent interactions between its sole activator Cdc24, the scaffold protein Bem1 and anionic lipids, including phosphatidylserine (PS) [1-3]. Similarly, in the fission yeast *Schizosaccharomyces pombe*, the localization and function of the two essential Rho-GTPases, Cdc42 and Rho1, depend on PS polarized distribution [4]. The importance of anionic lipids, and PS in particular, for cellular function and signaling encompasses kingdoms from fungi, to mammals [5] to plants [6]. In addition, PS has been reported to be critical for virulence in a broad spectrum of microbial pathogens (reviewed in [7, 8]). In particular, in the human fungal pathogen *Candida albicans*, the PS synthase Cho1, which is conserved in fungi but does not have an ortholog in Human, is required for virulence in a murine candidiasis model [9]. A *cho1* deletion mutant also exhibits increased exposure of β (1,3)-glucan *via* up-regulation of cell wall MAPK cascades, facilitating its detection by innate immune cells [10]. PS is synthesized in the endoplasmic reticulum (ER) and its cellular distribution is regulated both by lipid transfer proteins, which function at contact sites between the ER and the target cellular compartments, and lipid transporters, such as flippases that establish PS asymmetry between membrane leaflets (reviewed in [11]).

Lipid flippases are P4-ATPases, only found in eukaryotes, where they are similar in domain structures from fungi to Human (reviewed in [12]). These proteins actively transport phospholipids from the external/luminal to cytoplasmic membrane leaflets and play an important role in polarized growth (reviewed in [13]). There are

14 P4-ATPases in Human and only 5 in the yeast *S. cerevisiae* (Dnf1-3, Drs2, Neo1), with most of them regulated by non-catalytic subunits from the Cdc50/Lem3 family. For instance, in *S. cerevisiae*, Cdc50 forms a functional complex with Drs2 [14, 15] and very recently, the cryo-electron microscopy structure in different conformations of this complex was resolved at 2.8 to 3.7 Å [16]. This complex, which is well characterized, both *in vitro* and *in vivo*, primarily transports PS [17, 18]. The role of lipid flippases on membrane curvature and in trafficking has been extensively studied in *S. cerevisiae*, as well as in mammals (reviewed in [19]). In budding *S. cerevisiae*, Neo1, which is the sole essential flippase [20], localizes to the Golgi and endomembranes, Drs2 and Dnf3 to the trans-Golgi network (TGN) and Dnf1-2 to the PM [17, 21, 22]. A recent study indicates that Dnf3 can also be found at the PM in a cell-cycle dependent fashion, where it regulates, together with Dnf1-2, *S. cerevisiae* pseudohyphal growth [23]. Furthermore, in response to pheromone, it was shown that Dnf1, Dnf2 and Dnf3 localize to the shmoo tip, while Drs2 remains at the Golgi [24]. Interestingly, in the filamentous fungi *Aspergillus nidulans* and *Fusarium graminearum*, it was shown in particular that the Drs2 homolog, DnfB, localizes primarily to a cluster of vesicles at the hyphal apex, called Spitzenkorper (SPK), which is characteristic of fungi that can grow in a filamentous form [25, 26]. Together, these data indicate that flippases can localize to different distinct compartments in specific conditions of polarized growth.

Filamentous fungi are highly polarized organisms, in which the role of flippases has been investigated. For instance, in *A. nidulans*, the homologs of Dnf1 and Drs2, *i.e.* DnfA and DnfB, regulate growth and PS asymmetry [25], while in *Magnaporthe grisea*, MgAPT2, one of the 4 aminophospholipid translocase (APT) encoding genes related to Drs2, is required for plant infection but not filamentous

growth [27]. In *F. graminearum*, flippases play redundant as well as distinct roles in vegetative growth, where FgDnfA is critical, stress response, reproduction and virulence [26, 28, 29]. In the human fungal pathogen *C. albicans*, Neo1 is not essential and deletion of either Dnf1 or Dnf2 results in moderate increase sensitivity to copper [30]. The *drs2* deletion mutant is hypersensitive to copper [30], as well as to the antifungal drug fluconazole [31]. Deletion of Drs2 also results in altered PS distribution and impaired filamentous growth [31], and that of its Cdc50 subunit in altered filamentous growth and reduced virulence in a murine candidiasis model [32]. Here, we sought to determine the role of Drs2 in morphogenesis and whether membrane asymmetry is critical for this process.

Our results show that in response to serum, of the four flippases, Dnf1-3 and Drs2, only Drs2 is critical for filamentous growth, with the Dnf1 and Dnf2 together having a minor role in this process. Filamentous growth was largely recovered in the *drs2* mutant upon deletion of the lipid transfer protein Osh4, but not by that of other Osh proteins (Osh2, Osh3 and Osh7). Furthermore, our results demonstrate that the distributions of PS and of the phosphatidylinositol phosphate PI(4)P, which are both altered in the *drs2* mutant, were restored upon deletion of *OSH4*. These data indicate that the requirement for flippase activity across the lipid bilayer during filamentous growth can be specifically bypassed by lipid exchange between membrane compartments.

Results

Drs2 has a unique role in *C. albicans*

In *A. nidulans*, the Drs2 homolog DnfB, is not critical for hyphal growth [25]. In contrast, in *C. albicans*, Drs2 is required for filamentous growth and budding growth is largely unaffected (average doubling time of 90 min, compared to 80 min in the wild-type strain) [31]. To determine whether Drs2's role is specific, we investigated the importance of other flippases, *i.e.* Dnf1, Dnf2 and Dnf3, using loss of function mutants that we generated (Supplementary Figure S1A). As illustrated in Figure 1A, a *drs2* deletion mutant was not invasive on a serum-containing media, and reintroduction of *DRS2* in this mutant restored invasive growth (Figure 2A). In contrast, deletion of *DNF1* or *DNF3* did not alter serum-induced invasive growth, while deletion of *DNF2* resulted in reduced invasive growth, which was further reduced in a double *dnf1dnf2* deletion mutant. Over-expression of *DNF2* restored invasive growth both in the *dnf2* and *dnf1dnf2* mutants, but not in the *drs2* mutant, suggesting that Dnf2 and Drs2 function do not overlap in this invasive growth process. Upon serum-induced hyphal growth in liquid media (Figure 1B), the *dnf1*, *dnf2* and *dnf3* deletion mutants produced hyphae similar to the wild-type cells (79±4%, 78±7%, 76±10 % and 84±5 % respectively, compared to 18±3 % for the *drs2* mutant); hyphal formation in the *dnf1dnf2* mutant cells was somewhat reduced to 56±12%. The average hyphal filament length was nonetheless reduced in *dnf2* cells, as well as in *dnf1dnf2* cells (14±3 µm and 13±3 µm) compared to the WT, *dnf1* and *dnf3* cells (20±4 µm, 18±4 µm and 20±4 µm, respectively). These data indicate that, in contrast to the *drs2* deletion mutant, cells deleted for *DNF1*, *DNF2* and *DNF3* undergo hyphal invasive growth similar to the wild-type cells, albeit with a reduced efficiency for the *dnf2* mutant. Furthermore, Figure 1E shows that the *dnf1-3* mutants

also grew similar to the wild-type cells on cell wall perturbants, such as calcofluor white (CFW) and congo red (CR), and on antifungal drugs, such as caspofungin (Caspo) and fluconazole (FCZ), in contrast to the *drs2* mutant, which was hypersensitive to CFW and FCZ [31]. Together, these data indicate that Drs2 has a unique role in *C. albicans*.

Drs2 is critical for hyphal extension after septin ring formation

In response to serum, *drs2* cells appear to initiate filamentous growth, although they were unable to form hyphae [31]. Hence, we examined this mutant in a mouse model for systemic candidiasis and Figure 2B shows that the *drs2* mutant is avirulent. At the transcriptional level, hyphal growth is controlled by the hyphal specific gene *HGCI* [33], which itself is further regulated by *UME6* [34]. Both *hgc1* and *ume6* deletion mutants are defective in hyphal extension and attenuated for virulence in a mouse infection model [33, 35]. RT-PCR analyses in Figure 2C shows that the *drs2* mutant expressed *HGCI*, similar to that of the WT and complemented strains after 30 min serum-induction, but at a reduced level after 120 min, and a similar pattern was observed for *UME6* transcript levels. Expression of the peptide toxin candidalysin encoding *ECE1* gene, [36], which correlates with cell elongation, was reduced in *drs2* both at 30 and 120 min, the difference compared to control cells being greatest at 120 min. Expression of the secreted protease *SAP6*, which is mainly associated with hyphal growth [37], was also dramatically reduced after 120 min in *drs2* cells, but expression of the agglutinin-like (Als) adhesin gene *ALS3*, which is dispensable for hyphal formation [38], appeared to be unaffected compared to control cells. Together, our data are consistent with a defect in *drs2* hyphal extension.

To further characterize this defect at the molecular level, we used time-lapse microscopy to follow cells expressing fluorescent reporters for different cellular compartments. Figure 3A illustrates representative time courses of hyphal growth both in WT and *drs2* cells expressing the septin Cdc10 [39]. Measurement of the diameter of the filament compartments, apical and distal to the Cdc10 septin ring (Figure 3B) shows that, while their diameter was constant in WT cells ($\sim 1.8 \mu\text{m}$), the apical compartment specifically increased in *drs2* cells (to $\sim 2.5 \mu\text{m}$). This increase in diameter was associated with a reduced extension rate after appearance of the first septin ring ($0.09 \mu\text{m}/\text{min}$ in *drs2* cells, compared to $0.34 \mu\text{m}/\text{min}$ in WT cells; Figure 3C). These data are consistent with a defect in polarized growth in the *drs2* mutant after the first septin ring forms. In agreement with this, we observed that, upon filament extension, the localization of active Cdc42 [40] became depolarized in the *drs2* cells and that the Spitzenkörper (visualized with the myosin light chain Mlc1, [41, 42]), was not maintained at the tip of the filament following cell division, compared to the wild-type control cells (Figures 3D and 3E). Together, these data indicate that, subsequent to septin ring formation, the *drs2* mutant is unable to maintain polarized growth, which ultimately results in growth arrest and/or pseudohyphal growth.

Drs2 localizes to the hyphal tip

In *S. cerevisiae*, Drs2 localizes to the late Golgi during budding growth [20] and mating [24], while its homolog in *A. nidulans*, DnfB, localizes within the Spitzenkörper core [25]. To examine the distribution of Drs2 in *C. albicans*, we generated a strain that expresses a *DRS2-GFP* fusion, which was functional (Figure 4A). Given that the homolog of Dnf1-2 in *A. nidulans*, DnfA, also localizes to the

Spitzenkörper, albeit to the outer layer macrovesicles compared to DnfB [25], we also generated a strain that expressed a functional *DNF2-GFP* fusion (Figure 4A). Figure 4B shows that Drs2 was restricted to the apical region of the hyphal tip, as well as in internal structures, likely Golgi cisternae by analogy with *S. cerevisiae* [20]. Dnf2 was essentially localized to the plasma membrane at the apical cortex, similar to its localization in *S. cerevisiae* at the tip of buds and mating projections [24]. Both Dnf2 and Drs2 co-localized with a plasma membrane marker (a prenylated AFP fusion, AFP-CtRac1, [43]), although Drs2 localized to a smaller region at the hyphal tip than Dnf2 (Figure 4C) and, given the proximity of the Spitzenkörper to the plasma membrane, Drs2 also partially co-localized with the Spitzenkörper marker, the Myosin Light Chain Mlc1 (Figure 4D). Together, these data indicate that Drs2 and Dnf2 have distinct distributions at the filament apex.

The *drs2* mutant is altered for PI(4)P distribution

Drs2 is a P4-ATPase that flips selectively phosphatidylserine (PS) across the lipid bilayer *in vitro* and *in vivo* in *S. cerevisiae* [17, 18]. In *C. albicans*, using the reporter Lactadherin C2 [44-46], we observed that the distribution of PS was altered during hyphal growth in the *drs2* mutant, as the reporter was less associated with the plasma membrane and visible as intracellular punctae [31]. To determine the impact of the *DRS2* deletion on the distribution of other lipids shown to be critical for hyphal growth, such as the phosphatidylinositol phosphates PI(4P) and PI(4,5)P₂ [47, 48], as well as ergosterol [49], we used specific fluorescent reporters. The distribution of PI(4,5)P₂ appears to be similar in WT cells and *drs2* filamentous cells (Figure 5A), yet the distribution of PI(4)P was substantially less polarized in the mutant, compared to the wild-type or complemented strains (Figure 5B). This depolarization is further

illustrated by the graph in Figure 5B, which shows the relative concentration of PI(4)P, as a function of filament length. In contrast, PI(4)P at the Golgi appears similar in *drs2* and WT filamentous cells (Figure 5C). Furthermore, the number of Golgi cisternae was also similar (~7 cisternae per cell in *drs2* cells compared to ~9 per cell in the wild-type control), indicating that the Golgi structure was largely unaffected in this mutant (Figure 5D).

Using filipin staining, it was shown that membrane sterols are highly concentrated at the apex during *C. albicans* hyphal growth, with such a polarization not observed in budding and pseudohyphal cells [49]. We examined the sterol distribution in *drs2* cells, using both filipin staining and the genetically encoded biosensor D4H [50, 51]. Figures 6A and 6B show that sterols were highly concentrated at the apex of WT hyphal cells, whether visualized with filipin staining or the D4H reporter. In contrast, in the *drs2* mutant, while we observed a polarized distribution of sterols with filipin staining (Figure 6A), albeit less pronounced than in the WT cells, there was a striking difference with D4H, as this reporter preferentially labeled internal structures in *drs2* cells (Figure 6B). We attribute the difference in distribution of these reporters to different sterol accessibility from the inner PM leaflet [51]. The internal D4H associated signals were frequently observed at the filament apex and reintroduction of a copy of *DRS2* in the *drs2* mutant restored the ergosterol distribution to the PM (Figure 6C). Together, these data indicate that deletion of *DRS2* results not only in altered distribution of PS, but also of PI(4)P and ergosterol.

Deletion of *OSH4* recovers hyphal invasive filamentous growth in the *drs2* mutant

Lipid transfer proteins (LTPs), and more specifically oxysterol-binding protein (OSBP)-related proteins (ORPs), are important for membrane lipid composition, *via* non-vesicular traffic (reviewed in [52]), including for PS distribution (reviewed in [11]). LTPs can bind specific ligands such as PI(4)P, PS and sterol. For example, in *S. cerevisiae*, there are 7 oxysterol-binding homology (Osh) proteins, among which Osh6/Osh7 transports PS from cortical ER (cER) and PM [53], in counter-exchange with PI(4)P [54]. On the other hand, another Osh protein, Kes1/Osh4, which transports sterol in counter-exchange with PI(4)P [55] was proposed to act antagonistically with Drs2 to regulate the sterol distribution between PM and internal membranes in *S. cerevisiae* [56]. *C. albicans* has 5 Osh proteins (Osh1-4 and Osh7), with Osh4 and Osh7 sharing ~ 60% identity with their *S. cerevisiae* counterparts, and their importance is unknown in this organism. Note that the genes encoding *OHS7* (called *OBPA* and *OBPALPHA*) are located at the mating-type-like locus (MTL), similar to those encoding the Golgi phosphatidylinositol kinase Pik1 (*PIKA* and *PIKALPHA*).

To investigate the importance of Osh proteins in *C. albicans* invasive hyphal growth, we first generated *osh4* and *osh7* deletion mutants, as well as *drs2 osh4* and *drs2 osh7* double deletion mutants, and examined these mutants for invasive hyphal growth in response to serum induction. As illustrated in Figure 7, deletion of *OSH4* or *OSH7* alone did not alter invasive growth, yet deletion of *OSH4* in the *drs2* mutant background recovered invasive growth to a level similar to that of the WT (Figure 7A, upper panel). Reintroduction of a copy of *OSH4*, under the control of its own promoter in this *drs2 osh4* mutant resulted in non-filamentous colonies, similar to that of *drs2*. In serum-containing liquid media, we also observed a recovery of hyphal growth upon deletion of *OSH4* in the *drs2* mutant (Figure 7B-D), with 76±9%

filamentous cells, compared to $82\pm 8\%$ and $80\pm 6\%$ in the WT and the *osh4* mutant, respectively. In this *drs2 osh4* mutant, hyphal length was, however, slightly reduced compared to that of the WT and *osh4* cells (17 ± 3 μm , compared to 19 ± 1 μm for WT and *osh4* cells). Reintroduction of a copy of *OSH4* in the *drs2osh4* mutant resulted in a reduced percentage of hyphae to $54\pm 11\%$, with filament lengths of 16 ± 0.5 μm , compared to the *drs2 osh4* mutant, albeit higher than the percentage of hyphae in the *drs2* mutant ($18\pm 9\%$). The recovery of invasive filamentous growth in the *drs2* mutant was specific for the *OSH4* deletion, as deletion of *OSH7* did not recover invasive filamentous growth in the *drs2* mutant (Figure 7A, bottom panel).

To confirm the specificity of the *OSH4* deletion in recovering invasive growth in the *drs2* mutant, we also generated *drs2 osh2* and *drs2 osh3* double deletion mutants. *C. albicans OSH3* has been reported to be important for invasive growth in nutrient poor media (Spider media), but not in the presence of serum (Hur *et al.*, 2006). Similarly, we observed that mutants deleted for either *OSH2* or *OSH3* grew invasively in the presence of serum (Figure S2). In contrast to *OSH4* deletion, deletion of either *OSH2* or *OSH3* did not recover the *drs2* invasive growth defect. These data indicate that while Osh proteins (Osh2-4 and Osh7) are not required for serum-induced invasive filamentous growth, deletion of *OSH4* bypasses the *drs2* defect in this process.

While deletion of *OSH4* in the *drs2* mutant did also recover the growth defect on CFW, it did not recover growth on FCZ (Figure 7E), which remained similar to that of *drs2*, suggesting that Drs2 has specific roles that are not linked to Osh4 activity. The growth defect of *drs2* cells on FCZ could result from a mislocalization of multi-drug transporters, such as Cdr1 [57]. This is unlikely, as Figure 7F shows that a Cdr1-GFP fusion protein localized to the plasma membrane of *drs2* cells,

similar to that of WT cells. Together, these data indicate that *DRS2 per se* is not required for hyphal invasive growth, but rather that a balance in the activities of Drs2 and Osh4 regulate this process.

Drs2 is important for plasma membrane organization

To gain further insight into the mechanisms underlying the recovery of hyphal growth in the *drs2 osh4* mutant, we examined whether deletion of *OSH4* also restored the wild-type phospholipid distribution in the *drs2* mutant. Figure 8A shows that the distribution of PI(4)P was polarized in *drs2 osh4*, similar to that in WT and *osh4* cells. Similarly, the distribution of PS, as visualized with LactC2, appears to be also largely restored in *drs2 osh4*, as the internal punctae visualized in *drs2* cells were absent in these *drs2 osh4* cells, similar to the WT, complemented and *osh4* strains (Figure 8B). Quantification of the LactC2 signal in the *drs2* mutant indicates that the level of PS was both reduced at the PM and increased internally, compared to WT and *osh4* deleted cells, resulting in a decreased ratio of PM to intracellular signals (Figure 8C). Deletion of *OSH4* in these *drs2* cells significantly recovered the PS ratio of PM to intracellular signals, with an increase in PM and a decrease in internal signals (Figure 8C). Papuamide A (PapA) is a depsipeptide toxin that binds PS in the outer leaflet of the plasma membrane [58]. In *C. albicans*, the *chol* deletion mutant lacks the PS synthase and is less sensitive to PapA than WT cells [59]. As shown in Figure 8D, the *drs2* mutant was hypersensitive to PapA, compared to the WT strain, reflecting increased PS in the outer PM leaflet. Interestingly, the *drs2 osh4* mutant did not grow on PapA, similar to *drs2*, while the *osh4* mutant grew similar to the WT (Figure 8C). These results indicate that in this double mutant, the PS bilayer asymmetry was not

re-established and suggest that establishment of a PM PI(4)P gradient, rather than PS bilayer asymmetry, is critical for hyphal growth.

Deletion of both *DRS2* and *SAC1* results in a synthetic growth defect

To further investigate the relative importance of the PS bilayer asymmetry and the PM PI(4)P gradient in hyphal growth, we generated different mutants with the aim of altering each of these components. In an attempt to alter PS asymmetry, we generated strains expressing Drs2 mutated for the residues analogous to those specifically required for PS recognition in *S. cerevisiae*, Drs2^{F511Y} and Drs2^{QQ-GA} (Figure S3A; [60, 61]). Reintroduction of a copy of such a mutated version of *C. albicans* Drs2 (Drs2^{F520Y}) in *drs2*, restored growth on PapA, similar to that of the complemented and WT strains (Figures 8D). Furthermore, the mutants expressing either Drs2^{F520Y} or Drs2^{QQ-GA} had a PS distribution similar to that of the complemented strain and generated hyphae (Figures S3B and S3C), indicating that these residues are not critical for PS distribution and morphogenesis in *C. albicans*.

To alter the PM PI(4)P gradient, we generated mutants deleted for the lipid phosphatase Sac1, which dephosphorylates PI(4)P, and is responsible for regulating PM PI(4)P, both in yeast and mammalian cells [62, 63]. In *C. albicans*, Sac1 is critical for the steep PM PI(4)P gradient [47] and hyphal growth maintenance [47, 64]. In *S. cerevisiae*, deletion of either *OSH4* or *SAC1* is synthetically lethal in cells largely devoid of ER-PM contact sites [65], and cold-sensitive growth of a *drs2* deletion mutant is partially suppressed by deletion of either *SAC1* or the *OSH4* homolog, *KES1* [56]. As deletion of *OSH4* restored PI(4)P polarized distribution in *drs2*, as well as hyphal growth, we investigated the effect of *SAC1* deletion in *drs2*. Figures 9A and 9B show that budding growth was altered in such a *drs2 sac1* mutant,

with a doubling time that increased 3-fold, compared to the WT, *drs2* and *sac1* strains. Furthermore, the *drs2 sac1* strain did not form invasive colonies, similar to *sac1* (Figure 9C). However the *sac1* mutant formed filamentous cells in response to serum, albeit shorter than WT cells (Figure 9D; [47, 64]). In contrast, the *drs2 sac1* strain was unable to form filamentous cells, even after 270 min incubation (Figure 9D). RT-PCR confirmed the absence of *DRS2* and/or *SAC1* in the respective mutants (Figure 9E). Together, these data show that *DRS2* and *SAC1* genetically interact in *C. albicans*, indicating that they function in parallel pathways, and suggest that a PM PI(4)P gradient is critical in the absence of Drs2.

Materials and Methods

Growth conditions

Yeast extract-peptone dextrose (YEPD) or synthetic complete (SC) medium was used and strains were grown at 30°C, unless indicated otherwise. Filamentous growth induction was carried out as described previously either with 50% serum or 75% serum [66]. For filipin staining experiments, 10% of serum was used. Growth on YEPD plates containing Congo red, calcofluor white, caspofungin or fluconazole was examined as described [67]. Congo red, calcofluor white, filipin, hygromycin and fluconazole were from Fluka, Sigma-Aldrich, Saint Quentin Fallavier, France. Papuamide A was from University British Columbia.

Strains and plasmids

Strains and oligonucleotides used are listed in Tables S1 and S2, respectively. All strains were derived from BWP17 [68]. The deletion mutants were generated by homologous recombination. Each copy was replaced by either *HIS1*, *URA3*, *ARG4*, *SAT1* or *HYGB*, using knockout cassettes generated by amplification of pGem-*HIS1*, pGem-*URA3*, pGem-*CdARG4*, pFa-*ARG4*, pFa-*SAT1* and pBH1S [68-71] with primer pairs *DNF1.P1/DNF1.P2*, *DNF2.P1/DNF2.P2*, *DNF2.P3/DNF2.P4*, *DNF3.P1/DNF3.P2*, *OSH4.P1/OSH4.P2*, *OSH7A.P1/OSH7A.P2*, *OSH7 α .P1/OSH7 α .P2* and *SAC1.P1/SAC1.P2*. The *drs2 Δ /drs2 Δ* *osh4 Δ /osh4 Δ* , *drs2 Δ /drs2 Δ* *osh2 Δ /osh2 Δ* , *drs2 Δ /drs2 Δ* *osh3 Δ /osh3 Δ* , *drs2 Δ /drs2 Δ* *osh7a Δ /osh7 α Δ* and *drs2 Δ /drs2 Δ* *sac1 Δ /sac1 Δ* strains were generated from the *drs2 Δ /drs2 Δ* strain (PY3310 [31]) and the *dnf1 Δ /dnf1 Δ* *dnf2 Δ /dnf2 Δ* strain from the *dnf2 Δ /dnf2 Δ* strain (PY5804).

Plasmid *pDUP3-pADH1DNF2* was constructed by amplification from gDNA of the *DNF2* ORF, using primers with a unique *AscI* site at the 5' end (DNF2.P5) and a unique *MluI* site at the 3' end (DNF2.P6) and *pDUP3-pDRS2DRS2* by amplification from *pExp-pDRS2DRS2* [31] of the *DRS2* ORF together with 1 kb upstream and downstream, using primers with a unique *SpeI* site at the 5' end (DRS2.P3) and a unique *NotI* site at the 3' end (DRS2.P4). The fragments were subsequently cloned into *pDUP3-SAT1* [72], yielding to *pDUP3-pADH1DNF2* and *pDUP3-pDRS2DRS2*, respectively. Plasmid *pExp-pOSH4OSH4* was constructed by amplification from gDNA of the *OSH4* ORF, together with 1 kb upstream and downstream, using primers with a unique *SalI* site at the 5' end (OSH4.P3) and a unique *NotI* site at the 3' end (OSH4.P4) and subsequently cloned into *pExpARG4*, yielding to *pExp-pOSH4OSH4*. Site directed mutagenesis was used to mutate *Drs2* to *Drs2*^{F520Y} and *Drs2*^{QQ-GA}, using the primer pairs *DRS2.P7/DRS2.P8* and *DRS2.P9/DRS2.P10*, respectively, together with *pExp-pDRS2DRS2* [31]. To visualize *Drs2* and *Dnf2*, GFP γ was inserted by homologous recombination at the 3' end of *DRS2* or *DNF2* ORF in strains heterozygous for these genes (PY3303 and PY5677), respectively, after amplification of GFP γ from the plasmid *pFA-GFP γ -HIS1* [73], using the primers *DRS2.P5/DRS2.P6* or *DNF2.P7/DNF2.P8*. *pExp-pACT1CRIBGFP* [40], was used to transform the WT (BWP17) and *drs2/drs2* (PY3310) strains. *Cdr1-GFP*, *PH-FAPP1*^[E50A,H54A]-*GFP*, *GFP-(PH*^{OSH2[H340R]}*)*₂-*GFP* and *GFP-PHPLC δ 1-PHPLC δ 1-GFP* expressing strains were generated as described [47, 48]. *pDUP5-mScarlet-CtRac1* [74] was used to transform the *drs2/DRS2GFP* (PY4665) and *dnf2/DNF2GFP* (PY5746) strains. *Mlc1-mScarlet* and *Cdc10-mScarlet* were generated by amplification of *mScarlet-ARG4* from *pFA-mScarlet-ARG4* [75], using the primer pairs *MLC1.P1/MLC1.P2* and *CDC10.P1/CDC10.P2*, respectively. *mTurquoise-*

CtRac1 (mTrq-CtRac1) was constructed by replacing mScarlet in *pDUP5-pADH1-mScarlet-CtRac1* [74] with mTrq, and subsequently cloning mTrq-CtRac1 into *pDUP3* (Puerner, Bassilana & Arkowitz, in preparation). To visualize the distribution of phosphatidylserine, a fusion of GFP with the discoidin-like C2 domain of lactadherin (GFP-LactC2) was used, as previously described [31]. To visualize the distribution of ergosterol, we used filipin staining, as described [49], as well as the genetically encoded biosensor D4H [51]. D4H was amplified from plasmid pSM2244 [51], using primer pair D4H.P1 and D4H.P2 and cloned into plasmid *pExp-pACT1-mScarlet-CtRac1* [75], using AscI and MluI unique restriction sites, yielding *pExp-pACT1-mScarlet-D4H*. This plasmid was linearized with NcoI and integrated into the *RP10* locus. All other pExp plasmids were linearized with StuI and integrated into the *RP10* locus. pDUP3 and pDUP5 plasmids were digested with NgoMIV to release the cassette to be integrated into the *NEUTL5* locus.

Two independent clones of each strain were generated and confirmed by PCR. RT-PCR was also performed, where relevant, using the primers (GENE.pTm and GENE.mTm) listed in Table S2 or previously described [76] and RNA extraction was carried out using Master Pure yeast RNA extraction purification kit (Epicentre). All PCR amplified products were confirmed by sequencing (Eurofins MWG Operon, Ebersberg, Germany).

Microscopy analyses

Colony and cell morphology imaging were performed as described [66]. Briefly, plates were incubated for 3–6 days prior to imaging with a Leica MZ6 binocular (x20) and cells (budding or serum-induced) were imaged by differential interference

contrast with a microscope Leica DMR, using an ImagingSource DMK 23UX174 sCMOS camera.

Time lapses and fluorescent images were obtained using a spinning disk confocal microscope (inverted IX81 Olympus microscope with a 100X objective and a numerical aperture 1.45) and an EMCCD camera (Andor technology, UK). Z-stacks (images of 0.4 μm sections) acquired every 5 min, as described [47]. Maximum or sum intensity projections were generated from 21 z-sections with ImageJ software. Laser illuminations of 445 nm (Turquoise), 488 nm (GFP) and 561 nm (mScarlet) were used. CRIBGFP distribution experiments were carried out as described [40]. For filipin analyses, widefield images were acquired on an inverted ZEISS Axio Observer Z1 microscope with a 100X (1.3 NA) objective. Huygens professional software version 18.04 (Scientific-Volume Imaging) was used to deconvolve z-stack images of cells expressing PH-FAPP1^[E50A,H54A]-GFP. Bars are 5 μm .

Filament lengths and diameters were measured from DIC images, using image J software. Golgi cisternae were quantitated from deconvolved MAX projection images. Quantitation of PI4P distribution was performed on SUM projections, using the Matlab program HyphalPolarity [47]. Quantitation of PS plasma membrane and internal mean signals was performed on central z-sections, also using the Matlab program HyphalPolarity. Unless indicated otherwise, error bars represent the standard deviations.

Virulence assays

HDC was induced in 10 Balb/C mice (Charles Rivers, Italy) per group by injecting the lateral tail vein with an inoculum of 5×10^5 cells [77]. Animal body weight was

monitored daily and animals were sacrificed by cervical dislocation when they had lost more than 20% of their weight.

Ethics statement

Animal procedures were approved by the Bioethical Committee and Animal Welfare of the Instituto de Salud Carlos III (CBA2014_PA51) and of the Comunidad de Madrid (PROEX 330/14) and followed the current Spanish legislation (Real Decreto 53/2013) along with Directive 2010/63/EU.

Figure legends

Figure 1: Drs2 has a unique role in *C. albicans*. A) Invasive filamentous growth cannot be restored by overexpression of *DNF2* in the *drs2/drs2* mutant. Indicated strains were grown on agar-containing YEPD with FCS and images were taken after 6 days. Similar results were observed in 2 independent experiments. B) *DRS2* is critical for hyphal growth in response to serum. Cells from the indicated strains were incubated with FCS for 90 min at 37C. Bars are 5 μ m. C) and D). Graphs represent the percentage of hyphae (C) and the filament length (D) in the indicated strains after 90 min exposure to FCS at 37C. The percentage of hyphae is calculated as the mean \pm the SD of 3 experiments ($n = 150$ cells each) and the filament length was measured from the junction between cell body and filament (error bars indicate the mean \pm the SD of 3 experiments, $n \sim 50$ cells each). (E). The *drs2/drs2* mutant has increased susceptibility to fluconazole and calcofluor white. Serial dilutions of indicated strains were spotted on YEPD media containing 25 μ g/ml calcofluor white (CFW), 400 μ g/ml Congo red (CR), 125 ng/ml caspofungin (Caspo) or 10 μ g/ml fluconazole (FCZ). Images were taken after 2 days. Similar results were observed in 2 independent experiments.

Figure 2: Drs2 is critical for virulence in a mouse model of systemic candidiasis.

A) Reintroduction of *DRS2* complements the invasive growth defect of the *drs2/drs2* mutant. Indicated strains were grown as in Figure 1A. B) The *drs2/drs2* mutant has attenuated virulence in a mouse model of hematogenously disseminated candidiasis. Balb/C mice ($n = 10$) were injected with an inoculum (5×10^5 cells) of the indicated strains and the survival was assessed. C) Hyphal specific gene (HSGs) induction is reduced in the *drs2/drs2* mutant after cells were incubated 120 min with FCS. mRNA

and cDNA were prepared from the indicated strains. *HGCI*, *ECE1*, *SAP6* and *ALS3* transcripts were determined by RT-PCR using primer pairs described in Bassilana *et al.*, 2005, and *UME6* transcripts were determined using UME6.pTm/UME6.mTm (89 bp) primer pair. Actin (*ACT1*) transcript levels were used for normalization as in Bassilana *et al.*, 2005.

Figure 3: Drs2 is critical for maintaining polarized filament extension. A) The *drs2/drs2* mutant has altered morphology and exhibits reduced filament extension rate after septin ring formation. Time lapse of wild-type and *drs2/drs2* cells expressing Cdc10-mScarlet, incubated in the presence of FCS. Images were taken every 10 min and merges between DIC and sum projections of 21 z-sections are shown. Bars are 5 μ m. B) Graphs represent the filament diameter before (open circles) and after (solid circles) the first septin ring as a function of the times from the first image in which the septin ring is observed in wild-type (blue) and *drs2/drs2* (magenta) cells. Means +/- the SD of 25-50 cells are shown. C) The graph shows the filament extension rate in wild-type (blue) and *drs2/drs2* (magenta) cells calculated from the septin ring. Means +/- the SD of 30-60 cells are shown. D) and E) Polarized growth is altered in the *drs2/drs2* mutant. D) Time lapse of wild-type and *drs2/drs2* cells expressing Mlc1-mScarlet, incubated in the presence of FCS. Images were taken every 10 min and maximum projections of 21 z-sections are shown. E) Time lapse of wild-type and *drs2/drs2* cells expressing CRIB-GFP, incubated in the presence of FCS. Images were taken every 5 min and sum projections of 23 z-sections are shown.

Figure 4: Drs2 localizes preferentially to the filament apex. A) The Drs2-GFP and Dnf2-GFP fusions are functional. Indicated strains were grown as in Figure 1A. B)

and C) Drs2 and Dnf2 localize differently to the filament apex. Sum projections of 16 z-sections of representative cells expressing Drs2-GFP and Dnf2-GFP after 90 min FCS induction are shown and arrowheads indicate Golgi cisternae (B). Central z-sections and merge of representative cells expressing either Drs2-GFP or Dnf2-GFP, together with Trq-CtRac1, after 90 min FCS induction are shown (C). Bars are 5 μm . D) Drs2 partially overlaps with Mlc1. Sum projections of 16z-sections and central z-sections of representative cells expressing Drs2-GFP together with Mlc1-mScarlet, after 90 min FCS induction are shown.

Figure 5: Plasma membrane PI4P distribution is altered in the *drs2/drs2* mutant.

A) Plasma membrane PI_{4,5}P₂ distribution is not altered in the *drs2/drs2* mutant. Wild-type and *drs2/drs2* cells expressing GFP-PH_{PLC δ 1}-PH_{PLC δ 1}-GFP were incubated for 60 or 90 min, respectively, in the presence of FCS. Central z-sections and sum projections of (21 z-sections) of representative cells are shown. B) Plasma membrane PI4P distribution is altered in the *drs2/drs2* mutant. Indicated cells expressing GFP-(PH^{OSH2[H340R]})₂-GFP were incubated for 90 min in the presence of FCS. Sum projections of (21 z-sections) of representative cells are shown. The graph illustrates the means \pm the SEM of the relative concentration of plasma membrane PI4P as a function of filament length, normalized to the maximal signal for each cell ($n = 25-60$ cells). C) and D) The number of Golgi cisternae is not substantially affected in the *drs2/drs2* mutant. DIC and maximum projections (21 deconvolved z-sections) of representative cells of indicated strains expressing FAPP1^[E50A,H54A]-GFP and incubated for 60-90 min in the presence of FCS are shown (C). The number of Golgi cisternae per cell was determined in budding cells of the indicated strains from maximum projections of deconvolved images (21 z-sections). Bars in the graph indicate the

mean +/- the SD of 3 independent biological samples ($n = 100$ cells and ~700-800 cisternae for each strain) (D).

Figure 6: Distribution of ergosterol is altered in the *drs2/drs2* mutant. A) The ergosterol reporters Filipin and D4H localize similarly at the apex of the filament in wild-type cells. Left panel: Wild-type and *drs2/drs2* cells were induced with 10% FCS for 90 min prior to staining with filipin, as described in Material & Methods. Images were taken with a wide-field fluorescence microscope. Right panel: Wild-type and *drs2/drs2* cells expressing mScarlet-D4H together with Trq-CtRac1 were induced with 50% FCS for 90 min. Images were taken with a spinning disk confocal microscope and central z-sections, as well as merge images, are shown. B) Ergosterol distribution is altered in the *drs2/drs2* mutant. Images of the indicated strains expressing mScarlet-D4H were taken as in Figure 8A right panel.

Figure 7: Deletion of *OSH4* specifically rescues hyphal invasive growth in the *drs2/drs2* mutant. A) Invasive filamentous growth is specifically restored in the *drs2/drs2* mutant upon deletion of *OSH4*. Indicated strains were grown as in Figure 1A and images were taken after 6 days. Similar results were observed in 2 independent experiments. B) Hyphal growth is restored in the *drs2/drs2* mutant upon deletion of *OSH4*. Cells from the indicated strains were incubated with FCS for 90 min at 37°C. Bars are 5 μ m. C) and D). Graphs represent the percentage of hyphae (C) and the filament length (D) in the indicated strains, as in Figures 1C and 1D. The percentage of hyphae is calculated as the mean +/- the SD and the filament length was measured from the junction between cell body and filament, as in Fig. 1C & 1D. E) Deletion of *OSH4* does not rescue growth on fluconazole in the *drs2/drs2* mutant.

Serial dilutions of indicated strains were spotted on YEPD media containing 25 µg/ml calcofluor white (CFW), 10 µg/ml fluconazole (FCZ). Images were taken after 2 days. Similar results were observed in 2 experiments. F) The multidrug ABC transporter Cdr1 localizes to the plasma membrane in the *drs2/drs2* mutant. Central z-sections of representative WT and *drs2/drs2* cells expressing Cdr1-GFP are shown.

Figure 8: Deletion of *OSH4* rescues plasma membrane PI4P gradient and internal PS distribution in the *drs2/drs2* mutant. A) PI4P distribution is restored in the *drs2/drs2* mutant upon *OSH4* deletion. Indicated cells expressing GFP-(PH^{OSH2[H340R]})₂-GFP were incubated as in Figure 5B, with sum projections of representative cells shown. The graph illustrates the means +/- the SEM of the relative concentration of plasma membrane PI4P as a function of filament length, normalized to the maximal signal for each cell ($n = 100$ cells). B) Internal PS distribution is restored in the *drs2/drs2* mutant upon *OSH4* deletion. Indicated cells expressing GFP-LactC2 were incubated as in Figure 5B, with sum projections of representative cells shown. The graphs represent the relative internal and PM fractions of PS, as well as the ratio of the signal at the plasma membrane over the internal signal for the indicated strains ($n = 30-50$ cells each), and bars mean +/- the SD, in the indicated strains. C) Deletion of *OSH4* does not restore growth on Papuamide A of the *drs2/drs2* mutant. Serial dilutions of indicated strains were spotted on YEPD media containing 1 µg/ml papuamide A (PapA) and images were taken after 2 days. Similar results were observed in 2 experiments.

Figure 9: *DRS2* and *SAC1* genetically interact during *C. albicans* development.

A) Deletion of both *DRS2* and *SAC1* results in a synthetic growth defect. Serial

dilutions of indicated strains were spotted on YEPD and images were taken after 3 days. Similar results were observed in 2 independent experiments. B) Morphology of *drs2 sac1* budding cells. Cells from the indicated strains were grown to exponential phase in YEPD. The doubling time was ~90 min for WT, *drs2* and *sac1* strains and ~270 min for the *drs2 sac1* strain. Bars are 5 μ m. C) *SAC1* is critical for invasive growth in response to serum. Indicated strains were grown on agar-containing YEPD with FCS and images were taken after 6 days. Similar results were observed in 2 independent experiments. D) The *drs2 sac1* mutant does not generate hyphae in response to serum. Indicated strains were grown in the presence of FCS for 180 min. At 90 min, the percent of filamentous cells was 88%, 15%, 38% and 1% for the WT, *drs2*, *sac1* and *drs2 sac1* strains, respectively; n ~ 100 cells. Similar results were observed in 2 independent experiments. E) *DRS2* and *SAC1* transcript levels. Transcripts were determined by RT-PCR, using *SAC1.pTm/SAC1.mTm* (90 bp) and *DRS2.pTm/DRS2.mTm* (62 bp) primer pairs.

Figure S1: Flippase deletion mutant strains verification. A) *DRS2* and *DNF1-3* transcript levels. mRNA and cDNA were prepared from the indicated strains. *DRS2* and *DNF1-3* transcripts were determined by RT-PCR, using *DRS2.pTm/DRS2.mTm* (62 bp), *DNF1.pTm/DNF1.mTm* (73 bp), *DNF2.pTm/DNF2.mTm* (106 bp) and *DNF3.pTm/DNF3.mTm* (104 bp) primer pairs, respectively. Actin (*ACT1*) transcript levels (*ACT1.pTm/ACT1.mTm* primer pair) were used for normalization. B) *OSH4* and *OSH7* transcript levels. Transcripts were determined as in Figure S1A, using *OSH4.pTm/OSH4.mTm* (69 bp), *OSH7A.pTm/OSH7A.mTm* (84 bp), *OSH7 α .pTm/OSH7 α .mTm* (65 bp) primer pairs, respectively.

Figure S2: Deletion of *OSH2* and *OSH3* do not recover invasive growth in the *drs2* mutant. A) Invasive filamentous growth is not restored in the *drs2/drs2* mutant upon deletion of *OSH2* or *OSH3*. Indicated strains were grown on agar-containing YEPD with FCS and images were taken after 6 days. Similar results were observed in 2 independent experiments. B) *DRS2* and *OSH2-3* transcript levels. Transcripts were determined as in Figure S1A, using *OSH2.pTm/OSH2.mTm* (74 bp), *OSH3.pTm/OSH3.mTm* (74 bp) primer pairs, respectively.

Figure S3: Drs2 residues analogous to those of *S. cerevisiae* required for PS recognition are not critical for hyphal growth in *C. albicans*. A) Alignment of *S. cerevisiae* and *C. albicans* relevant Drs2 sequences with mutated residues indicated. The residues shown to specifically alter PS recognition in *S. cerevisiae*, Drs2^{F511Y} and Drs2^{QQ-GA} (Baldrige & Graham, 2012 & 2013) are located in conserved regions in *S. cerevisiae* Drs2's TMD3 and TMD1, respectively. *C. albicans* Drs2 has 66% overall identity with its *S. cerevisiae* counterpart and the mutated residues correspond to F520, Q242 and Q243. B) PS distribution in *drs2*^{F520Y} and *drs2*^{QQ-GA} mutant strains. Indicated cells expressing GFP-LactC2 were incubated as in Figure 5B, with sum projections of representative cells shown. C) Hyphal growth is not altered in *drs2*^{F520Y} and *drs2*^{QQ-GA} mutant strains. Cells from the indicated strains were incubated with FCS for 90 min at 37C. There was no difference in the percent of filamentous cells (75%, 80% and 85% for the *drs2* + *DRS2*, *drs2* + *drs2*^{F520Y} and *drs2* + *drs2*^{QQ-GA} strains, respectively, compared to 15% for the *drs2* strain; n ~ 100 cells) or the filament lengths (17 ±4 μm for the complemented strain, as well as the two strains expressing mutated versions of Drs2; n ~ 50 cells). Bars are 5 μm.

Table I: Strains used in the study.

STRAIN	RELEVANT GENEOTYPE	REFERENCE
BWP17	<i>ura3Δ::λimm434/ura3Δ::λimm434</i> <i>his1Δ::hisG/his1Δ::hisG</i> <i>arg4::hisG/arg4Δ::hisG</i>	[68]
PY1206	Same as BWP17 with <i>RP10::ARG4-pADH1-GFP-PHPLC81-PHPLC81-GFP</i>	[48]
PY2263	Same as BWP17 with <i>RP10:: ARG4 pACT1-CRIBGFP</i>	[40]
PY2045	Same as BWP17 with <i>RP10:: pADH1-FAPP1^[E50A,H54A] GFP</i>	[47]
PY3303	Same as BWP17 with <i>DRS2Δ::URA3/DRS2</i>	[31]
PY3239	Same as BWP17 with <i>RP10::ARG4-pACT1GFP-yeLactC2</i>	[31]
PY3310	Same as BWP17 with <i>drs2Δ::HIS1/drs2Δ::URA3</i>	[31]
PY3375	Same as PY3310 with <i>RP10::ARG4</i>	[31]
PY3873	Same as PY3310 with <i>RP10:: pADH1-FAPP1^[E50A,H54A] GFP</i>	[47]
PY3921	Same as BWP17 with <i>osh4Δ::URA3/osh4Δ::HIS1</i>	This study
PY3945	Same as BWP17 with <i>osh3Δ::HIS1/osh3Δ::URA3</i>	This study
PY3974	Same as PY3921 with <i>RP10::ARG4</i>	This study
PY3977	Same as PY3945 with <i>RP10::ARG4</i>	This study
PY3995	Same as BWP17 with <i>osh2Δ::HIS1/osh2Δ::URA3</i>	This study
PY4002	Same as PY3995 with <i>RP10::ARG4</i>	This study
PY4050	Same as PY3310 with <i>RP10::ARG4-pADH1-GFP-PHPLC81-PHPLC81-GFP</i>	This study
PY4665	Same as PY3303 (URA3) with <i>DRS2::DRS2-GFPγ-HIS1</i>	This study
PY4671	Same as PY3310 with <i>drs2Δ::HIS1/drs2Δ::SAT1</i>	This study
PY4861	<i>ura3Δ::λ imm434/ura3Δ::λ imm434</i> <i>his1::hisG/HIS1::his1::hisG</i> <i>arg4::hisG/URA3::ARG4::arg4::hisG</i>	[66]
PY4928	Same as PY4665 with <i>MLC1 /MLC1-mScarlet-ARG4</i>	This study
PY4946	Same as BWP17 with <i>dnf1Δ::SAT1/dnf1Δ::HYGB</i>	This study
PY4972	Same as PY3310 with <i>RP10:: ARG4 pACT1-CRIBGFP</i>	This study

PY5003	Same as PY3375 with <i>NEUT5L::SAT1-pADHDF2</i>	This study
PY5005	Same as PY4861 with <i>NEUT5L::SAT1-pADHDF2</i>	This study
PY5042	Same as PY3310 with <i>RP10::ARG4-pDRS2DRS2</i>	[31]
PY5045	Same as PY3310 with <i>RP10::ARG4-pDRS2DRS2F520Y</i>	This study
PY5134	Same as PY3310 with <i>NEUT5L::SAT1-pACT1GFP-yeLactC2</i>	This study
PY5151	Same as PY5134 with <i>RP10::ARG4-pDRS2DRS2</i>	This study
PY5156	Same as PY5134 with <i>RP10::ARG4-pDRS2DRS2F520Y</i>	This study
PY5218	Same as PY4676 with <i>MLC1/MLC1-mScarlet-ARG4</i>	This study
PY5246	Same as BWP17 with <i>osh7aΔ::SAT1/osh7αΔ::HIS1</i>	This study
PY5256	Same as PY5246 with <i>RP10::URA3 ARG4</i>	This study
PY5296	Same as PY4671 with <i>osh4Δ::URA3/osh4Δ::HYGB</i>	This study
PY5297	Same as PY4671 with <i>osh7αΔ::HYGB/OSH7aΔ::URA3</i>	This study
PY5336	Same as PY3921 with <i>RP10::ARG4-pACT1GFP-yeLactC2</i>	This study
PY5349	Same as PY4677 with <i>MLC1/MLC1-mScarlet-ARG4</i>	This study
PY5364	Same as PY5296 with <i>RP10::ARG4-pACT1GFP-yeLactC2</i>	This study
PY5539	Same as PY5296 with <i>RP10::ARG4</i>	This study
PY5568	Same as PY3310 with <i>RP10::ARG4-pADH1- GFP-(PH^{OSH2[H340R]})₂-GFP</i>	This study
PY5613	Same as BWP17 with <i>CDC10/CDC10::CDC10-mScarlet-ARG4</i> and <i>NEUT5L::SAT1-pADH1miRFP670CtRac1</i>	This study
PY5615	Same as 3310 with with <i>CDC10/CDC10::CDC10-mScarlet-ARG4</i> and <i>NEUT5L::SAT1-pADH1miRFP670CtRac1</i>	This study
PY5619	Same as BWP17 with <i>RP10::ARG4-pADH1- GFP-(PH^{OSH2[H340R]})₂-GFP</i>	[47]
PY5626	Same as PY3921 with <i>RP10::ARG4-pADH1- GFP-(PH^{OSH2[H340R]})₂-GFP</i>	This study
PY5630	Same as PY5296 with <i>RP10::ARG4-</i>	This study

	<i>pADH1-GFP-(PH^{OSH2[H340R]})₂-GFP</i>	
PY5674	Same as PY5296 with <i>RP10::ARG4-pOSH4OSH4</i>	This study
PY5677	Same as BWP17 with <i>DNF2Δ::HIS1/DNF2</i>	This study
PY5741	Same as BWP17 with <i>dnf3Δ::URA3/dnf3Δ::SAT1</i>	This study
PY5746	Same as PY5677 with <i>DNF2::DNF2-GFPγ-URA3</i>	This study
PY5801	Same as PY5741 with <i>RP10::ARG4-pExp</i> and <i>his1Δ::HIS1</i>	This study
PY5804	Same as BWP17 with <i>dnf2Δ::HIS1/dnf2Δ::ARG4</i>	This study
PY5814	Same as PY5804 with <i>NEUT5L::URA3</i>	This study
PY5915	Same as PY5746 with <i>MLC1/MLC1-mScarlet-ARG4</i>	This study
PY5919	Same as PY5814 with <i>NEUT5L::SAT1-pADHDNF2</i>	This study
PY5922	Same as PY5871 with <i>NEUT5L::SAT1-pADHDNF2</i>	This study
PY6037	Same as BWP17 with <i>RP10::ARG4-pACT1-mScarlet-D4H</i>	This study
PY6076	Same as PY3921 with <i>RP10::ARG4-pACT1-mScarlet-D4H</i>	This study
PY6083	Same as PY3310 with <i>RP10::ARG4-pACT1-mScarlet-D4H</i>	This study
PY6213	Same as PY6083 with <i>NEUT5L::pACT1-Turquoise-CtRAC1-SAT1</i>	This study
PY6218	Same as PY6083 with <i>NEUT5L::SAT1-pDRS2DRS2</i>	This study
PY6235	Same as PY4946 with <i>RP10::ARG4</i>	This study
PY6237	Same as PY6037 with <i>NEUT5L::pACT1-Turquoise-CtRAC1-SAT1</i>	This study
PY6239	Same as PY4665 with <i>NEUT5L::mScarlet-CtRAC1-SAT1</i>	This study
PY6241	Same as PY5746 with <i>NEUT5L::mScarlet-CtRAC1-SAT1</i>	This study
PY6260	Same as PY3310 with <i>RP10::ARG4-pDRS2DRS2QQ-GA</i>	This study
PY6284	Same as PY5134 with <i>RP10::ARG4-pDRS2DRS2QQ-GA</i>	This study
PY6286	Same as PY6083 with <i>osh4Δ::HYGB/osh4Δ::SAT1</i>	This study
PY6393	Same as PY4861 with <i>CDR1/CDR1::CDR1-GFP-SAT1</i>	This study
PY6395	Same as PY3375 with	This study

	<i>CDR1/CDR1::CDR1-GFP-SAT1</i>	
PY6400	Same as PY5804 with <i>dnf1Δ::URA3/dnf1Δ::HYGB</i>	This study
PY6407	Same as PY5568 with <i>NEUT5L::SAT1-pDRS2DRS2</i>	This study
PY6408	Same as PY4671 with <i>osh2Δ::URA3/osh2Δ::HYGB</i>	This study
PY6431	Same as PY4671 with <i>osh3Δ::URA3/osh3Δ::ARG4</i>	This study
PY6432	Same as PY4671 with <i>sac1Δ::ARG4/sac1Δ::HYGB</i>	This study
PY6436	Same as BWP17 with <i>sac1Δ::ARG4/sac1Δ::HYGB</i>	This study

Table II: Primer sequences

PRIMER	SEQUENCE
DNF1.P1	CAAGTGACAACCTCCAGTTAGCTCCTATTATTTGCATCGACCAAATCTAG AAGATCTTACTAGAACATCGAAAGTTGGAGTGACCATTTGCTGAAGCTTC GTACGCTGCAGGTC
DNF1.P2	CGAAAAATGTAAAACCGAAATCAAATGCAATGATACAATAAACTGAAACC CAATTACCACATAAAGTAGGTTAAGGATTCAAAGCTACACTATTCCTCTGA TATCATCGATGAATTCGAG
DNF2.P1	CACCTAATTCTACTTTATCCAATTCGAATTGCTATCCACACTCTTATGACT AAAAATAAGCACAATTCACGCGAAGCTTCGTACGCTGCAGGTC
DNF2.P2	CTTGATGTGTGTTTGTGTCTATAATGTTTTCTTTATGTTATGCAAATGA AAATTGCTGTTAATTCATTGAAGATACTCTCTGATATCATCGATGAATTCG AG
DNF2.P3	CACCTAATTCTACTTTATCCAATTCGAATTGCTATCCACACTCTTATGACT AAAAATAAGCACAATTCACGCTAAATAATAGTAGTGATGGAGTGTGGAA TTGTGAGCGGATA
DNF2.P4	GTATGTGTGTTTGTGTCTATAATGTTTTCTTTATGTTATGCAAATGAAAA TTGCTGTTAATTCATTGAAGATACTCTTTTTGATTTTCGTAGCTTATTCTA GATGCTCTTTCCAGTCACGACGTT
DNF3.P1	CTACAGATTCAACTTTATAGAATCCTACATTGAGTCACCTGTCTCATCATTT GGTCATTAATTTACAACACTACAGTGAATCATAAATTAGATTTGGAAGCTTC GTACGCTGCAGGTC
DNF3.P2	GCTCGGGTGAATTGAGACAATTTGATGTATCTTGTATATTTGTATAAATA CTTAGATGTACATTTCTTTGGTTTTGGAAACTCAATAGACACCTCTGATAT CATCGATGAATTCGAG
OSH4.P1	CTATATTTTAAAATAACACATCGTCTTCAAGCCAACAGTATATTTTTTTGTC ATGTCAAACCTCAAATCCAGTTCTGAAGTGTGGAATTGTGAGCGGATA
OSH4.P2	GATGTACTACTATTATAAACATTATTTTACGAAATTGAAAAAACCTACTCT AAATTCATTTAAAAGACTATTTCTTTCCAGTCACGACGTT
OSH7A.P1	CCCTTCCATTAAATCTCCCTGAGATTTGTTGTTTTTATCTGTATTCAGTAC GAAGTCAAGTTCACCATGGGTTTAACTGTGGAATTGTGAGCGGATA
OSH7A.P2	CGATTTCTAATCTAAACTAAAGATAAATATATAAAGAAGTACATTAATTTG CAATATATCAAAAACGAATTAAGTTTCTTCTTTCCAGTCACGACGTT
OSH7 α .P1	CCAGCGAACATGCACTTTTCTTTGTTGAAGGTTTCAGGTAATCAGTATGG GATTAACAGCTAAATTAGATAAGTGTGGAATTGTGAGCGGATA
OSH7 α .P2	TAAATTAGACAATACTACTTGATTCTAATTCAAATCTATTAATATGACCGT ATATTAAGTCCAACAATTAATTACTTTCCAGTCACGACGTT
OSH2.P1	CCATAATAAATTACTGATAAAACACTAACAACCTTAGAATAAACAGCTAAA ATCATGAATGATTCACCCCACTAAGTGCGAAGCTTCGTACGCTGCAGGT C
OSH2.P2	CAATCAACAATTAACAGTCTAAAATATGTCTCCCGTGTTCCGCAAATCT TGTGCCTTTCTTCTAGGCCAATACTCTGATATCATCGATGAATTCGAG
OSH3.P1	CCCACTCAATCCATTATTTCTTTCCCTTGACAGTTGAACTTTCCCATACCA ACTTGAAATATGGAACTTTAGAAGGAAGCTTCGTACGCTGCAGGTC
OSH3.P2	GGATTCTATGATCTAAATAATATAACGTCTAATAGATATGAAAAAGACAA

	AGAAATAGTAAAATTTACCACAATTTAATCTCTGATATCATCGATGAATTC GAG
SAC1.P1	AATATAAACACTATTTTTTCCACTTTCTTTAATCTAACCTTATACGCAACTAT ACAATTATATAACAGAAAATGGTGTTAGAAGCTTCGTACGCTGCAGGTC
SAC1.P2	ATCTATTATATAAAATAAGCAGCTACAACCTAAAGACAACCTTTCTAAAAAAA AAAACAACCCCCACAGCTAATCAATTCTTTCTGATATCATCGATGAATTCG AG
DNF2.P5	GGCGCGCCATGACTAAAAATAAGCACAATTTACGCG
DNF2.P6	ATACGCGTTTAATTCATTGAAGATACTCTTTTTG
DRS2.P3	TAAGTAGTCTTTTAATATAGCCGAATTCCTCCG
DRS2.P4	TATAGCGGCCGCGAGTTGGTTAATAACAAAATATCAG
OSH4.P3	ATGTCGACAAAACAACACAAGAAAGAGCTGCTGCTG
OSH4.P4	TATAGCGGCCGCGGTTAGTAACGCTCTTAGAACGTTGG
DRS2.P5	CAAGTTGAAGGTCAAGATCAAGATAAAATTGTTAGATTATATGATACTAC TAAAAAAGAGGAGTTTTTGGGAATTATCAGAAAGTAAGGGTGCTGGC GCAGGTGCTTC
DRS2.P6	GGGAGTGAGATAGTTGTATATCAAACAGTTCTATAGCTTTAAATAAATAA AAAAAACATTCATTGATTGCATTAATACTACTCATACTCTATTTATCTG ATATCATCGATGAATTCGAG
DNF2.P7	GGTAGCTACAGAAGAAATCCATTAGAAGATTTTGATGATGAACAAAAA GAGCATCTAGAATAAGCTACGAAAATCAAAAAGAGTATCTTCAATGAAT GGTGCTGGCGCAGGTGCTTC
DNF2.P8	CCTCTATTCTTTATATAAATATGCTTGAAATCTTGTATGTGTGTTTGTG TCTATAATGTTTTCTTTTATGTTATGCAAATGAAAATTGCTGTTATCTGATA TCATCGATGAATTCGAG
MLC1.P1	GATGAGTTATTAAGGGGTCAATGTAACCTCTGATGGAAATGTGGATTA TGTTGAATTTGTCAAATCAATTTTAGACCAAGGTGCTGGCGCAGGTGCTTC
MLC1.P2	CGAACAAGACTATACAATAACTATAATTTGTAAACTTGTAGTATATATAT TTCAATGGTTAATTGTAATTTTCTTTTATTCTGATATCATCGATGAATTCG AG
CDC10.P1	CAATCAAACCAAGATTTGAAGAACACCTCTGGTGTGCCAAATGCTCCTAT GTTCCAATCAACTACAGGTACTGCTGCTGCTAGAGGTGCTGGCGCAGGTG CTTC
CDC10.P2	CGCGTTTTGCTTTTCAACAAACACACAAAAGAAGAGGAATACAAAAAAGT AAAATCACATTATATCAATAACAAACCTGATATCATCGATGAATTCGAG
D4H.P1	ACGGCGCGCCGACTAGTGGATCCAAGGGAAAAATAAACTTAGATCATAG TGGAGCC
D4H.P2	GATACGCGTTAATTGTAAGTAATACTAGATCCAGGG
DRS2.P7	GGATTTTATTTTCCAATTTGGTACCCATTTTATTGTATGTCACGGTTGAATT GATCAAATAT
DRS2.P8	ATATTTGATCAATTCACCGTGACATACAATGAAATGGGTACCAAATTGG AAAATAAAATCC
DRS2.P9	GCCAATTTATTTTCTTGTACATCAATTATTGGAGCAGTACCTCATGTTT CCCCACAAATAG
DRS2.P10	CTATTTGTGGGGGAAACATGAGGTACTGCTCCAATAATTGATGTAACAAG GAAAAATAAATTGGC

RT.PCR	
DRS2.pTm	CGGCATTAGTGGTTACCATGT
DRS2.mTm	GCAGGATACCAACCTAACCATAA
DNF1.pTm	GCACAATCAACGGGAAGTCATAC
DNF1.mTm	AATGCCTGCACGTTTATCCAA
DNF2.pTm	TGACAAGACCGGGACATTA
DNF2.mTm	TCCGTAACCCAGCCAAT
DNF3.pTm	AAGCATCAATGGCAGGTCATC
DNF3.mTm	GCTGCCGTGCTTGTCTTG
OSH4.pTm	TTTGATTACTGCTGCTCCTT
OSH4.mTm	AATGTGACCACTGGATGCTT
OSH7a.pTm	TGAAGCAGCTGTCAAATCTAATGTG
OSH7a.mTm	CTGTCCCTCGTTATCCATTTTCATC
OSH7 α .pTm	GTAACTCGTCTGCAGCAATCATG
OSH7 α .mTm	CCTCGTTGTCCCATTTACCAA
OSH2.pTm	AAGCCAGAAAACAGAGGGAAGAT
OSH2.mTm	TCACTGGATGCTTTCTCTTAACAAA
OSH3.pTm	GGGTAACTTGCACCTACGGATT
OSH3.mTm	GCAGTGTCTGTATCTCCCTTTTCA
UME6.pTm	TGGCTCCACTTACAAATCATAGTGA
UME6.mTm	GCTTTACCAATCCTAGTCCCAACTC
SAC1.pTm	CCCATTCCACAGCAACAGATG
SAC1.mTm	TTCAACACCACCTCCAGTGT
ACT1.pTm	ATGTTCCCAGGTATTGCTGA
ACT1.mTm	ACATTTGTGGTGAACAATGG

References

1. Das A, Slaughter BD, Unruh JR, Bradford WD, Alexander R, Rubinstein B, et al. Flippase-mediated phospholipid asymmetry promotes fast Cdc42 recycling in dynamic maintenance of cell polarity. *Nat Cell Biol.* 2012;14(3):304-10. Epub 2012/02/22. doi: 10.1038/ncb2444. PubMed PMID: 22344035; PubMed Central PMCID: PMC3534761.
2. Fairn GD, Hermansson M, Somerharju P, Grinstein S. Phosphatidylserine is polarized and required for proper Cdc42 localization and for development of cell polarity. *Nat Cell Biol.* 2011;13(12):1424-30. Epub 2011/10/04. doi: 10.1038/ncb2351. PubMed PMID: 21964439.
3. Meca J, Massoni-Laporte A, Martinez D, Sartorel E, Loquet A, Habenstein B, et al. Avidity-driven polarity establishment via multivalent lipid-GTPase module interactions. *EMBO J.* 2019;38(3). Epub 2018/12/19. doi: 10.15252/embj.201899652. PubMed PMID: 30559330; PubMed Central PMCID: PMC6356062.
4. Haupt A, Minc N. Gradients of phosphatidylserine contribute to plasma membrane charge localization and cell polarity in fission yeast. *Mol Biol Cell.* 2017;28(1):210-20. Epub 2016/11/18. doi: 10.1091/mbc.E16-06-0353. PubMed PMID: 27852900; PubMed Central PMCID: PMC5221626.
5. Kay JG, Fairn GD. Distribution, dynamics and functional roles of phosphatidylserine within the cell. *Cell Commun Signal.* 2019;17(1):126. Epub 2019/10/17. doi: 10.1186/s12964-019-0438-z. PubMed PMID: 31615534; PubMed Central PMCID: PMC6792266.
6. Noack LC, Jaillais Y. Functions of Anionic Lipids in Plants. *Annu Rev Plant Biol.* 2020;71:71-102. Epub 2020/05/23. doi: 10.1146/annurev-arplant-081519-035910. PubMed PMID: 32442391.

7. Cassilly CD, Reynolds TB. PS, It's Complicated: The Roles of Phosphatidylserine and Phosphatidylethanolamine in the Pathogenesis of *Candida albicans* and Other Microbial Pathogens. *J Fungi (Basel)*. 2018;4(1). Epub 2018/02/21. doi: 10.3390/jof4010028. PubMed PMID: 29461490; PubMed Central PMCID: PMC5872331.
8. Rizzo J, Stanchev LD, da Silva VKA, Nimrichter L, Pomorski TG, Rodrigues ML. Role of lipid transporters in fungal physiology and pathogenicity. *Comput Struct Biotechnol J*. 2019;17:1278-89. Epub 2020/01/11. doi: 10.1016/j.csbj.2019.09.001. PubMed PMID: 31921394; PubMed Central PMCID: PMC6944739.
9. Chen YL, Montedonico AE, Kauffman S, Dunlap JR, Menn FM, Reynolds TB. Phosphatidylserine synthase and phosphatidylserine decarboxylase are essential for cell wall integrity and virulence in *Candida albicans*. *Mol Microbiol*. 2010;75(5):1112-32. Epub 2010/02/06. doi: 10.1111/j.1365-2958.2009.07018.x. PubMed PMID: 20132453.
10. Chen T, Jackson JW, Tams RN, Davis SE, Sparer TE, Reynolds TB. Exposure of *Candida albicans* beta (1,3)-glucan is promoted by activation of the Cek1 pathway. *PLoS Genet*. 2019;15(1):e1007892. Epub 2019/02/01. doi: 10.1371/journal.pgen.1007892. PubMed PMID: 30703081; PubMed Central PMCID: PMC6372213.
11. Lenoir G, D'Ambrosio JM, Dieudonne T, Copic A. Transport Pathways That Contribute to the Cellular Distribution of Phosphatidylserine. *Front Cell Dev Biol*. 2021;9:737907. Epub 2021/09/21. doi: 10.3389/fcell.2021.737907. PubMed PMID: 34540851; PubMed Central PMCID: PMC8440936.
12. Lyons JA, Timcenko M, Dieudonne T, Lenoir G, Nissen P. P4-ATPases: how an old dog learnt new tricks - structure and mechanism of lipid flippases. *Curr Opin*

Struct Biol. 2020;63:65-73. Epub 2020/06/04. doi: 10.1016/j.sbi.2020.04.001. PubMed PMID: 32492637.

13. Lopez-Marques RL. Lipid flippases in polarized growth. *Curr Genet.* 2021;67(2):255-62. Epub 2021/01/04. doi: 10.1007/s00294-020-01145-0. PubMed PMID: 33388852.

14. Lenoir G, Williamson P, Puts CF, Holthuis JC. Cdc50p plays a vital role in the ATPase reaction cycle of the putative aminophospholipid transporter Drs2p. *J Biol Chem.* 2009;284(27):17956-67. Epub 2009/05/05. doi: 10.1074/jbc.M109.013722. PubMed PMID: 19411703; PubMed Central PMCID: PMCPMC2709398.

15. Saito K, Fujimura-Kamada K, Furuta N, Kato U, Umeda M, Tanaka K. Cdc50p, a protein required for polarized growth, associates with the Drs2p P-type ATPase implicated in phospholipid translocation in *Saccharomyces cerevisiae*. *Mol Biol Cell.* 2004;15(7):3418-32. Epub 2004/04/20. doi: 10.1091/mbc.e03-11-0829. PubMed PMID: 15090616; PubMed Central PMCID: PMCPMC452594.

16. Timcenko M, Lyons JA, Janulienė D, Ulstrup JJ, Dieudonné T, Montigny C, et al. Structure and autoregulation of a P4-ATPase lipid flippase. *Nature.* 2019;571(7765):366-70. Epub 2019/06/28. doi: 10.1038/s41586-019-1344-7. PubMed PMID: 31243363.

17. Natarajan P, Wang J, Hua Z, Graham TR. Drs2p-coupled aminophospholipid translocase activity in yeast Golgi membranes and relationship to in vivo function. *Proc Natl Acad Sci U S A.* 2004;101(29):10614-9. Epub 2004/07/14. doi: 10.1073/pnas.0404146101. PubMed PMID: 15249668; PubMed Central PMCID: PMCPMC489982.

18. Zhou X, Graham TR. Reconstitution of phospholipid translocase activity with purified Drs2p, a type-IV P-type ATPase from budding yeast. *Proc Natl Acad Sci U S*

- A. 2009;106(39):16586-91. Epub 2009/10/07. doi: 10.1073/pnas.0904293106. PubMed PMID: 19805341; PubMed Central PMCID: PMCPMC2757829.
19. Best JT, Xu P, Graham TR. Phospholipid flippases in membrane remodeling and transport carrier biogenesis. *Curr Opin Cell Biol.* 2019;59:8-15. Epub 2019/03/22. doi: 10.1016/j.ceb.2019.02.004. PubMed PMID: 30897446; PubMed Central PMCID: PMCPMC6726550.
20. Hua Z, Fatheddin P, Graham TR. An essential subfamily of Drs2p-related P-type ATPases is required for protein trafficking between Golgi complex and endosomal/vacuolar system. *Mol Biol Cell.* 2002;13(9):3162-77. Epub 2002/09/11. doi: 10.1091/mbc.e02-03-0172. PubMed PMID: 12221123; PubMed Central PMCID: PMCPMC124150.
21. Chen CY, Ingram MF, Rosal PH, Graham TR. Role for Drs2p, a P-type ATPase and potential aminophospholipid translocase, in yeast late Golgi function. *J Cell Biol.* 1999;147(6):1223-36. Epub 1999/12/22. doi: 10.1083/jcb.147.6.1223. PubMed PMID: 10601336; PubMed Central PMCID: PMCPMC2168089.
22. Pomorski T, Lombardi R, Riezman H, Devaux PF, van Meer G, Holthuis JC. Drs2p-related P-type ATPases Dnf1p and Dnf2p are required for phospholipid translocation across the yeast plasma membrane and serve a role in endocytosis. *Mol Biol Cell.* 2003;14(3):1240-54. Epub 2003/03/13. doi: 10.1091/mbc.e02-08-0501. PubMed PMID: 12631737; PubMed Central PMCID: PMCPMC151593.
23. Frosig MM, Costa SR, Liesche J, Osterberg JT, Hanisch S, Nintemann S, et al. Pseudohyphal growth in *Saccharomyces cerevisiae* involves protein kinase-regulated lipid flippases. *J Cell Sci.* 2020;133(15). Epub 2020/07/15. doi: 10.1242/jcs.235994. PubMed PMID: 32661085.

24. Sartorel E, Barrey E, Lau RK, Thorner J. Plasma membrane aminoglycerolipid flippase function is required for signaling competence in the yeast mating pheromone response pathway. *Mol Biol Cell*. 2015;26(1):134-50. Epub 2014/11/08. doi: 10.1091/mbc.E14-07-1193. PubMed PMID: 25378585; PubMed Central PMCID: PMC4279224.
25. Schultzhaus Z, Yan H, Shaw BD. *Aspergillus nidulans* flippase DnfA is cargo of the endocytic collar and plays complementary roles in growth and phosphatidylserine asymmetry with another flippase, DnfB. *Mol Microbiol*. 2015;97(1):18-32. Epub 2015/04/08. doi: 10.1111/mmi.13019. PubMed PMID: 25846564.
26. Yun Y, Guo P, Zhang J, You H, Guo P, Deng H, et al. Flippases play specific but distinct roles in the development, pathogenicity, and secondary metabolism of *Fusarium graminearum*. *Mol Plant Pathol*. 2020;21(10):1307-21. Epub 2020/09/04. doi: 10.1111/mpp.12985. PubMed PMID: 32881238; PubMed Central PMCID: PMC7488471.
27. Gilbert MJ, Thornton CR, Wakley GE, Talbot NJ. A P-type ATPase required for rice blast disease and induction of host resistance. *Nature*. 2006;440(7083):535-9. Epub 2006/03/24. doi: 10.1038/nature04567. PubMed PMID: 16554820.
28. Li B, Dong X, Zhao R, Kou R, Zheng X, Zhang H. The t-SNARE protein FgPep12, associated with FgVam7, is essential for ascospore discharge and plant infection by trafficking Ca²⁺ ATPase FgNeo1 between Golgi and endosome/vacuole in *Fusarium graminearum*. *PLoS Pathog*. 2019;15(5):e1007754. Epub 2019/05/09. doi: 10.1371/journal.ppat.1007754. PubMed PMID: 31067272; PubMed Central PMCID: PMC6527245.
29. Zhang J, Yun Y, Lou Y, Abubakar YS, Guo P, Wang S, et al. FgAP-2 complex is essential for pathogenicity and polarised growth and regulates the apical localisation

of membrane lipid flippases in *Fusarium graminearum*. *Cell Microbiol.* 2019;21(8):e13041. Epub 2019/05/16. doi: 10.1111/cmi.13041. PubMed PMID: 31087807.

30. Douglas LM, Konopka JB. Plasma membrane architecture protects *Candida albicans* from killing by copper. *PLoS Genet.* 2019;15(1):e1007911. Epub 2019/01/12. doi: 10.1371/journal.pgen.1007911. PubMed PMID: 30633741; PubMed Central PMCID: PMC6345494.

31. Labbaoui H, Bogliolo S, Ghugtyal V, Solis NV, Filler SG, Arkowitz RA, et al. Role of Arf GTPases in fungal morphogenesis and virulence. *PLoS Pathog.* 2017;13(2):e1006205. Epub 2017/02/14. doi: 10.1371/journal.ppat.1006205. PubMed PMID: 28192532; PubMed Central PMCID: PMC5325608.

32. Xu D, Zhang X, Zhang B, Zeng X, Mao H, Xu H, et al. The lipid flippase subunit Cdc50 is required for antifungal drug resistance, endocytosis, hyphal development and virulence in *Candida albicans*. *FEMS Yeast Res.* 2019;19(3). Epub 2019/04/21. doi: 10.1093/femsyr/foz033. PubMed PMID: 31004489.

33. Zheng X, Wang Y, Wang Y. Hgc1, a novel hypha-specific G1 cyclin-related protein regulates *Candida albicans* hyphal morphogenesis. *EMBO J.* 2004;23(8):1845-56. Epub 2004/04/09. doi: 10.1038/sj.emboj.7600195. PubMed PMID: 15071502; PubMed Central PMCID: PMC394249.

34. Carlisle PL, Kadosh D. *Candida albicans* Ume6, a filament-specific transcriptional regulator, directs hyphal growth via a pathway involving Hgc1 cyclin-related protein. *Eukaryot Cell.* 2010;9(9):1320-8. Epub 2010/07/27. doi: 10.1128/EC.00046-10. PubMed PMID: 20656912; PubMed Central PMCID: PMC2937344.

35. Banerjee M, Thompson DS, Lazzell A, Carlisle PL, Pierce C, Monteagudo C, et al. UME6, a novel filament-specific regulator of *Candida albicans* hyphal extension and virulence. *Mol Biol Cell*. 2008;19(4):1354-65. Epub 2008/01/25. doi: 10.1091/mbc.E07-11-1110. PubMed PMID: 18216277; PubMed Central PMCID: PMC2291399.
36. Naglik JR, Gaffen SL, Hube B. Candidalysin: discovery and function in *Candida albicans* infections. *Curr Opin Microbiol*. 2019;52:100-9. Epub 2019/07/10. doi: 10.1016/j.mib.2019.06.002. PubMed PMID: 31288097; PubMed Central PMCID: PMC6687503.
37. Hube B, Monod M, Schofield DA, Brown AJ, Gow NA. Expression of seven members of the gene family encoding secretory aspartyl proteinases in *Candida albicans*. *Mol Microbiol*. 1994;14(1):87-99. Epub 1994/10/01. doi: 10.1111/j.1365-2958.1994.tb01269.x. PubMed PMID: 7830564.
38. Cleary IA, Reinhard SM, Miller CL, Murdoch C, Thornhill MH, Lazzell AL, et al. *Candida albicans* adhesin Als3p is dispensable for virulence in the mouse model of disseminated candidiasis. *Microbiology (Reading)*. 2011;157(Pt 6):1806-15. Epub 2011/03/26. doi: 10.1099/mic.0.046326-0. PubMed PMID: 21436220; PubMed Central PMCID: PMC3167918.
39. Gonzalez-Novo A, Jimenez J, Garcia MJ, Rios-Serrano I, Pla J, Jimenez A, et al. Dynamics of CaCdc10, a septin of *Candida albicans*, in living cells and during infection. *Int Microbiol*. 2004;7(2):105-12. Epub 2004/07/13. PubMed PMID: 15248158.
40. Corvest V, Bogliolo S, Follette P, Arkowitz RA, Bassilana M. Spatiotemporal regulation of Rho1 and Cdc42 activity during *Candida albicans* filamentous growth.

Mol Microbiol. 2013;89(4):626-48. Epub 2013/06/26. doi: 10.1111/mmi.12302. PubMed PMID: 23796158.

41. Crampin H, Finley K, Gerami-Nejad M, Court H, Gale C, Berman J, et al. *Candida albicans* hyphae have a Spitzenkorper that is distinct from the polarisome found in yeast and pseudohyphae. *J Cell Sci.* 2005;118(Pt 13):2935-47. Epub 2005/06/25. doi: 10.1242/jcs.02414. PubMed PMID: 15976451.

42. Puerner C, Serrano A, Wakade RS, Bassilana M, Arkowitz RA. A Myosin Light Chain Is Critical for Fungal Growth Robustness in *Candida albicans*. *mBio.* 2021;12(5):e0252821. Epub 2021/10/06. doi: 10.1128/mBio.02528-21. PubMed PMID: 34607458.

43. Vauchelles R, Stalder D, Botton T, Arkowitz RA, Bassilana M. Rac1 dynamics in the human opportunistic fungal pathogen *Candida albicans*. *PLoS One.* 2010;5(10):e15400. Epub 2010/11/10. doi: 10.1371/journal.pone.0015400. PubMed PMID: 21060846; PubMed Central PMCID: PMC2965673.

44. Del Vecchio K, Stahelin RV. Investigation of the phosphatidylserine binding properties of the lipid biosensor, Lactadherin C2 (LactC2), in different membrane environments. *J Bioenerg Biomembr.* 2018;50(1):1-10. Epub 2018/02/11. doi: 10.1007/s10863-018-9745-0. PubMed PMID: 29426977; PubMed Central PMCID: PMC5820145.

45. Leventis PA, Grinstein S. The distribution and function of phosphatidylserine in cellular membranes. *Annu Rev Biophys.* 2010;39:407-27. Epub 2010/03/03. doi: 10.1146/annurev.biophys.093008.131234. PubMed PMID: 20192774.

46. Yeung T, Gilbert GE, Shi J, Silvius J, Kapus A, Grinstein S. Membrane phosphatidylserine regulates surface charge and protein localization. *Science.*

2008;319(5860):210-3. Epub 2008/01/12. doi: 10.1126/science.1152066. PubMed PMID: 18187657.

47. Ghugtyal V, Garcia-Rodas R, Seminara A, Schaub S, Bassilana M, Arkowitz RA. Phosphatidylinositol-4-phosphate-dependent membrane traffic is critical for fungal filamentous growth. *Proc Natl Acad Sci U S A*. 2015;112(28):8644-9. Epub 2015/07/01. doi: 10.1073/pnas.1504259112. PubMed PMID: 26124136; PubMed Central PMCID: PMC4507248.

48. Vernay A, Schaub S, Guillas I, Bassilana M, Arkowitz RA. A steep phosphoinositide bis-phosphate gradient forms during fungal filamentous growth. *J Cell Biol*. 2012;198(4):711-30. Epub 2012/08/15. doi: 10.1083/jcb.201203099. PubMed PMID: 22891265; PubMed Central PMCID: PMC3514036.

49. Martin SW, Konopka JB. Lipid raft polarization contributes to hyphal growth in *Candida albicans*. *Eukaryot Cell*. 2004;3(3):675-84. Epub 2004/06/11. doi: 10.1128/EC.3.3.675-684.2004. PubMed PMID: 15189988; PubMed Central PMCID: PMC420133.

50. Kishimoto T, Mioka T, Itoh E, Williams DE, Andersen RJ, Tanaka K. Phospholipid flippases and Sfk1 are essential for the retention of ergosterol in the plasma membrane. *Mol Biol Cell*. 2021;32(15):1374-92. Epub 2021/05/27. doi: 10.1091/mbc.E20-11-0699. PubMed PMID: 34038161.

51. Marek M, Vincenzetti V, Martin SG. Sterol biosensor reveals LAM-family Ltc1-dependent sterol flow to endosomes upon Arp2/3 inhibition. *J Cell Biol*. 2020;219(6). Epub 2020/04/23. doi: 10.1083/jcb.202001147. PubMed PMID: 32320462; PubMed Central PMCID: PMC7265315.

52. Wong LH, Gatta AT, Levine TP. Lipid transfer proteins: the lipid commute via shuttles, bridges and tubes. *Nat Rev Mol Cell Biol.* 2019;20(2):85-101. Epub 2018/10/20. doi: 10.1038/s41580-018-0071-5. PubMed PMID: 30337668.
53. Maeda K, Anand K, Chiapparino A, Kumar A, Poletto M, Kaksonen M, et al. Interactome map uncovers phosphatidylserine transport by oxysterol-binding proteins. *Nature.* 2013;501(7466):257-61. Epub 2013/08/13. doi: 10.1038/nature12430. PubMed PMID: 23934110.
54. Moser von Filseck J, Vanni S, Mesmin B, Antonny B, Drin G. A phosphatidylinositol-4-phosphate powered exchange mechanism to create a lipid gradient between membranes. *Nat Commun.* 2015;6:6671. Epub 2015/04/08. doi: 10.1038/ncomms7671. PubMed PMID: 25849868.
55. de Saint-Jean M, Delfosse V, Douguet D, Chicanne G, Payrastré B, Bourguet W, et al. Osh4p exchanges sterols for phosphatidylinositol 4-phosphate between lipid bilayers. *J Cell Biol.* 2011;195(6):965-78. Epub 2011/12/14. doi: 10.1083/jcb.201104062. PubMed PMID: 22162133; PubMed Central PMCID: PMC3241724.
56. Muthusamy BP, Raychaudhuri S, Natarajan P, Abe F, Liu K, Prinz WA, et al. Control of protein and sterol trafficking by antagonistic activities of a type IV P-type ATPase and oxysterol binding protein homologue. *Mol Biol Cell.* 2009;20(12):2920-31. Epub 2009/05/01. doi: 10.1091/mbc.E08-10-1036. PubMed PMID: 19403696; PubMed Central PMCID: PMC2695799.
57. Prasad R, De Wergifosse P, Goffeau A, Balzi E. Molecular cloning and characterization of a novel gene of *Candida albicans*, CDR1, conferring multiple resistance to drugs and antifungals. *Curr Genet.* 1995;27(4):320-9. Epub 1995/03/01. doi: 10.1007/BF00352101. PubMed PMID: 7614555.

58. Parsons AB, Lopez A, Givoni IE, Williams DE, Gray CA, Porter J, et al. Exploring the mode-of-action of bioactive compounds by chemical-genetic profiling in yeast. *Cell*. 2006;126(3):611-25. Epub 2006/08/12. doi: 10.1016/j.cell.2006.06.040. PubMed PMID: 16901791.
59. Cassilly CD, Maddox MM, Cherian PT, Bowling JJ, Hamann MT, Lee RE, et al. SB-224289 Antagonizes the Antifungal Mechanism of the Marine Depsipeptide Papuamide A. *PLoS One*. 2016;11(5):e0154932. Epub 2016/05/18. doi: 10.1371/journal.pone.0154932. PubMed PMID: 27183222; PubMed Central PMCID: PMC4868317.
60. Baldrige RD, Graham TR. Identification of residues defining phospholipid flippase substrate specificity of type IV P-type ATPases. *Proc Natl Acad Sci U S A*. 2012;109(6):E290-8. Epub 2012/02/07. doi: 10.1073/pnas.1115725109. PubMed PMID: 22308393; PubMed Central PMCID: PMC3277569.
61. Baldrige RD, Graham TR. Two-gate mechanism for phospholipid selection and transport by type IV P-type ATPases. *Proc Natl Acad Sci U S A*. 2013;110(5):E358-67. Epub 2013/01/11. doi: 10.1073/pnas.1216948110. PubMed PMID: 23302692; PubMed Central PMCID: PMC3562821.
62. Stefan CJ, Manford AG, Baird D, Yamada-Hanff J, Mao Y, Emr SD. Osh proteins regulate phosphoinositide metabolism at ER-plasma membrane contact sites. *Cell*. 2011;144(3):389-401. Epub 2011/02/08. doi: 10.1016/j.cell.2010.12.034. PubMed PMID: 21295699.
63. Zewe JP, Wills RC, Sangappa S, Goulden BD, Hammond GR. SAC1 degrades its lipid substrate PtdIns4P in the endoplasmic reticulum to maintain a steep chemical gradient with donor membranes. *Elife*. 2018;7. Epub 2018/02/21. doi:

10.7554/eLife.35588. PubMed PMID: 29461204; PubMed Central PMCID: PMC5829913.

64. Zhang B, Yu Q, Jia C, Wang Y, Xiao C, Dong Y, et al. The actin-related protein Sac1 is required for morphogenesis and cell wall integrity in *Candida albicans*. *Fungal Genet Biol*. 2015;81:261-70. Epub 2015/01/13. doi: 10.1016/j.fgb.2014.12.007. PubMed PMID: 25575432.

65. Quon E, Sere YY, Chauhan N, Johansen J, Sullivan DP, Dittman JS, et al. Endoplasmic reticulum-plasma membrane contact sites integrate sterol and phospholipid regulation. *PLoS Biol*. 2018;16(5):e2003864. Epub 2018/05/22. doi: 10.1371/journal.pbio.2003864. PubMed PMID: 29782498; PubMed Central PMCID: PMC5983861.

66. Bassilana M, Blyth J, Arkowitz RA. Cdc24, the GDP-GTP exchange factor for Cdc42, is required for invasive hyphal growth of *Candida albicans*. *Eukaryot Cell*. 2003;2(1):9-18. Epub 2003/02/13. doi: 10.1128/EC.2.1.9-18.2003. PubMed PMID: 12582118; PubMed Central PMCID: PMC141177.

67. Ram AF, Klis FM. Identification of fungal cell wall mutants using susceptibility assays based on Calcofluor white and Congo red. *Nat Protoc*. 2006;1(5):2253-6. Epub 2007/04/05. doi: 10.1038/nprot.2006.397. PubMed PMID: 17406464.

68. Wilson RB, Davis D, Mitchell AP. Rapid hypothesis testing with *Candida albicans* through gene disruption with short homology regions. *J Bacteriol*. 1999;181(6):1868-74. Epub 1999/03/12. doi: 10.1128/JB.181.6.1868-1874.1999. PubMed PMID: 10074081; PubMed Central PMCID: PMC93587.

69. Bijlani S, Thevandavakkam MA, Tsai HJ, Berman J. Autonomously Replicating Linear Plasmids That Facilitate the Analysis of Replication Origin Function in *Candida albicans*. *mSphere*. 2019;4(2). Epub 2019/03/08. doi:

10.1128/mSphere.00103-19. PubMed PMID: 30842269; PubMed Central PMCID: PMC6403455.

70. Lai WC, Sun HF, Lin PH, Ho Lin HL, Shieh JC. A new rapid and efficient system with dominant selection developed to inactivate and conditionally express genes in *Candida albicans*. *Curr Genet*. 2016;62(1):213-35. Epub 2015/10/27. doi: 10.1007/s00294-015-0526-6. PubMed PMID: 26497136.

71. Schaub Y, Dunkler A, Walther A, Wendland J. New pFA-cassettes for PCR-based gene manipulation in *Candida albicans*. *J Basic Microbiol*. 2006;46(5):416-29. Epub 2006/09/30. doi: 10.1002/jobm.200510133. PubMed PMID: 17009297.

72. Gerami-Nejad M, Zacchi LF, McClellan M, Matter K, Berman J. Shuttle vectors for facile gap repair cloning and integration into a neutral locus in *Candida albicans*. *Microbiology (Reading)*. 2013;159(Pt 3):565-79. Epub 2013/01/12. doi: 10.1099/mic.0.064097-0. PubMed PMID: 23306673; PubMed Central PMCID: PMC3709822.

73. Li L, Zhang C, Konopka JB. A *Candida albicans* temperature-sensitive *cdc12-6* mutant identifies roles for septins in selection of sites of germ tube formation and hyphal morphogenesis. *Eukaryot Cell*. 2012;11(10):1210-8. Epub 2012/08/14. doi: 10.1128/EC.00216-12. PubMed PMID: 22886998; PubMed Central PMCID: PMC3485918.

74. Puerner C, Kukhaleishvili N, Thomson D, Schaub S, Noblin X, Seminara A, et al. Mechanical force-induced morphology changes in a human fungal pathogen. *BMC Biol*. 2020;18(1):122. Epub 2020/09/12. doi: 10.1186/s12915-020-00833-0. PubMed PMID: 32912212; PubMed Central PMCID: PMC7488538.

75. Silva PM, Puerner C, Seminara A, Bassilana M, Arkowitz RA. Secretory Vesicle Clustering in Fungal Filamentous Cells Does Not Require Directional Growth. *Cell*

Rep. 2019;28(8):2231-45 e5. Epub 2019/08/23. doi: 10.1016/j.celrep.2019.07.062.

PubMed PMID: 31433995.

76. Bassilana M, Hopkins J, Arkowitz RA. Regulation of the Cdc42/Cdc24 GTPase module during *Candida albicans* hyphal growth. *Eukaryot Cell*. 2005;4(3):588-603.

Epub 2005/03/10. doi: 10.1128/EC.4.3.588-603.2005. PubMed PMID: 15755921;

PubMed Central PMCID: PMCPMC1087799.

77. Sanchez AA, Johnston DA, Myers C, Edwards JE, Jr., Mitchell AP, Filler SG.

Relationship between *Candida albicans* virulence during experimental hematogenously disseminated infection and endothelial cell damage in vitro. *Infect Immun*. 2004;72(1):598-601. Epub 2003/12/23. doi: 10.1128/IAI.72.1.598-601.2004.

PubMed PMID: 14688143; PubMed Central PMCID: PMCPMC344013.

PubMed PMID: 14688143; PubMed Central PMCID: PMCPMC344013.

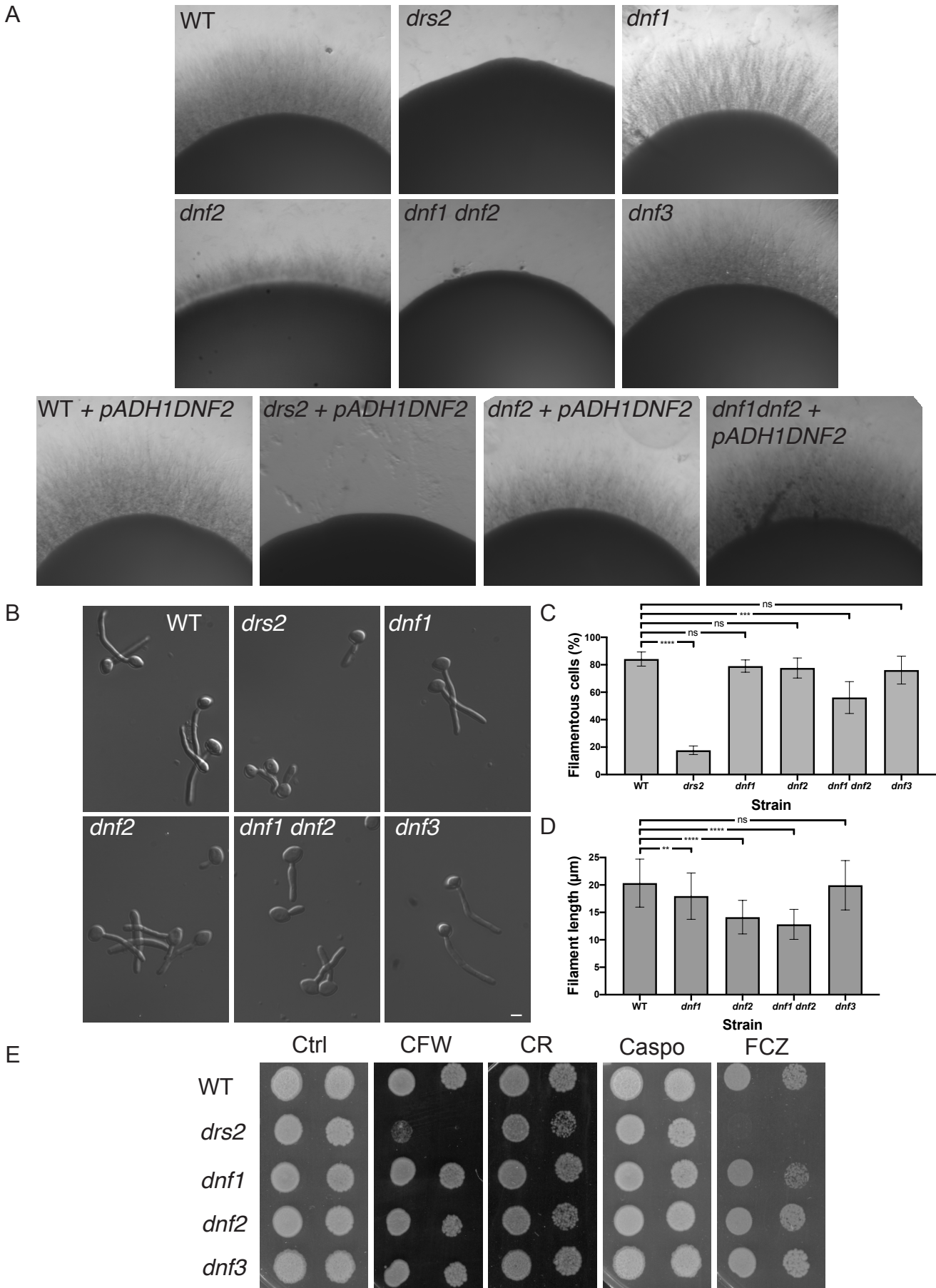


Figure 1

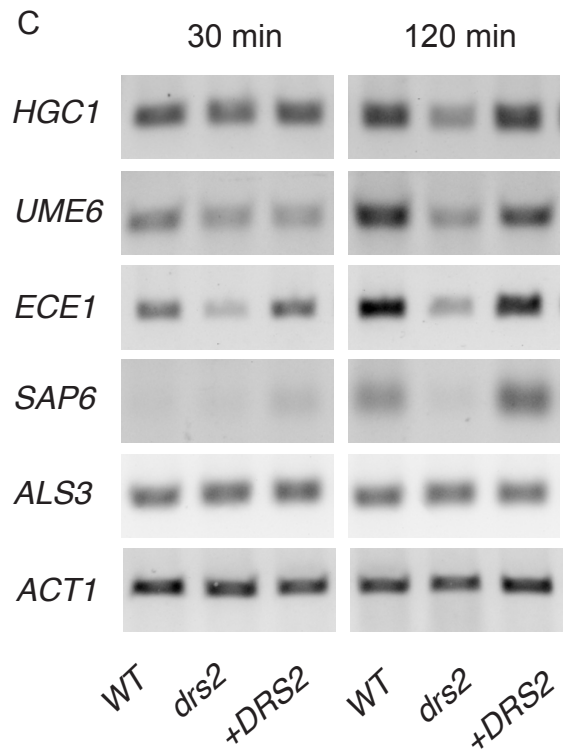
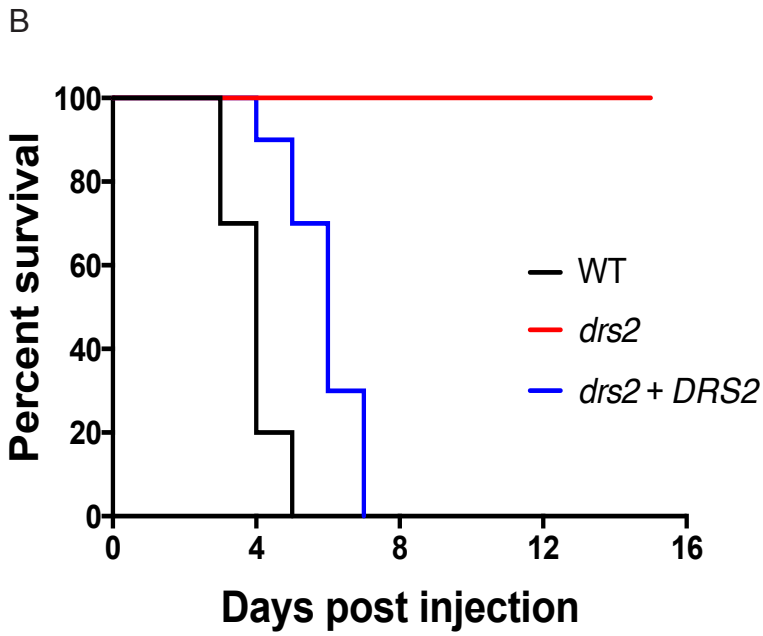
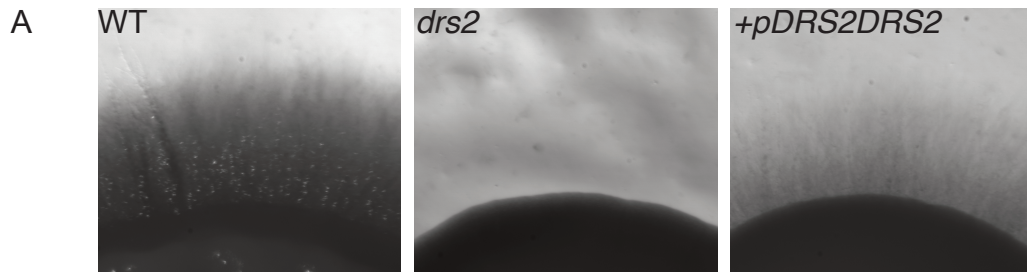


Figure 2

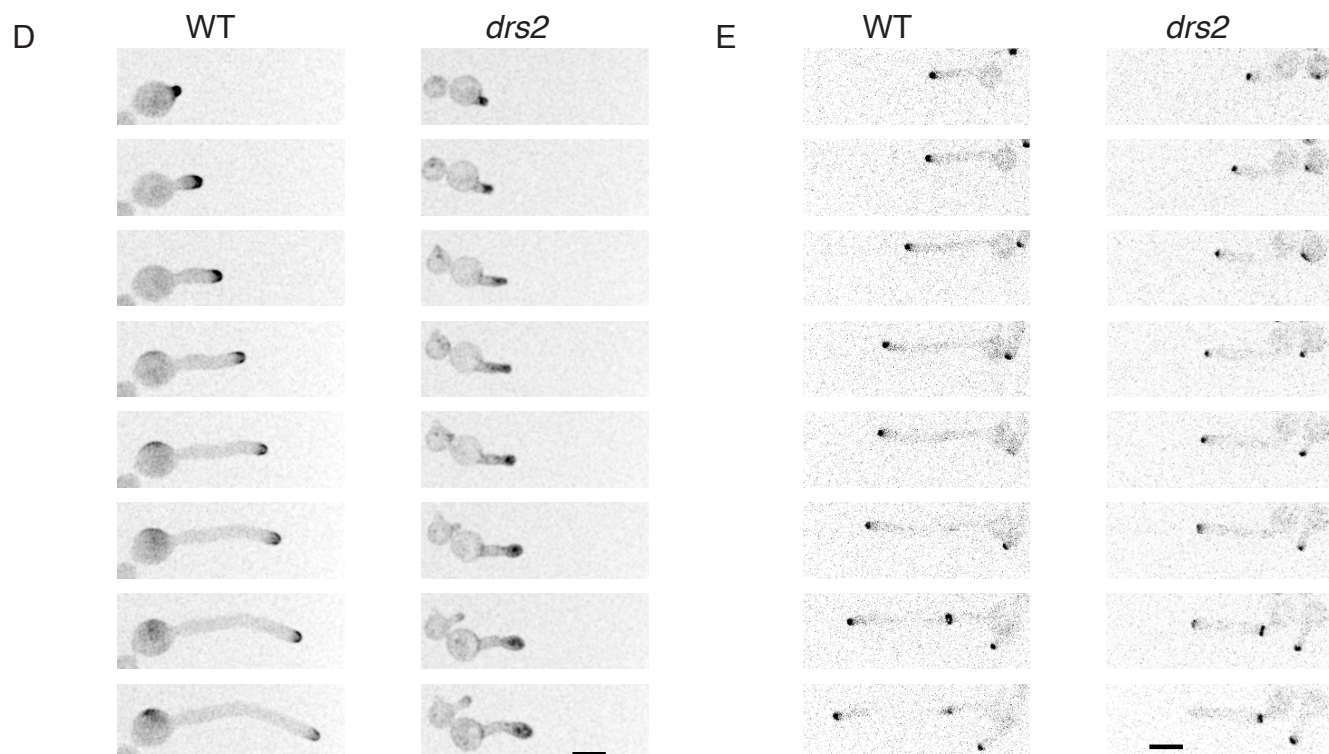
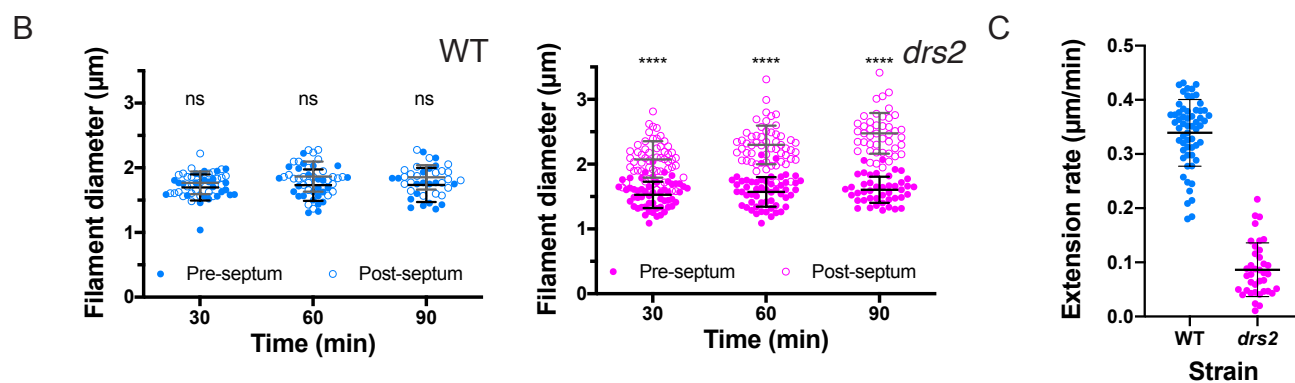
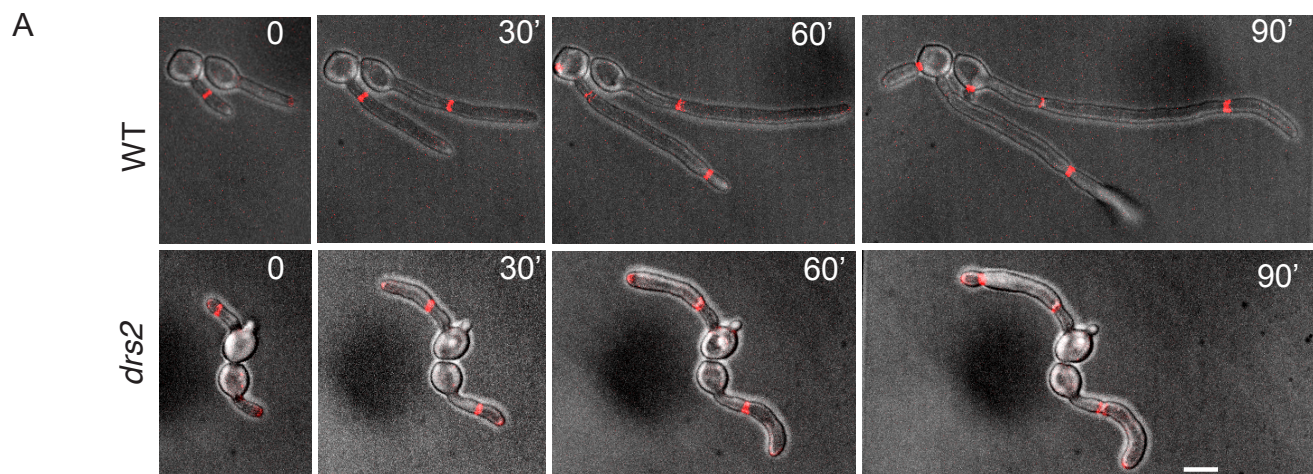


Figure 3

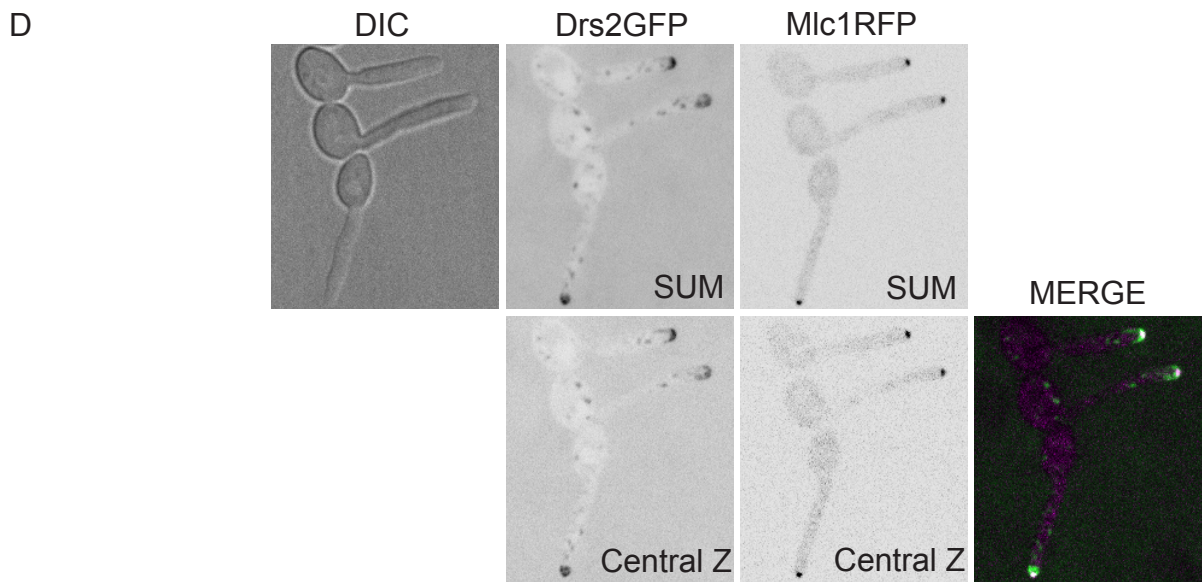
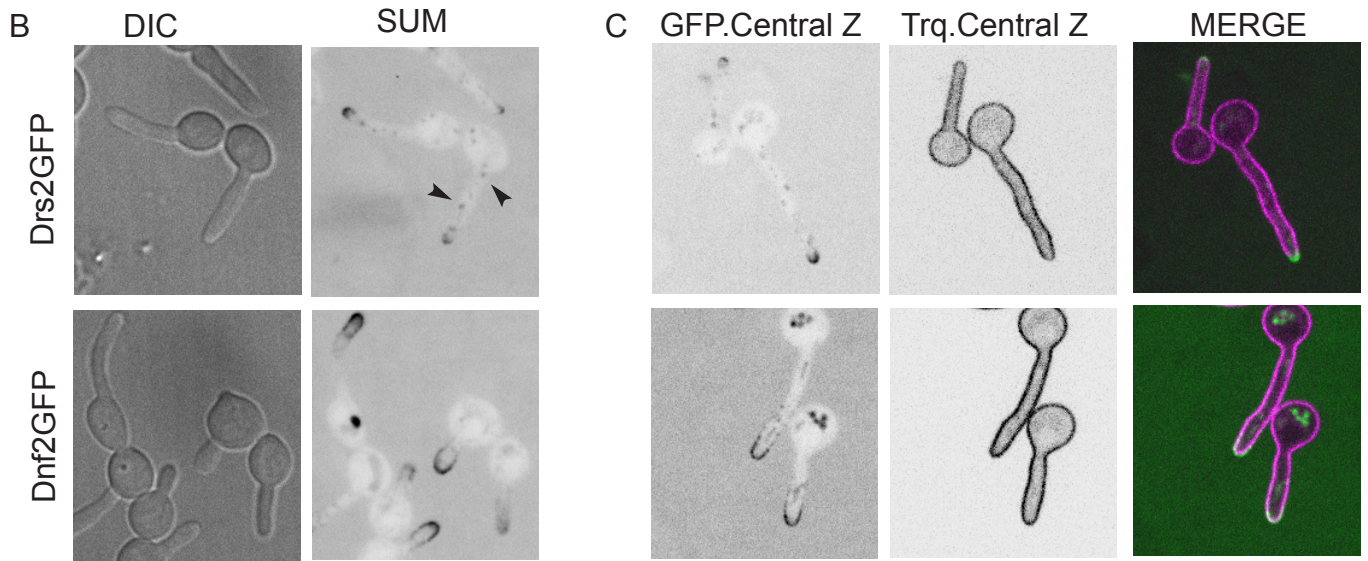
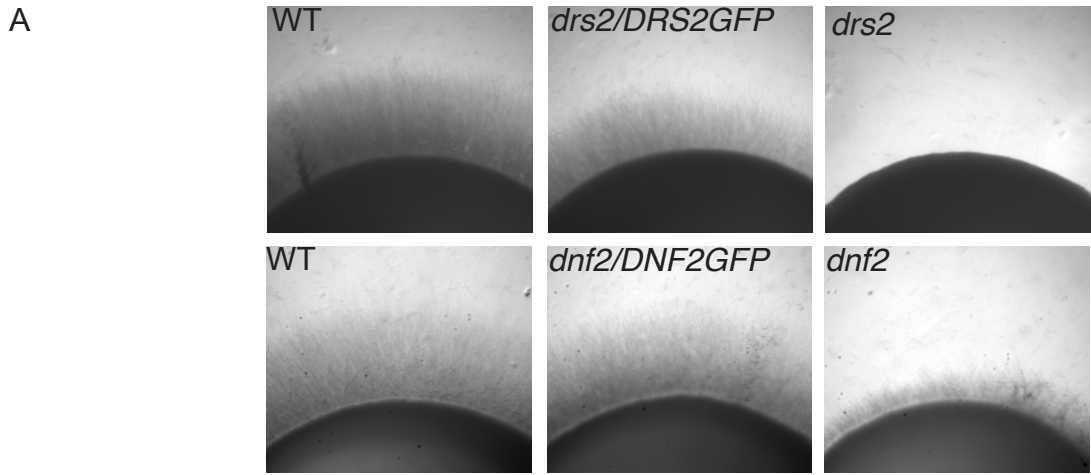


Figure 4

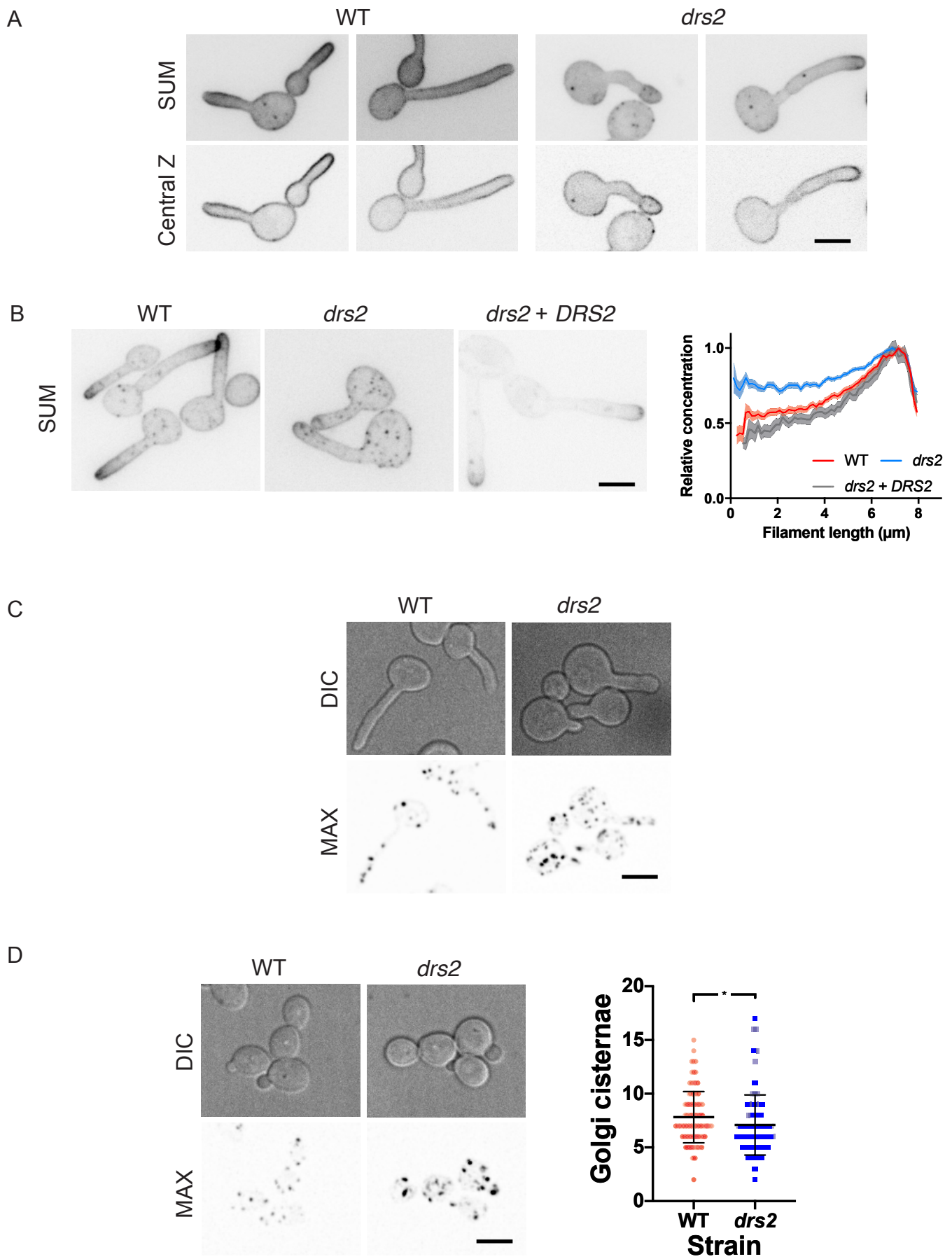


Figure 5

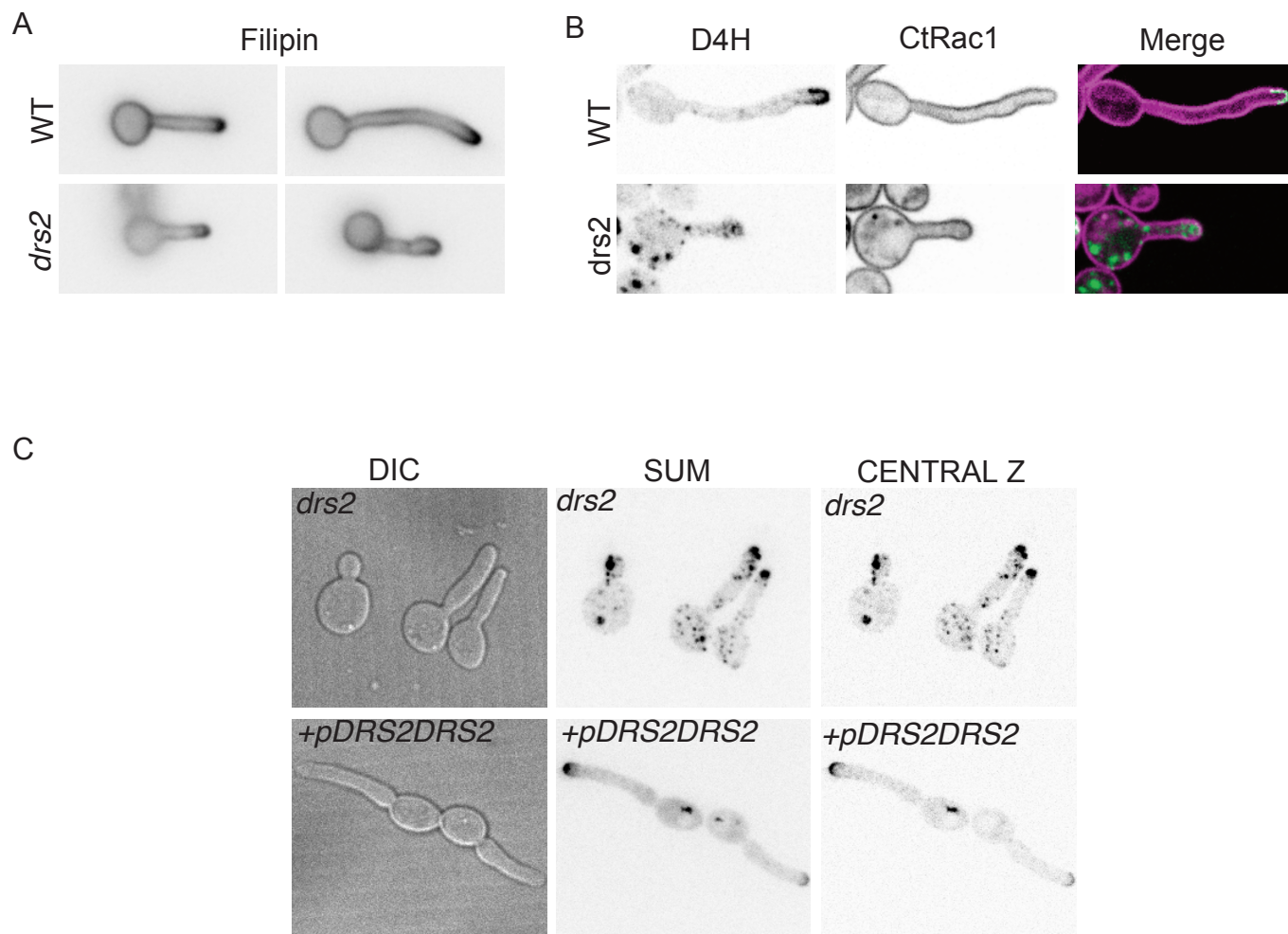


Figure 6

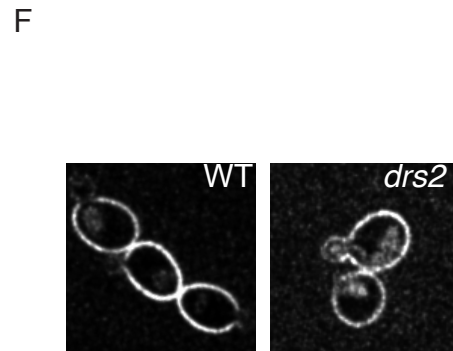
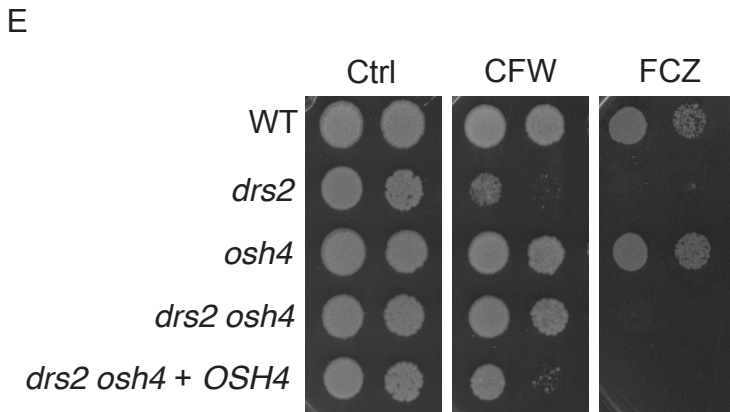
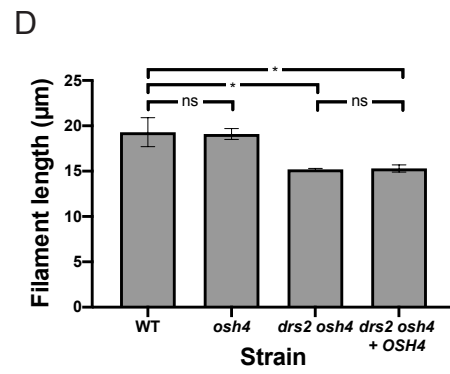
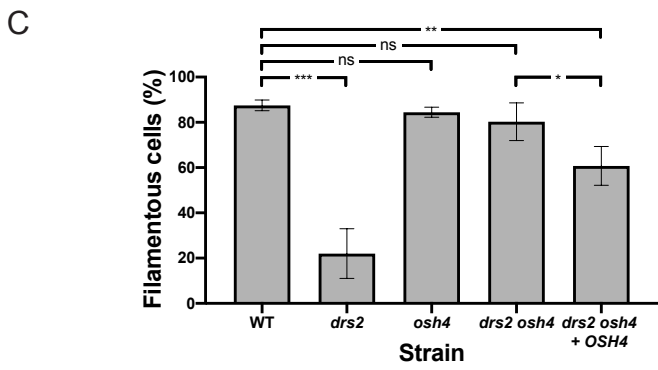
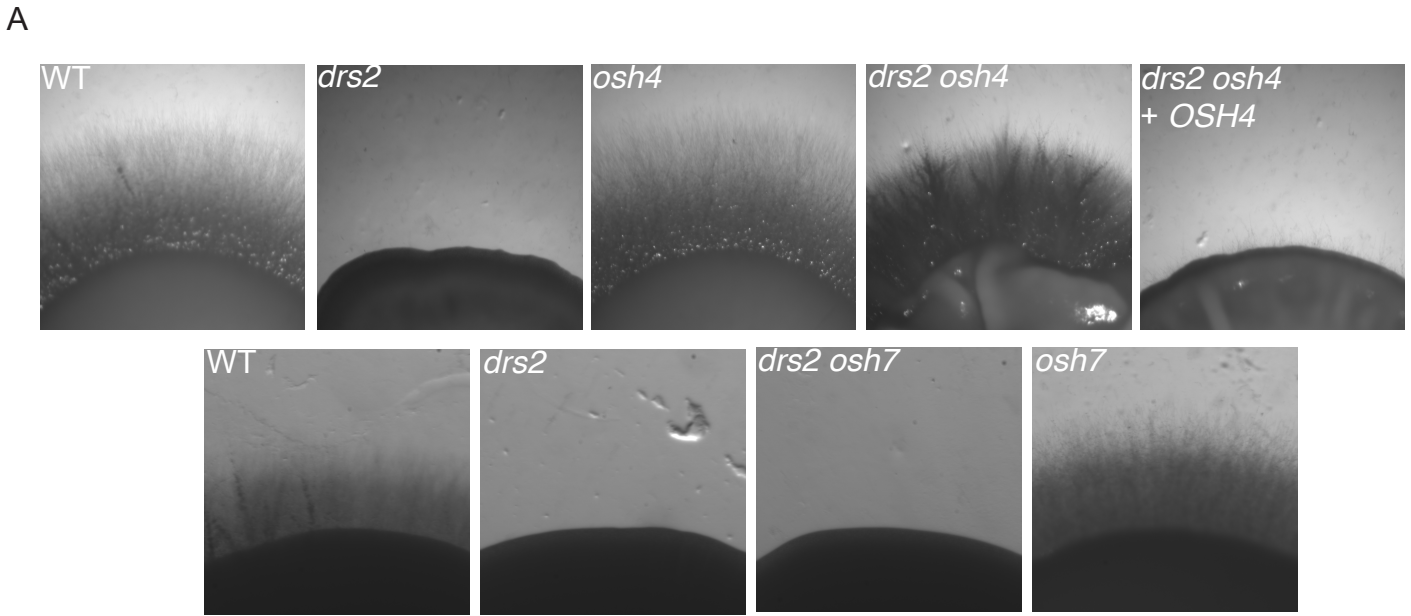


Figure 7

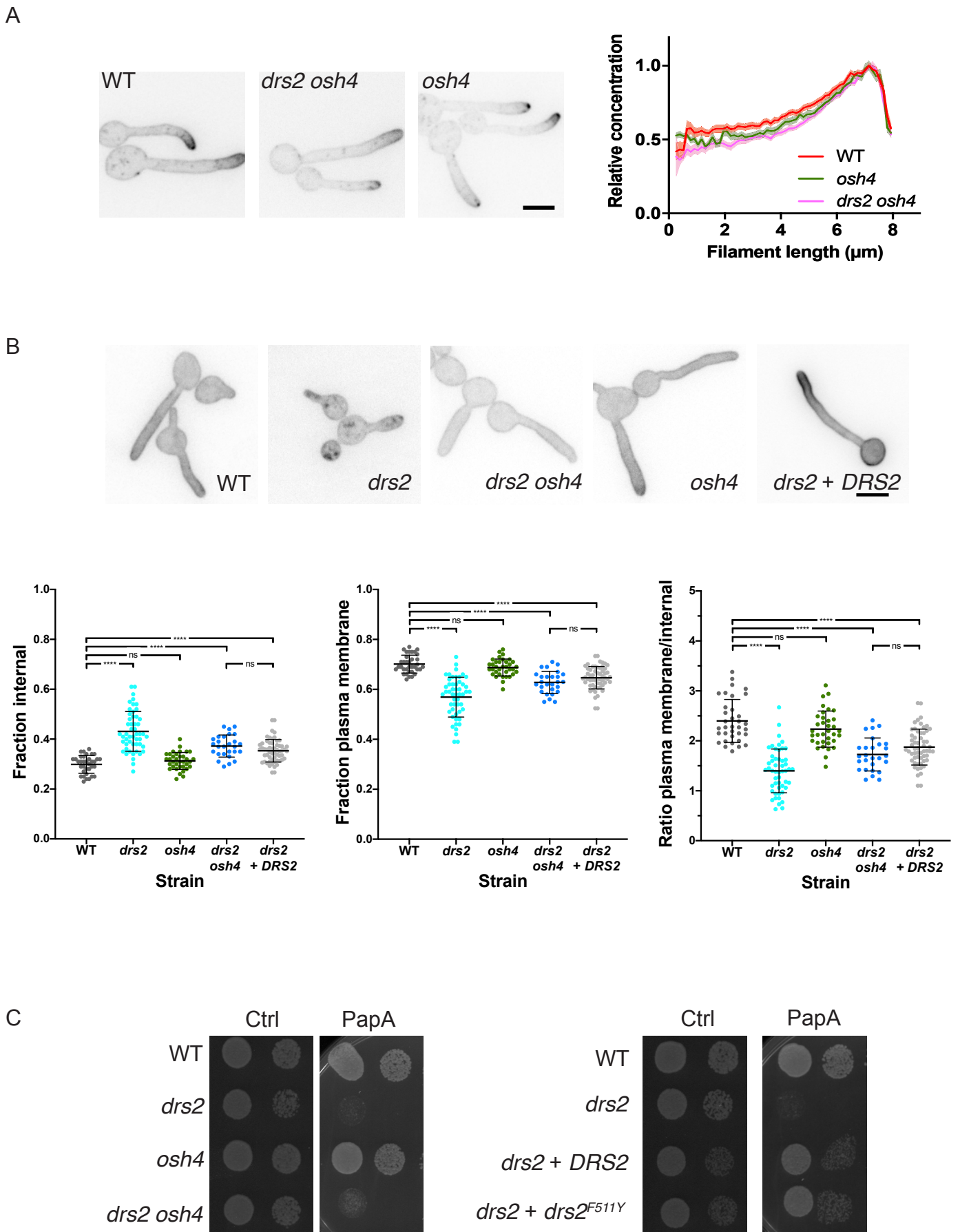
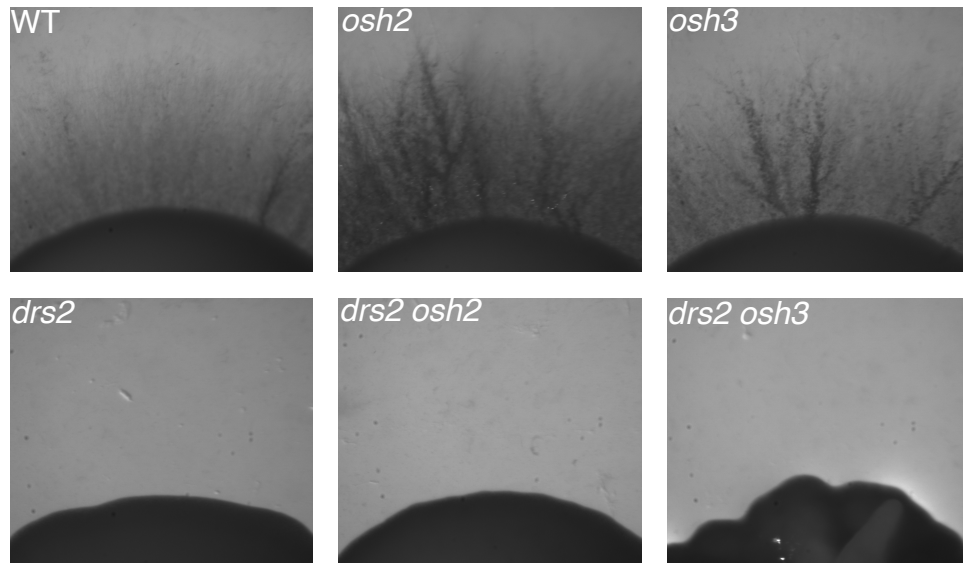


Figure 8

A



B

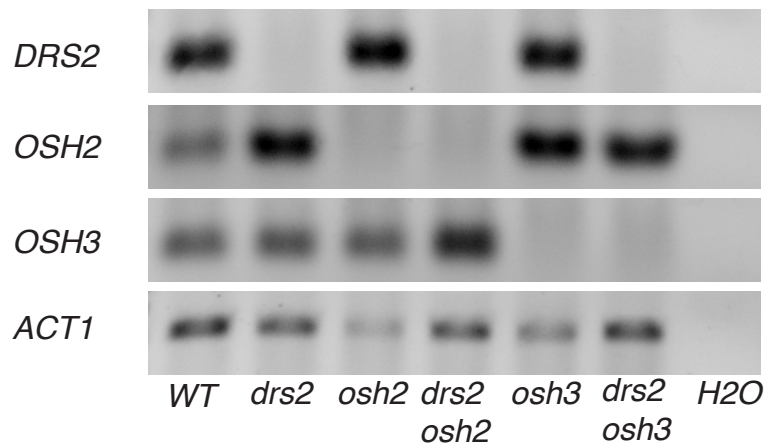
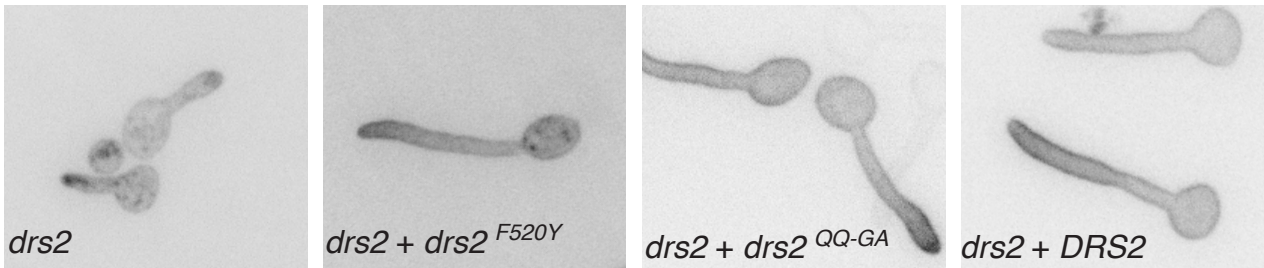


Figure S2

A

```
Sc: FSKYANLFFLCTSAIQQVPHVSPNRYTTIGTL 254  
FSKYANLFFL TS IQQVPHVSPNRYTTIGTL  
Ca: FSKYANLFFLVTSIIQQVPHVSPNRYTTIGTL 259  
  
Sc: WILFSNLVPISLFTVVELIKYYQAFMIGSDLD 530  
WILFSNLVPISLFTVVELIKYYQAFMIGSDLD  
Ca: WILFSNLVPISLFTVVELIKYYQAFMIGSDLD 539
```

B



C

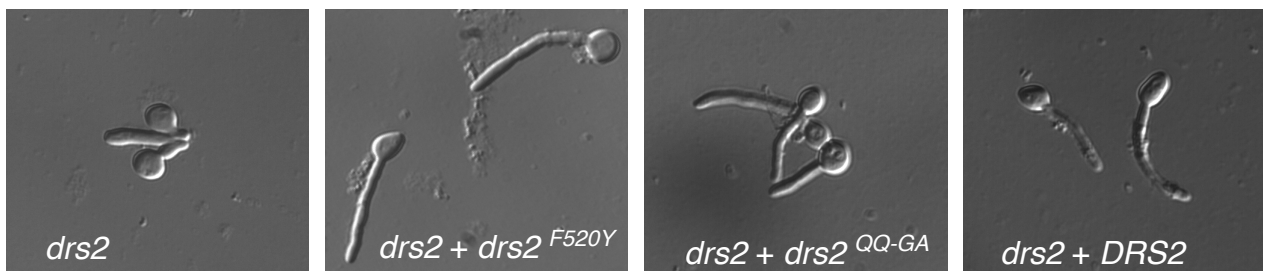


Figure S3

Additional results

These results correspond to additional and/or preliminary data obtained during my experimental work. They include further characterization of the *drs2* mutant, with respect to invasion and molecular analyses. Furthermore, I also investigated the importance of Drs2 localization for its function by targeting this flippase at the SPK constitutively.

Colony formation and invasion in the *drs2* mutant.

Drs2 is critical for hyphal, invasive growth (**Figures 2 & 3**). To further characterize this mutant, we investigated filamentous growth after 24h induction, on FCS containing 0.5% agar. While the WT (left panel) colonies have ~180 μm radius, with hyphae composed of ~30 μm long compartments, the *drs2* mutant colonies are smaller (~90 μm radius) with filaments, composed of thicker and shorter compartments (quantified in **Figure Ad1**, first and second graphs). Of note, the overall compartment volume of the *drs2* mutant is similar to that of the WT (**Figure Ad1**, third graph) and the distance between branches is shorter in the *drs2* cells (**Figure Ad1**, fourth graph). These results further confirmed the role of Drs2 in maintaining hyphal polarized growth.

Drs2 is necessary for polarization of exocytosis and endocytosis.

In *S. cerevisiae*, deletion of *DRS2* affects PM protein sorting at the TGN (Hankins et al., 2015b). In addition, deletion of *DRS2*, *DNF1* and *DNF2* result in an alteration of the endocytic uptake of FM4-64 (Pomorski et al., 2003). I showed that in a *drs2* mutant, active Cdc42 is depolarized (**Figure 3D**) and, consistently, this mutant cannot maintain hyphal growth (**Figure 3A**). Hence, I examined whether Drs2 is important for the organization of membrane traffic during hyphal growth, using exocytosis and endocytosis reporters.

We examined the distribution of endocytosis, by following the actin binding protein 1 (Abp1-GFP) (Ghugtyal et al., 2015; Martin et al., 2007). In WT cells, Abp1-GFP was tightly clustered

1–3 μm from the tip of germ tubes and longer filaments, as previously reported (Ghugtyal et al., 2015; Martin et al., 2007). However, in the *drs2* mutant, Abp1-GFP was less polarized, as shown in **Figure Ad.2.A**. The distribution of secretory vesicles was followed using a GFP fusion with the small Rab GTPase Sec4 (Li et al., 2007; Puerner et al., 2021a; Weiner et al., 2019). In germ tubes, both a *drs2* mutant and a complemented strain exhibited a cluster of Sec4 at the filament apex, corresponding to the SPK (**Figure Ad.2.B.**), yet there appears to be an increase in Sec4 vesicles throughout the filaments in the *drs2* mutant (**Figure Ad.2.B.**). Furthermore, Sec4 labeled vesicles were observed at the site of division in both WT and *drs2* cells. However, the Sec4 signal associated with the cell division site was more intense in the *drs2* mutant compared to the WT strain, and the signal at the tip was dramatically reduced in the mutant (**Figure Ad.2.B**).

As shown in **Figure 3E**, the SPK is also depolarized in *drs2* cells and I constructed a strain co-expressing fluorescently tagged Sec4 and Mlc1, to follow temporal dynamics of these two markers (**Figure Ad.3**). In WT cells, Mlc1 was found persistently at the hyphal tip during filamentous growth, however, when the maximal signal is observed, Mlc1 was also localized at the septum (**Figure Ad.3.A**; $t=5\text{min}$ and $t=10\text{min}$). This peak at the septum was transient, as at $t=25\text{ min}$, Mlc1 was again observed only at the hyphal tip (**Figure Ad.3.A**). GFP-Sec4 was also found persistently at the tip of the hypha and the signals at the septum, besides not being observed in all WT cells, were never higher than the signals at the tip. In contrast, in the *drs2* mutant, the signals associated with the SPK, both for Mlc1 and Sec4, decreased dramatically after septum recruitment; at 15-20 min little to no Mlc1 localized to the SPK (**Figure Ad.3.B**; $t=15$ and $t=20\text{ min}$). The GFP-Sec4 signal at the septum was also higher to that at the SPK (**Figure Ad.3.B**; $t=15\text{min}$ and $t=20\text{ min}$), which was not observed in the WT. Together these data suggest that membrane traffic is altered during filament extension in the *drs2* mutant, consistent with a defect in hyphal growth maintenance.

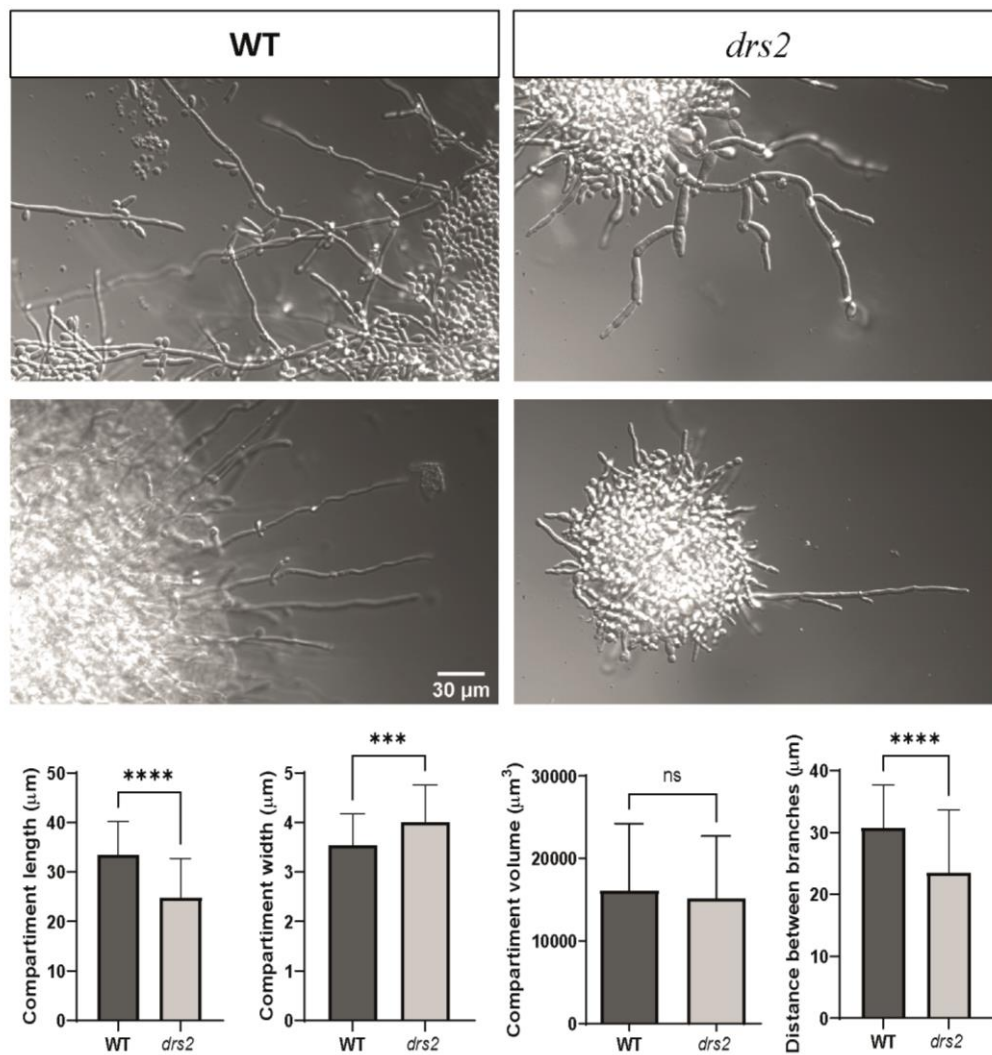


Figure Ad.12. Drs2 is required for maintaining hyphal filamentous growth. The *drs2* mutant filaments are altered in diameter and length. WT and *drs2* mutant cells were incubated on media containing 0.5% agar and 75% FCS on microscope slides (pads) and images were acquired with a 40X objective after an overnight incubation (24h). Filamentous length and diameter were determined, as well as the distance between branches, and plotted in the bottom graphs. Each compartment corresponds to a cell (delimited by septa). Cell volume was calculated as the volume of a cylinder ($V=h*\pi*r^2$). $n = 50$ cells. Bars indicate SD. *** indicates a P value of 0.0006; **** indicates a P value < 0.0001.

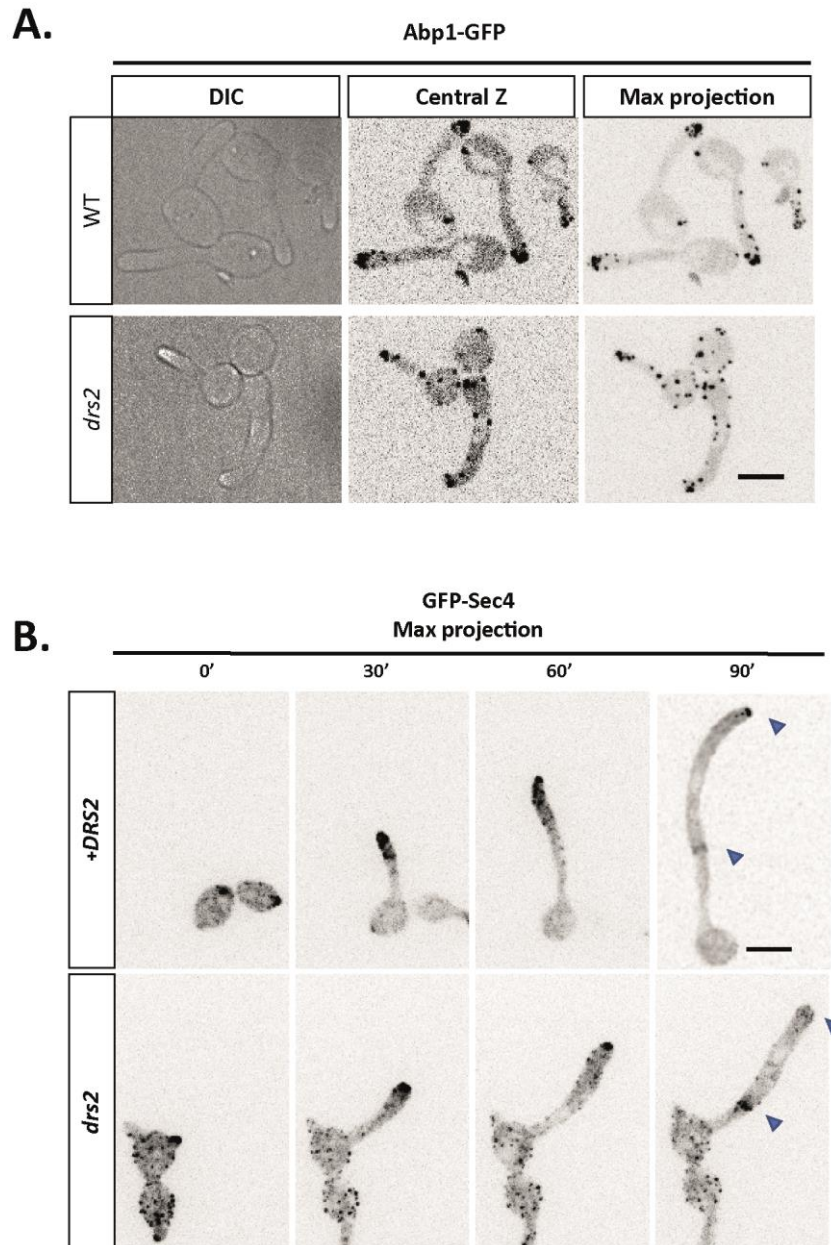
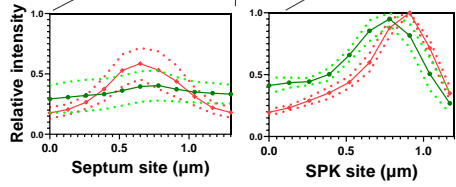
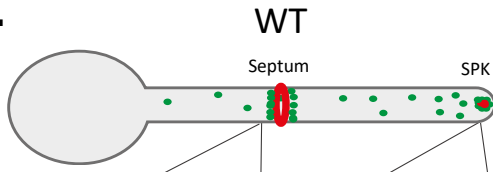
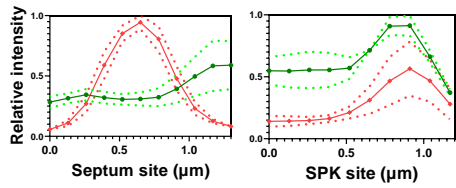


Figure Ad.2. Polarization of exocytosis and endocytosis is impaired in the *drs2* mutant. **A.** *Drs2* is necessary for the clustered distribution of endocytosis sites. WT and *drs2* cells after 60- and 90-min FCS induction, respectively, are shown. Central Z and maximum projection images (from 21 Z-sections) are shown for the indicated strains. **B.** *Drs2* is important for the distribution of secretory vesicles. Central Z and maximum projection images of *drs2* and *drs2* + *DRS2* cells expressing GFP-Sec4 over time. Blue arrowheads indicate the localization of the cluster of vesicles at the filament tip and at the septum. Scale bars correspond to 5 μ m.

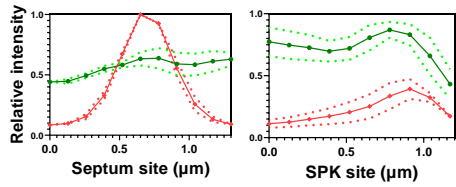
A.



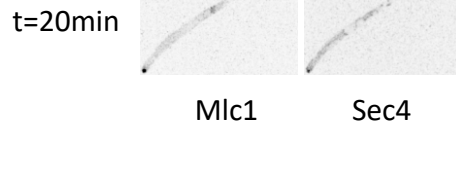
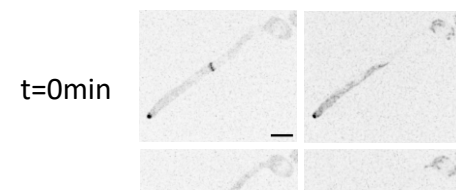
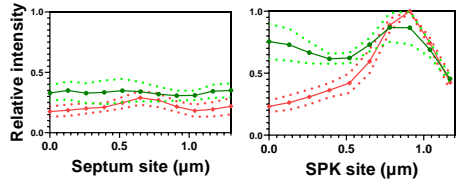
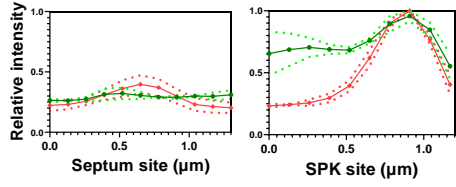
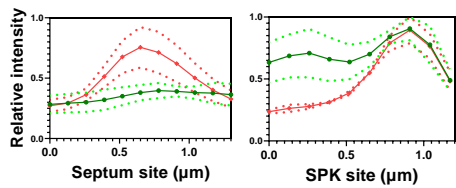
t=0min



t=10min



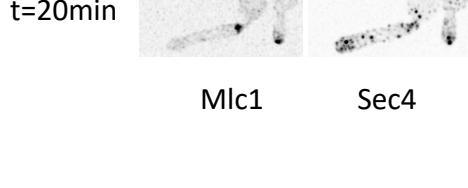
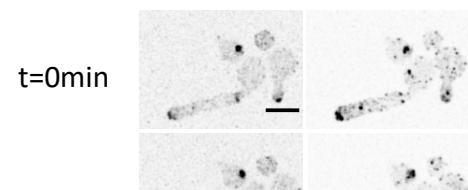
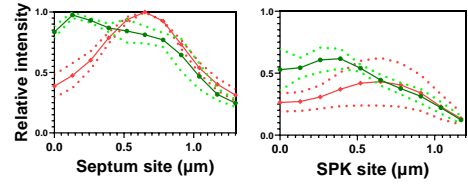
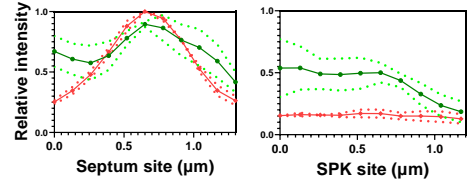
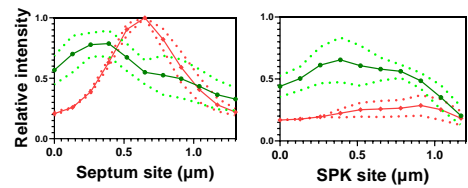
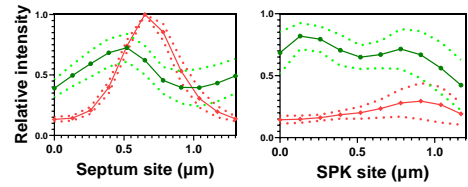
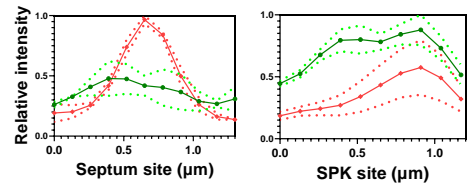
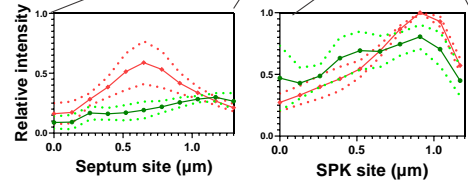
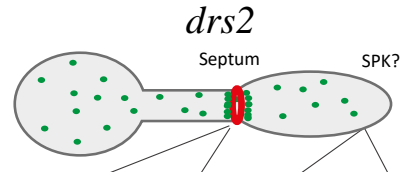
t=20min



Mlc1

Sec4

B.



Mlc1

Sec4

Figure Ad.3. Temporal dynamics of Mlc1 and Sec4. A and B. Cells co-expressing Mlc1-mScarlet and GFP-Sec4 were analyzed over time ($\Delta t = 5\text{min}$). Relative signals of each protein are plotted (Sec4 in green, Mlc1 in red) at two locations: the presumptive septum and SPK site. The septum graphs (left columns) correspond to a total of $\sim 1.3\ \mu\text{m}$, and the maximal peak correspond to the septum site (center values, $x = \sim 0.65\ \mu\text{m}$). The SPK graphs correspond to measurements in a total of $\sim 1.3\ \mu\text{m}$ from the apex, with the maximal signal near to the cell tip ($x = \sim 1\ \mu\text{m}$). 25 min of the time course are plotted: $t = 0$ represents the first appearance of Mlc1. A. shows the WT and B. *drs2* ($n = 3$ cells). Error bars are SEM. A scheme is shown (top) and representative images of WT and *drs2* cell are shown (bottom; Max projection of 21z-sections). Scale bars, $5\ \mu\text{m}$.

Constitutive targeting of Drs2 to the SPK is not deleterious for *C. albicans* filamentous growth.

We showed that Drs2 localizes at the hyphal tip as an apical crescent, most likely at the PM, given its co-localization with a prenylated mScarlet fusion, mSc-Ct_{Rac1}, (**Figure 4**), as well as partially co-localizes with Mlc1 (**Figure 4** and **Figure Ad.4.A.** and **B.**). To alter the distribution of Drs2, I used a synthetic physical interaction (SPI) to constitutively target Drs2 to the SPK, with a GFP nanobody (GNB) fused to a secretory vesicle component Mlc1, together with the far-red fluorescent protein miRFP₆₇₀ (miRFP) for visualization, as established by Puerner et al., 2021. GNB has high affinity for GFP, which it binds irreversibly (Rothbauer et al., 2006). In this strain expressing *MLC1*-miR-GNB, a tight localization of Drs2-GFP was observed at the SPK (**Figure Ad.4.C.** and **D.**), suggesting that Drs2 is constitutively targeted to this structure. Hence, we examined the effect of such a Drs2 distribution on filamentous growth in a strain where Drs2-GFP is the sole copy. As shown in **Figure Ad.4.D**, a small difference was observed in the percentage of filamentation in this strain ($64.6 \pm 3.2\%$) compared to that of a strain expressing Drs2-GFP ($73.3 \pm 2.5\%$). Together, these results suggest that the function of Drs2 in hyphal growth is unlikely to be limited solely to the PM.

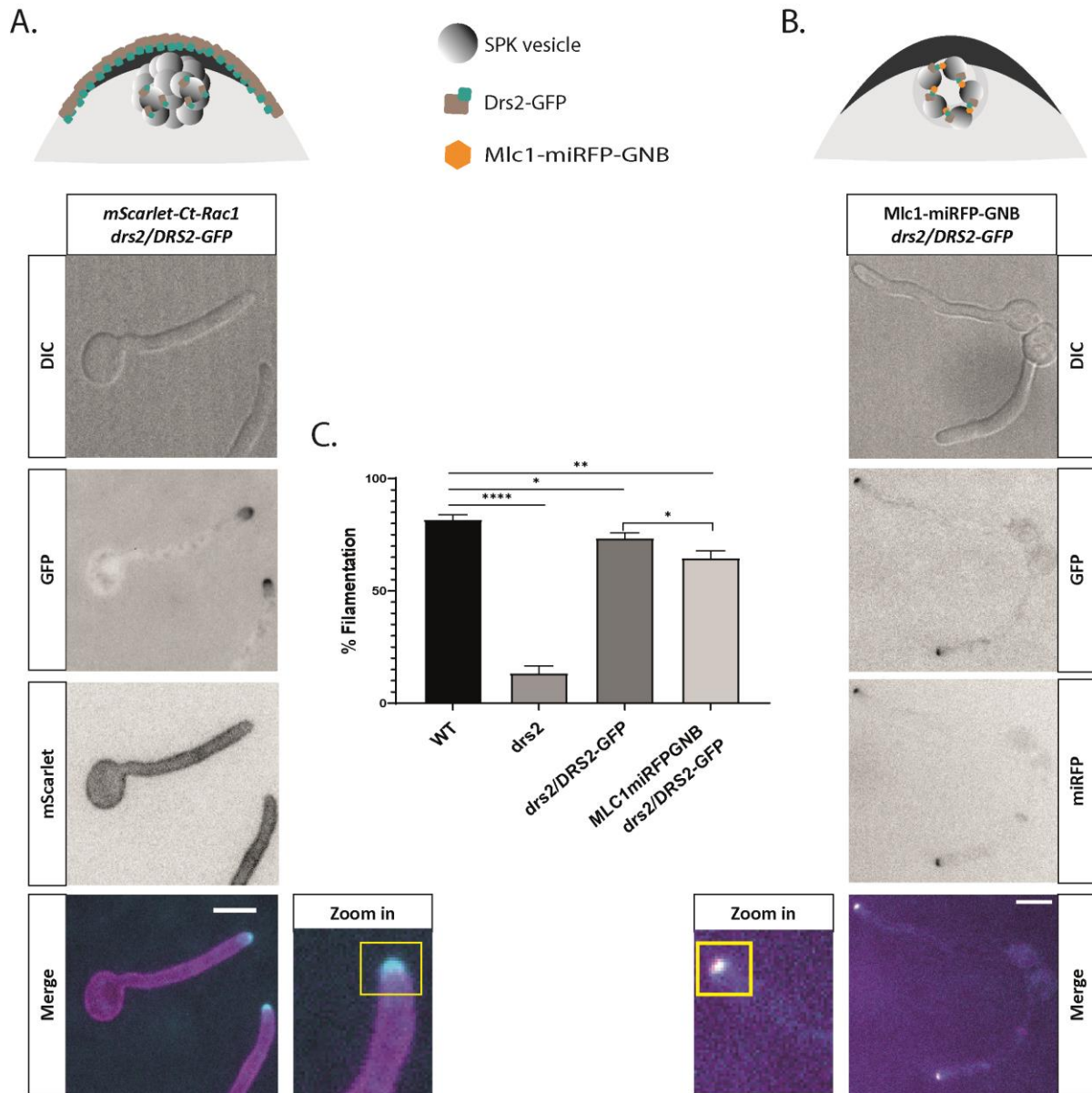


Figure Ad.4. Forced localization of Drs2 to the SPK does not substantially alter filamentous growth. **A.** Drs2-GFP localizes as a crescent at the hyphal tip, schematized on top. Images of cells expressing mScarlet-Ct_{Rac1}, together with Drs2-GFP after 90 min FCS induction. Images are sum projections of 16 z-sections. **B.** Drs2-GFP forced localization at the SPK. Images of cells expressing Drs2-GFP as the sole copy, as well as Mlc1-miRFP-GNB. Images are sum projections of 16 z-sections. Drs2-GFP distribution is shown in brown/green and Mlc1 in orange in the schematic on top. Scale bar is 5 μ m. **C.** Forced localization of Drs2 to the SPK does not substantially alter filamentous growth. The percentages of filamentous cells were determined for each strain. The mean percentage of hyphae +/- the SD (bars) from 3 experiments ($n = 100$ cells each).

The forced localization Osh4 to the SPK is not deleterious.

Using this GNB system, I attempted to artificially localize a specific lipid transporter, *i.e.* Osh4. Preliminary data are shown in **Figure Ad.5**. In *C. albicans*, while Osh4-GFP appeared homogeneously distributed throughout the cell (**Figure Ad.5.A.**), it is observed as a cluster at the SPK, when Osh4-GFP is expressed as a sole copy, together with Mlc1-miRFP-GNB (**Figure Ad.5.B.**). In these conditions, we did not observe an alteration of the percentage of filamentous cells, compared to that of a WT strain, suggesting that forced localization of Osh4 at the SPK is not deleterious for hyphal growth (**Figure Ad.5.C.**).

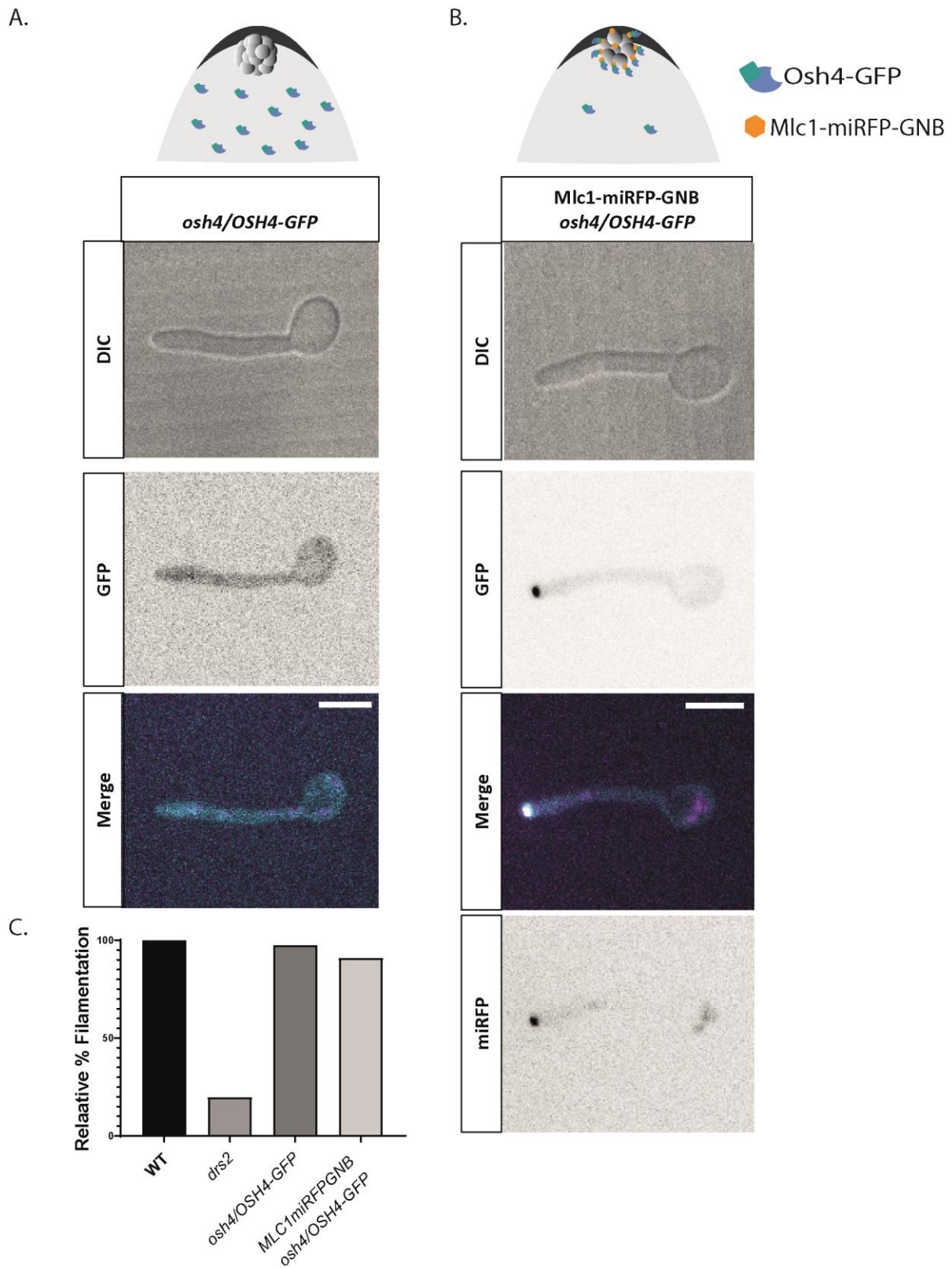


Figure Ad.13. Forced localization of Osh4 to the SPK do not alter filamentous growth. **A.** Osh4-GFP localizes in the cytosol. Image of a hyphal cell from a strain expressing Osh4-GFP as the sole copy. Sum projections of 16 z-sections are shown **B.** Synthetic physical interactions between Mlc1-miRFP-GNB and Osh4-GFP relocalizes Osh4 to the SPK. Sum projections of 16 z-sections are shown. **C.** Forced localization of Osh4 to the SPK does not alter filamentous growth. The percentage of filamentous cells was counted for each strain $n = 100$ cells.

DISCUSSION

In this work, I characterized the role of the flippases belonging to the P4-ATPase subfamily during polarized hyphal growth in the human opportunistic fungal pathogen *Candida albicans*. My results indicate that Drs2 plays a unique role in the maintenance of filamentous growth, which appears to be more critical after the first septum formation (**Figure D1**). Further characterization of the *drs2* deletion mutant shows in particular that, in addition to PS distribution, the distribution of PI(4)P at the PM is altered (**Figure D2**). Deletion of the lipid transfer protein Osh4, which exchanges PI(4)P and sterol, specifically recovers both PI(4)P polarized distribution at the PM, and hyphal invasive growth in *drs2* cells.

Importance of Drs2 for *C. albicans* filamentous growth and virulence

The deletion of the PS synthase Cho1 results in a defect in virulence in murine infection models (Chen et al., 2010; Davis et al., 2018). Additionally, the *cho1* mutant was trans-complemented with the *Arabidopsis thaliana* serine decarboxylase gene (AtSDC), providing this mutant with the capacity to capture enough ethanolamine to produce PS by a run backwards of the Psd1/2 enzymatic reaction, which rescues virulence (Davis et al., 2018), indicating that PS is critical for virulence. Consistent with this, we show now that Drs2 is also required for invasive growth and virulence in a murine model of systemic candidiasis (**Figure 2 and Ad.1**). In addition, it is possible that the reduced virulence of *drs2* could be due, at least in part, to the inability to maintain virulence attributes such as hyphal specific gene expression needed for tissue invasion, like Candidalysin (Ece1) or Sap6 (**Figure 2C**). Work on *Fusarium graminearum* also showed that flippases, including the Drs2 homologous, FgDnfB, are implicated in the production of virulence factors, such as the deoxynivalenol (DON) mycotoxin and in the expression of the genes implicated in DON production (Yun et al., 2020).

Drs2 is critical to maintain PS distribution in *C. albicans* (Labbaoui et al., 2017). PS plays key roles in the localization of polarity proteins in *S. cerevisiae*, such as Cdc42 (Fairn et al., 2011; Meca et al., 2019; Sartorel et al., 2018) that regulates the formin Bni1 (Chen et al., 2012). In *C. albicans*, Cdc42 is critical for hyphal growth initiation and maintenance (Bassilana et al., 2005, 2003b), Bni1 is necessary for hyphal growth maintenance (Li et al., 2005; Martin et al., 2005) and Mlc1 plays a role in regulating cell robustness necessary for invasive growth (Puerner et al., 2021a). Bni1, together with Mlc1, are components of the SPK (Crampin et al., 2005; Jones and Sudbery, 2010; Li et al., 2005; Martin et al., 2005; Puerner et al., 2021a) and our data show that in the *drs2* mutant, active Cdc42 (**Figure 3D**), Mlc1 and Sec4 (**Figure 3E** and **Figure Ad.3.**) are depolarized upon hyphal extension (Figure Ad.3.B). Hence, it is possible that the defect in maintaining hyphal growth in *drs2* results from active Cdc42 mis-localization, as a result of the alteration of PS distribution. Given that deletion of *DRS2* also results in the downregulation of *HGCI* (**Figure 2C**) and that the Hgc1-Cdc28 complex was found to regulate the Cdc42 GAP, Rga2 (Zheng et al., 2004, 2007), it is also possible that reduced *HGCI* expression contributes to the altered distribution of active Cdc42 in this mutant (**Figure D1**).

An important step to characterize a protein function is to examine its localization. In *S. cerevisiae*, Drs2 localizes to the TGN, during budding growth and mating (Alder-Baerens et al., 2006; Hua et al., 2002; Sartorel et al., 2015). In contrast, the Drs2 homologs localize at the SPK in filamentous *A. nidulans* and *F. graminearum* cells (Schultzhaus et al., 2015; Yun et al., 2020). Here, we showed that during serum-induced hyphal growth, Drs2 is found essentially at the filament apex, where it appears to localize at the plasma membrane and also partly at the SPK (**Figures 4C & 4D**). To understand where Drs2 is critical for its function in filamentous growth, I used a synthetic physical interaction system (Puerner et al., 2021a; Rothbauer et al., 2006), to restrain Drs2 at the SPK (**Figure Ad.4**). In these conditions, only a small reduction in the percent of filamentous cells was observed, suggesting that Drs2 PM localization is not

critical for this process. We could speculate that Drs2 is flipping PS on membrane vesicles at the SPK, which will subsequently contribute to the PS enrichment at the PM cytosolic leaflet.

Importance of Drs2 for plasma membrane and cell wall organization:

In the past decades, pivotal roles played by lipids in cell signaling and morphogenesis in fungi have been identified. PS, for example, is enriched at sites of polarized growth, such as the shmoo projection during mating of *S. cerevisiae* (Fairn et al., 2011) and *S. pombe* (Haupt and Minc, 2017), and the absence of this lipid compromises polarized growth (Fairn et al., 2011). Similarly, PS is enriched at the apex of *C. albicans* hyphae (Labbaoui et al., 2017) and the absence of PS, resulting from deletion of the PS synthase Cho1 impairs hyphal formation (Chen et al., 2010). The *drs2* mutant has an aberrant PS distribution (Labbaoui et al., 2017), with decreased PM and increased internal signal (**Figures 8B and C**), and is hypersensitive to Papuamide A (**Figure 8D**) which indicates an overexposure of PS at the external PM leaflet. This mutant is also hypersensitive to copper exposure (Douglas and Konopka, 2019), suggesting a defect in plasma membrane organization.

Loss of PS asymmetry has been associated with PM disorganization and is a common feature of strains defective for cortical actin organization and membrane trafficking (Douglas and Konopka, 2019). Consistently, the *drs2* mutant failed to maintain secretory vesicles and endocytic patches clustering during hyphal growth, indicative of a defect in membrane traffic (**Figure Ad.2.A. and Ad.3.B.**). In addition, a mutant of the Drs2 non-catalytic subunit, *cdc50* is altered for FM4-64 endocytic uptake (Xu et al., 2019) and several lines of evidence have linked an impaired endocytosis and altered PM lipid distribution to defects in hyphal morphogenesis and cell wall integrity (Douglas et al., 2009; Epp et al., 2013b; Knafler et al., 2019). PS absence in the *cho1* mutant also results in increased cell wall thickness (Chen et al., 2010) and in exposure of $\beta(1-3)$ -glucan (Davis et al., 2014). It is possible that altered PM PS asymmetry in *drs2* results in cell wall defects, as the *drs2* mutant is hypersensitive to calcofluor

white (CFW), a drug that binds to chitin and prevents its assembly, negatively impacting cell wall integrity. Of note, in filamentous fungi, P4-ATPases, including the Drs2 homolog DnfB, interact with the heterotetrameric complex AP-2, necessary for clathrin-mediated endocytosis (Martzoukou et al., 2017; Zhang et al., 2019), shown to be essential for cell wall integrity and polarity in different fungi (Chapa-y-Lazo et al., 2014; de León et al., 2016; Knafler et al., 2019; Martzoukou et al., 2017; Zhang et al., 2019).

Importance of Drs2 for phospholipid distribution and interaction with other lipid transporters.

In *S. cerevisiae*, the *DRS2/DNF* genes show a certain degree of redundancy for growth (Hua et al., 2002). Moreover, both Drs2 and the essential flippase Neo1 transport PS and PE, but they are functionally segregated due to the PQ-loop Any1-Neo1 interaction (Takar et al., 2019, 2016). In filamentous fungi such as *A. nidulans*, the deletion of the Drs2 homolog does not have a major defect in cell morphology or hyphal growth (Schultzhaus et al., 2015), yet the double deletion mutants *dnfA/dnfB* (Dnf1 and Drs2 homologs, respectively) and *dnfB/dnfD* (Drs2/Neo1 homologs, respectively) are non-viable (Schultzhaus et al., 2019, 2015), suggesting essential overlapping functions between these flippases. In *Fusarium graminearum*, despite the redundancies between FgDnfA, FgDnfB, and FgDnfD, these flippases play distinct and specific roles during toxosome biogenesis (Yun et al., 2020). In *C. albicans*, Drs2 appears to be particularly critical for maintaining hyphal growth, yet the importance of Neo1, which is not essential in this organism (Douglas & Konopka, 2019), should be investigated in this process. We could speculate that, in the absence of Drs2, Dnf1-3 and/or Neo1 contribute to hyphal growth during initiation, but, once filamentation is initiated, the function of Drs2 could not be compensated, resulting in a switch to isotropic growth (**Figure 3**).

Alteration of PM PI(4)P (Vernay et al., 2012) in the lipid kinase mutant *stt4* resulted in a defect in *C. albicans* hyphal growth (Vernay et al., 2012) and, similarly, loss of the PM PI(4)P

gradient, as well as a defect in filamentous growth, were observed in mutants deleted for the Sac1 phosphatase (Ghugtyal et al., 2015; Zhang et al., 2015). Although there was no apparent alteration of the distribution of PI(4,5)P₂ nor Golgi PI(4)P in *drs2*, we observed a decrease in the PM PI(4)P gradient at the apex that was rescued after complementation with the *DRS2* gene (**Figure 5**). Together, these data reinforced the importance of PM PI(4)P distribution in hyphal growth (**Figure D2**). Furthermore, given that deletion of *DRS2* and *SAC1* together result in a synthetic growth defect, these genes could function in parallel pathways (**Figure 9**). In *S. cerevisiae*, there is a cross-regulation of phospholipid levels. For example, deletion of the PI(4)P phosphatase, Sac1, leads to increased level of PS in endomembranes (Foti et al., 2001; Tani and Kuge, 2014), probably due to a misregulation of the lipid transfer protein Osh6/7, which exchanges PS to PI(4)P (J. Moser von Filseck et al., 2015). Deletion of the PM PI-4 kinase, Stt4, also increases PM PS levels (Trotter et al., 1998; Wang et al., 2020). Given that Drs2 has been shown to transport PS but not PI(4)P, it is likely that other lipid transporters are involved in regulating PI(4)P distribution in *drs2*. One could speculate that Osh4 regulates Osh7 that, by analogy with *S. cerevisiae*, would exchange PI(4)P and PS (Maeda et al., 2013; J. Moser von Filseck et al., 2015; Schulz et al., 2009) (**Figure D3**).

In *drs2*, we observed altered PM PI(4)P distribution, reduced PM PS and increased internal ergosterol (**Figure 5B, 6**). Drs2 has been proposed to genetically interact with the OSBP lipid transporter, Osh4, in *S. cerevisiae*, as Osh4 is hyperactive in the absence of Drs2 and *vice versa* (Hankins et al., 2015b; Muthusamy et al., 2009). Although none of the single *osh* deletion mutants was affected for serum-induced hyphal invasive growth (**Figure 7A-D and S2**), the deletion of *OSH4* rescued hyphal growth and restored the PM PI(4)P in *drs2* (**Figure 7A-D and S2**). Strikingly, the PS distribution was also restored in this *drs2osh4* (**Figure 8A and B**), yet the PS asymmetry was not, as this mutant was still sensitive to PapA, similar to *drs2* (**Figure 8C**). In an attempt to address the importance of PS asymmetry, we generated Drs2 mutants

analogous to those described in *S. cerevisiae* as critical for the PS specificity (Baldrige and Graham, 2013, 2012), yet, in such mutants, the PS distribution and growth on PapA were similar to that of the WT cells, precluding directly investigation of PS flipping activity in hyphal growth. Nonetheless, our results suggest that PS asymmetry is not critical for hyphal growth. However, given that the *drs2osh4* mutant is still hypersensitive to fluconazole, similar to *drs2*, one can propose that Drs2 has a role in plasma membrane organization that is independent of Osh4 and PI(4)P.

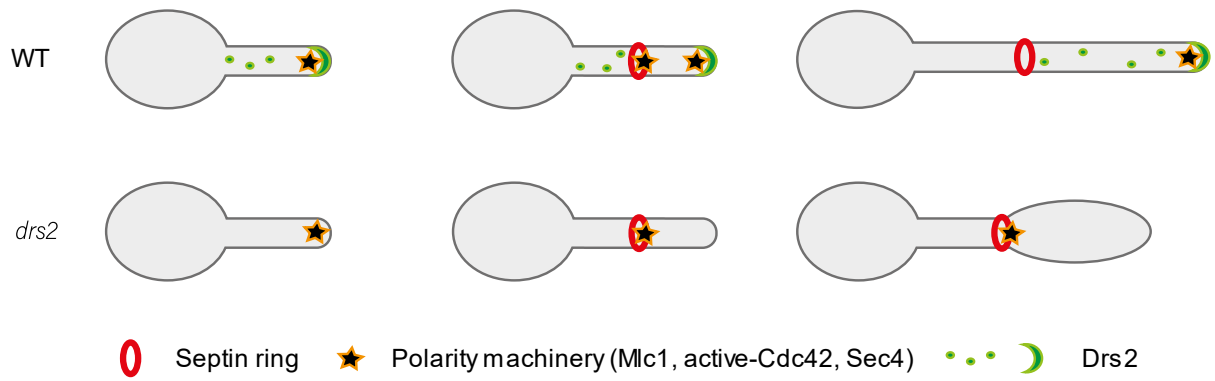


Figure D1. Drs2 is necessary for a correct localization of the polarity machinery. In WT cells, proteins implicated in polarized growth such as Cdc42, Mlc1 and Sec4 are required at the filament apex and, temporarily, at the septum site. In the *drs2* mutant, the absence of Drs2 leads to a misplacement of the polarity machine to the septum, losing completely the apical localization.

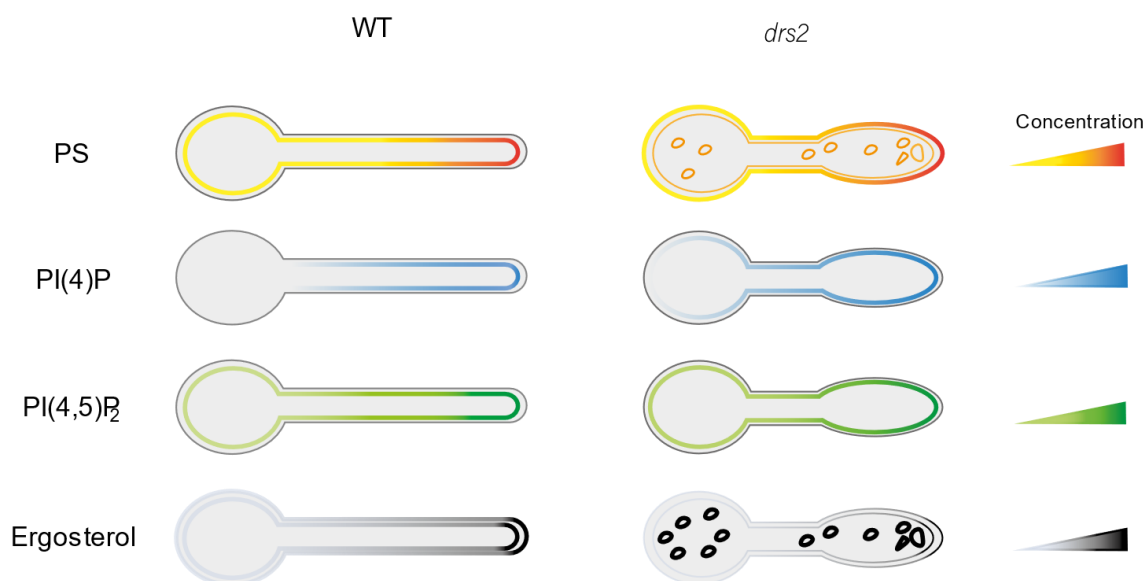


Figure D2. PM lipid distribution in the *drs2* mutant. In this schematic, the PM bilayer is represented with two lines. The thickness of these lines represents the asymmetric distribution of lipids across the membrane. The color gradient represents the lipid polarization. In WT cell, the represented phospholipids are more concentrated in the PM cytosolic leaflet and at the apex of the filament. Ergosterol levels are equivalent across the bilayer, however, there is a dramatic polarization at the hyphal apex. In the *drs2* mutant, PS is internalized to the cytoplasm, and it is exposed to the outer leaflet of the PM. Among the PIPs, only the polarized distribution of PI(4)P pool at the PM. Additionally, ergosterol levels at the PM are decreased and the cytoplasmic levels are augmented.

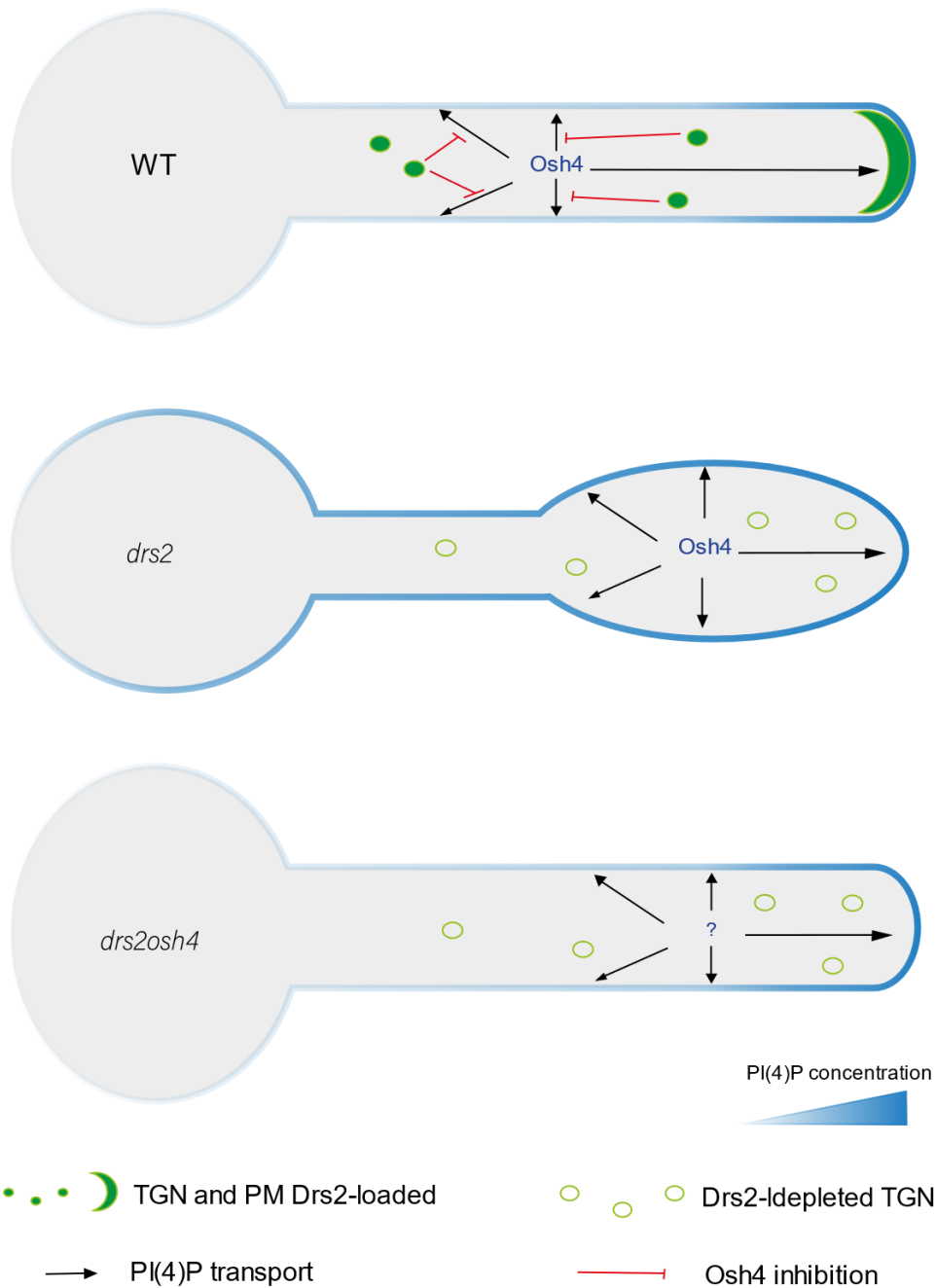


Figure D3. Drs2 negatively regulates Osh4 activity as PI(4)P transporter. In WT cells, Osh4 activity would be downregulated by Drs2. In the absence of the flippase, Osh4 hyperactively transport PI(4)P all over the PM dissolving the gradient. Deletion of OSH4 abolish the hyperactivity defect. “?” could be Osh7 exchanging PI(4)P, and PS.

CONCLUSION

In summary, we characterized the role of flippases during invasive hyphal growth in *Candida albicans*, with a particular focus on Drs2. We determined that Drs2 is critical for the distribution of phospholipids, such as PS and PI(4)P, as well as of ergosterol. Our results also show a genetic interaction between Drs2 and the lipid phosphatase Sac1, which regulates the PM PI(4)P gradient. In addition, we demonstrated that deletion of *OSH4* rescues the invasive hyphal growth defect of *drs2*, indicating that the requirement for flippase activity across the lipid bilayer can be specifically bypassed by lipid exchange between membrane compartments. However, given that deletion of *OSH4* did not rescue growth on papuamide A nor on fluconazole in *drs2*, this suggests that Drs2 has also specific functions in plasma membrane organization, independent of Osh4. Together, our results indicate that a critical balance between the activities of two classes of lipid transporters, as well as a lipid phosphatase, regulates hyphal growth and could be conserved during evolution.

BIBLIOGRAPHY

- Adhikari, H., Cullen, P.J., 2015. Role of phosphatidylinositol phosphate signaling in the regulation of the filamentous-growth mitogen-activated protein kinase pathway. *Eukaryot. Cell* 14, 427–440. <https://doi.org/10.1128/EC.00013-15>
- Alder-Baerens, N., Lisman, Q., Luong, L., Pomorski, T., Holthuis, J.C.M., 2006. Loss of P4 ATPases Drs2p and Dnf3p disrupts aminophospholipid transport and asymmetry in yeast post-Golgi secretory vesicles. *Mol. Biol. Cell* 17, 1632–1642. <https://doi.org/10.1091/mbc.e05-10-0912>
- Allert, S., Förster, T.M., Svensson, C.-M., Richardson, J.P., Pawlik, T., Hebecker, B., Rudolphi, S., Juraschitz, M., Schaller, M., Blagojevic, M., Morschhäuser, J., Figge, M.T., Jacobsen, I.D., Naglik, J.R., Kasper, L., Mogavero, S., Hube, B., 2018. *Candida albicans*-Induced Epithelial Damage Mediates Translocation through Intestinal Barriers. *mBio* 9. <https://doi.org/10.1128/mBio.00915-18>
- Alvarez, F., Douglas, L., Konopka, J., 2007. Sterol-Rich Plasma Membrane Domains in Fungi. *Eukaryot. Cell* 6, 755–63. <https://doi.org/10.1128/EC.00008-07>
- An, S.J., Rivera-Molina, F., Anneken, A., Xi, Z., McNellis, B., Polejaev, V.I., Toomre, D., 2021. An active tethering mechanism controls the fate of vesicles. *Nat. Commun.* 12, 5434. <https://doi.org/10.1038/s41467-021-25465-y>
- Araujo-Bazán, L., Peñalva, M.A., Espeso, E.A., 2008. Preferential localization of the endocytic internalization machinery to hyphal tips underlies polarization of the actin cytoskeleton in *Aspergillus nidulans*. *Mol. Microbiol.* 67, 891–905. <https://doi.org/10.1111/j.1365-2958.2007.06102.x>
- Araujo-Palomares, C.L., Riquelme, M., Castro-Longoria, E., 2009. The polarisome component SPA-2 localizes at the apex of *Neurospora crassa* and partially colocalizes with the Spitzenkörper. *Fungal Genet. Biol.* 46, 551–563. <https://doi.org/10.1016/j.fgb.2009.02.009>
- Arkowitz, R.A., Bassilana, M., 2019. Recent advances in understanding *Candida albicans* hyphal growth. *F1000Research* 8. <https://doi.org/10.12688/f1000research.18546.1>
- Atkinson, K., Fogel, S., Henry, S.A., 1980. Yeast mutant defective in phosphatidylserine synthesis. *J. Biol. Chem.* 255, 6653–6661.
- Atkinson, K.D., Jensen, B., Kolat, A.I., Storm, E.M., Henry, S.A., Fogel, S., 1980. Yeast mutants auxotrophic for choline or ethanolamine. *J. Bacteriol.* 141, 558–564. <https://doi.org/10.1128/jb.141.2.558-564.1980>
- Audhya, A., Foti, M., Emr, S.D., 2000. Distinct roles for the yeast phosphatidylinositol 4-kinases, Stt4p and Pik1p, in secretion, cell growth, and organelle membrane dynamics. *Mol. Biol. Cell* 11, 2673–2689. <https://doi.org/10.1091/mbc.11.8.2673>
- Bai, L., Kovach, A., You, Q., Hsu, H.-C., Zhao, G., Li, H., 2019. Autoinhibition and activation mechanisms of the eukaryotic lipid flippase Drs2p-Cdc50p. *Nat. Commun.* 10. <https://doi.org/10.1038/s41467-019-12191-9>
- Baldrige, R.D., Graham, T.R., 2013. Two-gate mechanism for phospholipid selection and transport by type IV P-type ATPases. *Proc. Natl. Acad. Sci. U. S. A.* 110, E358–367. <https://doi.org/10.1073/pnas.1216948110>
- Baldrige, R.D., Graham, T.R., 2012. Identification of residues defining phospholipid flippase substrate specificity of type IV P-type ATPases. *Proc. Natl. Acad. Sci.* 109, E290–E298. <https://doi.org/10.1073/pnas.1115725109>

- Balhadère, P.V., Talbot, N.J., 2001. PDE1 Encodes a P-Type ATPase Involved in Appressorium-Mediated Plant Infection by the Rice Blast Fungus *Magnaporthe grisea*. *Plant Cell* 13, 1987–2004. <https://doi.org/10.1105/TPC.010056>
- Banerjee, A., Pata, J., Sharma, S., Monk, B.C., Falson, P., Prasad, R., 2021. Directed Mutational Strategies Reveal Drug Binding and Transport by the MDR Transporters of *Candida albicans*. *J. Fungi Basel Switz.* 7, 68. <https://doi.org/10.3390/jof7020068>
- Banerjee, M., Thompson, D.S., Lazzell, A., Carlisle, P.L., Pierce, C., Monteagudo, C., López-Ribot, J.L., Kadosh, D., 2008. UME6, a Novel Filament-specific Regulator of *Candida albicans* Hyphal Extension and Virulence. *Mol. Biol. Cell* 19, 1354–1365. <https://doi.org/10.1091/mbc.E07-11-1110>
- Bansal, D., Bhatti, H.S., Sehgal, R., 2005. Role of cholesterol in parasitic infections. *Lipids Health Dis.* 4, 10. <https://doi.org/10.1186/1476-511X-4-10>
- Bard, F., Malhotra, V., 2006. The formation of TGN-to-plasma-membrane transport carriers. *Annu. Rev. Cell Dev. Biol.* 22, 439–455. <https://doi.org/10.1146/annurev.cellbio.21.012704.133126>
- Bassilana, M., Blyth, J., Arkowitz, R.A., 2003a. Cdc24, the GDP-GTP exchange factor for Cdc42, is required for invasive hyphal growth of *Candida albicans*. *Eukaryot. Cell* 2, 9–18. <https://doi.org/10.1128/ec.2.1.9-18.2003>
- Bassilana, M., Blyth, J., Arkowitz, R.A., 2003b. Cdc24, the GDP-GTP exchange factor for Cdc42, is required for invasive hyphal growth of *Candida albicans*. *Eukaryot. Cell* 2, 9–18. <https://doi.org/10.1128/EC.2.1.9-18.2003>
- Bassilana, M., Hopkins, J., Arkowitz, R.A., 2005. Regulation of the Cdc42/Cdc24 GTPase module during *Candida albicans* hyphal growth. *Eukaryot. Cell* 4, 588–603. <https://doi.org/10.1128/EC.4.3.588-603.2005>
- Bassilana, M., Puerner, C., Arkowitz, R.A., 2020. External signal-mediated polarized growth in fungi. *Curr. Opin. Cell Biol.* 62, 150–158. <https://doi.org/10.1016/j.ceb.2019.11.001>
- Basso, L.R., Bartiss, A., Mao, Y., Gast, C.E., Coelho, P.S.R., Snyder, M., Wong, B., 2010. Transformation of *Candida albicans* with a synthetic hygromycin B resistance gene. *Yeast Chichester Engl.* 27, 1039–1048. <https://doi.org/10.1002/yea.1813>
- Baumann, N.A., Sullivan, D.P., Ohvo-Rekilä, H., Simonot, C., Pottekat, A., Klaassen, Z., Beh, C.T., Menon, A.K., 2005. Transport of Newly Synthesized Sterol to the Sterol-Enriched Plasma Membrane Occurs via Nonvesicular Equilibration. *Biochemistry* 44, 5816–5826. <https://doi.org/10.1021/bi048296z>
- Beh, C.T., Cool, L., Phillips, J., Rine, J., 2001. Overlapping Functions of the Yeast Oxysterol-Binding Protein Homologues. *Genetics* 157, 1117–1140.
- Berepiki, A., Lichius, A., Read, N.D., 2011. Actin organization and dynamics in filamentous fungi. *Nat. Rev. Microbiol.* 9, 876–887. <https://doi.org/10.1038/nrmicro2666>
- Berg, J.M., Tymoczko, J.L., Stryer, L., 2002. Lipids and Many Membrane Proteins Diffuse Rapidly in the Plane of the Membrane. *Biochem.* 5th Ed.
- Bhattacharya, S., Esquivel, B.D., White, T.C., 2018. Overexpression or Deletion of Ergosterol Biosynthesis Genes Alters Doubling Time, Response to Stress Agents, and Drug Susceptibility in *Saccharomyces cerevisiae*. *mBio* 9, e01291-18. <https://doi.org/10.1128/mBio.01291-18>
- Bijlani, S., Thevandavakkam, M.A., Tsai, H.-J., Berman, J., 2019. Autonomously Replicating Linear Plasmids That Facilitate the Analysis of Replication Origin Function in *Candida albicans*. *mSphere* 4. <https://doi.org/10.1128/mSphere.00103-19>
- Binotti, B., Jahn, R., Pérez-Lara, Á., 2021. An overview of the synaptic vesicle lipid composition. *Arch. Biochem. Biophys.* 709, 108966. <https://doi.org/10.1016/j.abb.2021.108966>

- Bishop, A., Lane, R., Beniston, R., Chapa-y-Lazo, B., Smythe, C., Sudbery, P., 2010. Hyphal growth in *Candida albicans* requires the phosphorylation of Sec2 by the Cdc28-Ccn1/Hgc1 kinase. *EMBO J.* 29, 2930–2942. <https://doi.org/10.1038/emboj.2010.158>
- Bogdanov, M., Mileykovskaya, E., Dowhan, W., 2008. Lipids in the Assembly of Membrane Proteins and Organization of Protein Supercomplexes. *Subcell. Biochem.* 49, 197–239. https://doi.org/10.1007/978-1-4020-8831-5_8
- Bohnert, M., 2020. Tether Me, Tether Me Not—Dynamic Organelle Contact Sites in Metabolic Rewiring. *Dev. Cell* 54, 212–225. <https://doi.org/10.1016/j.devcel.2020.06.026>
- Boyne, J.R., Yosuf, H.M., Bieganowski, P., Brenner, C., Price, C., 2000. Yeast myosin light chain, Mlc1p, interacts with both IQGAP and class II myosin to effect cytokinesis. *J. Cell Sci.* 113, 4533–4543. <https://doi.org/10.1242/jcs.113.24.4533>
- Brand, A.C., Morrison, E., Milne, S., Gonia, S., Gale, C.A., Gow, N.A.R., 2014. Cdc42 GTPase dynamics control directional growth responses. *Proc. Natl. Acad. Sci.* 111, 811–816. <https://doi.org/10.1073/pnas.1307264111>
- Braun, B.R., Head, W.S., Wang, M.X., Johnson, A.D., 2000. Identification and characterization of TUP1-regulated genes in *Candida albicans*. *Genetics* 156, 31–44. <https://doi.org/10.1093/genetics/156.1.31>
- Braun, B.R., Kadosh, D., Johnson, A.D., 2001. NRG1, a repressor of filamentous growth in *C. albicans*, is down-regulated during filament induction. *EMBO J.* 20, 4753–4761. <https://doi.org/10.1093/emboj/20.17.4753>
- Bretscher, M.S., 1973. Membrane structure: some general principles. *Science* 181, 622–629. <https://doi.org/10.1126/science.181.4100.622>
- Brunke, S., Hube, B., 2013. Two unlike cousins: *Candida albicans* and *C. glabrata* infection strategies. *Cell. Microbiol.* 15, 701–708. <https://doi.org/10.1111/cmi.12091>
- Brunswik, H., 1924. Untersuchungen über die Geschlechts- und Kernverhältnisse bei der Hymenomyzetengattung *Coprinus*. G. Fischer, Jena.
- Bühler, N., Hagiwara, D., Takeshita, N., 2015. Functional Analysis of Sterol Transporter Orthologues in the Filamentous Fungus *Aspergillus nidulans*. *Eukaryot. Cell* 14, 908–921. <https://doi.org/10.1128/EC.00027-15>
- Butty, A.-C., Perrinjaquet, N., Petit, A., Jaquenoud, M., Segall, J.E., Hofmann, K., Zwahlen, C., Peter, M., 2002. A positive feedback loop stabilizes the guanine-nucleotide exchange factor Cdc24 at sites of polarization. *EMBO J.* 21, 1565–1576. <https://doi.org/10.1093/emboj/21.7.1565>
- Caballero-Lima, D., Kaneva, I.N., Watton, S.P., Sudbery, P.E., Craven, C.J., 2013. The spatial distribution of the exocyst and actin cortical patches is sufficient to organize hyphal tip growth. *Eukaryot. Cell* 12, 998–1008. <https://doi.org/10.1128/EC.00085-13>
- Caballero-Lima, D., Sudbery, P.E., 2014. In *Candida albicans*, phosphorylation of Exo84 by Cdk1-Hgc1 is necessary for efficient hyphal extension. *Mol. Biol. Cell* 25, 1097–1110. <https://doi.org/10.1091/mbc.e13-11-0688>
- Calderone, R.A. (Ed.), 2012. *Candida and candidiasis*, 2nd ed. ed. ASM Press, Washington, DC.
- Calera, J.A., Zhao, X.J., Calderone, R., 2000. Defective hyphal development and avirulence caused by a deletion of the SSK1 response regulator gene in *Candida albicans*. *Infect. Immun.* 68, 518–525. <https://doi.org/10.1128/iai.68.2.518-525.2000>
- Campanale, J.P., Sun, T.Y., Montell, D.J., 2017. Development and dynamics of cell polarity at a glance. *J. Cell Sci.* 130, 1201–1207. <https://doi.org/10.1242/jcs.188599>
- Carlisle, P.L., Kadosh, D., 2010. *Candida albicans* Ume6, a Filament-Specific Transcriptional Regulator, Directs Hyphal Growth via a Pathway Involving Hgc1 Cyclin-Related Protein. *Eukaryot. Cell* 9, 1320–1328. <https://doi.org/10.1128/EC.00046-10>

- Cavalheiro, M., Teixeira, M.C., 2018. *Candida* Biofilms: Threats, Challenges, and Promising Strategies. *Front. Med.* 5, 28. <https://doi.org/10.3389/fmed.2018.00028>
- Chantalat, S., Park, S.-K., Hua, Z., Liu, K., Gobin, R., Peyroche, A., Rambourg, A., Graham, T.R., Jackson, C.L., 2004. The Arf activator Gea2p and the P-type ATPase Drs2p interact at the Golgi in *Saccharomyces cerevisiae*. *J. Cell Sci.* 117, 711–722. <https://doi.org/10.1242/jcs.00896>
- Chapa-y-Lazo, B., Allwood, E.G., Smaczynska-de Rooij, I.I., Snape, M.L., Ayscough, K.R., 2014. Yeast endocytic adaptor AP-2 binds the stress sensor Mid2 and functions in polarized cell responses. *Traffic Cph. Den.* 15, 546–557. <https://doi.org/10.1111/tra.12155>
- Cheffings, T.H., Burroughs, N.J., Balasubramanian, M.K., 2016. Actomyosin Ring Formation and Tension Generation in Eukaryotic Cytokinesis. *Curr. Biol.* 26, R719–R737. <https://doi.org/10.1016/j.cub.2016.06.071>
- Chen, C.Y., Ingram, M.F., Rosal, P.H., Graham, T.R., 1999. Role for Drs2p, a P-type ATPase and potential aminophospholipid translocase, in yeast late Golgi function. *J. Cell Biol.* 147, 1223–1236. <https://doi.org/10.1083/jcb.147.6.1223>
- Chen, H., Kuo, C.-C., Kang, H., Howell, A.S., Zyla, T.R., Jin, M., Lew, D.J., 2012. Cdc42p regulation of the yeast formin Bni1p mediated by the effector Gic2p. *Mol. Biol. Cell* 23, 3814–3826. <https://doi.org/10.1091/mbc.E12-05-0400>
- Chen, H., Zhou, X., Ren, B., Cheng, L., 2020. The regulation of hyphae growth in *Candida albicans*. *Virulence* 11, 337–348. <https://doi.org/10.1080/21505594.2020.1748930>
- Chen, S., Wang, J., Muthusamy, B.-P., Liu, K., Zare, S., Andersen, R.J., Graham, T.R., 2006. Roles for the Drs2p-Cdc50p complex in protein transport and phosphatidylserine asymmetry of the yeast plasma membrane. *Traffic Cph. Den.* 7, 1503–1517. <https://doi.org/10.1111/j.1600-0854.2006.00485.x>
- Chen, Y.-L., Montedonico, A.E., Kauffman, S., Dunlap, J.R., Menn, F.-M., Reynolds, T.B., 2010. Phosphatidylserine synthase and phosphatidylserine decarboxylase are essential for cell wall integrity and virulence in *Candida albicans*. *Mol. Microbiol.* 75, 1112–1132. <https://doi.org/10.1111/j.1365-2958.2009.07018.x>
- Chiapparino, A., Maeda, K., Turei, D., Saez-Rodriguez, J., Gavin, A.-C., 2016. The orchestra of lipid-transfer proteins at the crossroads between metabolism and signaling. *Prog. Lipid Res.* 61, 30–39. <https://doi.org/10.1016/j.plipres.2015.10.004>
- Chiou, J., Balasubramanian, M.K., Lew, D.J., 2017. Cell Polarity in Yeast. *Annu. Rev. Cell Dev. Biol.* 33, 77–101. <https://doi.org/10.1146/annurev-cellbio-100616-060856>
- Cleary, I.A., Reinhard, S.M., Lazzell, A.L., Monteagudo, C., Thomas, D.P., Lopez-Ribot, J.L., Saville, S.P., 2016. Examination of the pathogenic potential of *Candida albicans* filamentous cells in an animal model of haematogenously disseminated candidiasis. *FEMS Yeast Res.* 16. <https://doi.org/10.1093/femsyr/fow011>
- Contreras, F.-X., Sánchez-Magraner, L., Alonso, A., Goñi, F.M., 2010. Transbilayer (flip-flop) lipid motion and lipid scrambling in membranes. *FEBS Lett.* 584, 1779–1786. <https://doi.org/10.1016/j.febslet.2009.12.049>
- Cooper, G.M., 2000. *The Mechanism of Vesicular Transport*. Cell Mol. Approach 2nd Ed.
- Corvest, V., Bogliolo, S., Follette, P., Arkowitz, R.A., Bassilana, M., 2013. Spatiotemporal regulation of Rho1 and Cdc42 activity during *Candida albicans* filamentous growth. *Mol. Microbiol.* 89, 626–648. <https://doi.org/10.1111/mmi.12302>
- Court, H., Sudbery, P., 2007. Regulation of Cdc42 GTPase activity in the formation of hyphae in *Candida albicans*. *Mol. Biol. Cell* 18, 265–281. <https://doi.org/10.1091/mbc.e06-05-0411>
- Crampin, H., Finley, K., Gerami-Nejad, M., Court, H., Gale, C., Berman, J., Sudbery, P., 2005. *Candida albicans* hyphae have a Spitzenkörper that is distinct from the

- polarisome found in yeast and pseudohyphae. *J. Cell Sci.* 118, 2935–2947.
<https://doi.org/10.1242/jcs.02414>
- Cutler, N.S., Heitman, J., Cardenas, M.E., 1997. STT4 is an essential phosphatidylinositol 4-kinase that is a target of wortmannin in *Saccharomyces cerevisiae*. *J. Biol. Chem.* 272, 27671–27677. <https://doi.org/10.1074/jbc.272.44.27671>
- Daleke, D.L., 2003. Regulation of transbilayer plasma membrane phospholipid asymmetry. *J. Lipid Res.* 44, 233–242. <https://doi.org/10.1194/jlr.R200019-JLR200>
- Dalle, F., Wächtler, B., L'Ollivier, C., Holland, G., Bannert, N., Wilson, D., Labruère, C., Bonnin, A., Hube, B., 2010. Cellular interactions of *Candida albicans* with human oral epithelial cells and enterocytes. *Cell. Microbiol.* 12, 248–271.
<https://doi.org/10.1111/j.1462-5822.2009.01394.x>
- D'Ambrosio, J.M., Albanèse, V., Lipp, N.-F., Fleuriot, L., Debayle, D., Drin, G., Čopič, A., 2020. Osh6 requires Ist2 for localization to ER-PM contacts and efficient phosphatidylserine transport in budding yeast. *J. Cell Sci.* 133, jcs243733.
<https://doi.org/10.1242/jcs.243733>
- Danielli, J.F., Davson, H., 1935. A contribution to the theory of permeability of thin films. *J. Cell. Comp. Physiol.* 5, 495–508. <https://doi.org/10.1002/jcp.1030050409>
- Das, A., Slaughter, B.D., Unruh, J.R., Bradford, W.D., Alexander, R., Rubinstein, B., Li, R., 2012. Flippase-mediated phospholipid asymmetry promotes fast Cdc42 recycling in dynamic maintenance of cell polarity. *Nat. Cell Biol.* 14, 304–310.
<https://doi.org/10.1038/ncb2444>
- Davis, S.E., Hopke, A., Minkin, S.C., Montedonico, A.E., Wheeler, R.T., Reynolds, T.B., 2014. Masking of $\beta(1-3)$ -glucan in the cell wall of *Candida albicans* from detection by innate immune cells depends on phosphatidylserine. *Infect. Immun.* 82, 4405–4413.
<https://doi.org/10.1128/IAI.01612-14>
- Davis, S.E., Tams, R.N., Solis, N.V., Wagner, A.S., Chen, T., Jackson, J.W., Hasim, S., Montedonico, A.E., Dinsmore, J., Sparer, T.E., Filler, S.G., Reynolds, T.B., 2018. *Candida albicans* Cannot Acquire Sufficient Ethanolamine from the Host To Support Virulence in the Absence of De Novo Phosphatidylethanolamine Synthesis. *Infect. Immun.* 86, e00815-17. <https://doi.org/10.1128/IAI.00815-17>
- de León, N., Hoya, M., Curto, M.-A., Moro, S., Yanguas, F., Doncel, C., Valdivieso, M.-H., 2016. The AP-2 complex is required for proper temporal and spatial dynamics of endocytic patches in fission yeast. *Mol. Microbiol.* 100, 409–424.
<https://doi.org/10.1111/mmi.13327>
- de Saint-Jean, M., Delfosse, V., Douguet, D., Chicanne, G., Payrastra, B., Bourguet, W., Antony, B., Drin, G., 2011. Osh4p exchanges sterols for phosphatidylinositol 4-phosphate between lipid bilayers. *J. Cell Biol.* 195, 965–978.
<https://doi.org/10.1083/jcb.201104062>
- Del Bel, L.M., Brill, J.A., 2018. Sac1, a lipid phosphatase at the interface of vesicular and nonvesicular transport. *Traffic Cph. Den.* 19, 301–318.
<https://doi.org/10.1111/tra.12554>
- Delfosse, V., Bourguet, W., Drin, G., 2020. Structural and Functional Specialization of OSBP-Related Proteins. *Contact* 3, 2515256420946627.
<https://doi.org/10.1177/2515256420946627>
- Delgado-Álvarez, D.L., Callejas-Negrete, O.A., Gómez, N., Freitag, M., Roberson, R.W., Smith, L.G., Mouriño-Pérez, R.R., 2010. Visualization of F-actin localization and dynamics with live cell markers in *Neurospora crassa*. *Fungal Genet. Biol.* 47, 573–586. <https://doi.org/10.1016/j.fgb.2010.03.004>
- Desai, J.V., 2018. *Candida albicans* Hyphae: From Growth Initiation to Invasion. *J. Fungi* 4, 10. <https://doi.org/10.3390/jof4010010>

- Desrivieres, S., Cooke, F.T., Parker, P.J., Hall, M.N., 1998. MSS4, a Phosphatidylinositol-4-phosphate 5-Kinase Required for Organization of the Actin Cytoskeleton in *Saccharomyces cerevisiae* *. *J. Biol. Chem.* 273, 15787–15793. <https://doi.org/10.1074/jbc.273.25.15787>
- Diaz-Rohrer, B.B., Levental, K.R., Simons, K., Levental, I., 2014. Membrane raft association is a determinant of plasma membrane localization. *Proc. Natl. Acad. Sci. U. S. A.* 111, 8500–8505. <https://doi.org/10.1073/pnas.1404582111>
- Diezmann, S., Cox, C.J., Schönian, G., Vilgalys, R.J., Mitchell, T.G., 2004. Phylogeny and evolution of medical species of *Candida* and related taxa: a multigenic analysis. *J. Clin. Microbiol.* 42, 5624–5635. <https://doi.org/10.1128/JCM.42.12.5624-5635.2004>
- Doktorova, M., Symons, J., Levental, I., 2020. Structural and functional consequences of reversible lipid asymmetry in living membranes. *Nat. Chem. Biol.* 16, 1321–1330. <https://doi.org/10.1038/s41589-020-00688-0>
- Douglas, L.M., Konopka, J.B., 2019. Plasma membrane architecture protects *Candida albicans* from killing by copper. *PLoS Genet.* 15, e1007911. <https://doi.org/10.1371/journal.pgen.1007911>
- Douglas, L.M., Konopka, J.B., 2016. Plasma membrane organization promotes virulence of the human fungal pathogen *Candida albicans*. *J. Microbiol. Seoul Korea* 54, 178–191. <https://doi.org/10.1007/s12275-016-5621-y>
- Douglas, L.M., Martin, S.W., Konopka, J.B., 2009. BAR Domain Proteins Rvs161 and Rvs167 Contribute to *Candida albicans* Endocytosis, Morphogenesis, and Virulence. *Infect. Immun.* 77, 4150–4160. <https://doi.org/10.1128/IAI.00683-09>
- Dunker, C., Polke, M., Schulze-Richter, B., Schubert, K., Rudolphi, S., Gressler, A.E., Pawlik, T., Prada Salcedo, J.P., Niemiec, M.J., Slesiona-Künzel, S., Swidergall, M., Martin, R., Dandekar, T., Jacobsen, I.D., 2021. Rapid proliferation due to better metabolic adaptation results in full virulence of a filament-deficient *Candida albicans* strain. *Nat. Commun.* 12, 3899. <https://doi.org/10.1038/s41467-021-24095-8>
- Dünkler, A., Wendland, J., 2007. *Candida albicans* Rho-type GTPase-encoding genes required for polarized cell growth and cell separation. *Eukaryot. Cell* 6, 844–854. <https://doi.org/10.1128/EC.00201-06>
- Epp, E., Nazarova, E., Regan, H., Douglas, L.M., Konopka, J.B., Vogel, J., Whiteway, M., 2013a. Clathrin- and Arp2/3-independent endocytosis in the fungal pathogen *Candida albicans*. *mBio* 4, e00476-00413. <https://doi.org/10.1128/mBio.00476-13>
- Epp, E., Nazarova, E., Regan, H., Douglas, L.M., Konopka, J.B., Vogel, J., Whiteway, M., 2013b. Clathrin- and Arp2/3-Independent Endocytosis in the Fungal Pathogen *Candida albicans*. *mBio* 4, e00476-13. <https://doi.org/10.1128/mBio.00476-13>
- Epp, E., Walther, A., Guylaine, L., Leon, Z., Mullick, A., Raymond, M., Wendland, J., Whiteway, M., 2010. Forward genetics in *Candida albicans* that reveals the Arp2/3 complex is required for hyphal formation, but not endocytosis. *Mol. Microbiol.* 75, 1182–1198. <https://doi.org/10.1111/j.1365-2958.2009.07038.x>
- Fahy, E., Cotter, D., Sud, M., Subramaniam, S., 2011. Lipid classification, structures and tools. *Biochim. Biophys. Acta* 1811, 637–647. <https://doi.org/10.1016/j.bbaliip.2011.06.009>
- Fahy, E., Subramaniam, S., Brown, H.A., Glass, C.K., Merrill, A.H., Murphy, R.C., Raetz, C.R.H., Russell, D.W., Seyama, Y., Shaw, W., Shimizu, T., Spener, F., Meer, G. van, VanNieuwenhze, M.S., White, S.H., Witztum, J.L., Dennis, E.A., 2005. A comprehensive classification system for lipids. *J. Lipid Res.* 46, 839–862. <https://doi.org/10.1194/jlr.E400004-JLR200>
- Fahy, E., Subramaniam, S., Murphy, R.C., Nishijima, M., Raetz, C.R.H., Shimizu, T., Spener, F., van Meer, G., Wakelam, M.J.O., Dennis, E.A., 2009. Update of the LIPID MAPS

- comprehensive classification system for lipids. *J. Lipid Res.* 50, S9–S14. <https://doi.org/10.1194/jlr.R800095-JLR200>
- Fairn, G.D., Hermansson, M., Somerharju, P., Grinstein, S., 2011. Phosphatidylserine is polarized and required for proper Cdc42 localization and for development of cell polarity. *Nat. Cell Biol.* 13, 1424–1430. <https://doi.org/10.1038/ncb2351>
- Fan, Y., He, H., Dong, Y., Pan, H., 2013. Hyphae-specific genes HGC1, ALS3, HWP1, and ECE1 and relevant signaling pathways in *Candida albicans*. *Mycopathologia* 176, 329–335. <https://doi.org/10.1007/s11046-013-9684-6>
- Feyder, S., De Craene, J.-O., Bär, S., Bertazzi, D.L., Friant, S., 2015. Membrane Trafficking in the Yeast *Saccharomyces cerevisiae* Model. *Int. J. Mol. Sci.* 16, 1509–1525. <https://doi.org/10.3390/ijms16011509>
- Filseck, J.M. von, Vanni, S., Mesmin, B., Antonny, B., Drin, G., 2015. A phosphatidylinositol-4-phosphate powered exchange mechanism to create a lipid gradient between membranes. *Nat. Commun.* 6, 1–12. <https://doi.org/10.1038/ncomms7671>
- Finley, K.R., Berman, J., 2005. Microtubules in *Candida albicans* hyphae drive nuclear dynamics and connect cell cycle progression to morphogenesis. *Eukaryot. Cell* 4, 1697–1711. <https://doi.org/10.1128/EC.4.10.1697-1711.2005>
- Fitzpatrick, D.A., Logue, M.E., Stajich, J.E., Butler, G., 2006. A fungal phylogeny based on 42 complete genomes derived from supertree and combined gene analysis. *BMC Evol. Biol.* 6, 99. <https://doi.org/10.1186/1471-2148-6-99>
- Flanagan, C.A., Schnieders, E.A., Emerick, A.W., Kunisawa, R., Admon, A., Thorner, J., 1993. Phosphatidylinositol 4-kinase: gene structure and requirement for yeast cell viability. *Science* 262, 1444–1448. <https://doi.org/10.1126/science.8248783>
- Florek, O.B., Clifton, L.A., Wilde, M., Arnold, T., Green, R.J., Frazier, R.A., 2018. Lipid composition in fungal membrane models: effect of lipid fluidity. *Acta Crystallogr. Sect. Struct. Biol.* 74, 1233–1244. <https://doi.org/10.1107/S2059798318009440>
- Foti, M., Audhya, A., Emr, S.D., 2001. Sac1 Lipid Phosphatase and Stt4 Phosphatidylinositol 4-Kinase Regulate a Pool of Phosphatidylinositol 4-Phosphate That Functions in the Control of the Actin Cytoskeleton and Vacuole Morphology. *Mol. Biol. Cell* 12, 2396–2411.
- Frøsig, M.M., Costa, S.R., Liesche, J., Østerberg, J.T., Hanisch, S., Nintemann, S., Sørensen, H., Palmgren, M., Pomorski, T.G., López-Marqués, R.L., 2020. Pseudohyphal growth in *Saccharomyces cerevisiae* involves protein kinase-regulated lipid flippases. *J. Cell Sci.* 133. <https://doi.org/10.1242/jcs.235994>
- Furuta, N., Fujimura-Kamada, K., Saito, K., Yamamoto, T., Tanaka, K., 2007. Endocytic Recycling in Yeast Is Regulated by Putative Phospholipid Translocases and the Ypt31p/32p–Rcy1p Pathway. *Mol. Biol. Cell* 18, 295–312. <https://doi.org/10.1091/mbc.E06-05-0461>
- Gall, W.E., Geething, N.C., Hua, Z., Ingram, M.F., Liu, K., Chen, S.I., Graham, T.R., 2002. Drs2p-Dependent Formation of Exocytic Clathrin-Coated Vesicles In Vivo. *Curr. Biol.* 12, 1623–1627. [https://doi.org/10.1016/S0960-9822\(02\)01148-X](https://doi.org/10.1016/S0960-9822(02)01148-X)
- Garcia-Bustos, J.F., Marini, F., Stevenson, I., Frei, C., Hall, M.N., 1994. PIK1, an essential phosphatidylinositol 4-kinase associated with the yeast nucleus. *EMBO J.* 13, 2352–2361.
- Garrenton, L.S., Stefan, C.J., McMurray, M.A., Emr, S.D., Thorner, J., 2010. Pheromone-induced anisotropy in yeast plasma membrane phosphatidylinositol-4,5-bisphosphate distribution is required for MAPK signaling. *Proc. Natl. Acad. Sci.* 107, 11805–11810. <https://doi.org/10.1073/pnas.1005817107>

- Garrenton, L.S., Young, S.L., Thorner, J., 2006. Function of the MAPK scaffold protein, Ste5, requires a cryptic PH domain. *Genes Dev.* 20, 1946–1958. <https://doi.org/10.1101/gad.1413706>
- Georgiev, A.G., Sullivan, D.P., Kersting, M.C., Dittman, J.S., Beh, C.T., Menon, A.K., 2011. Osh Proteins Regulate Membrane Sterol Organization but Are Not Required for Sterol Movement Between the ER and PM. *Traffic* 12, 1341–1355. <https://doi.org/10.1111/j.1600-0854.2011.01234.x>
- Gerami-Nejad, M., Zacchi, L.F., McClellan, M., Matter, K., Berman, J., 2013. Shuttle vectors for facile gap repair cloning and integration into a neutral locus in *Candida albicans*. *Microbiol. Read. Engl.* 159, 565–579. <https://doi.org/10.1099/mic.0.064097-0>
- Ghugtyal, V., Garcia-Rodas, R., Seminara, A., Schaub, S., Bassilana, M., Arkowitz, R.A., 2015. Phosphatidylinositol-4-phosphate-dependent membrane traffic is critical for fungal filamentous growth. *Proc. Natl. Acad. Sci.* 112, 8644–8649. <https://doi.org/10.1073/pnas.1504259112>
- Gilbert, M.J., Thornton, C.R., Wakley, G.E., Talbot, N.J., 2006. A P-type ATPase required for rice blast disease and induction of host resistance. *Nature* 440, 535–539. <https://doi.org/10.1038/nature04567>
- Gomez-Navarro, N., Miller, E., 2016. Protein sorting at the ER–Golgi interface. *J. Cell Biol.* 215, 769–778. <https://doi.org/10.1083/jcb.201610031>
- González-Novo, A., Aldana, C.V. de, Jiménez, J., 2009. Fungal septins: one ring to rule it all? *Open Life Sci.* 4, 274–289. <https://doi.org/10.2478/s11535-009-0032-2>
- González-Novo, A., Correa-Bordes, J., Labrador, L., Sánchez, M., Vázquez de Aldana, C.R., Jiménez, J., 2008. Sep7 is essential to modify septin ring dynamics and inhibit cell separation during *Candida albicans* hyphal growth. *Mol. Biol. Cell* 19, 1509–1518. <https://doi.org/10.1091/mbc.e07-09-0876>
- Gorter, E., Grendel, F., 1925. ON BIMOLECULAR LAYERS OF LIPOIDS ON THE CHROMOCYTES OF THE BLOOD. *J. Exp. Med.* 41, 439–443.
- Greig, J.A., Sudbery, I.M., Richardson, J.P., Naglik, J.R., Wang, Y., Sudbery, P.E., 2015. Cell Cycle-Independent Phospho-Regulation of Fkh2 during Hyphal Growth Regulates *Candida albicans* Pathogenesis. *PLOS Pathog.* 11, e1004630. <https://doi.org/10.1371/journal.ppat.1004630>
- Grinhagens, S., Dünkler, A., Wu, Y., Rieger, L., Brenner, P., Gronemeyer, T., Mulaw, M.A., Johnsson, N., 2020. A time-resolved interaction analysis of Bem1 reconstructs the flow of Cdc42 during polar growth. *Life Sci. Alliance* 3. <https://doi.org/10.26508/lsa.202000813>
- Grossmann, G., Opekarová, M., Malinsky, J., Weig-Meckl, I., Tanner, W., 2007. Membrane potential governs lateral segregation of plasma membrane proteins and lipids in yeast. *EMBO J.* 26, 1–8. <https://doi.org/10.1038/sj.emboj.7601466>
- Gu, R.-X., Baoukina, S., Tieleman, D.P., 2019. Cholesterol Flip-Flop in Heterogeneous Membranes. *J. Chem. Theory Comput.* 15, 2064–2070. <https://doi.org/10.1021/acs.jctc.8b00933>
- Guillas, I., Vernay, A., Vitagliano, J.-J., Arkowitz, R.A., 2013. Phosphatidylinositol 4,5-bisphosphate is required for invasive growth in *Saccharomyces cerevisiae*. *J. Cell Sci.* 126, 3602–3614. <https://doi.org/10.1242/jcs.122606>
- Guo, P.P., Yong, J.Y.A., Wang, Y.M., Li, C.R., 2016. Sec15 links bud site selection to polarised cell growth and exocytosis in *Candida albicans*. *Sci. Rep.* 6, 26464. <https://doi.org/10.1038/srep26464>
- Hankins, H.M., Baldrige, R.D., Xu, P., Graham, T.R., 2015a. Role of flippases, scramblases and transfer proteins in phosphatidylserine subcellular distribution. *Traffic Cph. Den.* 16, 35–47. <https://doi.org/10.1111/tra.12233>

- Hankins, H.M., Sere, Y.Y., Diab, N.S., Menon, A.K., Graham, T.R., 2015b. Phosphatidylserine translocation at the yeast trans-Golgi network regulates protein sorting into exocytic vesicles. *Mol. Biol. Cell* 26, 4674–4685. <https://doi.org/10.1091/mbc.E15-07-0487>
- Harayama, T., Riezman, H., 2018. Understanding the diversity of membrane lipid composition. *Nat. Rev. Mol. Cell Biol.* 19, 281–296. <https://doi.org/10.1038/nrm.2017.138>
- Has, C., Das, S.L., 2021. Recent developments in membrane curvature sensing and induction by proteins. *Biochim. Biophys. Acta BBA - Gen. Subj.* 1865, 129971. <https://doi.org/10.1016/j.bbagen.2021.129971>
- Haupt, A., Minc, N., 2017. Gradients of phosphatidylserine contribute to plasma membrane charge localization and cell polarity in fission yeast. *Mol. Biol. Cell* 28, 210–220. <https://doi.org/10.1091/mbc.E16-06-0353>
- Hazan, I., Liu, H., 2002. Hyphal Tip-Associated Localization of Cdc42 Is F-Actin Dependent in *Candida albicans*. *Eukaryot. Cell* 1, 856–864. <https://doi.org/10.1128/EC.1.6.856-864.2002>
- Hazan, I., Sepulveda-Becerra, M., Liu, H., 2002. Hyphal elongation is regulated independently of cell cycle in *Candida albicans*. *Mol. Biol. Cell* 13, 134–145. <https://doi.org/10.1091/mbc.01-03-0116>
- Hedges, S.B., 2002. The origin and evolution of model organisms. *Nat. Rev. Genet.* 3, 838–849. <https://doi.org/10.1038/nrg929>
- Heino, S., Lusa, S., Somerharju, P., Ehnholm, C., Olkkonen, V.M., Ikonen, E., 2000. Dissecting the role of the Golgi complex and lipid rafts in biosynthetic transport of cholesterol to the cell surface. *Proc. Natl. Acad. Sci.* 97, 8375–8380. <https://doi.org/10.1073/pnas.140218797>
- Holthuis, J.C.M., Menon, A.K., 2014. Lipid landscapes and pipelines in membrane homeostasis. *Nature* 510, 48–57. <https://doi.org/10.1038/nature13474>
- Homma, K., Terui, S., Minemura, M., Qadota, H., Anraku, Y., Kanaho, Y., Ohya, Y., 1998. Phosphatidylinositol-4-phosphate 5-kinase localized on the plasma membrane is essential for yeast cell morphogenesis. *J. Biol. Chem.* 273, 15779–15786. <https://doi.org/10.1074/jbc.273.25.15779>
- Horvath, S.E., Daum, G., 2013. Lipids of mitochondria. *Prog. Lipid Res.* 52, 590–614. <https://doi.org/10.1016/j.plipres.2013.07.002>
- Hoyer, L.L., Cota, E., 2016. *Candida albicans* Agglutinin-Like Sequence (Als) Family Vignettes: A Review of Als Protein Structure and Function. *Front. Microbiol.* 7. <https://doi.org/10.3389/fmicb.2016.00280>
- Hu, G., Caza, M., Bakkeren, E., Kretschmer, M., Bairwa, G., Reiner, E., Kronstad, J., 2017. A P4-ATPase subunit of the Cdc50 family plays a role in iron acquisition and virulence in *Cryptococcus neoformans*. *Cell. Microbiol.* 19, e12718. <https://doi.org/10.1111/cmi.12718>
- Hu, G., Kronstad, J.W., 2010. A putative P-type ATPase, Apt1, is involved in stress tolerance and virulence in *Cryptococcus neoformans*. *Eukaryot. Cell* 9, 74–83. <https://doi.org/10.1128/EC.00289-09>
- Hua, Z., Fatheddin, P., Graham, T.R., 2002. An essential subfamily of Drs2p-related P-type ATPases is required for protein trafficking between Golgi complex and endosomal/vacuolar system. *Mol. Biol. Cell* 13, 3162–3177. <https://doi.org/10.1091/mbc.e02-03-0172>
- Huang, Z., Feng, Z., Zou, Y., 2021. New wine in old bottles: current progress on P5 ATPases. *FEBS J.* <https://doi.org/10.1111/febs.16172>

- Hur, H., Ryu, J.-H., Kim, K.-H., Kim, J., 2006. Characterization of Osh3, an oxysterol-binding protein, in filamentous growth of *Saccharomyces cerevisiae* and *Candida albicans*. *J. Microbiol. Seoul Korea* 44, 523–529.
- Hurst, L.R., Fratti, R.A., 2020. Lipid Rafts, Sphingolipids, and Ergosterol in Yeast Vacuole Fusion and Maturation. *Front. Cell Dev. Biol.* 8, 539. <https://doi.org/10.3389/fcell.2020.00539>
- Ikeda, M., Kihara, A., Igarashi, Y., 2006. Lipid asymmetry of the eukaryotic plasma membrane: functions and related enzymes. *Biol. Pharm. Bull.* 29, 1542–1546. <https://doi.org/10.1248/bpb.29.1542>
- Inoue, H., Nojima, H., Okayama, H., 1990. High efficiency transformation of *Escherichia coli* with plasmids. *Gene* 96, 23–28. [https://doi.org/10.1016/0378-1119\(90\)90336-p](https://doi.org/10.1016/0378-1119(90)90336-p)
- Jacobson, K., Liu, P., Lagerholm, B.C., 2019. The Lateral Organization and Mobility of Plasma Membrane Components. *Cell* 177, 806–819. <https://doi.org/10.1016/j.cell.2019.04.018>
- Janmey, P.A., Kinnunen, P.K.J., 2006. Biophysical properties of lipids and dynamic membranes. *Trends Cell Biol.* 16, 538–546. <https://doi.org/10.1016/j.tcb.2006.08.009>
- Johnson, D.I., Pringle, J.R., 1990. Molecular characterization of CDC42, a *Saccharomyces cerevisiae* gene involved in the development of cell polarity. *J. Cell Biol.* 111, 143–152. <https://doi.org/10.1083/jcb.111.1.143>
- Jones, L.A., Sudbery, P.E., 2010. Spitzenkörper, Exocyst, and Polarisome Components in *Candida albicans* Hyphae Show Different Patterns of Localization and Have Distinct Dynamic Properties. *Eukaryot. Cell* 9, 1455–1465. <https://doi.org/10.1128/EC.00109-10>
- Jones, T., Federspiel, N.A., Chibana, H., Dungan, J., Kalman, S., Magee, B.B., Newport, G., Thorstenson, Y.R., Agabian, N., Magee, P.T., Davis, R.W., Scherer, S., 2004. The diploid genome sequence of *Candida albicans*. *Proc. Natl. Acad. Sci. U. S. A.* 101, 7329–7334. <https://doi.org/10.1073/pnas.0401648101>
- Kato, U., Emoto, K., Fredriksson, C., Nakamura, H., Ohta, A., Kobayashi, Toshihide, Murakami-Murofushi, K., Kobayashi, Tetsuyuki, Umeda, M., 2002. A novel membrane protein, Ros3p, is required for phospholipid translocation across the plasma membrane in *Saccharomyces cerevisiae*. *J. Biol. Chem.* 277, 37855–37862. <https://doi.org/10.1074/jbc.M205564200>
- Kim, K., Gadila, S.K.G., 2016. Cargo trafficking from the trans-Golgi network towards the endosome. *Biol. Cell* 108, 205–218. <https://doi.org/10.1111/boc.201600001>
- Klemm, R.W., Ejsing, C.S., Surma, M.A., Kaiser, H.-J., Gerl, M.J., Sampaio, J.L., de Robillard, Q., Ferguson, C., Proszynski, T.J., Shevchenko, A., Simons, K., 2009. Segregation of sphingolipids and sterols during formation of secretory vesicles at the trans-Golgi network. *J. Cell Biol.* 185, 601–612. <https://doi.org/10.1083/jcb.200901145>
- Klose, C., Surma, M.A., Gerl, M.J., Meyenhofer, F., Shevchenko, A., Simons, K., 2012. Flexibility of a eukaryotic lipidome--insights from yeast lipidomics. *PloS One* 7, e35063. <https://doi.org/10.1371/journal.pone.0035063>
- Klug, L., Daum, G., 2014. Yeast lipid metabolism at a glance. *FEMS Yeast Res.* 14, 369–388. <https://doi.org/10.1111/1567-1364.12141>
- Knafler, H.C., Rooij, I.I.S., Walker, L.A., Lee, K.K., Gow, N. a. R., Ayscough, K.R., 2019. AP-2-Dependent Endocytic Recycling of the Chitin Synthase Chs3 Regulates Polarized Growth in *Candida albicans*. *mBio* 10, e02421-18. <https://doi.org/10.1128/mBio.02421-18>
- Kobayashi, T., Menon, A.K., 2018. Transbilayer lipid asymmetry. *Curr. Biol. CB* 28, R386–R391. <https://doi.org/10.1016/j.cub.2018.01.007>

- Köhli, M., Galati, V., Boudier, K., Roberson, R.W., Philippsen, P., 2008. Growth-speed-correlated localization of exocyst and polarisome components in growth zones of *Ashbya gossypii* hyphal tips. *J. Cell Sci.* 121, 3878–3889. <https://doi.org/10.1242/jcs.033852>
- Kornitzer, D., 2019. Regulation of *Candida albicans* Hyphal Morphogenesis by Endogenous Signals. *J. Fungi* 5, 21. <https://doi.org/10.3390/jof5010021>
- Kudo, N., Kumagai, K., Tomishige, N., Yamaji, T., Wakatsuki, S., Nishijima, M., Hanada, K., Kato, R., 2008. Structural basis for specific lipid recognition by CERT responsible for nonvesicular trafficking of ceramide. *Proc. Natl. Acad. Sci. U. S. A.* 105, 488–493. <https://doi.org/10.1073/pnas.0709191105>
- Kullberg, B.J., Arendrup, M.C., 2015. Invasive Candidiasis. *N. Engl. J. Med.* 373, 1445–1456. <https://doi.org/10.1056/NEJMra1315399>
- Kusumi, A., Hyde, J.S., 1982. Spin-label saturation-transfer electron spin resonance detection of transient association of rhodopsin in reconstituted membranes. *Biochemistry* 21, 5978–5983. <https://doi.org/10.1021/bi00266a039>
- Labbaoui, H., Bogliolo, S., Ghugtyal, V., Solis, N.V., Filler, S.G., Arkowitz, R.A., Bassilana, M., 2017. Role of Arf GTPases in fungal morphogenesis and virulence. *PLOS Pathog.* 13, e1006205. <https://doi.org/10.1371/journal.ppat.1006205>
- Lai, W.-C., Sun, H.-F.S., Lin, P.-H., Ho Lin, H.L., Shieh, J.-C., 2016. A new rapid and efficient system with dominant selection developed to inactivate and conditionally express genes in *Candida albicans*. *Curr. Genet.* 62, 213–235. <https://doi.org/10.1007/s00294-015-0526-6>
- Lanze, C.E., Gandra, R.M., Foderaro, J.E., Swenson, K.A., Douglas, L.M., Konopka, J.B., 2020. Plasma Membrane MCC/Eisosome Domains Promote Stress Resistance in Fungi. *Microbiol. Mol. Biol. Rev.* MMBR 84, e00063-19. <https://doi.org/10.1128/MMBR.00063-19>
- Lenoir, G., D'Ambrosio, J.M., Dieudonné, T., Čopič, A., 2021. Transport Pathways That Contribute to the Cellular Distribution of Phosphatidylserine. *Front. Cell Dev. Biol.* 9, 737907. <https://doi.org/10.3389/fcell.2021.737907>
- Lenoir, G., Williamson, P., Puts, C.F., Holthuis, J.C.M., 2009. Cdc50p plays a vital role in the ATPase reaction cycle of the putative aminophospholipid transporter Drs2p. *J. Biol. Chem.* 284, 17956–17967. <https://doi.org/10.1074/jbc.M109.013722>
- Letts, V.A., Klig, L.S., Bae-Lee, M., Carman, G.M., Henry, S.A., 1983. Isolation of the yeast structural gene for the membrane-associated enzyme phosphatidylserine synthase. *Proc. Natl. Acad. Sci. U. S. A.* 80, 7279–7283. <https://doi.org/10.1073/pnas.80.23.7279>
- Lev, S., 2012. Nonvesicular lipid transfer from the endoplasmic reticulum. *Cold Spring Harb. Perspect. Biol.* 4, a013300. <https://doi.org/10.1101/cshperspect.a013300>
- Li, C.-R., Lee, R.T.-H., Wang, Y.-M., Zheng, X.-D., Wang, Y., 2007. *Candida albicans* hyphal morphogenesis occurs in Sec3p-independent and Sec3p-dependent phases separated by septin ring formation. *J. Cell Sci.* 120, 1898–1907. <https://doi.org/10.1242/jcs.002931>
- Li, C.R., Wang, Y.M., De Zheng, X., Liang, H.Y., Tang, J.C.W., Wang, Y., 2005. The formin family protein CaBni1p has a role in cell polarity control during both yeast and hyphal growth in *Candida albicans*. *J. Cell Sci.* 118, 2637–2648. <https://doi.org/10.1242/jcs.02393>
- Li, S., Ghosh, C., Xing, Y., Sun, Y., 2020. Phosphatidylinositol 4,5-bisphosphate in the Control of Membrane Trafficking. *Int. J. Biol. Sci.* 16, 2761–2774. <https://doi.org/10.7150/ijbs.49665>

- Lichius, A., Goryachev, A.B., Fricker, M.D., Obara, B., Castro-Longoria, E., Read, N.D., 2014. CDC-42 and RAC-1 regulate opposite chemotropisms in *Neurospora crassa*. *J. Cell Sci.* 127, 1953–1965. <https://doi.org/10.1242/jcs.141630>
- Ling, Y., Hayano, S., Novick, P., 2014. Osh4p is needed to reduce the level of phosphatidylinositol-4-phosphate on secretory vesicles as they mature. *Mol. Biol. Cell* 25. <https://doi.org/10.1091/mbc.E14-06-1087>
- Lingwood, D., Binnington, B., Róg, T., Vattulainen, I., Grzybek, M., Coskun, Ü., Lingwood, C.A., Simons, K., 2011. Cholesterol modulates glycolipid conformation and receptor activity. *Nat. Chem. Biol.* 7, 260–262. <https://doi.org/10.1038/nchembio.551>
- Lipp, N.-F., Ikhlef, S., Milanini, J., Drin, G., 2020. Lipid Exchangers: Cellular Functions and Mechanistic Links With Phosphoinositide Metabolism. *Front. Cell Dev. Biol.* 8, 663. <https://doi.org/10.3389/fcell.2020.00663>
- Lo, H.-J., Köhler, J.R., DiDomenico, B., Loebenberg, D., Cacciapuoti, A., Fink, G.R., 1997. Nonfilamentous *C. albicans* Mutants Are Avirulent. *Cell* 90, 939–949. [https://doi.org/10.1016/S0092-8674\(00\)80358-X](https://doi.org/10.1016/S0092-8674(00)80358-X)
- Lodish, H.F. (Ed.), 2008. *Molecular cell biology*, 6th ed. ed. W.H. Freeman, New York.
- López-Marqués, R.L., 2021. Lipid flippases as key players in plant adaptation to their environment. *Nat. Plants* 7, 1188–1199. <https://doi.org/10.1038/s41477-021-00993-z>
- Lopez-Marques, R.L., Theorin, L., Palmgren, M.G., Pomorski, T.G., 2014. P4-ATPases: lipid flippases in cell membranes. *Pflugers Arch.* 466, 1227–1240. <https://doi.org/10.1007/s00424-013-1363-4>
- Lorent, J.H., Levental, K.R., Ganesan, L., Rivera-Longworth, G., Sezgin, E., Doktorova, M., Lyman, E., Levental, I., 2020. Plasma membranes are asymmetric in lipid unsaturation, packing and protein shape. *Nat. Chem. Biol.* 16, 644–652. <https://doi.org/10.1038/s41589-020-0529-6>
- Lyons, J.A., Timcenko, M., Dieudonné, T., Lenoir, G., Nissen, P., 2020. P4-ATPases: how an old dog learnt new tricks - structure and mechanism of lipid flippases. *Curr. Opin. Struct. Biol.* 63, 65–73. <https://doi.org/10.1016/j.sbi.2020.04.001>
- Ma, M., Burd, C.G., 2020. Retrograde trafficking and plasma membrane recycling pathways of the budding yeast *Saccharomyces cerevisiae*. *Traffic Cph. Den.* 21, 45–59. <https://doi.org/10.1111/tra.12693>
- Maeda, K., Anand, K., Chiapparino, A., Kumar, A., Poletto, M., Kaksonen, M., Gavin, A.-C., 2013. Interactome map uncovers phosphatidylserine transport by oxysterol-binding proteins. *Nature* 501, 257–261. <https://doi.org/10.1038/nature12430>
- Mahmutefendić, H., Zagorac, G.B., Lučin, S.M. and P., 2018. Rapid Endosomal Recycling, Peripheral Membrane Proteins. *IntechOpen*. <https://doi.org/10.5772/intechopen.75685>
- Makarova, M., Owen, D.M., 2020. Asymmetry across the membrane. *Nat. Chem. Biol.* 16, 605–606. <https://doi.org/10.1038/s41589-020-0545-6>
- Malinsky, J., Opekarová, M., Grossmann, G., Tanner, W., 2013. Membrane microdomains, rafts, and detergent-resistant membranes in plants and fungi. *Annu. Rev. Plant Biol.* 64, 501–529. <https://doi.org/10.1146/annurev-arplant-050312-120103>
- Manik, M.K., Yang, H., Tong, J., Im, Y.J., 2017. Structure of Yeast OSBP-Related Protein Osh1 Reveals Key Determinants for Lipid Transport and Protein Targeting at the Nucleus-Vacuole Junction. *Structure* 25, 617-629.e3. <https://doi.org/10.1016/j.str.2017.02.010>
- Marek, M., Vincenzetti, V., Martin, S.G., 2020. Sterol biosensor reveals LAM-family Ltc1-dependent sterol flow to endosomes upon Arp2/3 inhibition. *J. Cell Biol.* 219. <https://doi.org/10.1083/jcb.202001147>
- Martin, R., Hellwig, D., Schaub, Y., Bauer, J., Walther, A., Wendland, J., 2007. Functional analysis of *Candida albicans* genes whose *Saccharomyces cerevisiae* homologues are

- involved in endocytosis. *Yeast* Chichester Engl. 24, 511–522.
<https://doi.org/10.1002/yea.1489>
- Martin, R., Walther, A., Wendland, J., 2005. Ras1-Induced Hyphal Development in *Candida albicans* Requires the Formin Bni1. *Eukaryot. Cell* 4, 1712–1724.
<https://doi.org/10.1128/EC.4.10.1712-1724.2005>
- Martin, S.G., 2019a. Quorum sensing with pheromones. *Nat. Microbiol.* 4, 1430–1431.
<https://doi.org/10.1038/s41564-019-0538-y>
- Martin, S.G., 2019b. Molecular mechanisms of chemotropism and cell fusion in unicellular fungi. *J. Cell Sci.* 132. <https://doi.org/10.1242/jcs.230706>
- Martin, S.G., Arkowitz, R.A., 2014. Cell polarization in budding and fission yeasts. *FEMS Microbiol. Rev.* 38, 228–253. <https://doi.org/10.1111/1574-6976.12055>
- Martin, S.W., Konopka, J.B., 2004a. Lipid raft polarization contributes to hyphal growth in *Candida albicans*. *Eukaryot. Cell* 3, 675–684. <https://doi.org/10.1128/EC.3.3.675-684.2004>
- Martin, S.W., Konopka, J.B., 2004b. Lipid Raft Polarization Contributes to Hyphal Growth in *Candida albicans*. *Eukaryot. Cell* 3, 675–684. <https://doi.org/10.1128/EC.3.3.675-684.2004>
- Martín-Hernández, E., Rodríguez-García, M.E., Camacho, A., Matilla-Dueñas, A., García-Silva, M.T., Quijada-Fraile, P., Corral-Juan, M., Tejada-Palacios, P., de Las Heras, R.S., Arenas, J., Martín, M.A., Martínez-Azorín, F., 2016. New ATP8A2 gene mutations associated with a novel syndrome: encephalopathy, intellectual disability, severe hypotonia, chorea and optic atrophy. *Neurogenetics* 17, 259–263.
<https://doi.org/10.1007/s10048-016-0496-y>
- Martzoukou, O., Amillis, S., Zervakou, A., Christoforidis, S., Diallynas, G., 2017. The AP-2 complex has a specialized clathrin-independent role in apical endocytosis and polar growth in fungi. *eLife* 6. <https://doi.org/10.7554/eLife.20083>
- McConnell, H.M., Kornberg, R.D., 1971. Inside-outside transitions of phospholipids in vesicle membranes. *Biochemistry* 10, 1111–1120.
<https://doi.org/10.1021/bi00783a003>
- McMahon, H.T., Boucrot, E., 2015. Membrane curvature at a glance. *J. Cell Sci.* 128, 1065–1070. <https://doi.org/10.1242/jcs.114454>
- McManus, B.A., Coleman, D.C., 2014. Molecular epidemiology, phylogeny and evolution of *Candida albicans*. *Infect. Genet. Evol. J. Mol. Epidemiol. Evol. Genet. Infect. Dis.* 21, 166–178. <https://doi.org/10.1016/j.meegid.2013.11.008>
- Meca, J., Massoni-Laporte, A., Martinez, D., Sartorel, E., Loquet, A., Habenstein, B., McCusker, D., 2019. Avidity-driven polarity establishment via multivalent lipid–GTPase module interactions. *EMBO J.* 38, e99652.
<https://doi.org/10.15252/embj.201899652>
- Mei, K., Guo, W., 2018. The exocyst complex. *Curr. Biol.* 28, R922–R925.
<https://doi.org/10.1016/j.cub.2018.06.042>
- Mendelsohn, S., Pinsky, M., Weissman, Z., Kornitzer, D., 2017. Regulation of the *Candida albicans* Hypha-Inducing Transcription Factor Ume6 by the CDK1 Cyclins Cln3 and Hgc1. *mSphere* 2, e00248-16. <https://doi.org/10.1128/mSphere.00248-16>
- Merlini, L., Khalili, B., Bendezú, F.O., Hurwitz, D., Vincenzetti, V., Vavylonis, D., Martin, S.G., 2016. Local Pheromone Release from Dynamic Polarity Sites Underlies Cell-Cell Pairing during Yeast Mating. *Curr. Biol. CB* 26, 1117–1125.
<https://doi.org/10.1016/j.cub.2016.02.064>
- Miller, K.E., Lo, W.-C., Chou, C.-S., Park, H.-O., 2019. Temporal regulation of cell polarity via the interaction of the Ras GTPase Rsr1 and the scaffold protein Bem1. *Mol. Biol. Cell* 30, 2543–2557. <https://doi.org/10.1091/mbc.E19-02-0106>

- Mizuno-Yamasaki, E., Medkova, M., Coleman, J., Novick, P., 2010. Phosphatidylinositol 4-phosphate controls both membrane recruitment and a regulatory switch of the Rab GEF Sec2p. *Dev. Cell* 18, 828–840. <https://doi.org/10.1016/j.devcel.2010.03.016>
- Moser von Filseck, Joachim, Čopič, A., Delfosse, V., Vanni, S., Jackson, C.L., Bourguet, W., Drin, G., 2015. INTRACELLULAR TRANSPORT. Phosphatidylserine transport by ORP/Osh proteins is driven by phosphatidylinositol 4-phosphate. *Science* 349, 432–436. <https://doi.org/10.1126/science.aab1346>
- Moser von Filseck, J., Drin, G., 2016. Running up that hill: How to create cellular lipid gradients by lipid counter-flows. *Biochimie* 130, 115–121. <https://doi.org/10.1016/j.biochi.2016.08.001>
- Moser von Filseck, J., opi, A., Delfosse, V., Vanni, S., Jackson, C.L., Bourguet, W., Drin, G., 2015. Phosphatidylserine transport by ORP/Osh proteins is driven by phosphatidylinositol 4-phosphate. *Science* 349, 432–436. <https://doi.org/10.1126/science.aab1346>
- Moyes, D.L., Richardson, J.P., Naglik, J.R., 2015. *Candida albicans*-epithelial interactions and pathogenicity mechanisms: scratching the surface. *Virulence* 6, 338–346. <https://doi.org/10.1080/21505594.2015.1012981>
- Moyes, D.L., Wilson, D., Richardson, J.P., Mogavero, S., Tang, S.X., Wernecke, J., Höfs, S., Gratacap, R.L., Robbins, J., Runglall, M., Murciano, C., Blagojevic, M., Thavaraj, S., Förster, T.M., Hebecker, B., Kasper, L., Vizcay, G., Iancu, S.I., Kichik, N., Häder, A., Kurzai, O., Luo, T., Krüger, T., Kniemeyer, O., Cota, E., Bader, O., Wheeler, R.T., Gutsmann, T., Hube, B., Naglik, J.R., 2016. Candidalysin is a fungal peptide toxin critical for mucosal infection. *Nature* 532, 64–68. <https://doi.org/10.1038/nature17625>
- Murad, A.M.A., Leng, P., Straffon, M., Wishart, J., Macaskill, S., MacCallum, D., Schnell, N., Talibi, D., Marechal, D., Tekaiia, F., d'Enfert, C., Gaillardin, C., Odds, F.C., Brown, A.J.P., 2001. NRG1 represses yeast–hypha morphogenesis and hypha-specific gene expression in *Candida albicans*. *EMBO J.* 20, 4742–4752. <https://doi.org/10.1093/emboj/20.17.4742>
- Muthusamy, B.-P., Raychaudhuri, S., Natarajan, P., Abe, F., Liu, K., Prinz, W.A., Graham, T.R., 2009. Control of Protein and Sterol Trafficking by Antagonistic Activities of a Type IV P-type ATPase and Oxysterol Binding Protein Homologue. *Mol. Biol. Cell* 20, 2920–2931. <https://doi.org/10.1091/mbc.E08-10-1036>
- Naglik, J., Albrecht, A., Bader, O., Hube, B., 2004. *Candida albicans* proteinases and host/pathogen interactions. *Cell. Microbiol.* 6, 915–926. <https://doi.org/10.1111/j.1462-5822.2004.00439.x>
- Naglik, J.R., Challacombe, S.J., Hube, B., 2003. *Candida albicans* secreted aspartyl proteinases in virulence and pathogenesis. *Microbiol. Mol. Biol. Rev.* MMBR 67, 400–428, table of contents. <https://doi.org/10.1128/MMBR.67.3.400-428.2003>
- Naglik, J.R., Gaffen, S.L., Hube, B., 2019. Candidalysin: discovery and function in *Candida albicans* infections. *Curr. Opin. Microbiol.* 52, 100–109. <https://doi.org/10.1016/j.mib.2019.06.002>
- Nakano, K., Yamamoto, T., Kishimoto, T., Noji, T., Tanaka, K., 2008. Protein Kinases Fpk1p and Fpk2p are Novel Regulators of Phospholipid Asymmetry. *Mol. Biol. Cell* 19, 1783–1797. <https://doi.org/10.1091/mbc.e07-07-0646>
- Nakayama, H., Mio, T., Nagahashi, S., Kokado, M., Arisawa, M., Aoki, Y., 2000. Tetracycline-Regulatable System To Tightly Control Gene Expression in the Pathogenic Fungus *Candida albicans*. *Infect. Immun.* 68, 6712–6719.
- Natarajan, P., Liu, K., Patil, D.V., Sciorra, V.A., Jackson, C.L., Graham, T.R., 2009. Regulation of a Golgi flippase by phosphoinositides and an ArfGEF. *Nat. Cell Biol.* 11, 1421–1426. <https://doi.org/10.1038/ncb1989>

- Nicolson, G.L., 2014. The Fluid—Mosaic Model of Membrane Structure: Still relevant to understanding the structure, function and dynamics of biological membranes after more than 40years. *Biochim. Biophys. Acta BBA - Biomembr., Membrane Structure and Function: Relevance in the Cell's Physiology, Pathology and Therapy* 1838, 1451–1466. <https://doi.org/10.1016/j.bbamem.2013.10.019>
- Noble, S.M., Gianetti, B.A., Witchley, J.N., 2017. *Candida albicans* cell type switches and functional plasticity in the mammalian host. *Nat. Rev. Microbiol.* 15, 96–108. <https://doi.org/10.1038/nrmicro.2016.157>
- Pande, K., Chen, C., Noble, S.M., 2013. Passage through the mammalian gut triggers a phenotypic switch that promotes *Candida albicans* commensalism. *Nat. Genet.* 45, 1088–1091. <https://doi.org/10.1038/ng.2710>
- Pantazopoulou, A., Peñalva, M.A., 2009. Organization and Dynamics of the *Aspergillus nidulans* Golgi during Apical Extension and Mitosis. *Mol. Biol. Cell* 20, 4335–4347. <https://doi.org/10.1091/mbc.E09-03-0254>
- Pappas, P.G., Lionakis, M.S., Arendrup, M.C., Ostrosky-Zeichner, L., Kullberg, B.J., 2018. Invasive candidiasis. *Nat. Rev. Dis. Primer* 4, 1–20. <https://doi.org/10.1038/nrdp.2018.26>
- Perry, A.M., Hernday, A.D., Nobile, C.J., 2020. Unraveling How *Candida albicans* Forms Sexual Biofilms. *J. Fungi Basel Switz.* 6, E14. <https://doi.org/10.3390/jof6010014>
- Pike, L.J., 2006. Rafts defined: a report on the Keystone Symposium on Lipid Rafts and Cell Function. *J. Lipid Res.* 47, 1597–1598. <https://doi.org/10.1194/jlr.E600002-JLR200>
- Pointer, B.R., Boyer, M.P., Schmidt, M., 2015. Boric acid destabilizes the hyphal cytoskeleton and inhibits invasive growth of *Candida albicans*. *Yeast Chichester Engl.* 32, 389–398. <https://doi.org/10.1002/yea.3066>
- Pomorski, T., Lombardi, R., Riezman, H., Devaux, P.F., van Meer, G., Holthuis, J.C.M., 2003. Drs2p-related P-type ATPases Dnf1p and Dnf2p are required for phospholipid translocation across the yeast plasma membrane and serve a role in endocytosis. *Mol. Biol. Cell* 14, 1240–1254. <https://doi.org/10.1091/mbc.e02-08-0501>
- Pomorski, T.G., Menon, A.K., 2016. Lipid somersaults: Uncovering the mechanisms of protein-mediated lipid flipping. *Prog. Lipid Res.* 64, 69–84. <https://doi.org/10.1016/j.plipres.2016.08.003>
- Poulsen, L.R., López-Marqués, R.L., McDowell, S.C., Okkeri, J., Licht, D., Schulz, A., Pomorski, T., Harper, J.F., Palmgren, M.G., 2008. The Arabidopsis P4-ATPase ALA3 localizes to the golgi and requires a beta-subunit to function in lipid translocation and secretory vesicle formation. *Plant Cell* 20, 658–676. <https://doi.org/10.1105/tpc.107.054767>
- Pöyry, S., Vattulainen, I., 2016. Role of charged lipids in membrane structures — Insight given by simulations. *Biochim. Biophys. Acta BBA - Biomembr., Biosimulations of lipid membranes coupled to experiments* 1858, 2322–2333. <https://doi.org/10.1016/j.bbamem.2016.03.016>
- Prinz, W.A., 2010. Lipid trafficking sans Vesicles: where, why, how? *Cell* 143, 870–874. <https://doi.org/10.1016/j.cell.2010.11.031>
- Proszynski, T.J., Klemm, R., Bagnat, M., Gaus, K., Simons, K., 2006. Plasma membrane polarization during mating in yeast cells. *J. Cell Biol.* 173, 861–866. <https://doi.org/10.1083/jcb.200602007>
- Puerner, C., 2020. Croissance invasive d'un champignon pathogène de l'Homme: forces mécaniques et réorganisation cellulaire.
- Puerner, C., Serrano, A., WAKADE, R., Bassilana, M., Arkowitz, R.A., 2021a. A myosin light chain is critical for fungal growth robustness in *Candida albicans*. *MBio*.

- Puerner, C., Serrano, A., Wakade, R.S., Bassilana, M., Arkowitz, R.A., 2021b. A Myosin Light Chain Is Critical for Fungal Growth Robustness in *Candida albicans*. *mBio* 0, e02528-21. <https://doi.org/10.1128/mBio.02528-21>
- Pulver, R., Heisel, T., Gonia, S., Robins, R., Norton, J., Haynes, P., Gale, C.A., 2013. Rsr1 focuses Cdc42 activity at hyphal tips and promotes maintenance of hyphal development in *Candida albicans*. *Eukaryot. Cell* 12, 482–495. <https://doi.org/10.1128/EC.00294-12>
- Ramage, G., VandeWalle, K., López-Ribot, J.L., Wickes, B.L., 2002. The filamentation pathway controlled by the Efg1 regulator protein is required for normal biofilm formation and development in *Candida albicans*. *FEMS Microbiol. Lett.* 214, 95–100. <https://doi.org/10.1111/j.1574-6968.2002.tb11330.x>
- Rida, P.C.G., Nishikawa, A., Won, G.Y., Dean, N., 2006. Yeast-to-hyphal transition triggers formin-dependent Golgi localization to the growing tip in *Candida albicans*. *Mol. Biol. Cell* 17, 4364–4378. <https://doi.org/10.1091/mbc.e06-02-0143>
- Ripmaster, T.L., Vaughn, G.P., Woolford, J.L., 1993. DRS1 to DRS7, novel genes required for ribosome assembly and function in *Saccharomyces cerevisiae*. *Mol. Cell. Biol.* 13, 7901–7912. <https://doi.org/10.1128/mcb.13.12.7901-7912.1993>
- Riquelme, M., Aguirre, J., Bartnicki-García, S., Braus, G.H., Feldbrügge, M., Fleig, U., Hansberg, W., Herrera-Estrella, A., Kämper, J., Kück, U., Mouriño-Pérez, R.R., Takeshita, N., Fischer, R., 2018. Fungal Morphogenesis, from the Polarized Growth of Hyphae to Complex Reproduction and Infection Structures. *Microbiol. Mol. Biol. Rev.* 82, e00068-17. <https://doi.org/10.1128/MMBR.00068-17>
- Riquelme, M., Sánchez-León, E., 2014. The Spitzenkörper: a choreographer of fungal growth and morphogenesis. *Curr. Opin. Microbiol., Host–microbe interactions: fungi/parasites/viruses* 20, 27–33. <https://doi.org/10.1016/j.mib.2014.04.003>
- Rodríguez-Cerdeira, C., Martínez-Herrera, E., Carnero-Gregorio, M., López-Barcenas, A., Fabbrocini, G., Fida, M., El-Samahy, M., González-Cespón, J.L., 2020. Pathogenesis and Clinical Relevance of *Candida* Biofilms in Vulvovaginal Candidiasis. *Front. Microbiol.* 11, 544480. <https://doi.org/10.3389/fmicb.2020.544480>
- Roelants, F.M., Baltz, A.G., Trott, A.E., Fereres, S., Thorner, J., 2010. A protein kinase network regulates the function of aminophospholipid flippases. *Proc. Natl. Acad. Sci.* 107, 34–39. <https://doi.org/10.1073/pnas.0912497106>
- Roland, B.P., Graham, T.R., 2016. Decoding P4-ATPase substrate interactions. *Crit. Rev. Biochem. Mol. Biol.* 51, 513–527. <https://doi.org/10.1080/10409238.2016.1237934>
- Rothbauer, U., Zolghadr, K., Tillib, S., Nowak, D., Schermelleh, L., Gahl, A., Backmann, N., Conrath, K., Muylldermans, S., Cardoso, M.C., Leonhardt, H., 2006. Targeting and tracing antigens in live cells with fluorescent nanobodies. *Nat. Methods* 3, 887–889. <https://doi.org/10.1038/nmeth953>
- Saito, K., Fujimura-Kamada, K., Furuta, N., Kato, U., Umeda, M., Tanaka, K., 2004. Cdc50p, a Protein Required for Polarized Growth, Associates with the Drs2p P-Type ATPase Implicated in Phospholipid Translocation in *Saccharomyces cerevisiae*. *Mol. Biol. Cell* 15, 3418–3432. <https://doi.org/10.1091/mbc.E03-11-0829>
- Saito, K., Fujimura-Kamada, K., Hanamatsu, H., Kato, U., Umeda, M., Kozminski, K.G., Tanaka, K., 2007. Transbilayer Phospholipid Flipping Regulates Cdc42p Signaling during Polarized Cell Growth via Rga GTPase-Activating Proteins. *Dev. Cell* 13, 743–751. <https://doi.org/10.1016/j.devcel.2007.09.014>
- Santiago-Tirado, F.H., Legesse-Miller, A., Schott, D., Bretscher, A., 2011. PI4P and Rab inputs collaborate in myosin-V-dependent transport of secretory compartments in yeast. *Dev. Cell* 20, 47–59. <https://doi.org/10.1016/j.devcel.2010.11.006>

- Santos, A.X.S., Riezman, H., 2012. Yeast as a model system for studying lipid homeostasis and function. *FEBS Lett.* 586, 2858–2867. <https://doi.org/10.1016/j.febslet.2012.07.033>
- Santos, F.C., Marquês, J.T., Bento-Oliveira, A., Almeida, R.F.M. de, 2020. Sphingolipid-enriched domains in fungi. *FEBS Lett.* 594, 3698–3718. <https://doi.org/10.1002/1873-3468.13986>
- Sartorel, E., Barrey, E., Lau, R.K., Thorner, J., 2015. Plasma membrane aminoglycerolipid flippase function is required for signaling competence in the yeast mating pheromone response pathway. *Mol. Biol. Cell* 26, 134–150. <https://doi.org/10.1091/mbc.E14-07-1193>
- Sartorel, E., Ünlü, C., Jose, M., Massoni-Laporte, A., Meca, J., Sibarita, J.-B., McCusker, D., 2018. Phosphatidylserine and GTPase activation control Cdc42 nanoclustering to counter dissipative diffusion. *Mol. Biol. Cell* 29, 1299–1310. <https://doi.org/10.1091/mbc.E18-01-0051>
- Schaub, Y., Dünkler, A., Walther, A., Wendland, J., 2006. New pFA-cassettes for PCR-based gene manipulation in *Candida albicans*. *J. Basic Microbiol.* 46, 416–429. <https://doi.org/10.1002/jobm.200510133>
- Schink, K.O., Tan, K.-W., Stenmark, H., 2016. Phosphoinositides in Control of Membrane Dynamics. *Annu. Rev. Cell Dev. Biol.* 32, 143–171. <https://doi.org/10.1146/annurev-cellbio-111315-125349>
- Schultzhaus, Z., Cunningham, G.A., Mouriño-Pérez, R.R., Shaw, B.D., 2019. The phospholipid flippase DnfD localizes to late Golgi and is involved in asexual differentiation in *Aspergillus nidulans*. *Mycologia* 111, 13–25. <https://doi.org/10.1080/00275514.2018.1543927>
- Schultzhaus, Z., Yan, H., Shaw, B.D., 2015. *Aspergillus nidulans* flippase DnfA is cargo of the endocytic collar and plays complementary roles in growth and phosphatidylserine asymmetry with another flippase, DnfB. *Mol. Microbiol.* 97, 18–32. <https://doi.org/10.1111/mmi.13019>
- Schultzhaus, Z., Zheng, W., Wang, Z., Mouriño-Pérez, R., Shaw, B., 2017. Phospholipid flippases DnfA and DnfB exhibit differential dynamics within the *A. nidulans* Spitzenkörper. *Fungal Genet. Biol.* 99, 26–28. <https://doi.org/10.1016/j.fgb.2016.12.007>
- Schulz, T.A., Choi, M.-G., Raychaudhuri, S., Mears, J.A., Ghirlando, R., Hinshaw, J.E., Prinz, W.A., 2009. Lipid-regulated sterol transfer between closely apposed membranes by oxysterol-binding protein homologues. *J. Cell Biol.* 187, 889–903. <https://doi.org/10.1083/jcb.200905007>
- Schweizer, A., Rupp, S., Taylor, B.N., Röllinghoff, M., Schröppel, K., 2000. The TEA/ATTS transcription factor CaTec1p regulates hyphal development and virulence in *Candida albicans*. *Mol. Microbiol.* 38, 435–445. <https://doi.org/10.1046/j.1365-2958.2000.02132.x>
- Sezgin, E., Levental, I., Mayor, S., Eggeling, C., 2017. The mystery of membrane organization: composition, regulation and roles of lipid rafts. *Nat. Rev. Mol. Cell Biol.* 18, 361–374. <https://doi.org/10.1038/nrm.2017.16>
- Shafaq-Zadah, M., Dransart, E., Johannes, L., 2020. Clathrin-independent endocytosis, retrograde trafficking, and cell polarity. *Curr. Opin. Cell Biol.* 65, 112–121. <https://doi.org/10.1016/j.ceb.2020.05.009>
- Shlomovitz, I., Speir, M., Gerlic, M., 2019. Flipping the dogma - phosphatidylserine in non-apoptotic cell death. *Cell Commun. Signal. CCS* 17, 139. <https://doi.org/10.1186/s12964-019-0437-0>

- Silva, P.M., Puerner, C., Seminara, A., Bassilana, M., Arkowitz, R.A., 2019. Secretory Vesicle Clustering in Fungal Filamentous Cells Does Not Require Directional Growth. *Cell Rep.* 28, 2231-2245.e5. <https://doi.org/10.1016/j.celrep.2019.07.062>
- Simons, K., Ikonen, E., 1997. Functional rafts in cell membranes. *Nature* 387, 569–572. <https://doi.org/10.1038/42408>
- Simons, K., Sampaio, J.L., 2011. Membrane organization and lipid rafts. *Cold Spring Harb. Perspect. Biol.* 3, a004697. <https://doi.org/10.1101/cshperspect.a004697>
- Singer, S.J., Nicolson, G.L., 1972. The Fluid Mosaic Model of the Structure of Cell Membranes. *Science* 175, 720–731. <https://doi.org/10.1126/science.175.4023.720>
- Sinha, I., Wang, Y.-M., Philp, R., Li, C.-R., Yap, W.H., Wang, Y., 2007. Cyclin-Dependent Kinases Control Septin Phosphorylation in *Candida albicans* Hyphal Development. *Dev. Cell* 13, 421–432. <https://doi.org/10.1016/j.devcel.2007.06.011>
- Smindak, R.J., Heckle, L.A., Chittari, S.S., Hand, M.A., Hyatt, D.M., Mantus, G.E., Sanfelippo, W.A., Kozminski, K.G., 2017. Lipid-dependent regulation of exocytosis in *S. cerevisiae* by OSBP homolog (Osh) 4. *J Cell Sci* 130, 3891–3906. <https://doi.org/10.1242/jcs.205435>
- Smith, G.R., Givan, S.A., Cullen, P., Sprague Jr., G.F., 2002. GTPase-Activating Proteins for Cdc42. *Eukaryot. Cell* 1, 469–480. <https://doi.org/10.1128/EC.1.3.469-480.2002>
- Staab, J.F., Bahn, Y.-S., Tai, C.-H., Cook, P.F., Sundstrom, P., 2004. Expression of Transglutaminase Substrate Activity on *Candida albicans* Germ Tubes through a Coiled, Disulfide-bonded N-terminal Domain of Hwp1 Requires C-terminal Glycosylphosphatidylinositol Modification. *J. Biol. Chem.* 279, 40737–40747. <https://doi.org/10.1074/jbc.M406005200>
- Staab, J.F., Bradway, S.D., Fidel, P.L., Sundstrom, P., 1999. Adhesive and Mammalian Transglutaminase Substrate Properties of *Candida albicans* Hwp1. *Science* 283, 1535–1538. <https://doi.org/10.1126/science.283.5407.1535>
- Stefan, C.J., Manford, A.G., Baird, D., Yamada-Hanff, J., Mao, Y., Emr, S.D., 2011. Osh Proteins Regulate Phosphoinositide Metabolism at ER-Plasma Membrane Contact Sites. *Cell* 144, 389–401. <https://doi.org/10.1016/j.cell.2010.12.034>
- Stefan, T., G, D., K, R., P, D.C., S, C., Am, V., J, L.-S., Tp, L., Db, I., Fr, M., Ce, F., Er, E., D, J., Ar, van V., P, A., Sa, T., A, S., Hm, M., 2017. Membrane dynamics and organelle biogenesis-lipid pipelines and vesicular carriers. *BMC Biol.* 15, 102–102. <https://doi.org/10.1186/s12915-017-0432-0>
- Steinberg, G., 2007. On the move: endosomes in fungal growth and pathogenicity. *Nat. Rev. Microbiol.* 5, 309–316. <https://doi.org/10.1038/nrmicro1618>
- Sudbery, P.E., 2011. Growth of *Candida albicans* hyphae. *Nat. Rev. Microbiol.* 9, 737–748. <https://doi.org/10.1038/nrmicro2636>
- Sugiura, T., Takahashi, C., Chuma, Y., Fukuda, M., Yamada, M., Yoshida, U., Nakao, H., Ikeda, K., Khan, D., Nile, A.H., Bankaitis, V.A., Nakano, M., 2019. Biophysical Parameters of the Sec14 Phospholipid Exchange Cycle. *Biophys. J.* 116, 92–103. <https://doi.org/10.1016/j.bpj.2018.11.3131>
- Sun, Y., Drubin, D.G., 2012. The functions of anionic phospholipids during clathrin-mediated endocytosis site initiation and vesicle formation. *J. Cell Sci.* 125, 6157–6165. <https://doi.org/10.1242/jcs.115741>
- Sundstrom, P., Balish, E., Allen, C.M., 2002. Essential Role of the *Candida albicans* Transglutaminase Substrate, Hyphal Wall Protein 1, in Lethal Oropharyngeal Candidiasis in Immunodeficient Mice. *J. Infect. Dis.* 185, 521–530. <https://doi.org/10.1086/338836>

- Surma, M.A., Klose, C., Klemm, R.W., Ejsing, C.S., Simons, K., 2011. Generic sorting of raft lipids into secretory vesicles in yeast. *Traffic Cph. Den.* 12, 1139–1147. <https://doi.org/10.1111/j.1600-0854.2011.01221.x>
- Surma, M.A., Klose, C., Simons, K., 2012. Lipid-dependent protein sorting at the trans-Golgi network. *Biochim. Biophys. Acta BBA - Mol. Cell Biol. Lipids, Lipids and Vesicular Transport* 1821, 1059–1067. <https://doi.org/10.1016/j.bbalip.2011.12.008>
- Swidergall, M., Filler, S.G., 2017. Oropharyngeal Candidiasis: Fungal Invasion and Epithelial Cell Responses. *PLoS Pathog.* 13, e1006056. <https://doi.org/10.1371/journal.ppat.1006056>
- Takar, M., Huang, Y., Graham, T.R., 2019. The PQ-loop protein Any1 segregates Drs2 and Neol functions required for viability and plasma membrane phospholipid asymmetry. *J. Lipid Res.* 60, 1032–1042. <https://doi.org/10.1194/jlr.M093526>
- Takar, M., Wu, Y., Graham, T.R., 2016. The Essential Neol Protein from Budding Yeast Plays a Role in Establishing Aminophospholipid Asymmetry of the Plasma Membrane. *J. Biol. Chem.* 291, 15727–15739. <https://doi.org/10.1074/jbc.M115.686253>
- Takeshita, N., 2016. Coordinated process of polarized growth in filamentous fungi. *Biosci. Biotechnol. Biochem.* 80, 1693–1699. <https://doi.org/10.1080/09168451.2016.1179092>
- Tani, M., Kuge, O., 2014. Involvement of Sac1 phosphoinositide phosphatase in the metabolism of phosphatidylserine in the yeast *Saccharomyces cerevisiae*. *Yeast* 31, 145–158. <https://doi.org/10.1002/yea.3004>
- TerBush, D.R., Maurice, T., Roth, D., Novick, P., 1996. The Exocyst is a multiprotein complex required for exocytosis in *Saccharomyces cerevisiae*. *EMBO J.* 15, 6483–6494.
- Thomson, D.D., Berman, J., Brand, A.C., 2016. High frame-rate resolution of cell division during *Candida albicans* filamentation. *Fungal Genet. Biol.* 88, 54–58. <https://doi.org/10.1016/j.fgb.2016.02.001>
- Timcenko, M., Dieudonné, T., Montigny, C., Boesen, T., Lyons, J.A., Lenoir, G., Nissen, P., 2021. Structural Basis of Substrate-Independent Phosphorylation in a P4-ATPase Lipid Flippase. *J. Mol. Biol., Inroads Into Membrane Physiology Through Transport Nanomachines* 433, 167062. <https://doi.org/10.1016/j.jmb.2021.167062>
- Timcenko, M., Lyons, J.A., Janulienė, D., Ulstrup, J.J., Dieudonné, T., Montigny, C., Ash, M.-R., Karlsen, J.L., Boesen, T., Kühlbrandt, W., Lenoir, G., Moeller, A., Nissen, P., 2019. Structure and autoregulation of a P4-ATPase lipid flippase. *Nature* 571, 366–370. <https://doi.org/10.1038/s41586-019-1344-7>
- Tong, J., Manik, M.K., Yang, H., Im, Y.J., 2016. Structural insights into nonvesicular lipid transport by the oxysterol binding protein homologue family. *Biochim. Biophys. Acta* 1861, 928–939. <https://doi.org/10.1016/j.bbalip.2016.01.008>
- Trotter, P.J., Wu, W.I., Pedretti, J., Yates, R., Voelker, D.R., 1998. A genetic screen for aminophospholipid transport mutants identifies the phosphatidylinositol 4-kinase, STT4p, as an essential component in phosphatidylserine metabolism. *J. Biol. Chem.* 273, 13189–13196. <https://doi.org/10.1074/jbc.273.21.13189>
- Tsai, P.-C., Hsu, J.-W., Liu, Y.-W., Chen, K.-Y., Lee, F.-J.S., 2013. Arl1p regulates spatial membrane organization at the trans-Golgi network through interaction with Arf-GEF Gea2p and flippase Drs2p. *Proc. Natl. Acad. Sci. U. S. A.* 110, E668–677. <https://doi.org/10.1073/pnas.1221484110>
- Tsuji, T., Cheng, J., Tatematsu, T., Ebata, A., Kamikawa, H., Fujita, A., Gyobu, S., Segawa, K., Arai, H., Taguchi, T., Nagata, S., Fujimoto, T., 2019. Predominant localization of phosphatidylserine at the cytoplasmic leaflet of the ER, and its TMEM16K-dependent

- redistribution. *Proc. Natl. Acad. Sci. U. S. A.* 116, 13368–13373.
<https://doi.org/10.1073/pnas.1822025116>
- Upadhyay, S., Shaw, B.D., 2008. The role of actin, fimbrin and endocytosis in growth of hyphae in *Aspergillus nidulans*. *Mol. Microbiol.* 68, 690–705.
<https://doi.org/10.1111/j.1365-2958.2008.06178.x>
- Urbani, L., Simoni, R.D., 1990. Cholesterol and vesicular stomatitis virus G protein take separate routes from the endoplasmic reticulum to the plasma membrane. *J. Biol. Chem.* 265, 1919–1923.
- Ushinsky, S.C., Harcus, D., Ash, J., Dignard, D., Marcil, A., Morchhauser, J., Thomas, D.Y., Whiteway, M., Leberer, E., 2002. CDC42 Is Required for Polarized Growth in Human Pathogen *Candida albicans*. *Eukaryot. Cell* 1, 95–104.
<https://doi.org/10.1128/EC.1.1.95-104.2002>
- Valtz, N., Herskowitz, I., 1996. Pea2 protein of yeast is localized to sites of polarized growth and is required for efficient mating and bipolar budding. *J. Cell Biol.* 135, 725–739.
<https://doi.org/10.1083/jcb.135.3.725>
- van Meer, G., 2011. Dynamic Transbilayer Lipid Asymmetry. *Cold Spring Harb. Perspect. Biol.* 3, a004671. <https://doi.org/10.1101/cshperspect.a004671>
- van Meer, G., Voelker, D.R., Feigenson, G.W., 2008. Membrane lipids: where they are and how they behave. *Nat. Rev. Mol. Cell Biol.* 9, 112–124.
<https://doi.org/10.1038/nrm2330>
- Vernay, A., Schaub, S., Guillas, I., Bassilana, M., Arkowitz, R.A., 2012. A steep phosphoinositide bis-phosphate gradient forms during fungal filamentous growth. *J. Cell Biol.* 198, 711–730. <https://doi.org/10.1083/jcb.201203099>
- Wang, A., Raniga, P.P., Lane, S., Lu, Y., Liu, H., 2009. Hyphal Chain Formation in *Candida albicans*: Cdc28-Hgc1 Phosphorylation of Efg1 Represses Cell Separation Genes. *Mol. Cell. Biol.* 29, 4406–4416. <https://doi.org/10.1128/MCB.01502-08>
- Wang, H., Huang, Z.-X., Yong, J.Y.A., Zou, H., Zeng, G., Gao, J., Wang, Yanming, Wong, A.H.-H., Wang, Yue, 2016. CDK phosphorylates the polarisome scaffold Spa2 to maintain its localization at the site of cell growth. *Mol. Microbiol.* 101, 250–264.
<https://doi.org/10.1111/mmi.13386>
- Wang, Y., 2016. Hgc1-Cdc28—how much does a single protein kinase do in the regulation of hyphal development in *Candida albicans*? *J. Microbiol.* 54, 170–177.
<https://doi.org/10.1007/s12275-016-5550-9>
- Wang, Y., Yuan, P., Grabon, A., Tripathi, A., Lee, D., Rodriguez, M., Lönnfors, M., Eisenberg-Bord, M., Wang, Z., Man Lam, S., Schuldiner, M., Bankaitis, V.A., 2020. Noncanonical regulation of phosphatidylserine metabolism by a Sec14-like protein and a lipid kinase. *J. Cell Biol.* 219, e201907128.
<https://doi.org/10.1083/jcb.201907128>
- Warena, A.J., Kauffman, S., Sherrill, T.P., Becker, J.M., Konopka, J.B., 2003. *Candida albicans* Septin Mutants Are Defective for Invasive Growth and Virulence. *Infect. Immun.* 71, 4045–4051. <https://doi.org/10.1128/IAI.71.7.4045-4051.2003>
- Warena, A.J., Konopka, J.B., 2002. Septin Function in *Candida albicans* Morphogenesis. *Mol. Biol. Cell* 13, 2732–2746. <https://doi.org/10.1091/mbc.E02-01-0013>
- Weiner, A., Orange, F., Lacas-Gervais, S., Rechav, K., Ghugtyal, V., Bassilana, M., Arkowitz, R.A., 2019. On-site secretory vesicle delivery drives filamentous growth in the fungal pathogen *Candida albicans*. *Cell. Microbiol.* 21, e12963.
<https://doi.org/10.1111/cmi.12963>
- Wild, A.C., Yu, J.W., Lemmon, M.A., Blumer, K.J., 2004. The p21-activated Protein Kinase-related Kinase Cla4 Is a Coincidence Detector of Signaling by Cdc42 and

- Phosphatidylinositol 4-Phosphate*. *J. Biol. Chem.* 279, 17101–17110.
<https://doi.org/10.1074/jbc.M314035200>
- Wilhelm, L.P., Wendling, C., Védie, B., Kobayashi, T., Chenard, M.-P., Tomasetto, C., Drin, G., Alpy, F., 2017. STARD3 mediates endoplasmic reticulum-to-endosome cholesterol transport at membrane contact sites. *EMBO J.* 36, 1412–1433.
<https://doi.org/10.15252/embj.201695917>
- Wilson, R.B., Davis, D., Enloe, B.M., Mitchell, A.P., 2000. A recyclable *Candida albicans* URA3 cassette for PCR product-directed gene disruptions. *Yeast Chichester Engl.* 16, 65–70. [https://doi.org/10.1002/\(SICI\)1097-0061\(20000115\)16:1<65::AID-YEA508>3.0.CO;2-M](https://doi.org/10.1002/(SICI)1097-0061(20000115)16:1<65::AID-YEA508>3.0.CO;2-M)
- Wilson, R.B., Davis, D., Mitchell, A.P., 1999. Rapid Hypothesis Testing with *Candida albicans* through Gene Disruption with Short Homology Regions. *J. Bacteriol.* 181, 1868–1874.
- Witte, K., Strickland, D., Glotzer, M., 2017. Cell cycle entry triggers a switch between two modes of Cdc42 activation during yeast polarization. *eLife* 6, e26722.
<https://doi.org/10.7554/eLife.26722>
- Wolfe, K.H., Shields, D.C., 1997. Molecular evidence for an ancient duplication of the entire yeast genome. *Nature* 387, 708–713. <https://doi.org/10.1038/42711>
- Woods, B., Lew, D.J., 2019. Polarity establishment by Cdc42: Key roles for positive feedback and differential mobility. *Small GTPases* 10, 130–137.
<https://doi.org/10.1080/21541248.2016.1275370>
- Wu, Y., Takar, M., Cuentas-Condori, A.A., Graham, T.R., 2016. Neo1 and phosphatidylethanolamine contribute to vacuole membrane fusion in *Saccharomyces cerevisiae*. *Cell. Logist.* 6, e1228791. <https://doi.org/10.1080/21592799.2016.1228791>
- Xie, Y., Loh, Z.Y., Xue, J., Zhou, F., Sun, J., Qiao, Z., Jin, S., Deng, Y., Li, H., Wang, Y., Lu, L., Gao, Y., Miao, Y., 2020. Orchestrated actin nucleation by the *Candida albicans* polarisome complex enables filamentous growth. *J. Biol. Chem.* 295, 14840–14854.
<https://doi.org/10.1074/jbc.RA120.013890>
- Xie, Y., Sun, J., Han, X., Turšić-Wunder, A., Toh, J.D.W., Hong, W., Gao, Y.-G., Miao, Y., 2019. Polarisome scaffold Spa2-mediated macromolecular condensation of Aip5 for actin polymerization. *Nat. Commun.* 10, 5078. <https://doi.org/10.1038/s41467-019-13125-1>
- Xu, D., Zhang, X., Zhang, B., Zeng, X., Mao, H., Xu, H., Jiang, L., Li, F., 2019. The lipid flippase subunit Cdc50 is required for antifungal drug resistance, endocytosis, hyphal development and virulence in *Candida albicans*. *FEMS Yeast Res.* 19.
<https://doi.org/10.1093/femsyr/foz033>
- Xu, P., Baldrige, R.D., Chi, R.J., Burd, C.G., Graham, T.R., 2013. Phosphatidylserine flipping enhances membrane curvature and negative charge required for vesicular transport. *J. Cell Biol.* 202, 875–886. <https://doi.org/10.1083/jcb.201305094>
- Yashiroda, Y., Yoshida, M., 2019. Intraspecies cell–cell communication in yeast. *FEMS Yeast Res.* 19. <https://doi.org/10.1093/femsyr/foz071>
- Yoshida, S., Ohya, Y., Goebel, M., Nakano, A., Anraku, Y., 1994. A novel gene, STT4, encodes a phosphatidylinositol 4-kinase in the PKC1 protein kinase pathway of *Saccharomyces cerevisiae*. *J. Biol. Chem.* 269, 1166–1172.
- Yun, Y., Guo, Pusheng, Zhang, J., You, H., Guo, Pingting, Deng, H., Hao, Y., Zhang, L., Wang, X., Abubakar, Y.S., Zhou, J., Lu, G., Wang, Z., Zheng, W., 2020. Flippases play specific but distinct roles in the development, pathogenicity, and secondary metabolism of *Fusarium graminearum*. *Mol. Plant Pathol.* 21, 1307–1321.
<https://doi.org/10.1111/mpp.12985>

- Zhang, B., Yu, Q., Jia, C., Wang, Y., Xiao, C., Dong, Y., Xu, N., Wang, L., Li, M., 2015. The actin-related protein Sac1 is required for morphogenesis and cell wall integrity in *Candida albicans*. *Fungal Genet. Biol.* 81, 261–270. <https://doi.org/10.1016/j.fgb.2014.12.007>
- Zhang, C., Konopka, J.B., 2010. A Photostable Green Fluorescent Protein Variant for Analysis of Protein Localization in *Candida albicans*. *Eukaryot. Cell* 9, 224–226. <https://doi.org/10.1128/EC.00327-09>
- Zhang, J., Yun, Y., Lou, Y., Abubakar, Y.S., Guo, P., Wang, S., Li, C., Feng, Y., Adnan, M., Zhou, J., Lu, G., Zheng, W., 2019. FgAP-2 complex is essential for pathogenicity and polarised growth and regulates the apical localisation of membrane lipid flippases in *Fusarium graminearum*. *Cell. Microbiol.* 21, e13041. <https://doi.org/10.1111/cmi.13041>
- Zhang, X., Orlando, K., He, B., Xi, F., Zhang, J., Zajac, A., Guo, W., 2008. Membrane association and functional regulation of Sec3 by phospholipids and Cdc42. *J. Cell Biol.* 180, 145–158. <https://doi.org/10.1083/jcb.200704128>
- Zhang, X.C., Zhang, H., 2019. P-type ATPases use a domain-association mechanism to couple ATP hydrolysis to conformational change. *Biophys. Rep.* 5, 167–175. <https://doi.org/10.1007/s41048-019-0087-1>
- Zhao, X., Oh, S.-H., Cheng, G., Green, C.B., Nuessen, J.A., Yeater, K., Leng, R.P., Brown, A.J.P., Hoyer, L.L., 2004. ALS3 and ALS8 represent a single locus that encodes a *Candida albicans* adhesin; functional comparisons between Als3p and Als1p. *Microbiology*, 150, 2415–2428. <https://doi.org/10.1099/mic.0.26943-0>
- Zhao, X., Oh, S.-H., Yeater, K.M., Hoyer, L.L., 2005. Analysis of the *Candida albicans* Als2p and Als4p adhesins suggests the potential for compensatory function within the Als family. *Microbiology*, 151, 1619–1630. <https://doi.org/10.1099/mic.0.27763-0>
- Zheng, P., Nguyen, T.A., Wong, J.Y., Lee, M., Nguyen, T.-A., Fan, J.-S., Yang, D., Jedd, G., 2020. Spitzenkörper assembly mechanisms reveal conserved features of fungal and metazoan polarity scaffolds. *Nat. Commun.* 11, 2830. <https://doi.org/10.1038/s41467-020-16712-9>
- Zheng, X., Wang, Yanming, Wang, Yue, 2004. Hgc1, a novel hypha-specific G1 cyclin-related protein regulates *Candida albicans* hyphal morphogenesis. *EMBO J.* 23, 1845–1856. <https://doi.org/10.1038/sj.emboj.7600195>
- Zheng, X.-D., Lee, R.T.H., Wang, Y.-M., Lin, Q.-S., Wang, Y., 2007. Phosphorylation of Rga2, a Cdc42 GAP, by CDK/Hgc1 is crucial for *Candida albicans* hyphal growth. *EMBO J.* 26, 3760–3769. <https://doi.org/10.1038/sj.emboj.7601814>
- Zheng, X.-D., Wang, Y.-M., Wang, Y., 2003. CaSPA2 is important for polarity establishment and maintenance in *Candida albicans*. *Mol. Microbiol.* 49, 1391–1405. <https://doi.org/10.1046/j.1365-2958.2003.03646.x>
- Zhu, W., Filler, S.G., 2010. Interactions of *Candida albicans* with epithelial cells. *Cell. Microbiol.* 12, 273–282. <https://doi.org/10.1111/j.1462-5822.2009.01412.x>